



**Determination of
hydrology and erosion
model parameters:
Natural site adjacent to
Pit #1 at ERA Ranger
Mine, Northern Territory,
Australia**

Lyndon SJ Bell
Garry R Willgoose

January 1998



**Determination of Hydrology and Erosion Model Parameters -
Natural Site Adjacent to Pit #1 at ERA Ranger Mine Northern
Territory, Australia.**

by

Lyndon S.J. Bell & Garry R. Willgoose

**Department of Civil, Surveying and Environmental Engineering,
University of Newcastle
Callaghan NSW 2308**

January 1998

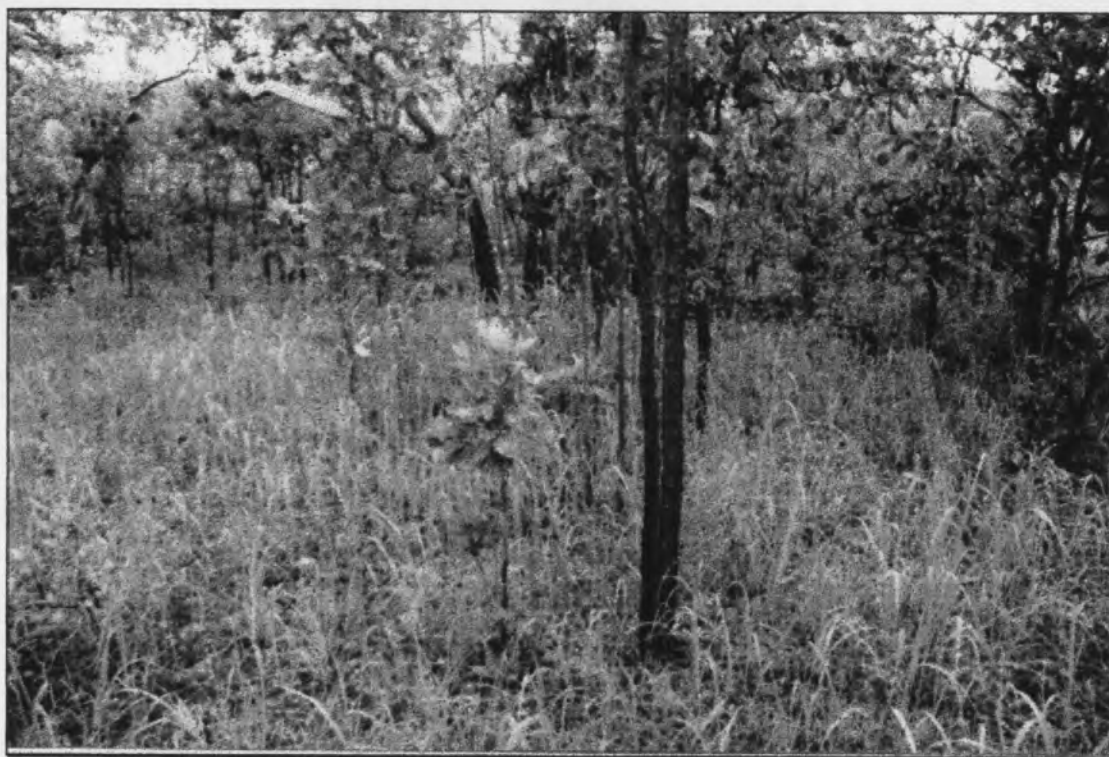
File Reference: JR-05-236



ENVIRONMENTAL RESEARCH INSTITUTE OF THE SUPERVISING SCIENTIST



ERA Ranger Mine, Pit 1.



Vegetation and ground-cover on undisturbed bushland beside Pit 1.

Acknowledgments

Acknowledgment is given to the invaluable support provided by my supervisor at the University of Newcastle, Dr. G. Willgoose, and my supervisor at *eriss*, Mr K. Evans (Senior Professional Officer, Erosion and Hydrology Section).

The support at *eriss* of Mr D. Moliere, Mr M. Saynor and Mr B. Smith, (Erosion and Hydrology Section) and Mr T. House and Mr T Mount (Information Technology Section) is also gratefully acknowledged.

Mr G. Cramb, ERA Environmental Services (ERAES) is thanked for his assistance and liaison between ERA Ranger Mine and *eriss*. Mr R. McAllister (ERAES) and Mr G. McKenzie (ERARM) are thanked for technical advice.

ERARM is thanked for the provision of; data-logging equipment, field plot construction materials, and earthmoving equipment.

My thanks are extended to Mr J Bell, Mr J Foster and Ms S Hickling, for their assistance in data acquisition and processing. Finally, the ANCA volunteers whom were involved in the initial construction of the field plot are thanked for their assistance.

Executive Summary

The current study involved erosion and hydrology data collection and parameter estimation on a 600 square metre field plot adjacent to Pit No. 1, at ERA Ranger Mine. Runoff and sediment loss data, resulting from natural rainfall, were collected during the 1996/1997 wet season and utilised to derive parameters for the Field Williams hydrology model, DISTFW; and the overland flow erosion and total sediment loss, sediment transportation models from the landform evolution model SIBERIA.

The kinematic wave and infiltrative loss parameters from DISTFW, were estimated from rainfall and runoff data utilising the non-linear regression analysis package NLFIT. The mean values for the DISTFW parameters were ascertained from eight storm events which had peak discharges in excess of 1 L/s, and a well defined duration. The mean values of the kinematic wave parameters C_r and e_m , were 4.98 and 1.82, respectively. The mean values of the infiltrative loss parameters S_ϕ and ϕ , were $1.67 \text{ mm/hr}^{1/2}$ and 14.55 mm/hr , respectively.

A comparison between DISTFW parameters obtained from the current study and the Tin Camp Creek study (comprising two field plots, the Quartz and Mica sites) was undertaken to ascertain if there were any differences in modelled hydrological behaviour. A 95% posterior probability comparison of kinematic wave parameters from eight individual storm events from the current study, and four storm events (compressed into only two sets of parameters) from both the Mica and Quartz sites, highlighted no conclusive trends, even though the Quartz site was considered to be a possible outlier. The comparison of the infiltrative loss parameters between four individual storms from the current study, and the two sets of parameters from the Mica and Quartz sites, highlighted that the Mica site was notably outside the general trend and was considered to be significantly different.

Sediment transportation rate estimation on the natural site was quantified with two similar models; the overland flow erosion; and the total sediment loss models.

The overland flow erosion model is of the form.

$$Q_s = \beta_1 W^{(1-m_1)} Q^{m_1} S^{n_1}$$

The parameters of the overland flow erosion model were estimated from a regression analysis utilising all of the collected suspended sediment experimental data from eight observed storm events.

$$Q_s = 0.917 W^{(1-0.854)} Q^{0.854} S^{0.69} \quad (r^2=0.74, df=169, p<0.001)$$

The total sediment loss erosion model is of the form.

$$T = \beta_1 W^{(1-m_1)} S^{n_1} \int Q^{m_1} dt$$

The parameters of the total sediment loss model were estimated from a regression analysis utilising both the bedload and suspended sediment experimental data from five significant storm events.

$$T = 1.171 W^{(1-1.120)} S^{0.69} \int Q^{1.120} dt \quad (r^2=0.99, df=4, p<0.001)$$

The magnitude of the erosion parameters β_1 and m_1 , from the current study compare well to previous studies on the Northern Waste Rock Dump of ERARM and in the Tin Camp Creek area, and enables quantification of the trend that the exposed waste rock material will experience decreasing rates of erosion over time.

Table of Contents

<i>Acknowledgments</i>	<i>ii</i>
<i>Executive Summary</i>	<i>iii</i>
<i>Table of Contents</i>	<i>v</i>
<i>List of Figures</i>	<i>vii</i>
<i>List of Tables</i>	<i>x</i>
1.0 Introduction	1
1.1 General Overview	1
1.2 Erosion and Hydrology	3
1.3 Research Objectives	6
2.0 Rainfall-Runoff Experimental Field Plot	11
2.1 General Overview	11
2.2 Experimental Field Plot	14
3.0 DISTFW-NLFIT Rainfall-Runoff Model	24
3.1 Introduction	24
3.2 DISTFW-NLFIT	27
3.2.1 Infiltration	27
3.2.2 Routing of Overland Flow - Hillslope Run-off	32
3.2.3 Routing of Channel Flow	34
3.3 DISTFW Data Requirements	39
3.4 DISTFW-NLFIT Calibration Procedure	45
3.5 NLFIT-General and Least Squares Error Models	48
3.6 Data	54
3.7 Parameter Comparison	63

4.0 Sediment Transport Model Parameter Fitting	75
4.1 Introduction	75
4.2 Sediment Transportation Models	76
4.3 Data	78
4.4 Parameter Comparison	86
5.0 Evaluation of the Effect of Vegetation Growth Over Wet Season	90
6.0 Further Work	97
7.0 References	98

Appendix 3.A: DISTFW Rainfall and Runoff Input Files and Predicted Versus Observed Output Hydrographs and Accompanying Statistics.

Appendix 4.A: Suspended and Bedload Sediment Data and Sample Processing Procedure.

Appendix 4.B: Particle Size Analysis.

Appendix 4.C: Regression Analysis for Overland Flow Erosion and Total Sediment Loss Models.

List of Figures

Figure 1.1.1: The locality of ERARM within the Northern Territory. The mine-site is approximately 270 kilometres East of Darwin (after Finnegan, 1993).	2
Figure 1.2.1: Mean monthly rainfall and evaporation at Jabiru Airport, approximately 5 kilometres West of ERARM (after Finnegan, 1993).	3
Figure 1.3.1: Each study listed is assumed to represent the weathered state of waste rock material after a certain number of years of exposure.	7
Figure 1.3.2: The 4 square kilometre, 17 metre high post-mining rehabilitation structure prior to erosion commencement is featured at the top of this Figure. Featured at the bottom of this Figure is the landform after 1000 years of simulated erosion by SIBERIA (after Willgoose and Riley, 1993). The initiation of gully erosion is also highlighted in this Figure.	9
Figure 2.1.1: The undisturbed natural field plot is approximately 50 metres from the edge of Pit No. 1, ERARM. The eriss staff member featured in the background of this Figure, is standing along the access road.	11
Figure 2.1.2: Schematic diagram highlighting the position of the field plot relative to the SWRD, Pit No.1, and the access road. The large cross, indicates the position of Figure 2.1.1. The position of the drainage channel and raingauge that were installed during the monitoring program are also featured in this Figure.	12
Figure 2.1.3: Three dimensional topographic surface of the 30m by 20m erosion and hydrology field plot which collected both surface run-off and transported sediment at the downslope end of the plot with a 300mm diameter PVC pipe. The dimension listed on the x, y, and z axes are a function of the computer program and are only relative to each other.	13
Figure 2.2.1: The 20 cm wide bituminous aluminium building product, (damp-coarse), was bent in a letter 'L' shape, and nailed to the soil surface, and supported with concrete. The field plot was thus hydraulically isolated from the surrounding bushland.	14
Figure 2.2.2: One half of a 300 mm diameter, 20 m long PVC pipe was buried at the down-slope end of the field plot. Additional damp-coarse material was attached to the PVC pipe to prevent overflow of surface runoff. A concrete lip was installed to allow unhindered transport of sediment and surface runoff into the PVC pipe.	15
Figure 2.2.3: Featured in the foreground is the trapezoidal hydraulic control structure which was connected to a concrete reservoir which accumulated sediment, and partially controlled the run-off.	16
Figure 2.2.4: The concrete reservoir was served a dual purpose; to collect bedload sediment that was transported during rain events and steady the flow entering the weir. Surface runoff that is leaving the PVC pipe, (highlighted by a large arrow to the left of the Figure), enters the concrete reservoir and is quickly steadied.	17
Figure 2.2.5: The concrete reservoir serves as an aid to steady the flow of water across the trapezoidal weir, and as a storage area for bedload sediment.	18
Figure 2.2.6: Considerable quantities of surface run-off are transported from the field plot, the change in direction of flow, and the length of the reservoir both serve to control and steady the flow.	18
Figure 2.2.7: Cross-sectional view of the hydraulic control structure, with a base of 150 mm. The depth of water, with respect to cross-sectional area, is utilised to determine the discharge through the structure.	19
Figure 2.2.8: Run-off is still occurring in the foreground of this Figure after a storm event. The position of the hydraulic inlet that is connected to the stilling well containing the water level sensing device is also featured in this Figure.	20
Figure 2.2.9: Featured to the left of this Figure is the discharge trench that was constructed to carry runoff away from the experimental area. Attached to the star picket in the background of this Figure is the manual raingauge, and the steel cylinder sitting atop a pedestal, in the middle of the Figure, is the electronic tipping bucket raingauge.	22
Figure 2.2.10: A schematic of a tipping bucket raingauge featuring two L-shaped plastic buckets in a back to back configuration attached to a fulcrum, a magnet attached to the plastic bucket mechanism, and a magnetic sensitive switch which was connected to an electronic data logger.	23
Figure 3.1.1: Numerous mechanisms for water movement exist on hill-slopes including overland and subsurface pathways (after Gerrard, 1981).	24

Figure 3.1.2: Four module conceptual arrangement of the rainfall-runoff model, DISTFW, incorporating non-linear surface and linear groundwater storage, and kinematic wave hillslope and channel routing (after Willgoose et al, 1995).	26
Figure 3.2.1: Typical infiltration rate curves for different soil matrix compositions under ponded infiltration (Gerrard, 1981).	27
Figure 3.2.2: The infiltration envelope highlighted in this Figure, defines the time to ponding for rainfalls of different hypothetical intensities (Smith, 1972; cited in Kirkby and Morgan, 1980).	29
Figure 3.2.3: Incremental precipitation rate and its dissociation into amounts of infiltration, depression storage, and overland flow (Fetter, 1994).	31
Figure 3.2.4: A schematic of a hillslope which illustrates the principal of temporary storage of surface run-off, infiltration and subsurface flow (Kuczera 1996).	34
Figure 3.2.5: Combination of four different cross sectional profiles illustrating A) Constant depth sheet flow, B) Irregular depth sheet flow, C) Triangular rill flow, and D) Irregular depth rill flow (after Willgoose and Kuczera, 1995).	37
Figure 3.3.1: Regression analysis of the results obtained from the calibration experiment performed on the water level sensing device (capacitance rod), prior to installation on-site.	39
Figure 3.3.2: An extract from a raw data file unloaded from the UNIDATA data-logger highlighting the number of tips from the electronic raingauge, and the water level via a capacitance reading. It should be noted that the number in the column after the 'D', representing a data-entry line, represents the channel that each device was connected to within the data-logger.	40
Figure 3.3.3: The 30 m in length, and 20 m in width, 600 m ² field plot was divided into ten equally proportioned sub-catchments and upstream and downstream elevation information was entered into the 'Field Williams' file. The Northing and Eastings including topographic measurements can only be conservative to one another.	42
Figure 3.3.4: A typical Field Williams input file, containing topographic information on the field plot, and the rainfall and runoff input file names for a particular storm event.	43
Figure 3.3.5: A DISTFW rainfall input file featuring a title, and cumulative rainfall with accompanying time stamp in decimal hours since the commencement of the event.	44
Figure 3.3.6: A DISTFW runoff input file featuring a title, and discharge, (m ³ /s), with accompanying time stamp in decimal hours since the commencement of the event.	44
Figure 3.4.1: The global optimisation of the objective function $\psi(\gamma)$, involves the search vector moving in a down-gradient direction until a minimum is reached, denoted by an 'X' (Kuczera, 1994).	45
Figure 3.5.1: Plot of standardised residuals versus predicted response for a least squares model of the 1 st January 1997 event. The increasing spread of standardised residuals versus predicted response indicates that the residual variance is increasing with predicted response thus violating the least squares model assumption. The number 'X' in this plot refers to 'X' residuals occupying virtually the same position.	49
Figure 3.5.2: Plot of time versus standardised residuals for the 1 st January 1997 event. The Z statistic being -9.5, exceeds the test value of 2 , indicating that the standardised residuals are not independent.	50
Figure 3.5.3: A normal probability plot for the storm event occurring on the 1 st January 1997 with a Kolmogorov-Smirnov statistic of 0.1091, and a 5% exceedance value of 0.0690. As the Kolmogorov-Smirnov statistic exceeds the 5% test value, the residuals are considered not to be normally distributed.	51
Figure 3.5.4: Residual autocorrelation plot for the 1 st January storm event, which highlights the time dependence of the residuals, in this case the assumption of the residuals being statistically independent is not consistent with the data.	52
Figure 3.5.5: Residual cumulative periodogram plot for the 1 st January 1997 storm event, which should be linear assuming that the residuals are independent and constant (an assumption of the least squares error model).	53
Figure 3.6.1: Observed and predicted discharge, (m ³ /s), and cumulative rainfall, (mm), for the storm event occurring on the 1 st January 1997. The large arrow indicates a reduction in rainfall that resulted in a subsequent decrease in observed and predicted discharge from the field plot.	56

Figure 3.6.2: The ill-defined duration of the overnight storm event occurring over the 23 rd -24 th January, resulted in the considerable differences between the observed and predicted hydrographs.	57
Figure 3.6.3: The predicted hydrograph of the storm event occurring on the 19 th February, does not compare well with the observed hydrograph. Considerable fluctuation in the observed hydrograph over an extended period of time virtually negates the possibility of a smooth predicted response curve.	60
Figure 3.6.4: The inclination limb of the storm event occurring on the 28 th January, is well estimated, with a slight drop in discharge resulting from a fluctuation in rainfall, highlighted by an arrow. The recession limb is dominated by fluctuations in the observed hydrograph, highlighted by an arrow, resulting from intermittent rainfall occurring at the 1.5 hour mark.	61
Figure 3.6.4: The inclination limb of the second storm event of the 21 st January is adequately fitted, however the peak and the recession limb is poorly approximated. A large second discharge peak is predicted at the 0.5 hour mark and considerable under-prediction is evident beyond the 0.75 hour mark.	62
Figure 3.7.1: 95% posterior probability plot of the kinematic wave parameters, C , and e_m for the ten storm events listed from the current study and two parameter sets from the Mica and Quartz sites (Table 3.7.1).	69
Figure 3.7.2: The predicted hydrograph for the storm event occurring on the 4 th January, exhibits considerable deviation from the observed hydrograph in both the peak and the recession limb. Differences in the volume of the predicted hydrograph compared to that which was observed is believed to have been the origin of the large standard deviations of the infiltrative loss parameters listed in Table 3.7.2 for this event.	70
Figure 3.7.3: The end of predicted hydrograph for the storm event occurring on the 22 nd February was non-zero, due to an error in the DISTFW runoff input file. This was believed to have resulted in difficulties in the estimation of the volume of the hydrograph which was translated into large standard deviations for the infiltrative loss parameters, S_p and ϕ .	72
Figure 3.7.4: The predicted hydrograph for the storm event occurring on the 23 rd February, exhibits considerable deviation from the observed hydrograph in both the peak and in the recession limb. Differences in the volume of the predicted hydrograph compared to that which was observed is believed to be the origin of the large deviations of the infiltrative loss parameters, S_p and ϕ .	73
Figure 3.7.5: 95% posterior probability plot of the infiltrative parameters, S_p and ϕ , for four storm events from the natural site, 1 st and 3 rd January, 20 th and 22 nd pm February, and the Quartz and Mica sites from Tin Camp Creek.	74
Figure 4.3.1: Plot of the suspended sediment concentration, (g/L), and discharge, (m^3/s), versus time, (hours), for a storm event occurring on the 1 st January 1997.	79
Figure 4.3.2: A log-log regression analysis of ' Q ', discharge, (L/s), versus ' Q_s ', sediment discharge, (g/s), Equation (4.3.2), was performed utilising all the suspended sediment samples from eight storm events (Table 4.3.1).	80
Figure 4.3.3: A log-log regression analysis of the integration of $Q^{m1} dt$, (L^{m1}), against the total sediment loss, ' T ', (g), was performed utilising the five storm events listed in Table 4.3.2.	84
Figure 5.1: Natural field plot, 5 th December 1996.	90
Figure 5.2: Natural field plot, 30 th December 1996.	91
Figure 5.3: Natural field plot, 29 th January 1997.	91
Figure 5.4: Decomposing leaf litter from the previous wet season slowly breaks down during the course of the year and provides considerable coverage of the soil surface.	92
Figure 5.1: 95% posterior probability plot of the kinematic wave parameters C , and e_m for the eight storm events listed in Table 5.1. The eight storm events were divided into two groups, those occurring at the start and at the end of the wet season, each with their on defined mean.	94
Figure 5.2: Plot of the S_p values fitted from DISTFW-NLFIT, for eight storm events that occurred over the wet season that are listed in Table 5.1.	95
Figure 5.3: Plot of the ϕ values fitted from DISTFW-NLFIT, for eight storm events that occurred over the wet season that are listed in Table 5.1.	96

List of Tables

<i>Table 3.4.1: DISTFW model parameter initial calibration magnitudes and designation as to whether an estimation of the parameter was sought or whether the parameter's value was permanently fixed.</i>	46
<i>Table 3.6.1: Recorded storm events during the 1996/1997 wet season with associated total rainfall, (mm), peak discharge, (L/s) and storm duration (hours).</i>	54
<i>Table 3.6.2: Summary of infiltration and kinematic wave parameter values for all storm events that had a peak discharge in excess of 1L/s, and a definite storm duration.</i>	58
<i>Table 3.7.1: Mean and standard deviations for the kinematic wave and infiltrative loss DISTFW parameters for all the storm events from the current study listed in Table 3.6.2 (neglecting 22/1/97nd, 23-24/1/97, and 28/1/97) and the Tin Camp Creek study (Moliere et al, 1996).</i>	64
<i>Table 3.7.2: Summary of infiltration and kinematic wave parameter values for eight representative storm events from the natural site and from the Tin Camp Creek study.</i>	68
<i>Table 4.3.1: Storm events and respective rainfall and runoff characteristics for eight monitored storm events from the natural site.</i>	78
<i>Table 4.3.2: Eight observed storm events from the natural site and their respective total runoff, (L), total suspended and bedload sediment, (g).</i>	83
<i>Table 4.4.1: Comparison between the fitted erosion parameters β_1 and m_1, from the overland flow erosion and the total sediment loss model.</i>	86
<i>Table 4.4.2: Comparison between the fitted erosion parameters β_1 and m_1, from the overland flow erosion model for the Tin Camp Creek, utilising the complete data set, and data with discharge values less than 10L/s, and the natural site study.</i>	86
<i>Table 4.4.3: Comparison between the fitted erosion parameters β_1 and m_1, from the total sediment loss model for studies conducted on the Northern Waste Rock Dump, in the Tin Camp Creek area, and the current study.</i>	87
<i>Table 5.1: Summary of kinematic wave parameter values for eight storm events from the current study that occurred at the start of January and the end of February.</i>	93

1.0 Introduction

1.1 General Overview

The Energy Resources of Australia Ranger Mine (ERARM), is situated approximately 11 kilometres East of the township of Jabiru, enclosed by, but not a part of, the world heritage listed Kakadu National Park, in the Northern Territory. The mine-site is approximately 270 kilometres East of Darwin and occupies a 78 square kilometre lease, which incorporates both the current Ranger operation and the future Jabiluka operation (Figure 1.1.1).

The landscape within the Kakadu National Park is diverse and contrasting, ranging from the massive sandstone escarpment of the Arnhem land plateau, to flat open woodland, to expansive wetlands and billabongs that spill into the coastal fringe.

The Commonwealth body, the Office of the Supervising Scientist, of which the Alligator Rivers Region Research Institute (ARRRI) was a part of, was established to monitor and assess the environmental impact of the uranium mine on the surrounding environment. The ARRRI was renamed in 1993 as the Environmental Research Institute for the Supervising Scientist (*eriss*), (which is now a part of the Commonwealth Environment Department), from amendments to the Environmental Protection (Alligators Rivers Region) Act, (1978), to reflect the broadened role of the organisation. The program of research at *eriss*, is broadly outlined in Johnston (1995), and includes; the impact of mining on the environment, the protection and management of wetlands, and general environment protection research.

The Erosion and Hydrology Section at *eriss* has focussed, in recent years, on landform evolution modelling, which requires the input of data concerning the erosion and hydrology of such landforms (Johnston, 1995).

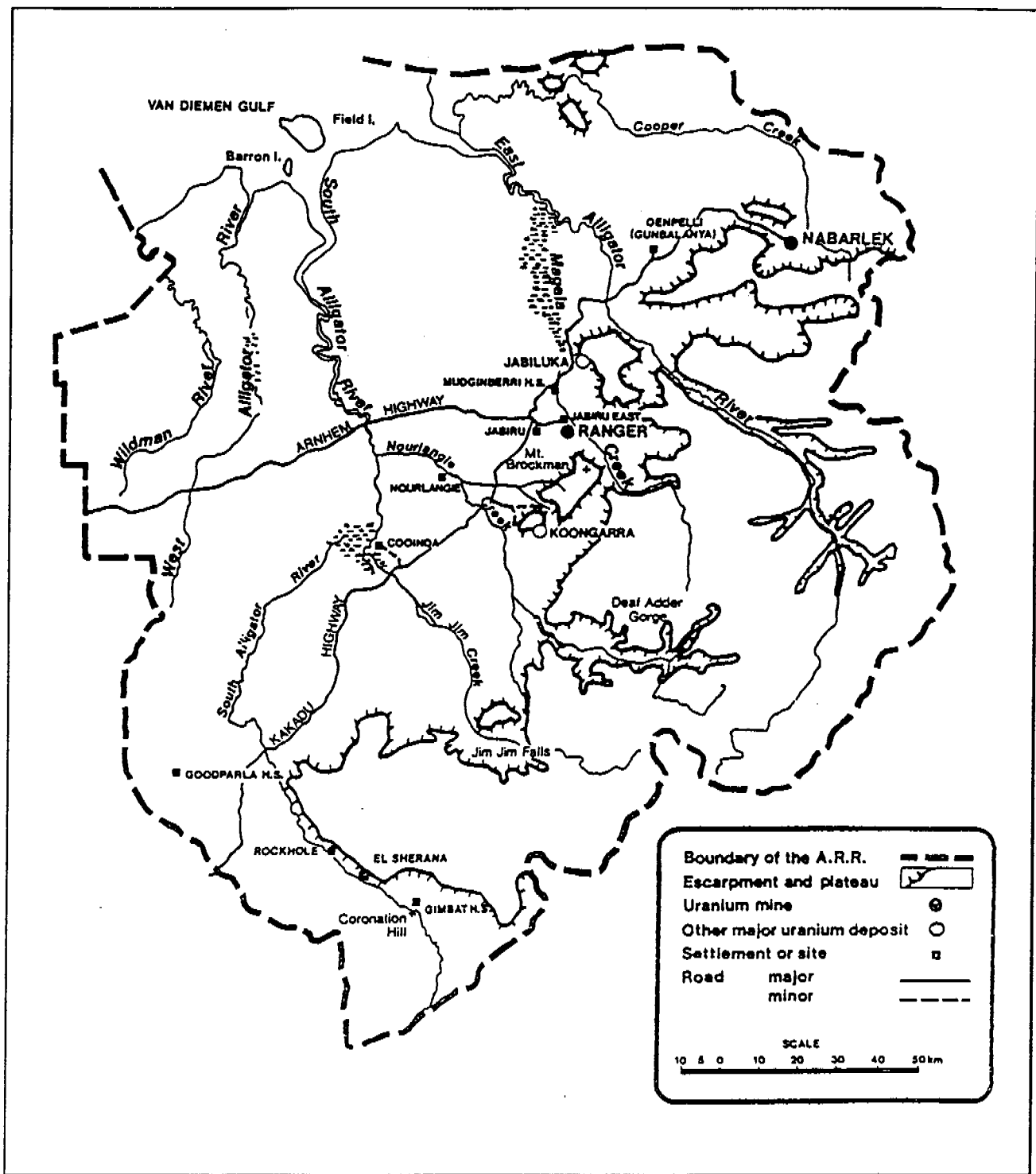


Figure 1.1.1: The locality of ERARM within the Northern Territory. The mine-site is approximately 270 kilometres East of Darwin (after Finnegan, 1993).

1.2 Erosion and Hydrology

The climatic fluctuations that occur within the Kakadu National Park are regarded as extreme. The annual rainfall characteristics of the region can be divided into distinct wet and dry seasons. The average temperature fluctuates between 25-35°C in the wet season and 17-30°C in the dry season. The wet season is characterised by a three to four month period of intensive rainfall from November to March, followed by the extended dry season, from April to October (Figure 1.2.1).

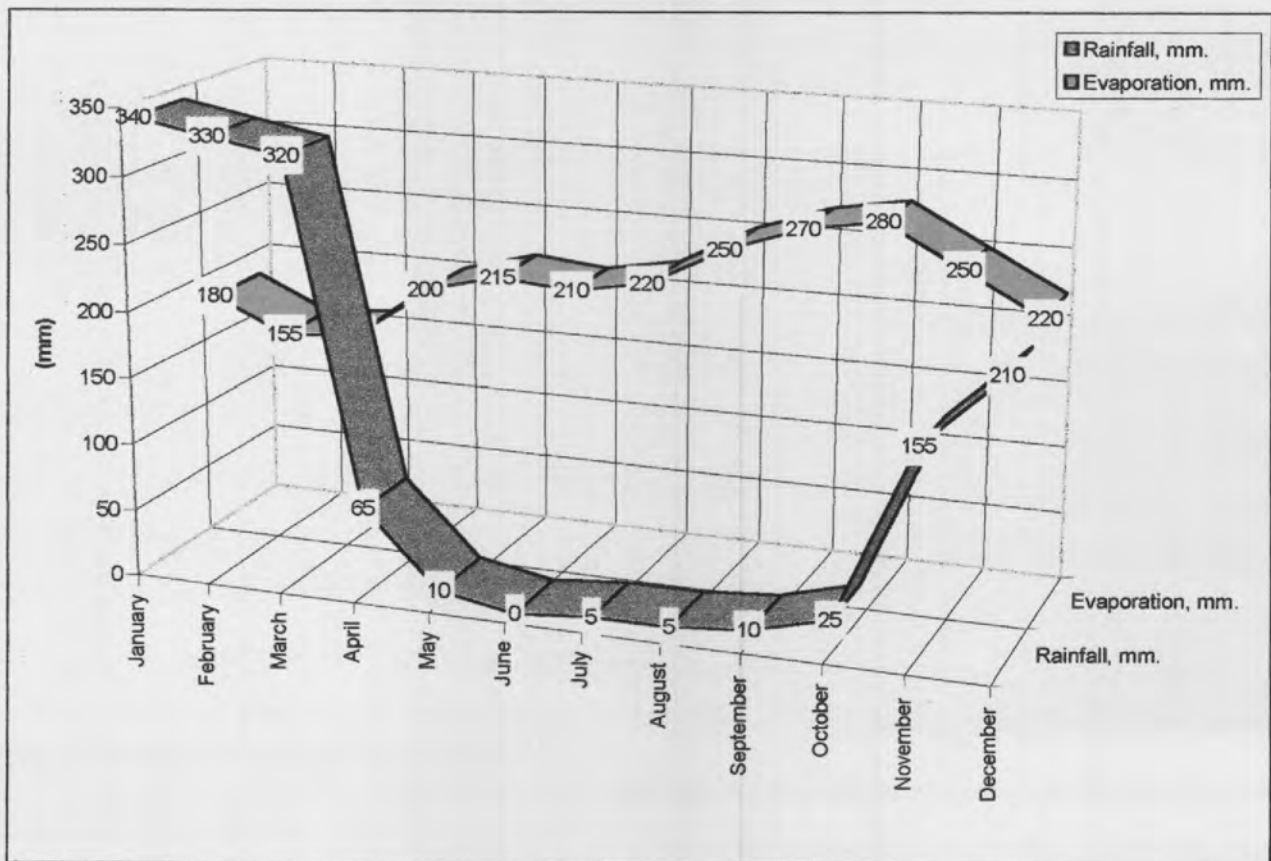


Figure 1.2.1: Mean monthly rainfall and evaporation at Jabiru Airport, approximately 5 kilometres West of ERARM (after Finnegan, 1993).

It can be observed from Figure 1.2.1, that the rates of evaporation across the year are fairly consistent, and that approximately 60% of the average annual rainfall of 1481 mm (20 year average) falls during the period January to March.

The distinct extremes between the wet and dry seasons of the region, has a considerable influence on the erodibility of the landscape. During the 1996/1997 wet season for example, considerable periods of intensive rainfall were noted, such as 60 mm of rainfall in less than one hour at the start of January, and 40 mm in just 18 minutes at the end of January.

In contrast, during the long periods of the dry season where there is virtually no rainfall, considerable quantities of sediment accumulate on the surface from accelerated weathering believed to be due to large temperature fluctuations between the day and night and the highly weatherable nature of the soil material.

The quantity and intensity of surface run-off is a major function governing sediment transportation (Willgoose and Riley, 1993). The magnitude of rainfall intensities previously reported, highlights the considerable potential for surface erosion in the region from rainfall.

ERARM exploits a stratabound uranium deposit hosted by the lower member of the Early Proterozoic Cahill Formation (Evans, Willgoose and Riley, 1995). The waste rock material from the ERARM operation comprises of carbonates, carbonaceous schists and mica, and quartz feldspar schist from that lower member (Needham, 1988; cited in Evans *et al*, 1995). Milnes (1988; cited in Evans, *et al*, 1995) noted that this waste rock material is highly weatherable, and large components of the chloritic schist fragments break down into medium and fine gravel and clay rich detritus within a two to three year period.

Willgoose and Riley (1993) noted that by circa 2012, when the all economic uranium ore has been extracted from the first and third orebodies at ERARM, there will remain approximately 100 million tonnes of tailings, waste material, and sub-economic grade ore. There are numerous alternatives for long-term containment of this material, one option is the creation of a 4 square kilometre, 17 metre high landform, termed the "above ground option" (Willgoose and Riley, 1993). Any surface landform configuration will be subjected to considerable erosion due to extremes of temperature and erosive rainfall.

Willgoose and Riley (1993) identified both short and long term possible erosion hazards which could be experienced after the cessation of mining at ERARM;

- Sediment influx into the local fluvial system from short-term erosion of waste rock material, and
- Radioactive and heavy metal contamination from long-term erosion of the tailings dam.

1.3 Research Objectives

Hydrological and geomorphological studies have been previously conducted by the Erosion and Hydrology Section of *eriss*, to ascertain reasonable estimates of erosion rates that the rehabilitated landform would experience over time. Studies have occurred on both the Northern Waste Rock Dump (NWRD) of ERARM (Willgoose and Riley, 1993; Saynor, Evans, Smith, and Willgoose, 1995; and Evans, Saynor and Riley, 1996) and in the Tin Camp Creek area (Moliere, Evans, Riley, and Willgoose, 1996). Tin Camp Creek, a tributary of the East Alligator River, is situated approximately 25 kilometres south west of Nabarlek (Figure 1.1.1).

Riley (1992; cited in Moliere *et al*, 1996) noted that weathering studies conducted on the NWRD may not reflect the long-term erosion rate of the landform, as the surfaces are relatively immature, having only had 5 to 8 years of exposure. Another more mature surface was sought that would reflect the state of the weathered waste rock material after a considerable time period. Uren (1992; cited in Moliere *et al*, 1996) stated that the Tin Camp Creek site would most likely reflect the erosional characteristics of a rehabilitated (including re-vegetation) structure at ERARM in the long term.

The current investigation involved similar hydrological and geomorphological studies as previously conducted at Tin Camp Creek and on the NWRD. Natural rainfall event monitoring on a 600 square metre field plot adjacent to Pit No. 1, at ERARM was conducted over the 1996/1997 wet season and constitutes the current project. It should be noted that the current study is also referred to as the natural site.

Willgoose (pers. comm.) noted that the three studies previously mentioned could be considered on a geological time-scale. Willgoose emphasised that the NWRD has been exposed for approximately ten years and represents the virtually unweathered nature of the waste rock material.

Evans, Riley, and Willgoose (1993; cited in Moliere *et al*, 1996) noted that the Tin Camp Creek site was assumed to represent waste rock material after at least 1,000 years of weathering and the development of natural vegetation.

Willgoose (pers. comm.) considered the natural site to represent waste rock material after approximately 10,000 to 100,000 years of weathering and the development of natural vegetation. Figure 1.3.1 highlights the three studies with respect to a geological time scale.

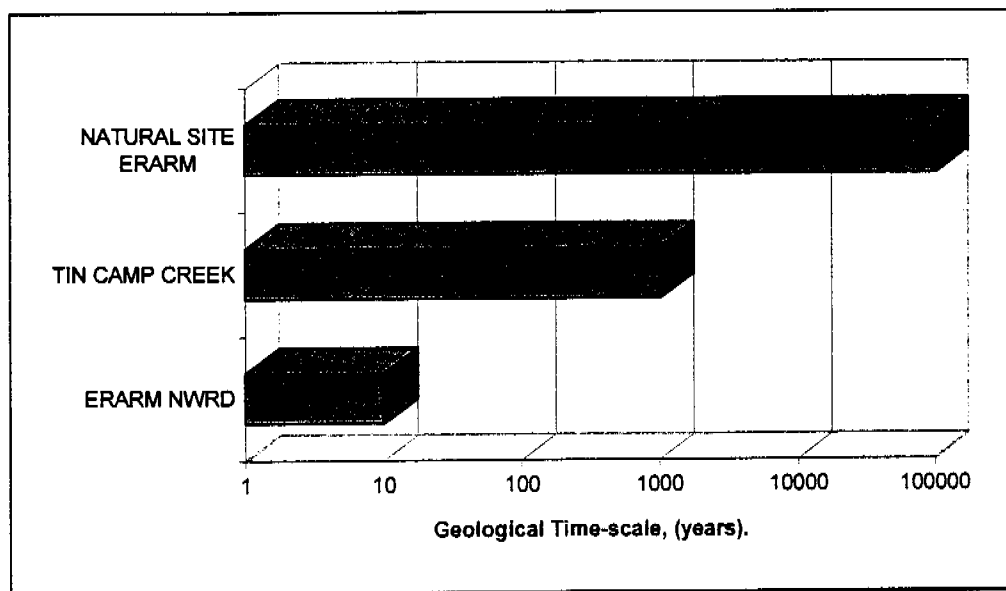


Figure 1.3.1: Each study listed is assumed to represent the weathered state of waste rock material after a certain number of years of exposure.

The specific research objectives of this study were;

- 1) Establishment of an erosion and runoff plot adjacent to Pit No.1 in undisturbed bushland;
- 2) Field monitoring on the plot by collecting rainfall, sediment (suspended and bedload) loss, and runoff data under natural rainfall.

- 3) Hydrological data collected was to be used to determine Distributed Field Williams (DISTFW) (Willgoose, Kuczera, and Williams, 1995) rainfall-runoff model parameters; and
- 4) Sediment loss data collected was to be used to determine parameters in sediment transportation equations from the landform evolution model, SIBERIA (Willgoose, Bras, and Rodriguez-Iturbe, 1989).

The DISTFW-NLFIT package (Willgoose *et al*, 1995) utilised in this study incorporates the DISTFW rainfall-runoff model with the nonlinear Bayesian regression analysis package, NLFIT (Kuczera, 1989). The package is able to estimate values for Field Williams hydrology model parameters that describe a discharge hydrograph. This hydrograph is calibrated to an observed hydrograph for a given rainfall event.

The landform evolution model, SIBERIA, is a computer model that can be used to predict the erosional development of catchments and their channel networks over time (Willgoose and Riley, 1993). Figure 1.3.2 illustrates the possible state of the post-mining rehabilitation structure after 1000 years of simulated erosion utilising SIBERIA.

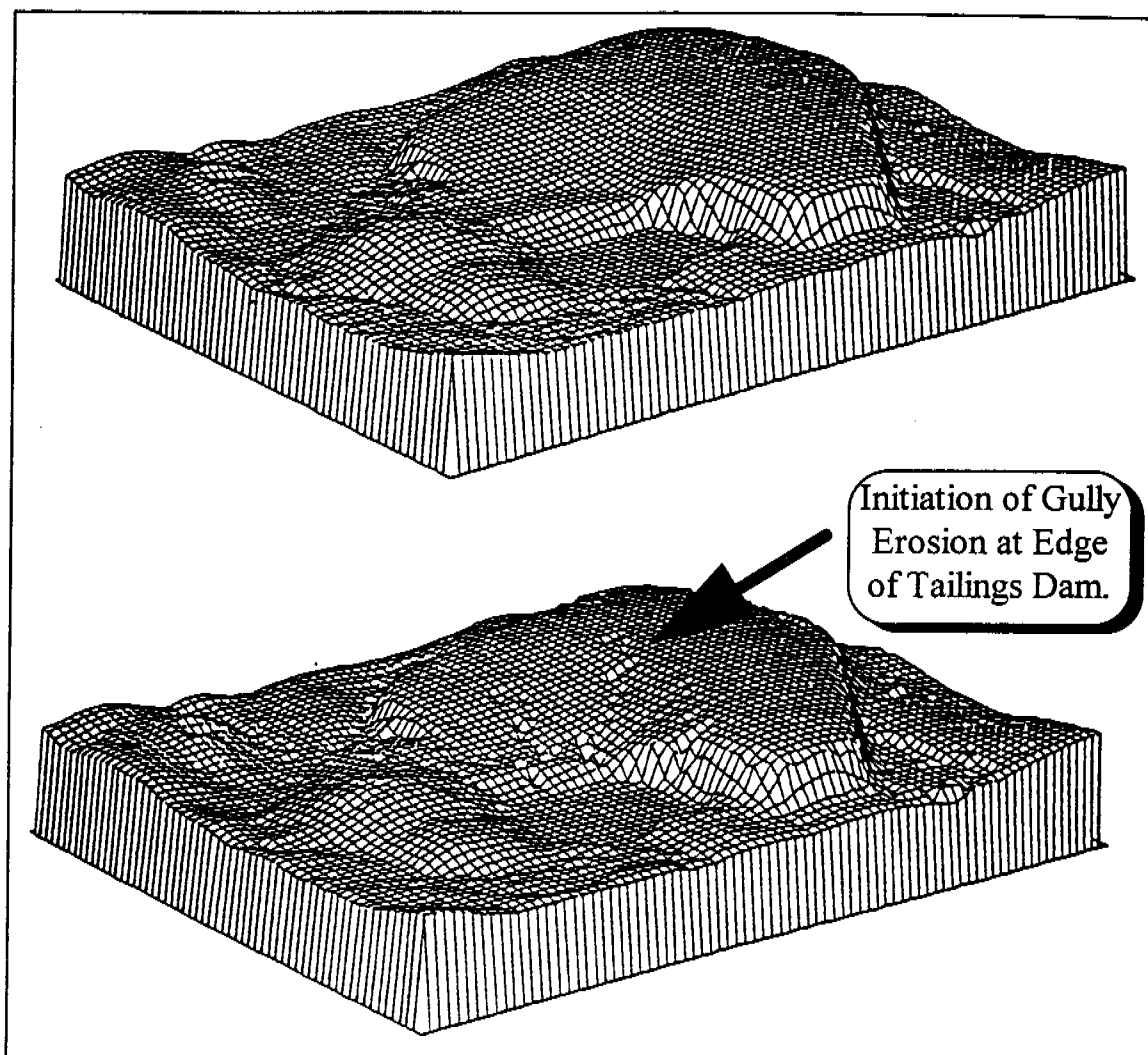


Figure 1.3.2: The 4 square kilometre, 17 metre high post-mining rehabilitation structure prior to erosion commencement is featured at the top of this Figure. Featured at the bottom of this Figure is the landform after 1000 years of simulated erosion by SIBERIA (after Willgoose and Riley, 1993). The initiation of gully erosion is also highlighted in this Figure.

It can be observed in the lower DTM plot of the rehabilitated landform (highlighted by a large arrow in Figure 1.3.2), that gully erosion is predicted to occur. The breach of the tailings dam wall and the subsequent release of radioactive and heavy metal tailings from gully erosion, was identified by Willgoose and Riley (1993) as a potential threat to the surrounding environment in the long term.

Over a geological time scale (Figure 1.3.2), SIBERIA simulates the erosional evolution of the rehabilitation structure. Over such a long period of time, rates of erosion are going to change, through the development of vegetation cover and changes in the physical composition of the erodible material. It is therefore important to compare the similarity of the natural site and the Tin Camp Creek site with respect to infiltration properties, to ascertain whether a long term trend in hydrologic behaviour is likely to exist, which may affect the erosion rates predicted by SIBERIA. A comparison between the predicted rates of sediment transportation utilising the overland flow erosion model and the total sediment loss model, from studies on the NWRD, in the Tin Camp Creek area, and the on the natural site is presented in Section 4.0.

Other minor objectives of the current study include the evaluation of the effect of vegetation growth on the hydrological characteristics of the field plot during the course of the wet season (Section 5.0). Previous studies (George, 1996) have been conducted to evaluate the effect of vegetation growth on a ripped, topsoiled site on the NWRD of ERARM. An evaluation of the deficiencies of the use of the least squares error model has also been conducted (Section 3.0). In a complex hydrologic model such as DISTFW, most of the distributions of errors in data sets violate the assumptions of the least squares model indicating that a more general error model should be used. The DISTFW-NLFIT package incorporates diagnostic statistics to assess the violations of least square error model assumptions and enables the selection of the appropriate form of a more general error model (Box-Cox transformation or an Auto-Regressive Moving Average) for a particular data set.

2.0 Rainfall-Runoff Experimental Field Plot

2.1 General Overview

Hydrology and sediment loss data was collected from a 600 square metre rainfall-runoff plot purposefully constructed in undisturbed bushland approximately 50 metres from the edge of Pit No.1, ERARM (Figure 2.1.1).

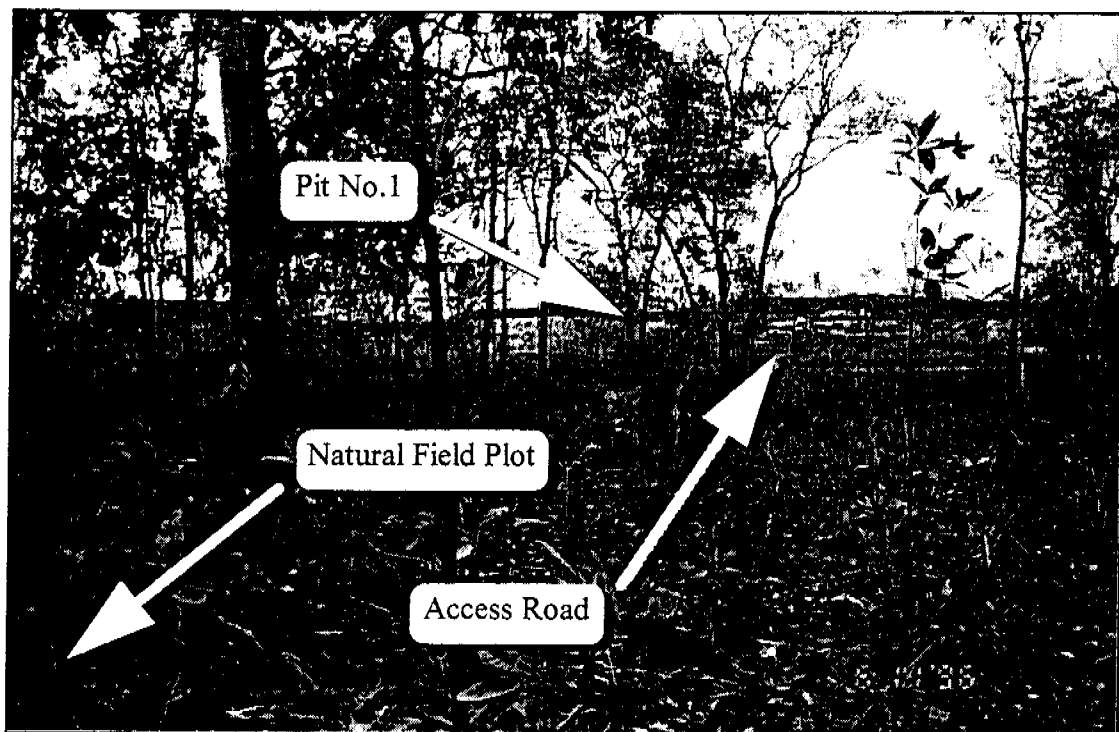


Figure 2.1.1: The undisturbed natural field plot is approximately 50 metres from the edge of Pit No. 1, ERARM. The *eriss* staff member featured in the background of this Figure, is standing along the access road.

Figure 2.1.1 illustrates the undisturbed character of the field plot area, prior to construction in early November 1996. The large open space in the background of Figure 2.1.1, is Pit No.1 which is approximately 700 metres in diameter. The vegetative ground-cover in the area is sparse to non-existent prior to the commencement of the monsoonal wet season.

The determination of the position of the field site involved meeting a number of criteria;

- The site had to be totally undisturbed, containing original vegetation;
- The site was not to be unduly sheltered from surrounding landform structures, such as the Southern Waste Rock Dump (SWRD);
- The general slope of the site must be conducive to the establishment of an experimental field plot; and
- The site must be representative of the landscape present before the commencement of mining operations.

The position of the field plot with respect to the SWRD, and Pit No.1, is illustrated in Figure 2.1.2.

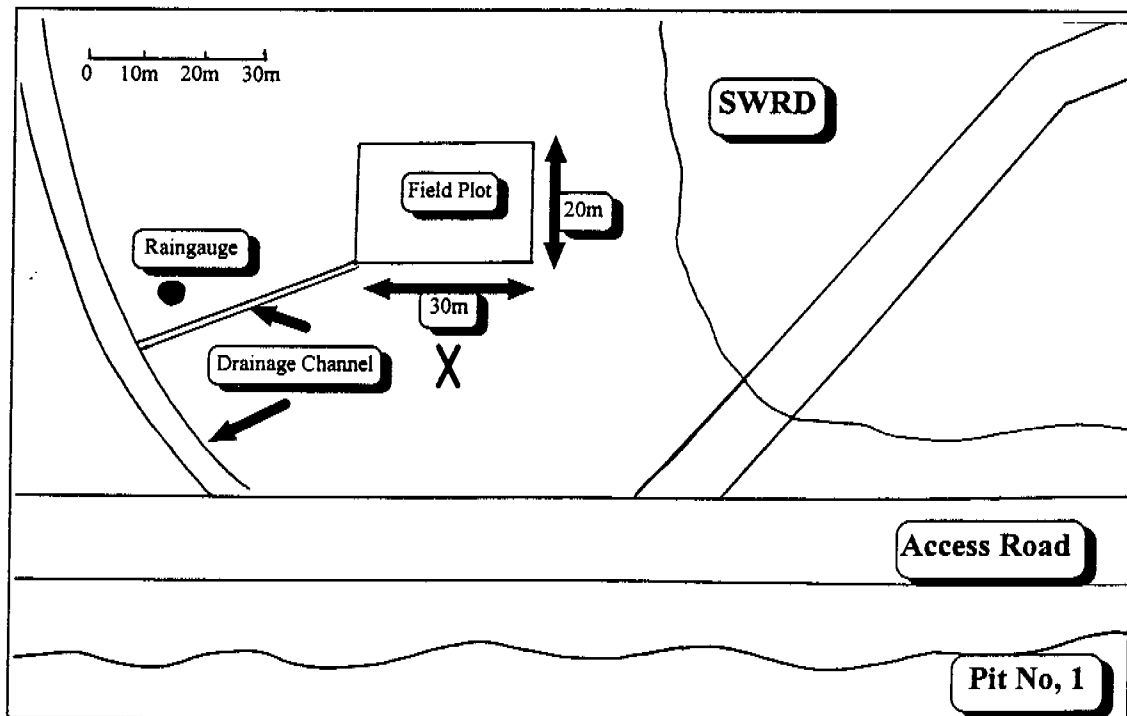


Figure 2.1.2: Schematic diagram highlighting the position of the field plot relative to the SWRD, Pit No.1, and the access road. The large cross, indicates the position of Figure 2.1.1. The position of the drainage channel and raingauge that were installed during the monitoring program are also featured in this Figure.

It can be observed from Figure 2.1.1 that the criteria that the plot should contain undisturbed vegetation was satisfied. Figure 2.1.2 highlights that the position of the field plot is sufficiently distant from the 15 metre high SWRD. The SWRD was not believed to have any notable shadowing effects upon rainfall falling upon the site. The vegetative characteristics of the field plot, were considered to be representative of other portions of undisturbed bushland around and outside the confines of ERARM.

The general topography of the field plot was ascertained in a survey using a TopCon total station theodolite (Figure 2.1.3). The average slope was calculated to be 0.027 metre drop per metre, thus satisfying the criteria of a gently sloping field plot.

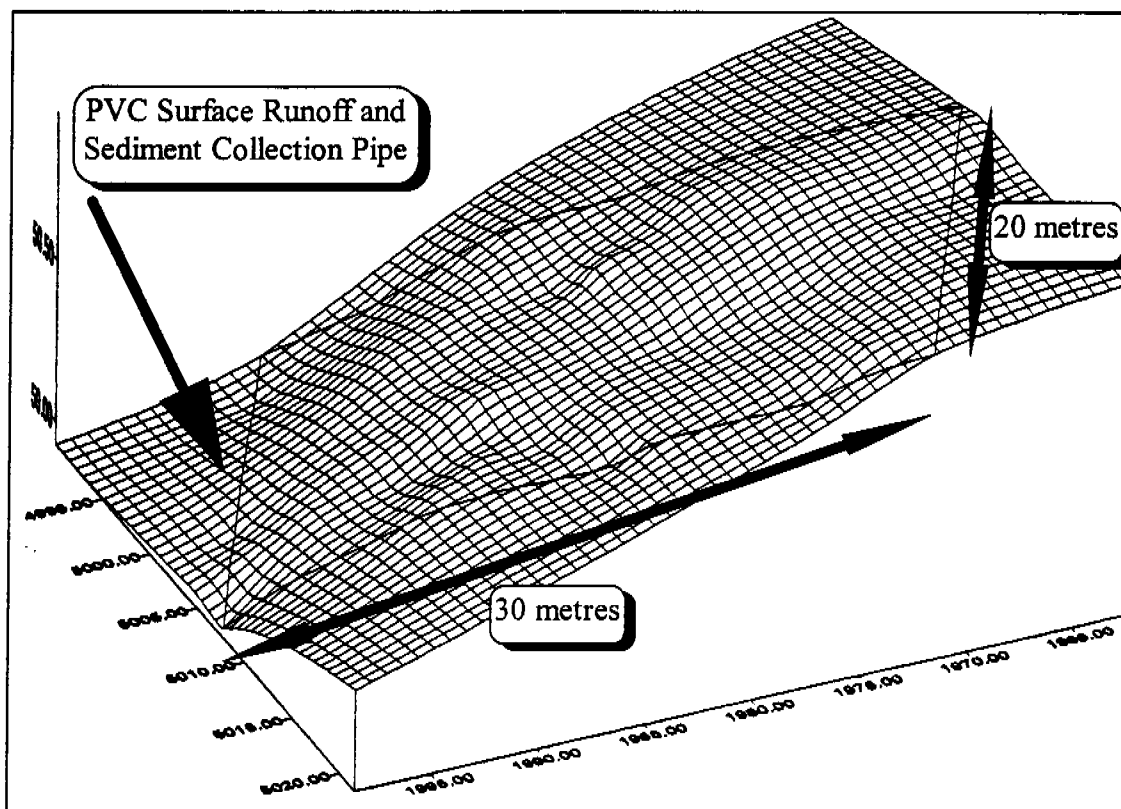


Figure 2.1.3: Three dimensional topographic surface of the 30m by 20m erosion and hydrology field plot which collected both surface run-off and transported sediment at the downslope end of the plot with a 300mm diameter PVC pipe. The dimension listed on the x, y, and z axes are a function of the computer program and are only relative to each other.

2.2 Experimental Field Plot

The 20 metre by 30 metre rainfall-runoff plot was hydraulically isolated from the surrounding bushland with damp-coarse, a bituminous coated aluminium building material. The material was approximately 20 centimetre wide, and a 5 centimetre section was bent at 90° and secured to the ground with large nails. The flattened edge of the material was set in place with concrete (Figure 2.2.1).

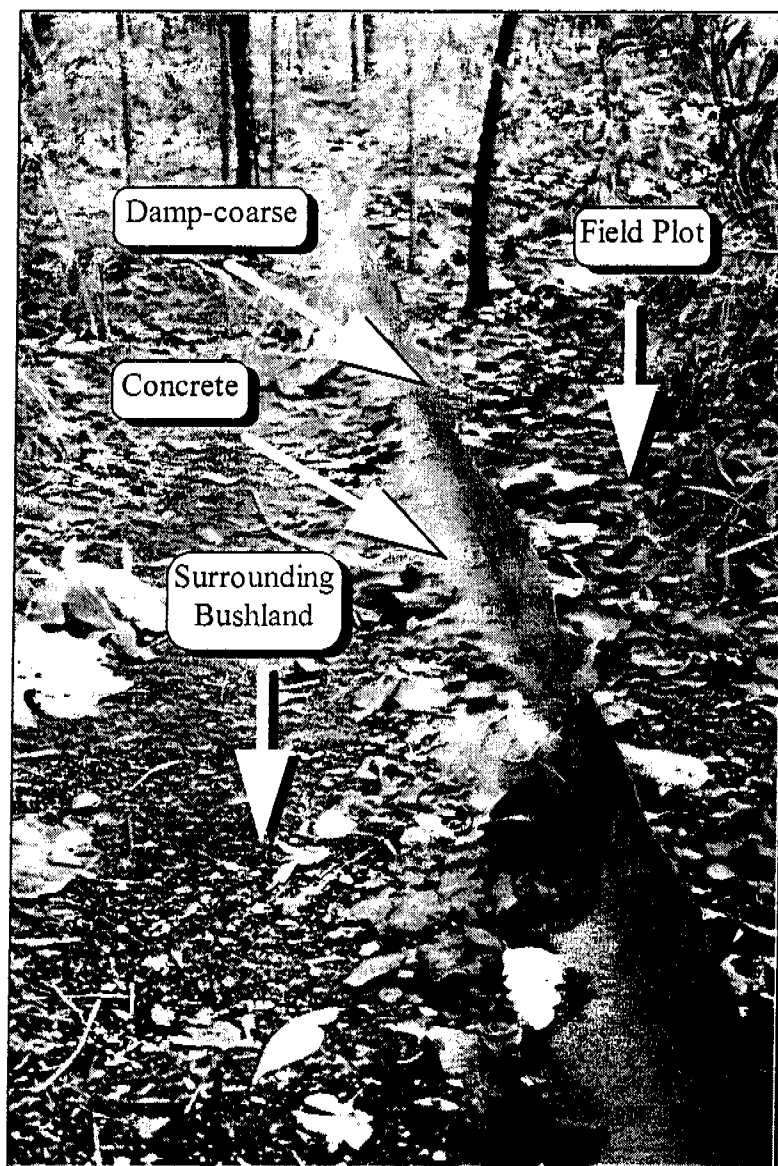


Figure 2.2.1: The 20 cm wide bituminous aluminium building product, (damp-coarse), was bent in a letter 'L' shape, and nailed to the soil surface, and supported with concrete. The field plot was thus hydraulically isolated from the surrounding bushland.

The damp-coarse material prevented the ingress of surface overland flow from the surrounding bushland. Sub-surface flow was not considered to be significant source of water.

The position of the field plot was purposefully chosen such that the general topography featured decreasing elevation (Figure 2.1.3). One half of a large PVC drainage pipe was buried into the ground at the down-slope end of the plot for the collection of surface run-off and sediment that was transported by the surface run-off.

The PVC pipe was 300 millimetres in diameter and 20 metres in length, and was donated by ERARM for the experiment. Figure 2.2.2 illustrates the downslope end of the field plot where the PVC pipe was installed.

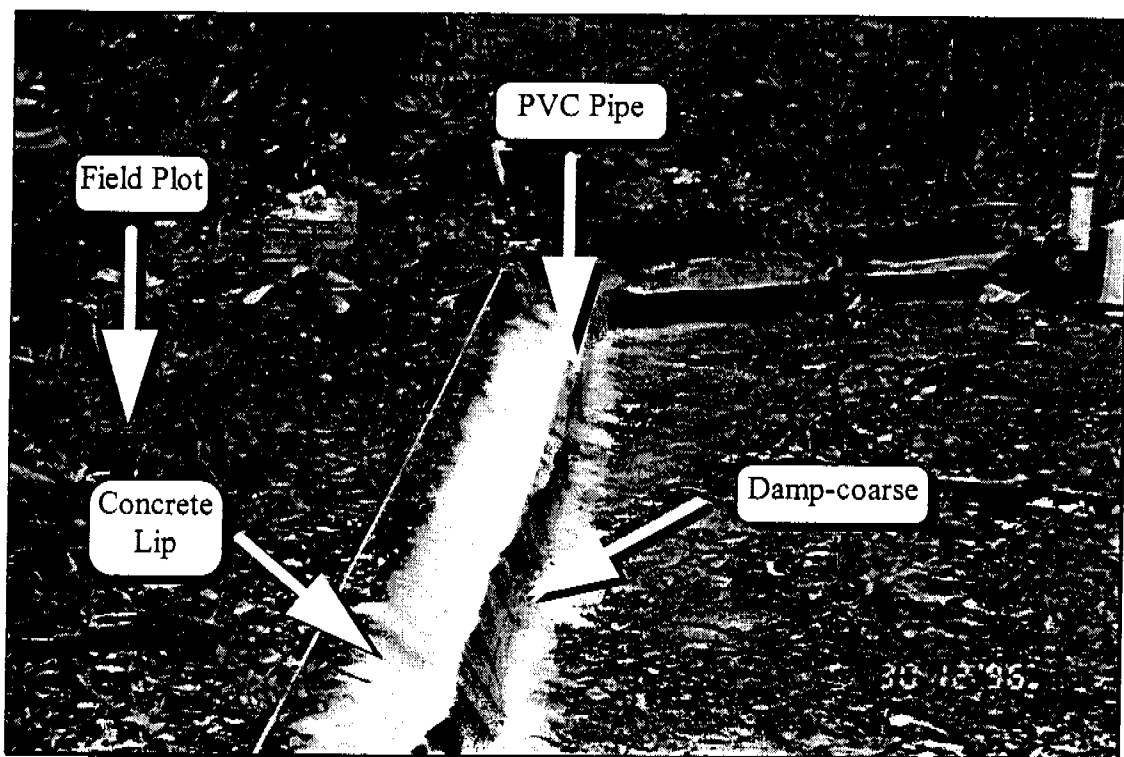


Figure 2.2.2: One half of a 300 mm diameter, 20 m long PVC pipe was buried at the down-slope end of the field plot. Additional damp-coarse material was attached to the PVC pipe to prevent overflow of surface runoff. A concrete lip was installed to allow unhindered transport of sediment and surface runoff into the PVC pipe.

The PVC pipe served a dual purpose, to conduct surface run-off from the plot and to provide temporary storage for sediment transported by that surface run-off. The nature of the installation of the half PVC pipe, buried at an angle, necessitated the construction of a concrete lip on the field plot side of the pipe for a smooth transition between the field plot and the pipe (Figure 2.2.2). Extra damp-coarse material was added to the right hand side of the PVC pipe (Figure 2.2.2), to prevent surface runoff from overflowing out of the pipe. During construction and rainfall event monitoring of the field plot, the ground surface was disturbed as least as possible. Figure 2.2.3 illustrates the concrete reservoir and hydraulic control structure which was visible in the background of Figure 2.2.2.

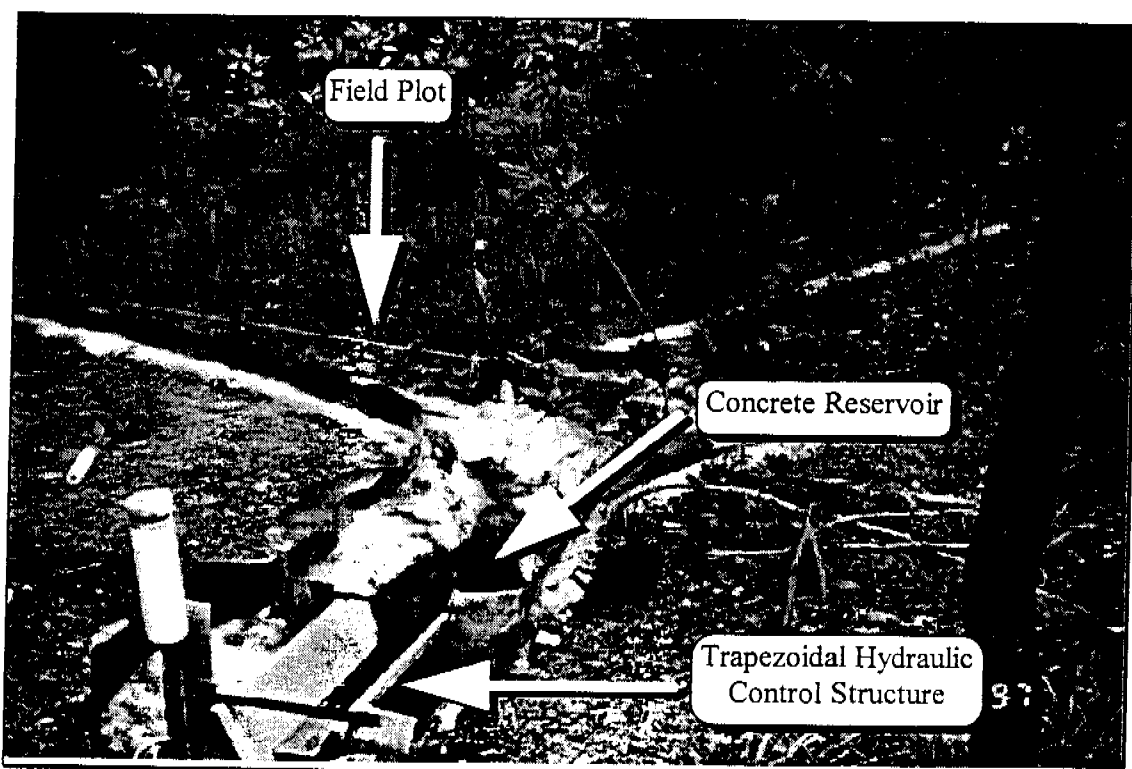


Figure 2.2.3: Featured in the foreground is the trapezoidal hydraulic control structure which was connected to a concrete reservoir which accumulated sediment, and partially controlled the run-off.

The concrete reservoir (Figure 2.2.3), collected bedload sediment that was swept into the PVC pipe from the plot and steadied the flow entering the trapezoidal hydraulic control structure. The concrete reservoir was hydraulically sealed with slight imperfections in the walls of the reservoir being filled with marine silicon sealant. The reservoir had an approximate volume of 20 litres.

Figure 2.2.4 illustrates the concrete reservoir after the cessation of a natural rain event. The turbulent water, highlighted by the large arrow to the left of Figure 2.2.4, is surface run-off flowing from the PVC pipe into the reservoir.

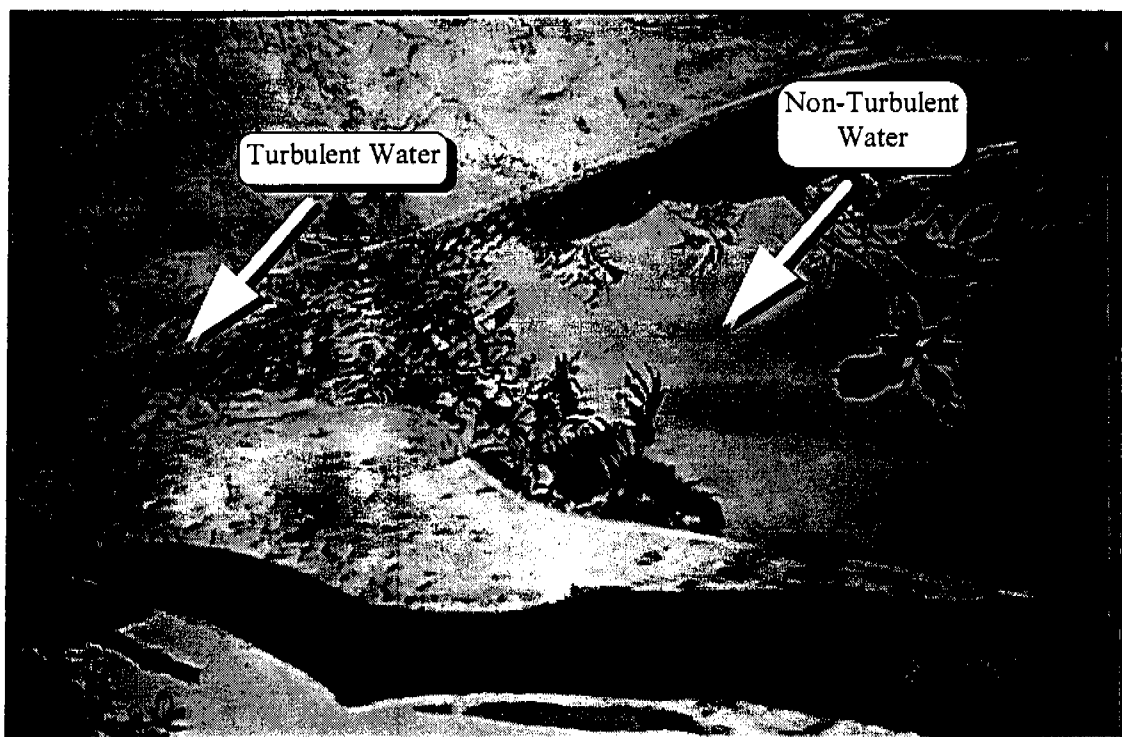


Figure 2.2.4: The concrete reservoir served a dual purpose; to collect bedload sediment that was transported during rain events and steady the flow entering the hydraulic control structure. Surface runoff that is leaving the PVC pipe, (highlighted by an arrow to the left of the Figure), enters the concrete reservoir and is quickly steadied, (highlighted by an arrow to the right of the Figure).

The reservoir was rectangular in plan view, with the PVC pipe supplying water at one end, highlighted by an arrow to the left of Figure 2.2.4. Figure 2.2.5 illustrates a cross-sectional schematic of the flow steadying ability of the reservoir trapezoidal weir system.

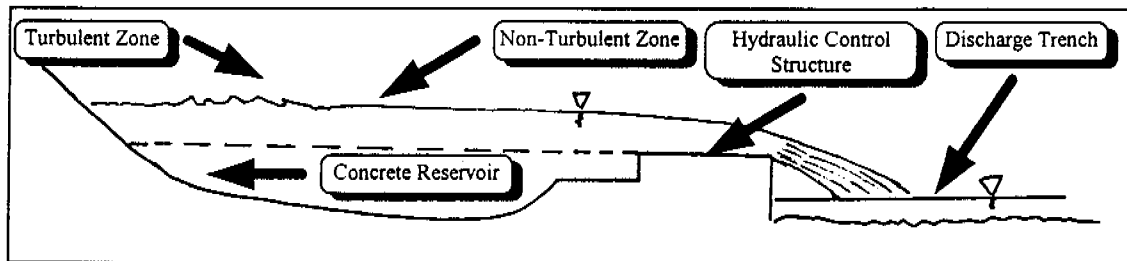


Figure 2.2.5: The concrete reservoir serves to steady the flow of water across the hydraulic control structure, and as a storage area for bedload sediment.

Figure 2.2.6 illustrates the behaviour of the reservoir and control structure system during large storm activity.

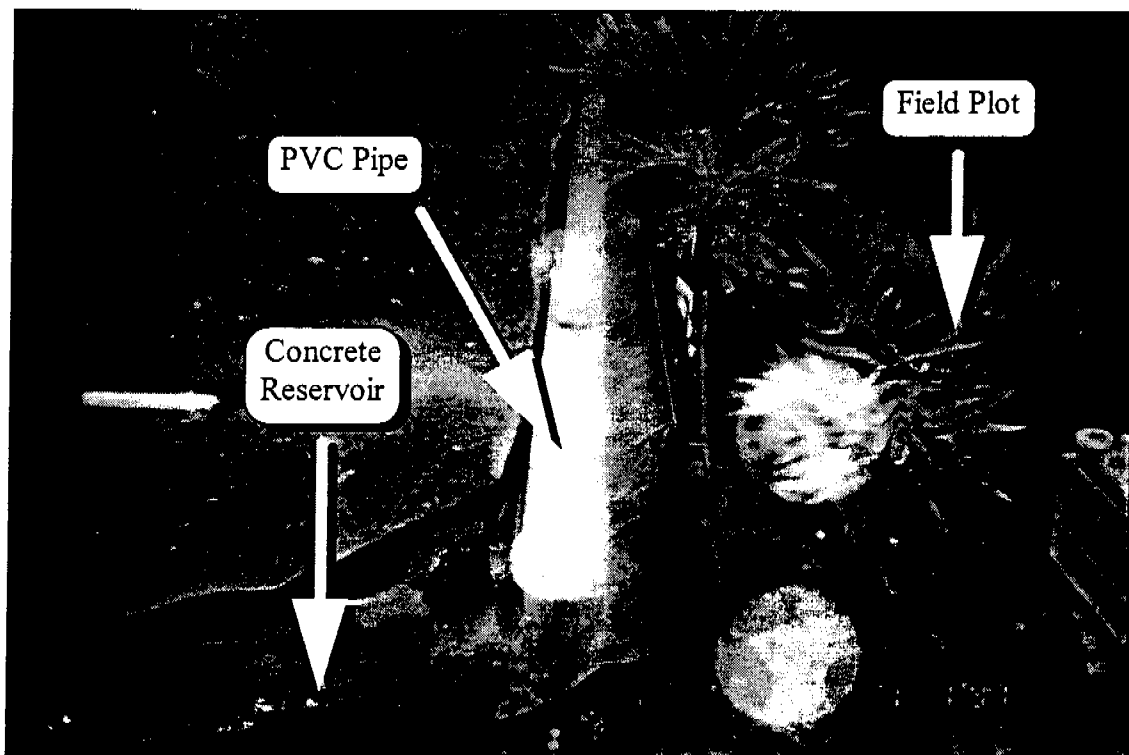


Figure 2.2.6: Considerable quantities of surface run-off are transported from the field plot, the change in direction of flow, and the length of the reservoir both serve to control and steady the flow.

The water level in the reservoir was refilled before the commencement of each monitored storm event, so that any initial surface run-off occurring could be recorded accurately by the control structure. The discharge trench featured in Figures 2.1.1 and 2.2.5, comprised of a large ditch dug out roughly with a back-hoe, (ERARM), to allow run-off from the experimental area to be transported away.

The trapezoidal hydraulic control structure installed following the concrete reservoir, provided a method for the determination of the quantity of discharge, via a water level height measurement. The control structure utilised in this study was a “150 mm RBC flume” (Bos *et al*, 1984; cited in Evans and Riley, 1993) and was constructed of galvanised steel. Figure 2.2.7 illustrates a cross-sectional view of the RBC flume.

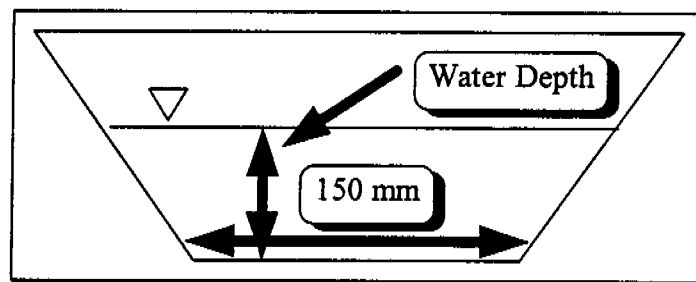


Figure 2.2.7: Cross-sectional view of the hydraulic control structure, with a base of 150 mm. The depth of water, with respect to cross-sectional area, is utilised to determine the discharge through the structure.

The relationship between the depth of water, ‘h’, (m), and the quantity of discharge , ‘Q’, (m³/s), was previously determined (Equation 2.2.1), (Evans and Riley, 1993).

$$Q = 18.4 \times h + 940 \times h^2 \quad (r^2 = 1) \quad (2.2.1)$$

where

Q = Discharge, (m³/s), and

h = Depth of water, (m).

Figure 2.2.8 illustrates the trapezoidal control structure, the concrete reservoir, the discharge trench, and the water level sensing probe, termed a capacitance rod.

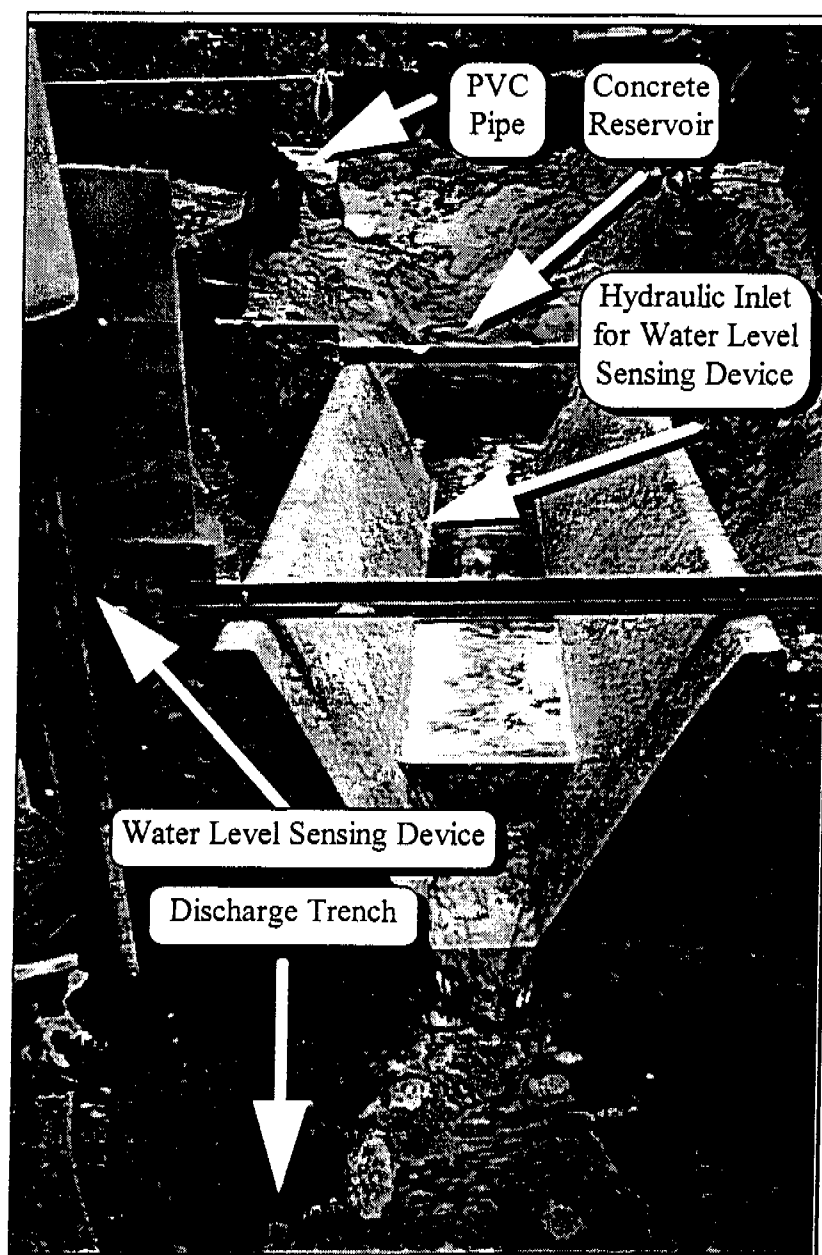


Figure 2.2.8: Run-off is still occurring in the foreground of this Figure after a storm event. The position of the hydraulic inlet that is connected to the stilling well containing the water level sensing device is also featured in this Figure.

It was generally observed that for a considerable period of time after the cessation of rainfall, surface run-off continued to occur (Figure 2.2.8). Surface run-off flowing from the control structure is directed into the discharge trench and carried away from the site (Figures 2.1.1, and 2.2.5).

In the left foreground of Figure 2.2.8, a small section of white PVC stormwater pipe sits atop a small clear plastic cylinder, termed a stilling well. The stilling well contained the water level sensing probe, which had an insulated core that was wrapped with a thin, bare wire. Minute changes in resistance, detected by the connected electronic data logger, due to more or less of the bare wire contacting water within the stilling well, yielded a measurement of the water level. The relative resistance reading was stored by the data-logger along with a time signature. The stilling well housing the sensor, was hydraulically connected to the base of the control structure (Figure 2.2.8). Manual water level readings were taken using a measuring tape attached to side of the stilling well. The water within the stilling well was coloured with a fluorescent dye for ease of reading.

The DISTFW rainfall-runoff model required input of information pertaining to the topography of the catchment, and time related discharge and rainfall data. Rainfall data was recorded utilising an electronic and a manual raingauge, that were positioned approximately 20 metres from the field plot (Figure 2.2.9).

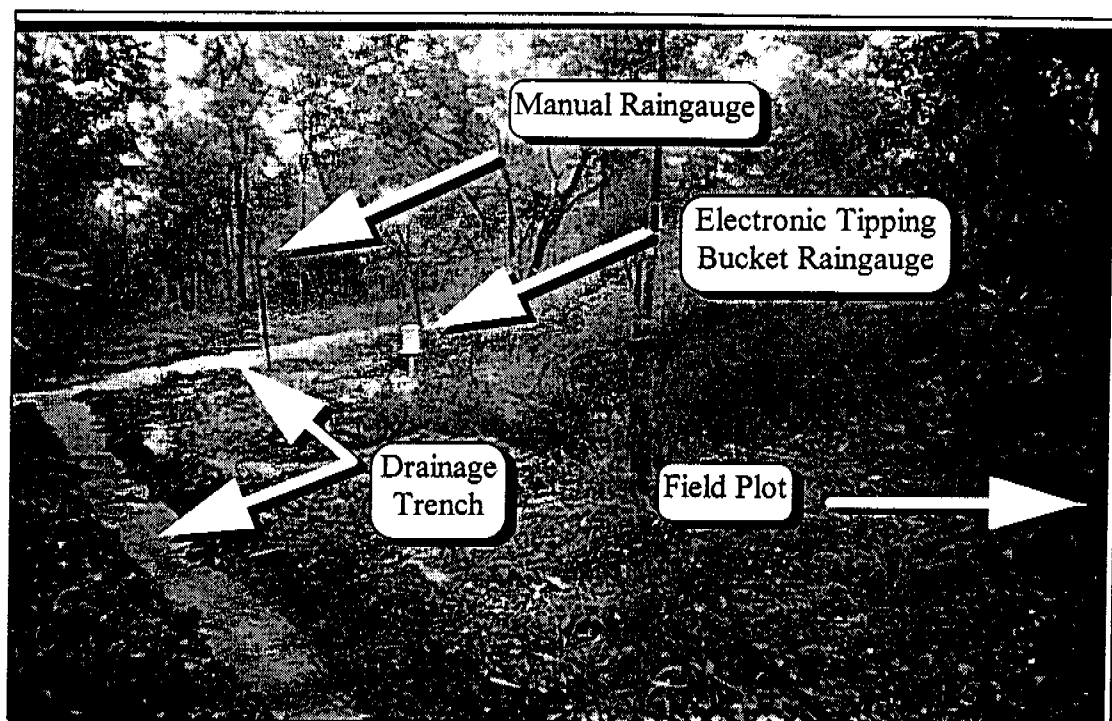


Figure 2.2.9: Featured to the left of this Figure is the discharge trench that was constructed to carry runoff away from the experimental area. Attached to the star picket in the background of this Figure is the manual raingauge, and the steel cylinder sitting atop a pedestal, in the middle of the Figure, is the electronic tipping bucket raingauge.

The electronic tipping bucket raingauge consisted of two L-shaped plastic buckets (in a back to back formation) that held 0.2 mm of rainfall each; a magnet; and a magnetic sensitive switch. When 0.2 mm of rainfall accumulated in one L-shaped bucket, from the feed mechanism, the two bucket mechanism pivoted via a fulcrum, and emptied one bucket, and the other bucket began to fill. A magnet was attached to the base of the two L-shaped buckets and tripped a magnetic sensitive switch when the buckets moved. Signals from the magnetic switch were recorded by a connected data logger. Figure 2.2.10 presents a schematic of a typical electronic tipping bucket raingauge.

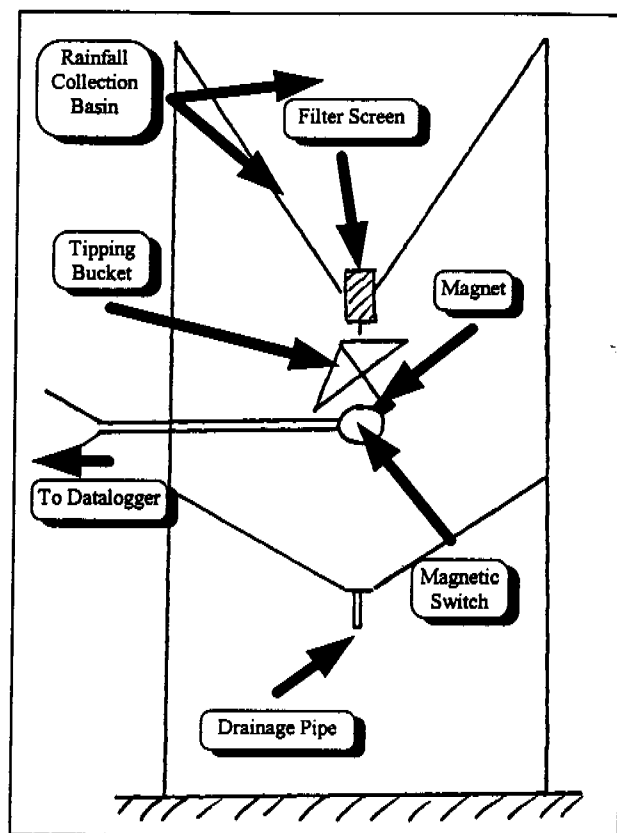


Figure 2.2.10: A schematic of a tipping bucket raingauge featuring two L-shaped plastic buckets in a back to back configuration attached to a fulcrum, a magnet attached to the plastic bucket mechanism, and a magnetic sensitive switch which was connected to an electronic data logger.

The filter screen featured in Figure 2.2.10 at the base of the collection basin, ensured the exclusion of leaves and twigs from the raingauge. The tall vegetation surrounding the electronic raingauge (Figure 2.2.9), was partially cleared to ensure that the gauge was not shadowed. The electronic data-logger recorded the cumulative tip number along with a time signature. Manual rainfall data was collected in a NYLEX "1000" plastic rain-gauge which was factory calibrated to allow direct readings of rainfall in millimetre increments.

3.0 DISTFW-NLFIT Rainfall-Runoff Model

3.1 Introduction

The movement of water via surface and sub-surface mechanisms on slopes is a function of rainfall intensity, vegetation, slope length and form, and soil properties.

The generally accepted mechanisms for water movement on slopes are considered to be Hortonian and Saturated Overland Flow, and unsaturated and saturated throughflow, which are illustrated in Figure 3.1.1.

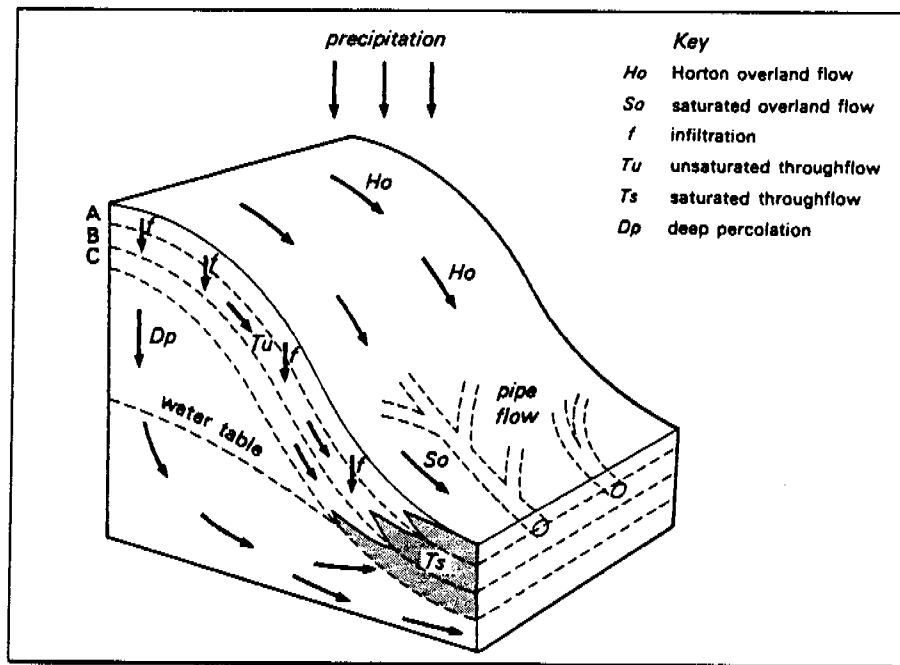


Figure 3.1.1: Numerous mechanisms for water movement exist on hill-slopes including overland and subsurface pathways (after Gerrard, 1981).

The quantity and intensity of surface run-off is a major function governing sediment transportation, thus the accuracy of the estimation of surface run-off is important (Willgoose and Riley, 1993).

The hydrology model utilised in this study and in previous related work on the NWRD (Willgoose and Riley, 1993; Saynor *et al*, 1995; and Evans *et al*, 1996) and in the Tin Camp Creek area (Moliere *et al*, 1996) is the rainfall-runoff model, DISTFW (Willgoose *et al*, 1995). DISTFW, as in previous studies on the NWRD and in Tin Camp Creek, was calibrated to hydrologic and hyetographic field data collected from the natural site.

The DISTFW model which was extended to use digital terrain elevation data (Willgoose *et al*, 1995), is based on the Field-Williams model one-dimensional kinematic wave flood routing model (Field and Williams, 1987). The model was originally called the generalised kinematic catchment model (GKCM) and is a runoff-routing model which has a conceptually more sound basis than other similar models widely used in Australia, namely RORB, and RAFTS, (Kuczera, 1996).

The DISTFW conceptual rainfall-runoff model includes a number of features;

- Flow from surface storage to a channel,
- Flow from groundwater storage to a channel,
- Non-linear storage of water on the hillslope surface,
- Philip infiltration from surface storage to a linear groundwater store, and
- Run-off routing down a channel by use of the kinematic wave.

(Willgoose and Riley, 1995)

The DISTFW rainfall runoff model can be divided into four modules; non-linear surface storage, kinematic wave hillslope routing and channel routing, and linear groundwater storage (Figure 3.1.2). Detailed evaluation of each module of DISTFW is presented in Section 3.2.

The DISTFW-NLFIT model can be used for a standard sub-catchment, a constant width plot, or a DTM based catchment (Willgoose *et al*, 1995). The current study involved a constant width 20 metre by 30 metre rectangular field plot, and the model was adjusted accordingly.

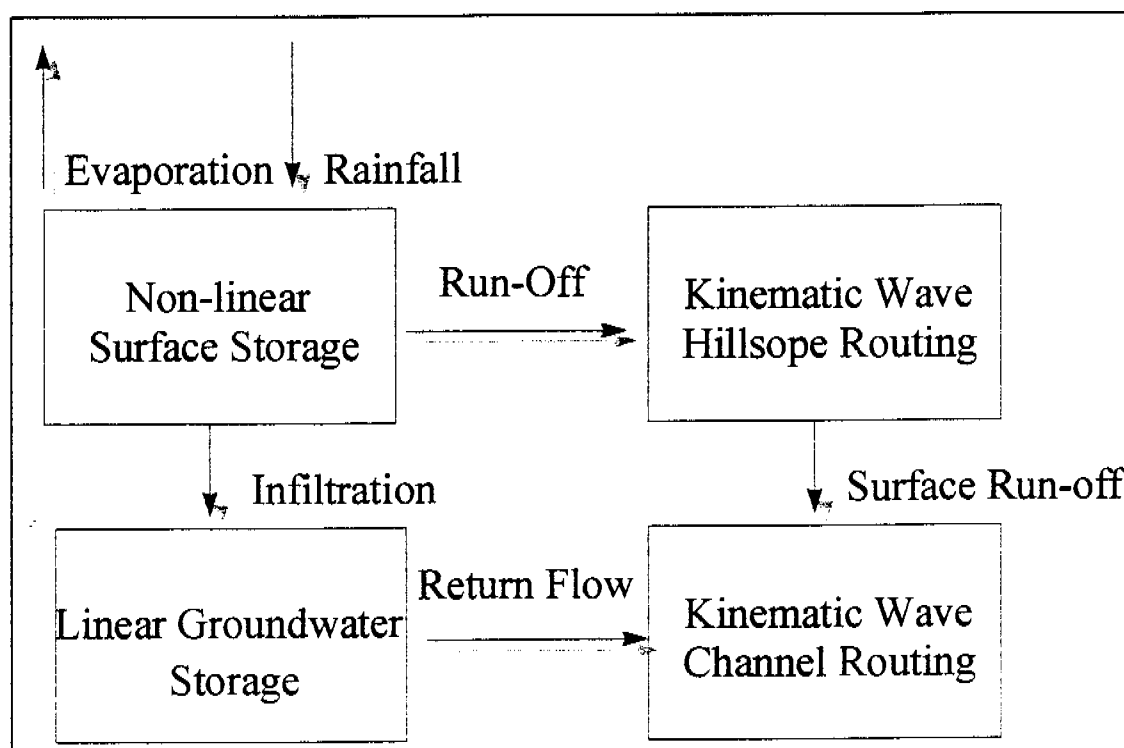


Figure 3.1.2: Four module conceptual arrangement of the rainfall-runoff model, DISTFW, incorporating non-linear surface and linear groundwater storage, and kinematic wave hillslope and channel routing (after Willgoose *et al*, 1995).

3.2 DISTFW-NLFIT

An evaluation of the DISTFW-NLFIT model can be divided into an examination of the processes of infiltration, the routing of overland flow, the routing of sub-surface flow, and channel routing using the kinematic wave approximation.

3.2.1 Infiltration

Gerrard (1981) defined infiltration as the process of water entering the soil, and infiltration capacity as the maximum flux of water across the soil surface. The infiltration properties of the soil tend to govern the volume of surface run-off leaving a catchment (Willgoose and Kuczera, 1995).

A typical infiltration rate curve for a soil under ponded conditions, will feature a period of rapid infiltration followed by an asymptotic decrease until the infiltration rate approaches the infiltration capacity of the soil. Figure 3.2.1 illustrates the infiltration rate of various soils under ponded conditions with respect to time.

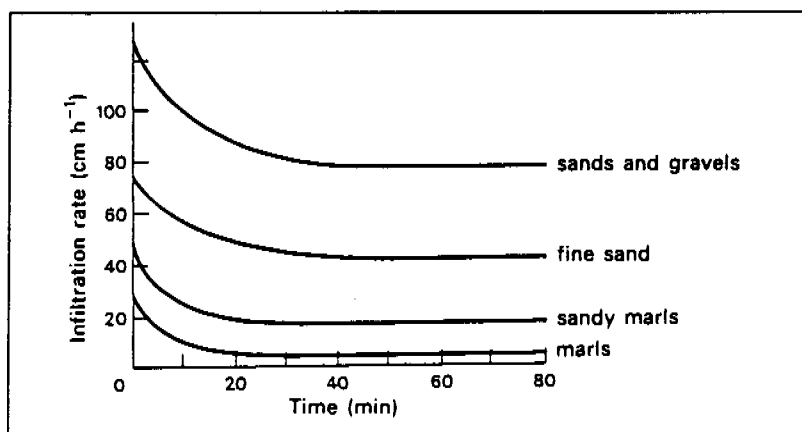


Figure 3.2.1: Typical infiltration rate curves for different soil matrix compositions under ponded infiltration (Gerrard, 1981).

Comparison of the ponded infiltration rate curves for the different soil types featured Figure 3.2.1, highlights that there is only a linear difference between them.

Bodman and Coleman (1943; cited in Gerrard, 1981) divided a typical soil profile into three components in an attempt to quantify the asymptotic behaviour of ponded infiltration rate curves similar to those illustrated in Figure 3.2.1.

Bodman and Coleman postulated that;

- The upper portion of the wetted soil matrix, is merely a transmission zone, which only conducts water from the surface, as it is completely saturated.
- The middle portion of the soil matrix comprises an intermediate zone where the moisture gradient increases with depth.
- The final component of the soil matrix, is the irregular surface of the wetting front, which is characterised by a very high potential moisture gradient.

There are a number of models that attempt to emulate ponded infiltration, namely the Green and Ampt, Kostikov, Horton, and Philip models (Gerrard, 1981).

There is a clear distinction with infiltration rate behaviour under ponding and non-ponding conditions. Thorne (cited in Kirkby and Morgan, 1980) noted that if the rainfall intensity subjected to a soil is lower than its maximum infiltration under ponded conditions, then non-ponded and pre-ponded infiltration will be prevalent. Figure 3.2.2 illustrates the division of infiltration into four different types; pre-ponding, non-ponding, ponding, and flooding infiltration.

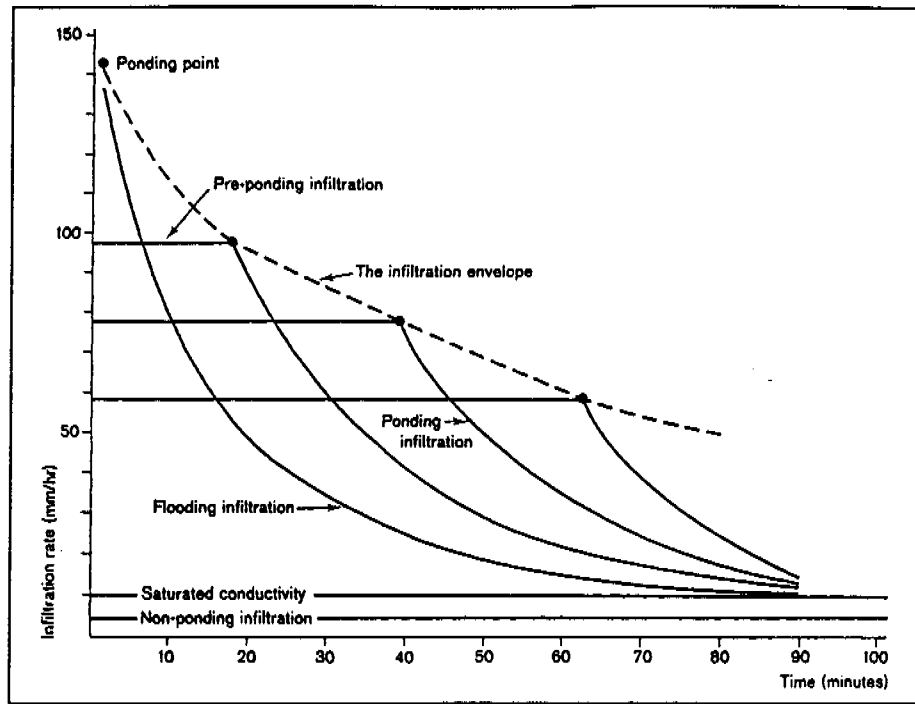


Figure 3.2.2: The infiltration envelope highlighted in this Figure, defines the time to ponding for rainfalls of different hypothetical intensities (Smith, 1972; cited in Kirkby and Morgan, 1980).

The infiltration rate, 'i', (m/s), of rainfall into the soil matrix that is modelled in DISTFW, can be divided into the two processes, ponded and non-ponded, at any timestep, Δt , (Equation 3.2.1), (Kuczera, 1996).

$$i = \begin{cases} f & \text{if ponding occurs, namely } p\Delta t + h^s \geq f\Delta t \\ p + \frac{h^s}{\Delta t} & \text{otherwise} \end{cases} \quad (3.2.1)$$

where

i = Infiltration rate, (m/s),

f = Soil infiltration capacity, (m/s),

h^s = Average depth of surface storage, (m),

p = Rainfall intensity, (m/s), and

Δt = Timestep, (s).

Under conditions of ponding, the DISTFW model assumes that the infiltration capacity of the soil is governed by the Philip's equation (Equation 3.2.2), which takes the form of the flooding infiltration rate curve of Figure 3.2.2.

$$f = \frac{S_\phi}{2\sqrt{t}} + \phi \quad (3.2.2)$$

where

S_ϕ = Sorptivity, (m/s^{1/2}),

ϕ = Continuing loss rate, (m/s), and

t = Time since commencement of ponding, (s).

Field and Williams (1987) noted that sorptivity is a soil parameter which describes the initial dryness of the soil, and that the continuing loss rate, is a parameter that represents the saturated hydraulic conductivity of the soil.

Equation (3.2.2) has the underlying assumption that a condition of ponding will be prevalent throughout a storm event, which is not the case in reality. A time compression algorithm was utilised to find an approximate solution to this problem, such that 'F', the soil infiltration capacity, (m/s), can be expressed as a function of the cumulative infiltrated depth, 'F', (m), (Equation 3.2.3), (Field and Williams, 1987).

$$\begin{aligned} F &= \int_0^t \left[\frac{1}{2} S_\phi V^{-\frac{1}{2}} + \phi \right] dv \\ F &= S_\phi t^{\frac{1}{2}} + \phi t \end{aligned} \quad (3.2.3)$$

where

F = Cumulative infiltrated depth, (m), and

V = Velocity of the wetting front, (m/s).

Willgoose and Kuczera (1995) noted that the instantaneous infiltration rate, 'f', (m/s), as a function of the cumulative infiltration, 'F', (m), from DISTFW can be rearranged as Equation 3.2.4.

$$f = \phi + \frac{S_{\phi}^2}{4F} \left(1 + \left(1 + \left(\frac{4F\phi}{S_{\phi}^2} \right)^{\frac{1}{2}} \right) \right) \quad (3.2.4)$$

Rainfall that does not infiltrate and overcomes depression storage becomes overland flow, which is modelled as a Hortonian process in DISTFW. Willgoose and Kuczera (1995) stressed that changes in infiltration rates mainly influence the volume of runoff that occurs at the outlet of the catchment.

The process of rainfall becoming overland flow, is schematically illustrated in Figure 3.2.3 (Fetter, 1994).

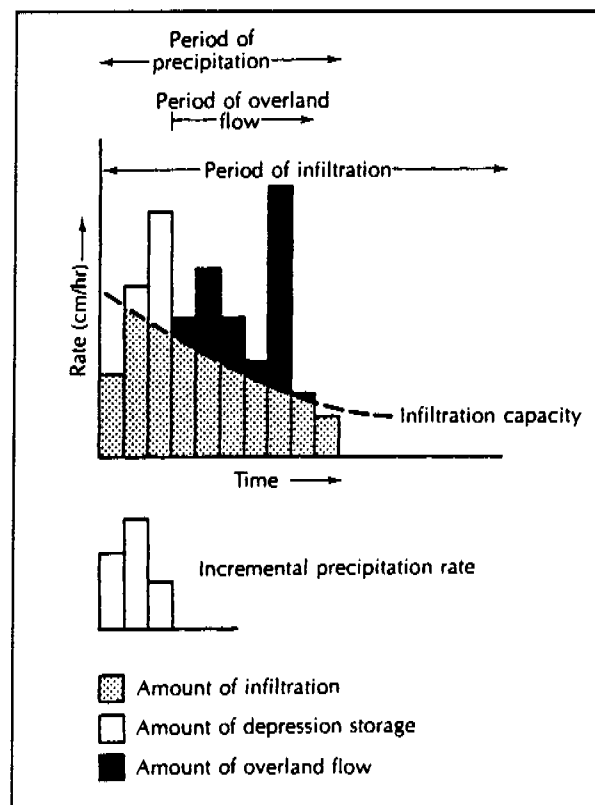


Figure 3.2.3: Incremental precipitation rate and its dissociation into amounts of infiltration, depression storage, and overland flow (Fetter, 1994).

Figure 3.2.3 illustrates that overland flow will continue past the point of the cessation of rainfall, and that infiltration will continue past the point of the cessation of overland flow.

3.2.2 Routing of Overland Flow - Hillslope Run-off

Surface overland flow modelled in DISTFW is based on the concept of Hortonian overland flow. Field and Williams (1987) noted that this type of flow mechanism can only be observed on disturbed or scantily vegetated surfaces. They continued that on natural undisturbed surfaces, overland flow is likely to be dominated by saturation overland flow rather than Hortonian flow. They concluded however that, although there is a conceptual limitation between modelling saturation overland flow as Hortonian flow, the rainfall runoff model can be successfully calibrated to catchments where there is domination of the saturation overland flow process due to similarities between the processes.

Willgoose and Kuczera (1995) emphasised that the original Field-Williams model was designed to be an event model which was extended to model continuous flow series through the addition of infiltration recovery and evaporation components to Equation 3.2.4 in DISTFW, which is illustrated in the four module schematic of the model (Figure 3.1.2).

As the overland flow moves down-slope it encounters resistance which establishes temporary storage, which results in rainfall in excess of the maximum infiltration capacity, being delayed and attenuated (Kuczera, 1996). Field and Williams (1987) noted that DISTFW approximates the dynamics of the delay and attenuation of excess rainfall by utilising a non-linear level-pool routing mechanism.

Willgoose and Kuczera (1995) noted the non-linear level-pool routing mechanism can be defined with respect to the discharge per unit area of surface storage, 's^s', (m/s), as Equation (3.2.5).

$$s^s = \left(\frac{h^s}{C_s B^\gamma} \right)^{\frac{1}{\gamma}} \quad (3.2.5)$$

where

B = Width of the catchment element, (m),

C_s = Surface supply parameter, (m^(1-2γ)s^γ),

h^s = Average depth of surface storage, (m), and

γ = Parameter to be determined from observations on actual catchments.

Field and Williams (1987) emphasised that the parameters C_s and γ, can only be estimated through calibration to observed storm events. Willgoose and Kuczera (1995) noted that Equation (3.2.5) can be used to model surface depressions such as deep rip patterns on rehabilitated mine surfaces.

Figure 3.2.4 illustrates the principle of the delay and attenuation of rainfall excess in the form of temporary storage of surface water on a hillslope.

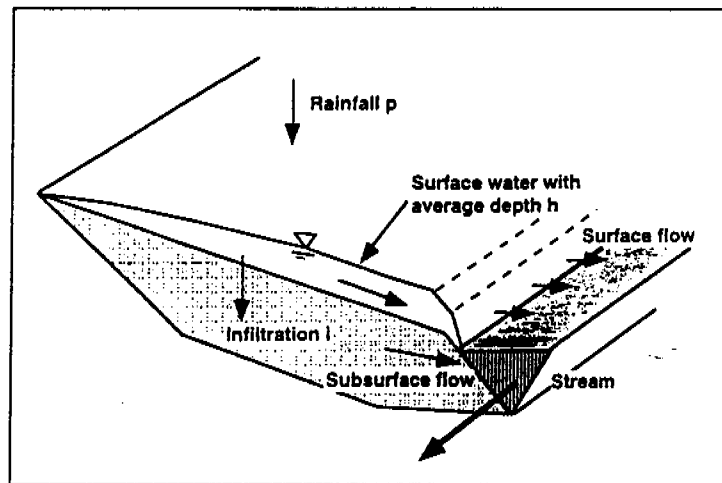


Figure 3.2.4: A schematic of a hillslope which illustrates the principal of temporary storage of surface run-off, infiltration and subsurface flow (Kuczera 1996).

Field and Williams (1987) noted that a mass balance may be applied to surface water moving in an overland flow manner toward a 'stream', illustrated in Figure 3.2.4. Figure 3.2.4 also highlights that the non-linear surface storage of water is the source of water for the routing component, the kinematic wave (Willgoose and Kuczera, 1995).

3.2.3 Routing of Channel Flow

Chaudhry (1993) noted that flood routing can be referred to as the computation of the height and velocity of a flood wave as it propagates in a body of water (channel, lake, stream, reservoir etc.). Finnegan (1993) observed that the routing of channel flow is developed from theories of unsteady flow, which generally involve transitory waves. These transitory waves are gravity waves that occur within channels that cause particles of fluid to be displaced in a direction parallel to the flow. Chaudhry (1993) noted that the simultaneous solving of the continuity equation with a simplified form of the momentum equation assuming steady uniform conditions, is referred to as the kinematic routing procedure.

Derivation of the kinematic wave channel routing component of the DISTFW model can be found in Field and Williams (1987), Finnegan (1993), and Kuczera (1996).

The conveyance properties of hillslopes and channels in DISTFW differ and are permitted to change with respect to discharge (Willgoose and Kuczera, 1995). They continued that changes in those conveyance properties allows DISTFW to predict behaviour of overbank flow regions in flooded rills or channels.

The Manning's equation is utilised to determine discharge, coupled with the kinematic wave assumption that the pressure and inertia terms of the momentum equation are negligible when compared to the gravity and friction terms. If the slope is not so mild that the pressure term becomes appreciable, not less than approximately 0.05%, and that the transitory wave does not rise and fall too quickly (ie the assumption of negligible vertical acceleration holds) then the assumption that the friction slope is equal to the bed slope is valid.

Equation (3.2.6) represents Manning's equation with the assumption that the friction slope, ' S_f ' is equal to the bed slope, ' S_0 '.

$$q = \frac{1}{n} \left(R^{\frac{2}{3}} S^{\frac{1}{2}} P \right) \quad (3.2.6)$$

where

n = Manning's roughness coefficient,

q = Discharge per unit width of hillslope, ($m^3/s/m$),

R = Hydraulic radius, (m),

P = Wetted perimeter, (m), and

S = Bed slope, (m/m).

As the hydraulic radius is equal to the cross sectional area of flow divided by the wetted perimeter, then Equation (3.2.6) can be re-expressed as Equation (3.2.7).

$$q = \frac{1}{n} \left(A^{\frac{2}{3}} S^{\frac{1}{2}} P^{\frac{2}{3}} \right) \quad (3.2.7)$$

where

A = Cross sectional area of flow, (m^2).

Incorporation of the cross sectional area and wetted perimeter terms of Equation (3.2.7), into the channel conveyance term, ' K ', (m^3/s), (Willgoose and Kuczera, 1995), allows the discharge per unit width, ' q ', (m^3/s) to be simply stated (Equation 3.2.8).

$$q = KS^{\frac{1}{2}} \quad (3.2.8)$$

where

K = Channel conveyance, (m^3/s).

The channel conveyance can be approximated by a power law function involving the cross sectional area of flow (Equation 3.2.9), (Willgoose and Kuczera, 1995).

$$K = C_r A^{e_m} \quad (3.2.9)$$

The parameters C_r and e_m are defined by the flow geometry and surface roughness and have non-dimensional units, but together define the kinematic wave component of DISTFW. It can be observed from Equation (3.2.9), that as the magnitude of C_r increase the rate of discharge also increases.

Figure 3.2.5 illustrates the cross sectional flow geometries of four different overland sheetflow and rillflow profiles.

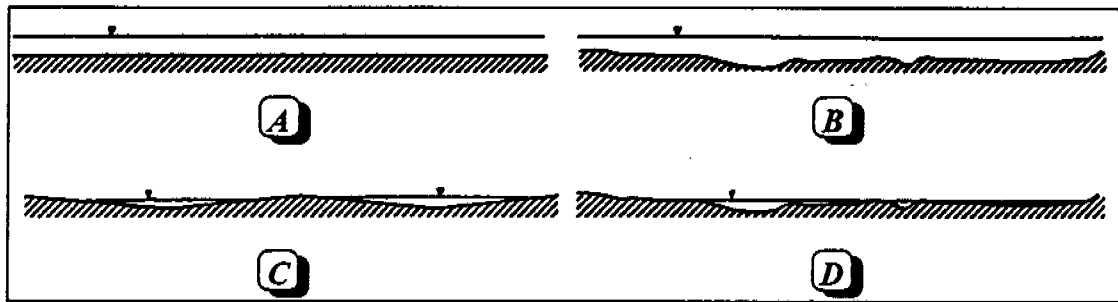


Figure 3.2.5: Combination of four different cross sectional profiles illustrating A) Constant depth sheet flow, B) Irregular depth sheet flow, C) Triangular rill flow, and D) Irregular depth rill flow (after Willgoose and Kuczera, 1995).

It can be observed from Figure 3.2.5 that cases 'A' and 'B', are cross sectional profiles which exhibit sheet flow. Surface water in these two cases, has a constant or irregular depth over the entire width of the hillslope (Willgoose and Kuczera, 1995), and the cross sectional area is proportional to the wetted perimeter. They continue that if, with an increase in discharge, the wetted perimeter per unit width remains virtually constant, then C_r and e_m can be defined as Equation (3.2.10).

$$\begin{aligned} C_r &= \frac{1}{P^{0.67} n} \\ e_m &= 1.67 \end{aligned} \quad (3.2.10)$$

It can be observed from Figure 3.2.5 that the cross sectional profile for case 'C', is one of triangular rillflow. Surface water in this case does not have a constant or irregular depth over the entire width of the hillslope, rather the flow is concentrated in rivulets, that is, only a small proportion of the hillslope is contributing to surface runoff (Willgoose and Kuczera, 1995).

They continued that in this case, the cross sectional area is proportional to the square of the wetted perimeter, and for a channel with a side slope of $1:\alpha$ and 'N' number of rills per unit width, C_r and e_m can be defined as Equation (3.2.11).

$$\boxed{\begin{aligned} C_r &= N \left(\frac{\left(\frac{\alpha}{4(1 + \alpha^2)} \right)^{0.33}}{n} \right) \\ e_m &= 1.33 \end{aligned}} \quad (3.2.11)$$

The final cross sectional profile to be considered is that of a natural surface, case 'D' (Figure 3.2.5). Willgoose and Kuczera (1995) noted that C_r and e_m can be derived from the analysis of cross sections that are perpendicular to the direction of flow. The relationship between the cross sectional area and the wetted perimeter for a natural field plot is reported in Equation (3.2.12), (derived by Parsons, Abrahams, and Luk, 1990; cited in Willgoose and Kuczera, 1995).

$$\boxed{\begin{aligned} A &= 0.0076P^{1.49} \quad R^2 = 0.88 \\ C_r &= \frac{0.113}{n} \\ e_m &= 1.21 \end{aligned}} \quad (3.2.12)$$

Willgoose and Kuczera (1995) emphasised that a kinematic wave response close to linearity would be expected with surface irregularities rather than the sheetflow kinematic wave assumption generally accepted in hydrologic models such as KINCAT (Field and Williams, 1987).

3.3 DISTFW Data Requirements

The DISTFW-NLFIT package utilised in this study is the same as used in previous studies on the NWRD of ERARM, (Willgoose and Riley, 1993; and Saynor *et al*, 1995) and in the Tin Camp Creek area (Moliere *et al*, 1996).

A UNIDATA data-logger, provided by ERAES, was programmed utilising a connected laptop computer and accompanying data-logger software. The data-logger was programmed to accept two channels of input; a tipping bucket raingauge and a water level sensing device (capacitance rod), (Section 2.0).

A laboratory calibration experiment was conducted prior to the installation of the capacitance rod on-site to establish a relationship between the capacitance reading, (Hz), and the relative water level, (mm), (Figure 3.3.1).

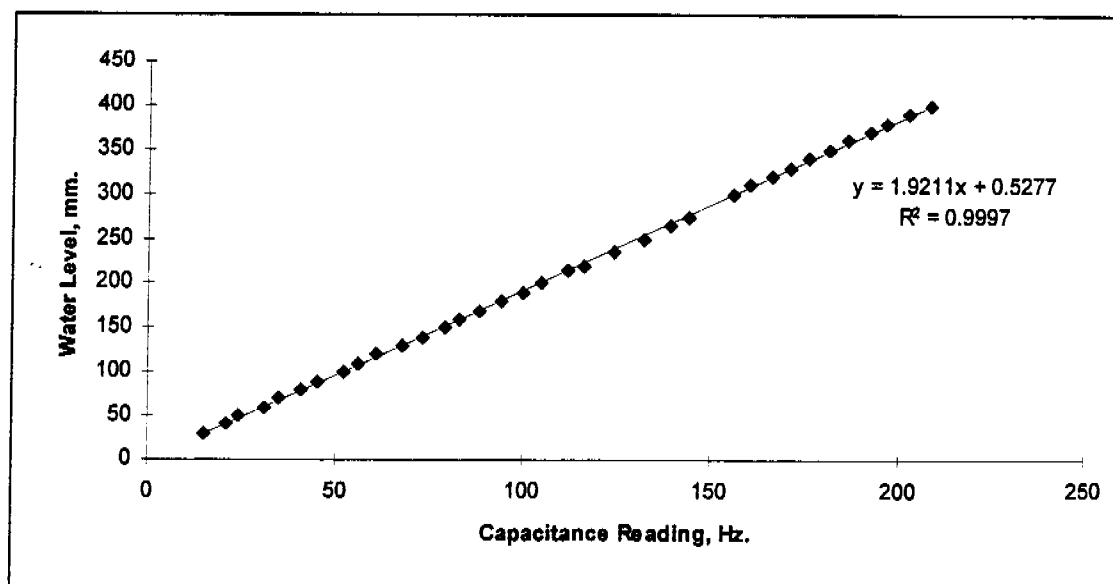


Figure 3.3.1: Regression analysis of the results obtained from the calibration experiment performed on the water level sensing device (capacitance rod), prior to installation on-site.

In previous studies it was suggested that readings from the capacitance rod had a dependency upon water temperature within the stilling well. A separate experiment was undertaken to evaluate the effect of stilling well water temperature but was not reported, and found no temperature dependency of readings from the capacitance rod utilised for the natural site.

The water level, (m), as a function of resistance reading, (Hz), is presented as Equation (3.3.1).

$$\text{Water Level(m)} = 1.9211 \times \text{Reading(Hz)} + 0.5277 \quad (r^2 = 1.0) \quad (3.3.1)$$

The rainfall data recorded by the data-logger was stored in the form of the number of cumulative tips that had occurred since the previous logger reset, with an accompanying time signature. The runoff data recorded, was in the form of a resistance value, (Hz), from the capacitance rod, which varied according to the water height, (m), moving through the hydraulic control structure. Figure 3.3.2, illustrates an extract of a raw data file, illustrating the two data sources; rainfall and runoff.

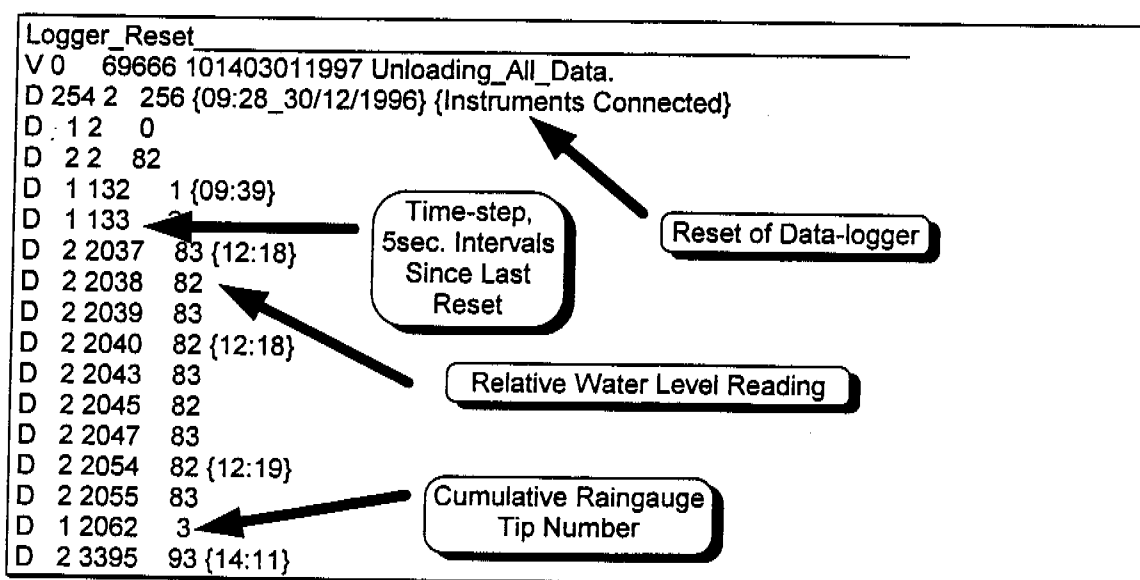


Figure 3.3.2: An extract from a raw data file unloaded from the UNIDATA data-logger highlighting the number of tips from the electronic raingauge, and the water level via a capacitance reading. It should be noted that the number in the column after the 'D', representing a data-entry line, represents the channel that each device was connected to within the data-logger.

Raw rainfall and runoff data similar to the extract (Figure 3.3.2), was obtained from the UNIDATA data-logger at regular intervals by transferring data to a laptop computer. The data-logger was reset with the accompanying software and re-sealed. The discharge, (m^3/s), and cumulative rainfall, (mm), data was arranged in DISTFW rainfall and runoff file format.

The DISTFW-NLFIT model required data pertaining to the topography of the catchment and the runoff response from the catchment, under certain rainfall.

The 'Field Williams' input file (a *.fw file), could be considered as the controlling file, and containing information on; the sub-catchment number and their relative size; upstream/downstream elevation; linkage from one sub-catchment to another; storm duration; rainfall and runoff input file names; and erosion parameters and calibration data. It should be noted that the erosion component of the DISTFW model was not utilised in this study. Further discussion pertaining to the prediction of erosion from the field plot are considered in Section 4.0 of this report.

The topographical characteristics of the field plot were determined by a survey with a TopCon total station theodolite. Figure 3.3.3 highlights the division of the field plot into ten equal sub-catchments that were entered into the 'Field Williams' input file.

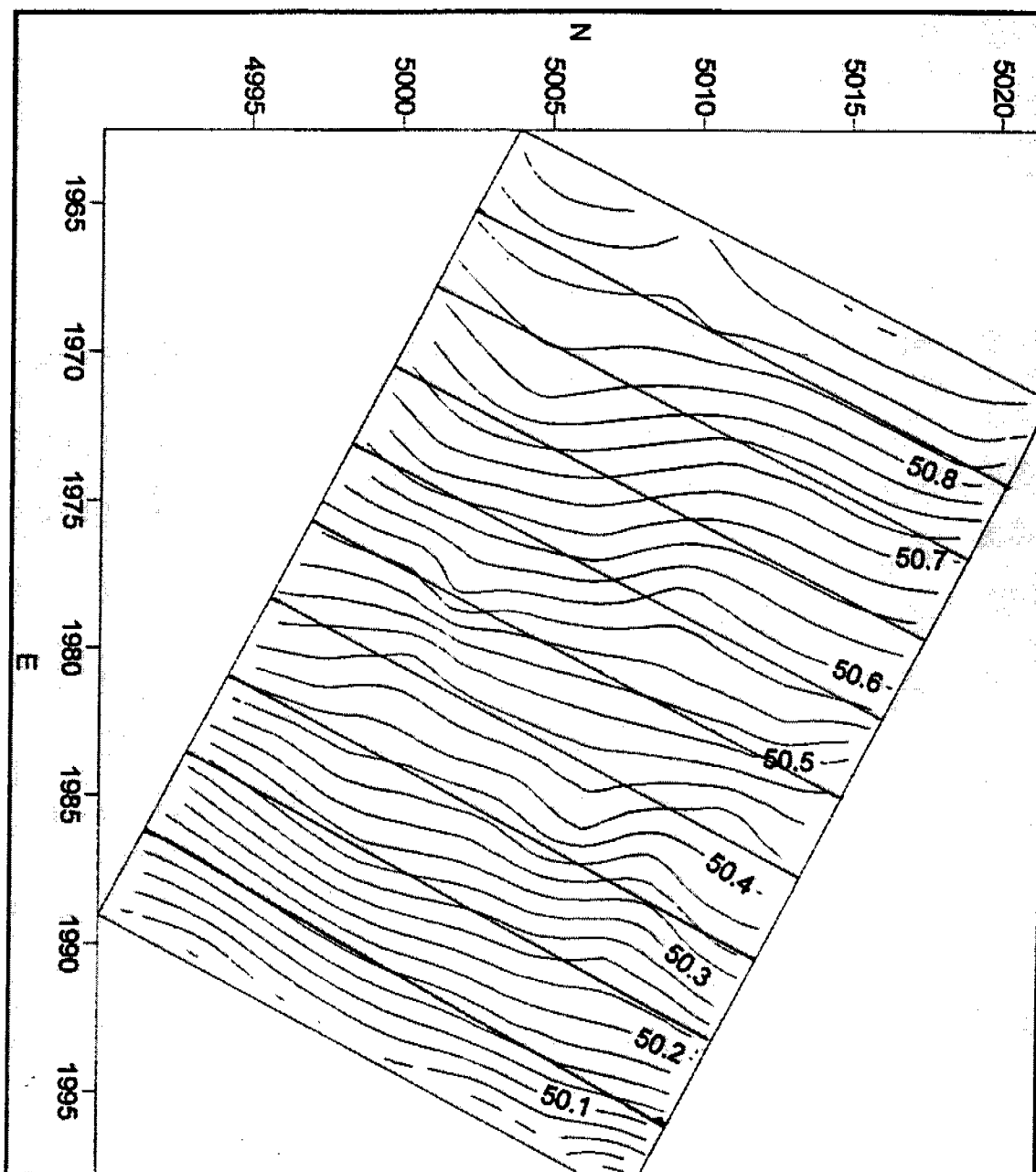


Figure 3.3.3: The 30 m in length, and 20 m in width, 600 m² field plot was divided into ten equally proportioned sub-catchments and upstream and downstream elevation information was entered into the 'Field Williams' file. The Northing and Eastings including topographic measurements can only be conservative to one another.

Each sub-catchment had a length of 3 metres and a width of 20 metres, with a total area of 60 square metres. The 'Field Williams' input file was especially modified to accept sub-catchments that were connected together in the form of a field plot, as there was no specific main channel for discharge as in a normal catchment (Willgoose *et al*, 1995).

The typical features of a 'Field Williams' file are illustrated in Figure 3.3.4.

```

Data file is for a rainfall simulation plot (plot version)
RUMPIT 1 large scale plot Monitoring
01/01/97 1550hrs
PLOT
# No of elements, No of reservoirs, no of u/s elements
10      0      1
# No of U/S element draining into D/S elements
#
# zero time (hrs), timestep (minutes), time of duration of storm (hrs)
#
0 0.05 1.9
#
# OUTPUT PARAMETERS
#
# no of pts for output discharge, psteps
1 1
# subareas at which discharge requested
10
# maximum discharge on output graph
0.002
#
INCIDENCES
0 1 2 3 4 5 6 7 8 9
PARAMETERS
# Kind of element
0
# No Area Length U/S D/S SWSupply Gamma Sorpt Phi GWSupply
# Elevation Elevation
#
1 60.0 3.0 50.9 50.825 1.0 1.0 1.0 1.0 1.0
2 60.0 3.0 50.825 50.725 1.0 1.0 1.0 1.0 1.0
3 60.0 3.0 50.725 50.65 1.0 1.0 1.0 1.0 1.0
4 60.0 3.0 50.65 50.575 1.0 1.0 1.0 1.0 1.0
5 60.0 3.0 50.575 50.50 1.0 1.0 1.0 1.0 1.0
6 60.0 3.0 50.50 50.425 1.0 1.0 1.0 1.0 1.0
7 60.0 3.0 50.425 50.35 1.0 1.0 1.0 1.0 1.0
8 60.0 3.0 50.35 50.225 1.0 1.0 1.0 1.0 1.0
9 60.0 3.0 50.225 50.125 1.0 1.0 1.0 1.0 1.0
10 60.0 3.0 50.125 50.025 1.0 1.0 1.0 1.0 1.0
# Hillslope and Channel conveyances
# 1st set are hillslope conveyances
# 2nd set are channel conveyances
# Element No, No of conveyances
# CR, EM, CONVEY
#
CONVEYANCES
1 2
0.136 1. 0.
0.136 1. 1000.
#
# Parameter Multipliers
# Ch-CR Ch-EM SWSupply SWGamma Sorptivity Phi GWSupply timing(sec)
MULTIPLIERS
7.8 1.33 0.03 0.375 0.00001 6.5 1000. 0.0
1
0.0 0.0
# No of pluvios
RAINFALL #1
1
CUMPLUVIO 1197.rf
1.00 1.00 1.00 1.00 1.00 1.00 1.00 1.00 1.00
# No of known initial flows at stations
INITIALQ
title line 1
title line 2
title line 3
1
# stations at which flows known and initial flow (cumecs)
10 0.0
# No of stations with known inflows
INFLOWQ NONE
# Hydrograph to calibrate with (no of values)
CALIB #1 1197.ro
END

```

Storm duration and timestep

Subcatchment Topography

Parameter Multipliers

Rainfall Input File Name

Runoff Input File Name

Figure 3.3.4: A typical Field Williams input file, containing topographic information on the field plot, and the rainfall and runoff input file names for a particular storm event.

The rainfall and runoff input files for the DISTFW model, contain the cumulative rainfall, (mm), and discharge at the outlet of the catchment, (m^3/s), respectively. The outlet of the catchment in this case is the PVC discharge trench, as featured in Figure 2.2.2. Every data point in the rainfall and runoff files has a time signature, in decimal hours associated with it. Figures 3.3.5, and 3.3.6 respectively illustrate typical DISTFW rainfall and runoff input data files.

RUM 96-97 Monitoring pit 1 site		Storm Event Details
Rainfall 1/1/97 1550hrs		
168	Number of Lines of Data	
0.0000 0.0		
0.0167 0.2		
0.0250 0.4		
0.0417 0.8		
0.0500 1.0	Cumulative Rainfall, mm	
0.0583 1.2		
0.0667 1.6	Time, decimal hours	
0.0750 2.2		
0.0833 2.4		

Figure 3.3.5: A DISTFW rainfall input file featuring a title, and cumulative rainfall with accompanying time stamp in decimal hours since the commencement of the event.

RUM 96-97 Monitoring pit 1 site		Storm Event Details
Runoff 1/1/97 1550hrs		
168	Number of Lines of Data	
0.000 0.00000		
0.017 0.00001		
0.025 0.00001		
0.042 0.00001		
0.050 0.00005		
0.058 0.00005	Discharge, (m^3/s)	
0.067 0.00005		
0.075 0.00005	Time, (decimal hours)	

Figure 3.3.6: A DISTFW runoff input file featuring a title, and discharge, (m^3/s), with accompanying time stamp in decimal hours since the commencement of the event.

All DISTFW rainfall, runoff and Field Williams files utilised in this study appear in Appendix 3.A.

3.4 DISTFW-NLFIT Calibration Procedure

The DISTFW model was calibrated according to the procedure outlined in Willgoose *et al* (1995), and Saynor *et al* (1995). The magnitudes and standard deviations of the two kinematic wave parameters, Cr and e_m , and the two infiltration parameters, S_ϕ and ϕ , were primarily of interest in this study.

Parameters were estimated with the DISTFW-NLFIT package by means of a descent method, which evaluated the gradient direction of the response surface at each iteration and progressively stepped in a downhill direction until the objective function reached a minimum (Johnston and Pilgram, 1976). Figure 3.4.1 features the global optimisation of the hypothetical objective function $\psi(\gamma)$, which comprises of a three dimensional response surface with contours of constant of $\psi(\gamma)$ whose magnitude is a function of the two hypothetical parameters, γ_1 and γ_2 .

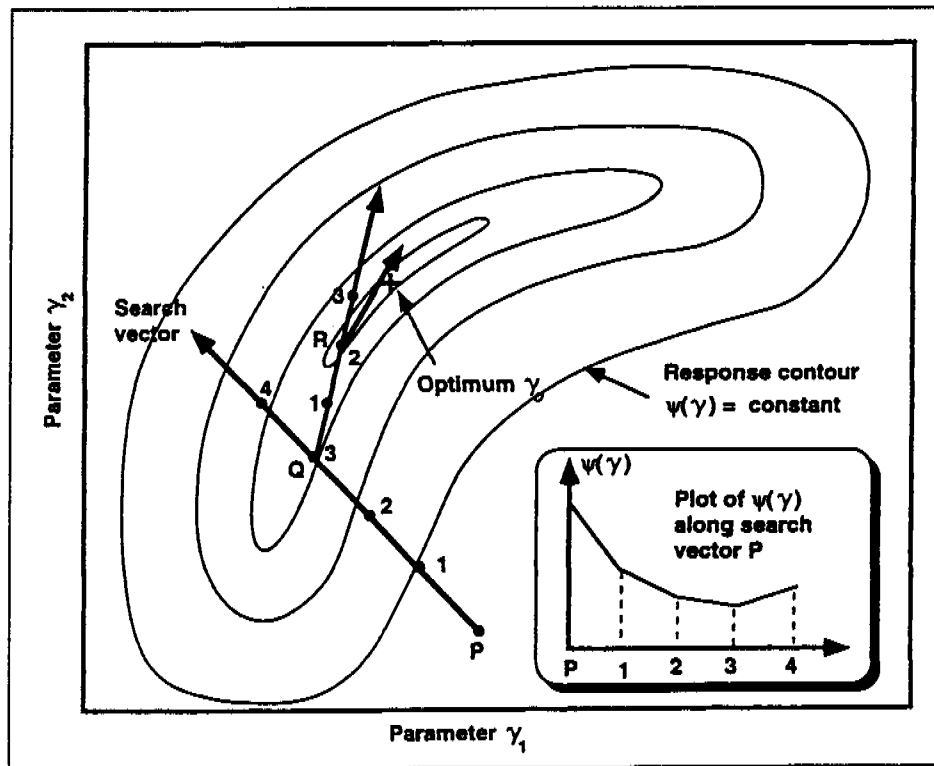


Figure 3.4.1: The global optimisation of the objective function $\psi(\gamma)$, involves the search vector moving in a down-gradient direction until a minimum is reached, denoted by an 'X' (Kuczera, 1994).

The value of parameters from the DISTFW model can be estimated with NLFIT, as illustrated in Figure 3.4.1. Parameters of the DISTFW model include; C_r , e_m , C_s , γ , S_ϕ , ϕ , C_g , 'timing' and 'initial wetness'; where C_s is a coefficient and γ is the exponent from the surface storage equation (Equation 3.2.5); and C_g is a coefficient from the groundwater storage equation, which was not considered in the current study; 'timing' is a factor to account for differences in time between rainfall and runoff data (usually associated with data from different sources); and 'initial wetness', is only applicable in multiple fitted storm events (where it accounts for differences in catchment response from various states of initial wetness). Only the kinematic wave and infiltrative loss parameters, C_r , e_m , S_ϕ , and ϕ were estimated in this study.

Table 3.4.1, highlights the initial starting values for the parameters utilised in the DISTFW model as recommended in Willgoose *et al* (1995).

Table 3.4.1: DISTFW model parameter initial calibration magnitudes and designation as to whether an estimation of the parameter was sought or whether the parameter's value was permanently fixed.

Parameter	Magnitude	Permanently Fixed
C_r	10	No
e_m	1.67	No
C_s	0.003	Yes
γ	0.375	Yes
S_ϕ	0.001	No
ϕ	0.001	No
C_g	1000	Yes
Timing	0.001	Yes
Initial Wetness	0.001	Yes

Willgoose and Kuczera (1995) noted that during simulations, only one of the non-linear or kinematic wave stores should be enabled due to parameter identification difficulties that could be encountered. As such the magnitudes of the surface storage parameters of C_s and γ were permanently fixed in this study.

The groundwater storage equation was not considered in this study, as over normal short storm durations groundwater contribution to catchment runoff was negligible.

Willgoose *et al* (1995) noted that due to stability problems associated with the DISTFW model, the parameters of C_r , C_s , S_ϕ , ϕ , and 'initial wetness', must not have magnitudes less than or equal to 0.0. They continue that if S_ϕ becomes relatively large and is incorporated into the Philip's infiltration model then the root of a negative number will attempt to be found and will cause program instabilities.

The following calibration procedure was adopted due to the severe parameter interactions within the DISTFW model (Willgoose *et al*, 1995);

- Fit C_r and ϕ , to approximate the timing and volume of the hydrograph,
- Fit S_ϕ and ϕ , to better approximate the volume of the hydrograph,
- Fit C_r and e_m , to achieve a better approximate of the routing of the hydrograph, and
- Fit all parameters, to achieve a polished approximation of the hydrograph.

A least squares error model was chosen initially for each storm event calibration. In many cases, because of a lack of statistical normality in the distribution of errors, a more general error model needed to be adopted. Kuczera (1994) noted that the adequacy of the least squares error model could be evaluated through simple diagnostic residual plots. The DISTFW-NLFIT package utilised in this study incorporated these diagnostic residual plots. Comparisons were made between each error model to determine the one that yielded the most accurate predicted hydrograph compared to that which was observed, and that satisfied the most diagnostic residual plots. Due to the complexity of the statistics associated with the NLFIT package, reference is made to Kuczera (1994) for further information beyond the summary presented in Section 3.5.

3.5 NLFIT-General and Least Squares Error Models

Kuczera (1994) noted that the least squares error model assumes that; the expected value of the random error ' ε_t ' is zero; and the variance of ' ε_t ' equals a constant ' σ^2 '; the errors are statistically independent of each other; and are normally distributed. The least squares error model is summarised as Equation (3.5.1)

$$\varepsilon_t \sim N(0, \sigma^2) \quad (3.5.1)$$

A residual is an estimate of the true random error ' ε_t '. The standardised residual ' Z_t ' is defined in Equation (3.5.2) (Kuczera, 1994).

$$Z_t = \frac{\hat{\varepsilon}_t}{\sigma} \quad (3.5.2)$$

Kuczera (1994) continued that if a least squares model is adequate in predicting error, then the standardised residuals should have a normal distribution, $Z_t \sim N(0,1)$. This normal distribution implies that 95% of the ' Z_t ' values should fall within the range -2 and 2. If the absolute value of ' Z_t ' is beyond 2, then a more general error model should be investigated.

Kuczera (1994) considered the most informative diagnostic output is a plot of predicted response versus standardised residuals, where a randomly scattered pattern is evidence of least squares model adequacy. Figure 3.5.1 illustrates a residual versus predicted response plot for the parameter estimation of storm event occurring on the 1/1/97, utilising a least squares error model.

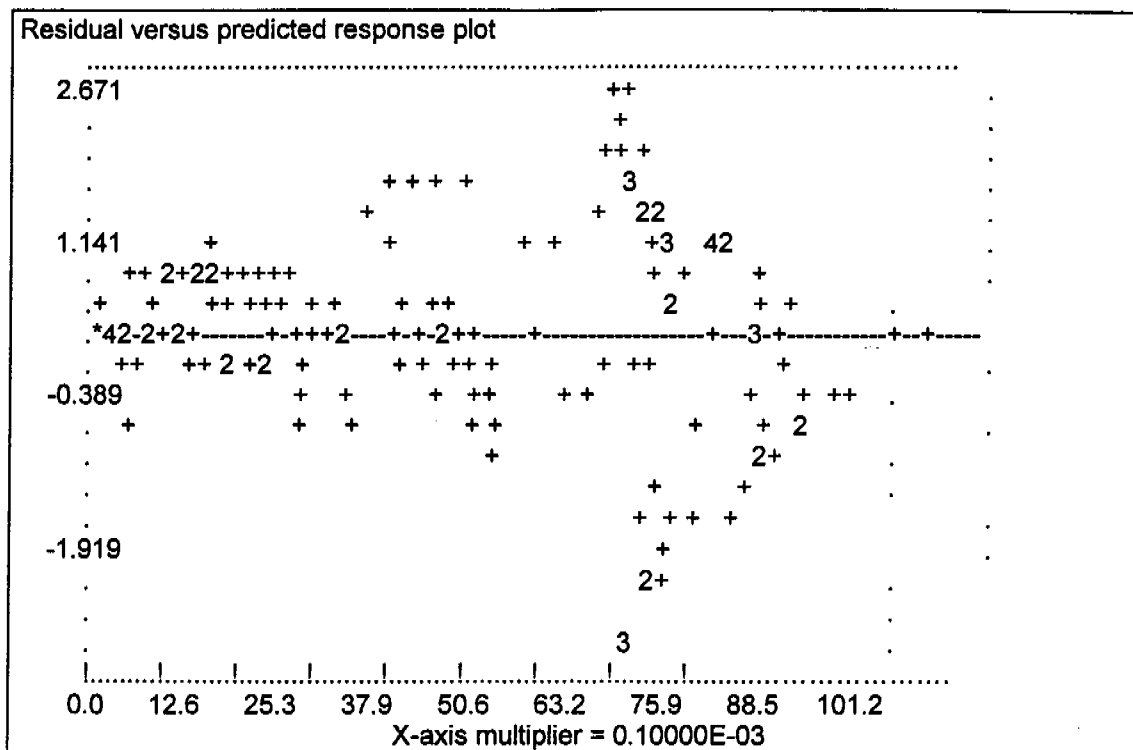


Figure 3.5.1: Plot of standardised residuals versus predicted response for a least squares model of the 1st January 1997 event. The increasing spread of standardised residuals versus predicted response indicates that the residual variance is increasing with predicted response thus violating the least squares model assumption. The number 'X' in this plot refers to 'X' residuals occupying virtually the same position.

It can be observed in Figure 3.5.1, that there is an increasing scatter of standardised residuals as the predicted response increases, indicating a violation of the least squares model. The corrections for violations of the simple residual plots are presented later in this Section.

Kuczera (1994) noted that a plot of time versus standardised residuals is useful for the detection of trends and periodicity in standardised residuals, and another tool for the evaluation of the adequacy of the least squares model. The number 'X' in the plot of standardised residuals versus predicted response (Figure 3.5.1), highlights that there are 'X' residuals occupying virtually the same position. Figure 3.5.2, illustrates a plot of time versus standardised residuals for the same storm event.

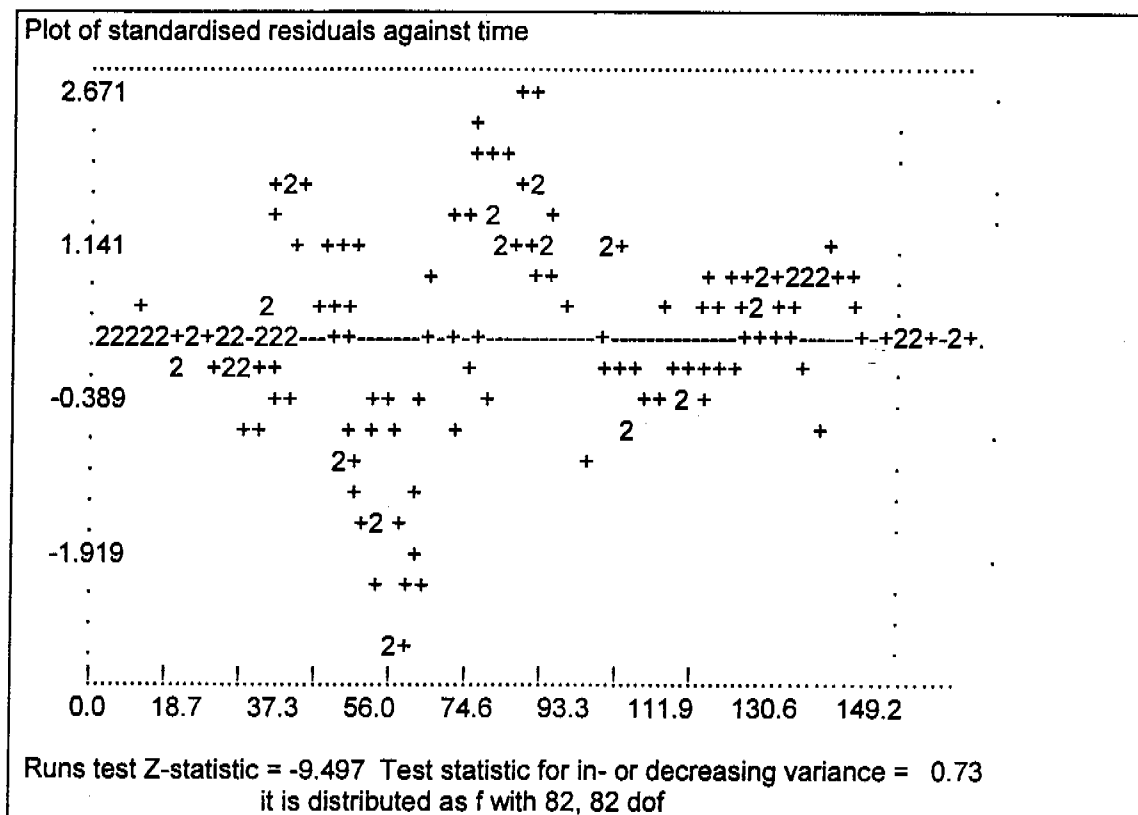


Figure 3.5.2: Plot of time versus standardised residuals for the 1st January 1997 event. The Z statistic being -9.5, exceeds the test value of |2|, indicating that the standardised residuals are not independent.

A pattern of scatter of increasing magnitude with time or the absolute value of the Z statistic exceeding 2 (as in the case of Figure 3.5.2), is an implication that the standardised residuals are probably not independent (Kuczera, 1994), a key assumption of the least squares model.

The normal probability of standardised residuals should, in a large sample, plot as a straight line, implying normality. The assessment of linearity is considered to be difficult (Kuczera, 1994), hence a Kolmogorov-Smirnov statistic and a 5% exceedance test value is used as an indicator of linearity. The normal probability plot for the 1st January storm event is presented in Figure 3.5.3.

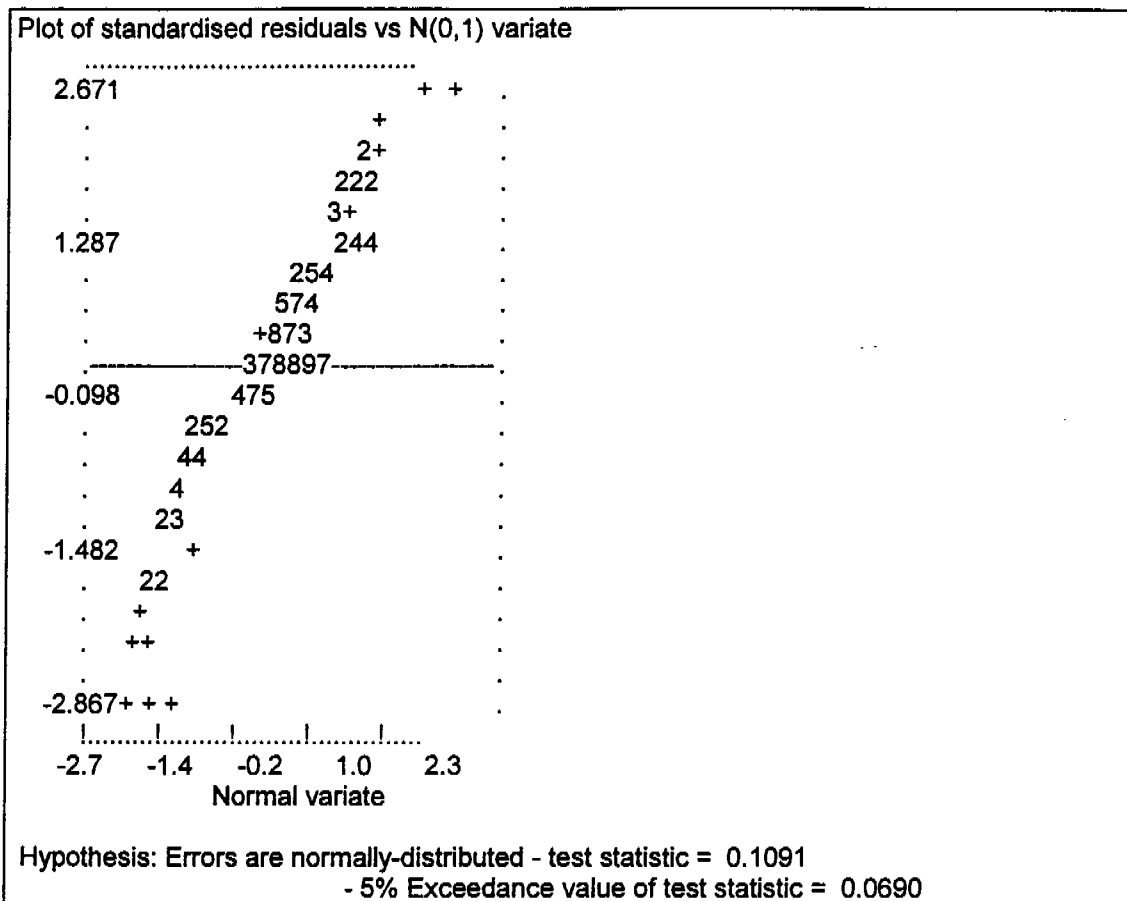


Figure 3.5.3: A normal probability plot for the storm event occurring on the 1st January 1997 with a Kolmogorov-Smirnov statistic of 0.1091, and a 5% exceedance value of 0.0690. As the Kolmogorov-Smirnov statistic exceeds the 5% test value, the residuals are considered not to be normally distributed.

If Kolmogorov-Smirnov statistic exceeds the 5% test value then it can be argued that the residuals are probably not normally distributed (Kuczera, 1994).

Plots of autocorrelation and partial autocorrelation give insight into the time dependence of standardised residuals. The 95% confidence limits on the autocorrelation function are represented by the dashed lines on Figure 3.5.4. Kuczera (1994) noted that if most of the autocorrelation plot falls inside the 95% limits, then the assumption that the standardised residuals are statistically independent is not inconsistent with the data.

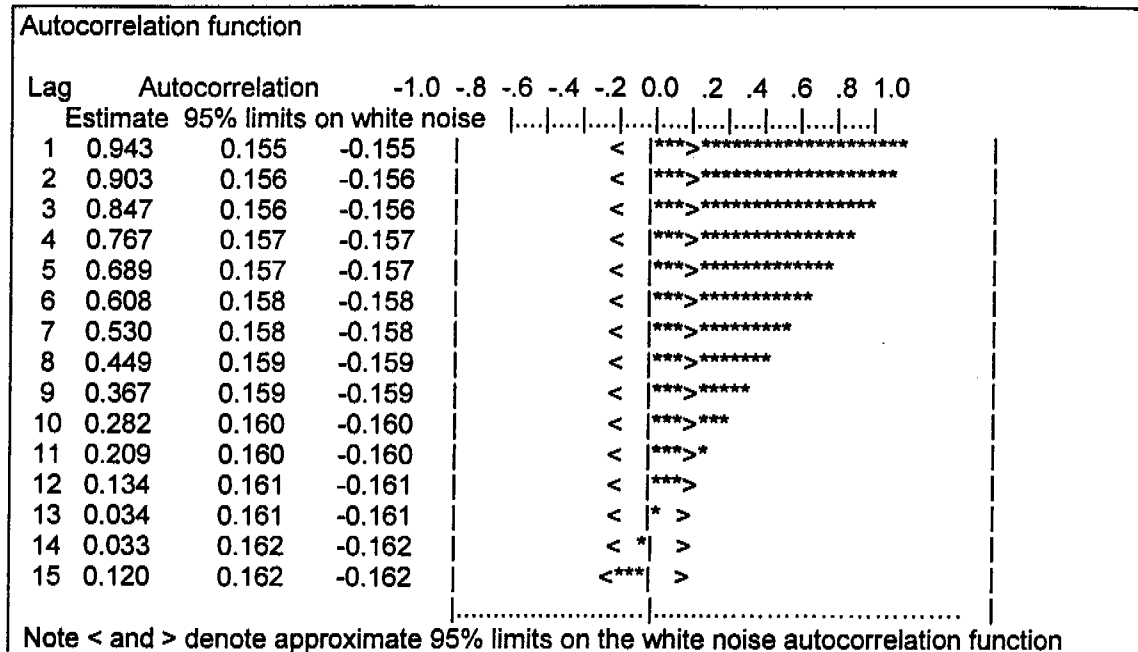


Figure 3.5.4: Residual autocorrelation plot for the 1st January storm event, which highlights the time dependence of the residuals, in this case the assumption of the residuals being statistically independent is not consistent with the data.

Divergence of residuals beyond the 95% prediction limits (Figure 3.5.4), suggests that an alternative to the least squares error model should be used. The partial autocorrelation plot from the storm event occurring on the 1st January is not presented.

Figure 3.5.5 highlights a cumulative periodogram plot for the 1st January storm event, which is analogous to the normal probability plot, but is particularly sensitive to periodicities in standardised residuals with constant variance (Kuczera, 1994).

Kuczera (1994) noted that although the theoretical periodogram should be a straight line assuming that the residuals are independent and constant, but for small samples, the plot deviates from the straight line due merely to sampling variability. The sample space was considered sufficiently large, so Figure 3.5.5 implies another violation of the least squares error model assumptions.

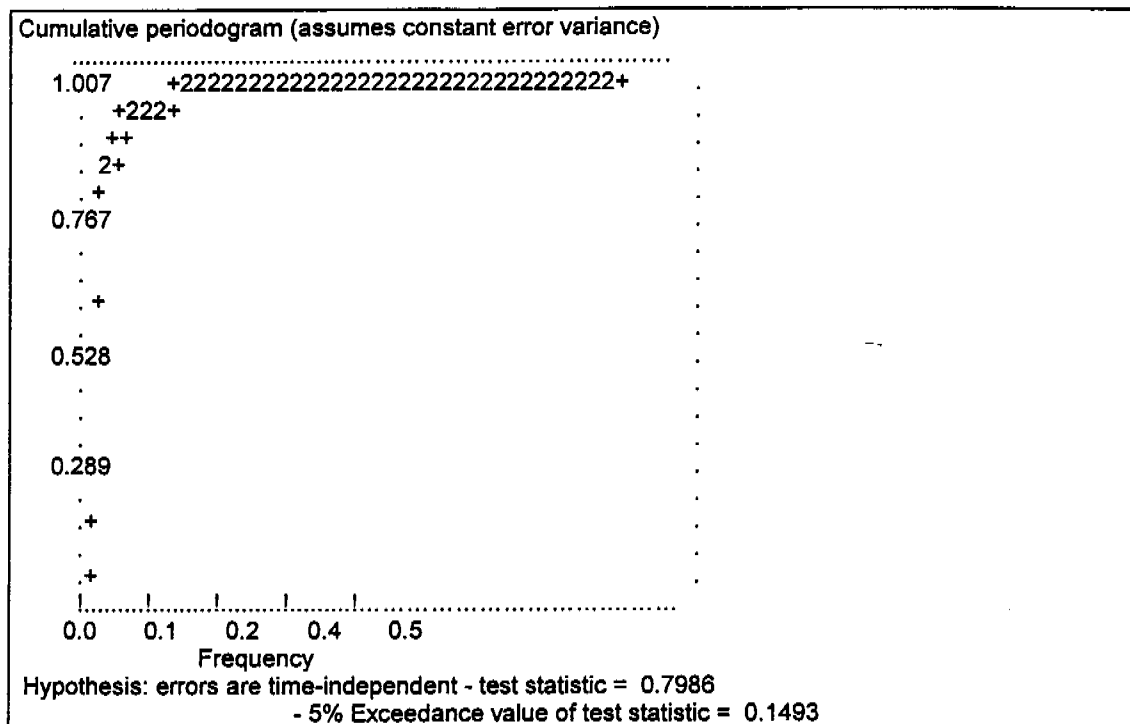


Figure 3.5.5: Residual cumulative periodogram plot for the 1st January 1997 storm event, which should be linear assuming that the residuals are independent and constant (an assumption of the least squares error model).

Kuczera (1994) noted that when the least squares model is invalidated, two options in NLFIT, in the form more general error models, can be employed to modify the errors so that the residuals conform more adequately with the least squares assumptions;

- To correct for non-stationary residual variance, when the scatter of the standardised residual versus predicted response plot is not in a uniform band, a Box-Cox transformation can be used. The Box-Cox model transforms the data in such a way that the variance of the random error and the transformed error are constant. Stabilisation of the residual variances often induces normality in the residuals (Kuczera, 1994).
- Kuczera continued that if the diagnostic plots infer a time dependence, then a complex ARMA (Auto Regressive Moving Average) time series model may be employed for correction.

3.6 Data

Natural rainfall event monitoring over the 1996/1997 wet season resulted in the accumulation of rainfall, runoff, and sediment loss data from numerous storm events. The raw hydrological data was transformed into DISTFW rainfall, runoff, and Field Williams files, and listed in Appendix 3.A (as previously reported in Section 3.3).

Table 3.6.1 lists the storm events (designated by the date of occurrence), the total rainfall recorded, (mm), the peak discharge, (L/s), and the approximate duration of the storm, (hours).

Table 3.6.1: Recorded storm events during the 1996/1997 wet season with associated total rainfall, (mm), peak discharge, (L/s) and storm duration (hours).

Storm Event.	Total Rainfall, mm.	Peak Runoff, L/s.	Duration, hours.
1/1/97	70.2	11.00	1.90
3/1/97 ^a	58.4	6.00	4.90
3/1/97pm ^a	14.4	0.90	4.10
4/1/97	12.2	1.30	3.90
11-12/1/97	37.6	3.50	4.10
12/1/97 ^a	5.0 ^b	0.25	0.10
12/1/97pm ^a	16.5 ^b	0.55	0.55
17/1/97	29.6	0.35	1.50
19/1/97	19.6	0.60	1.90
21/1/97 ^{st, c}	11.8	0.40	0.77
21/1/97 ^{nd, c}	22.4	1.70	1.50
22/1/97	30.8	0.70	8.20
23/1/97	43.8	12.00	2.60
23-24/1/97	40.6	3.00	6.30
28/1/97	28.2	2.50	4.00
19/2/97	64.6	1.20	4.50
20/2/97	32.4	4.00	2.20
22/2/97	29.0	4.00	3.50
22/2/97pm	26.8	3.70	4.20
23/2/97	23.0	3.30	4.10

^a Afternoon and morning storm events occurred.

^b No cumulative rainfall was available due to electronic raingauge failure.

^c Two afternoon events.

It can be observed from Table 3.6.1, that there was considerable variation in the magnitude of rainfall events experienced during the monitoring season, with peak discharges ranging from 0.25 to 11 L/s. The cumulative rainfall listed in Table 3.6.1, although of similar magnitude, differed significantly with respect to intensity. Surface runoff from the field plot was observed to continue for a considerable period of time after the cessation of rainfall. The storm durations listed in Table 3.6.1, refer to the cessation of surface runoff, not the cessation of rainfall.

The DISTFW model required the input of the rainfall and runoff data for each storm event (Section 3.3), selection of appropriate initial estimates of parameter values (Table 3.4.1), and the choice of an error model. In all cases the "least squares" error model was chosen initially and a more general error model was selected in subsequent runs based on the results from the simple diagnostic residual plots produced as an output from the modelling process, and summarised for each storm event in Appendix 3.A. The output from the DISTFW-NLFIT model that was of primary interest in the current study was the mean and standard deviations of the kinematic wave parameters C_r and e_m and the infiltration parameters S_ϕ , and ϕ .

All storm durations listed in Table 3.6.1, were fitted with the DISTFW model utilising various error models and appear in Appendix 3.A in the form of Figure 3.6.1. Featured in Figure 3.6.1, is a plot of the cumulative rainfall, (mm), the observed hydrograph, (m^3/s), and the hydrograph predicted by DISTFW, (m^3/s), for a storm event occurring on the 1st January 1997.

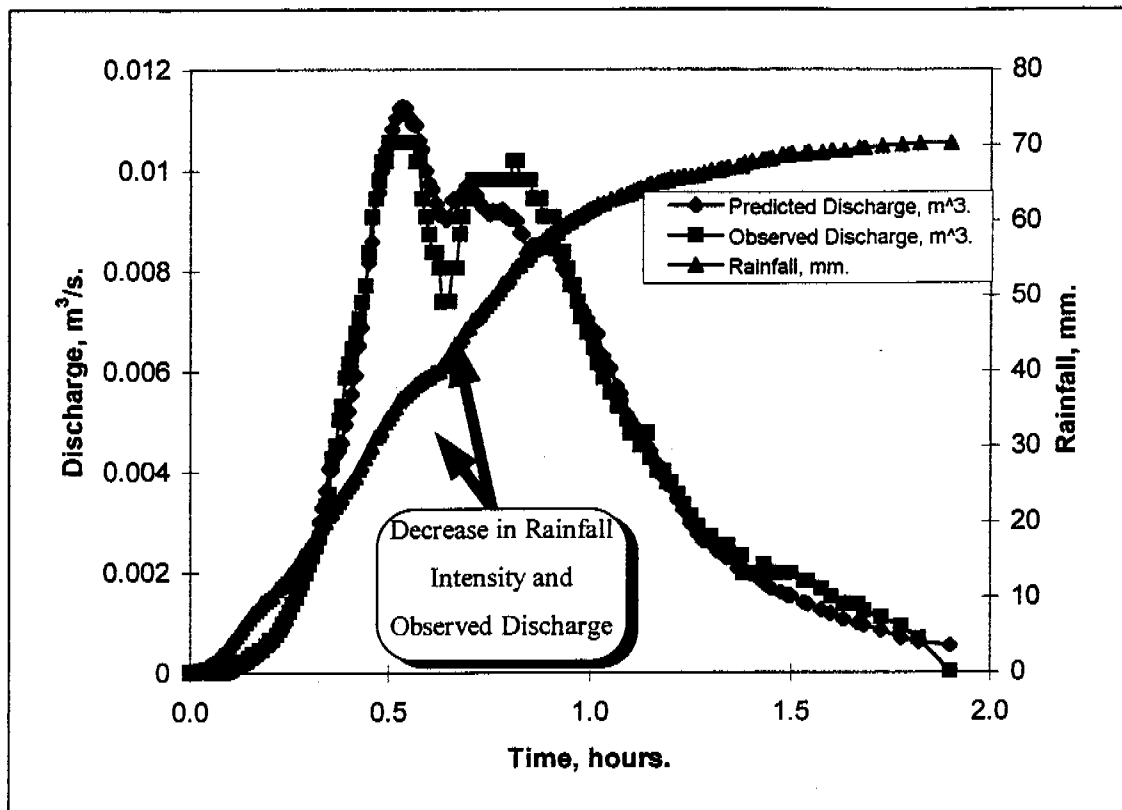


Figure 3.6.1: Observed and predicted discharge, (m^3/s), and cumulative rainfall, (mm), for the storm event occurring on the 1st January 1997. The large arrow indicates a reduction in rainfall that resulted in a subsequent decrease in observed and predicted discharge from the field plot.

Figure 3.6.1 highlights that the predicted hydrograph is very similar to that which was observed, especially in the incline and recession limbs. The over-prediction of the first peak and the under-prediction of the second peak is only of a minor concern. The large arrow in Figure 3.6.1 that is pointing towards the cumulative rainfall curve, indicates a slight reduction in rainfall intensity at the three-quarters of an hour mark after the commencement of rainfall. Corresponding to the slight reduction in rainfall intensity is the slightly delayed dip in surface runoff, yet as the rainfall re-intensifies, discharge increases accordingly.

Table 3.6.2 illustrates the kinematic wave and infiltration parameter values and their corresponding standard deviations for a select number of fitted storm events which fulfilled the criteria of the peak discharge exceeding 1 L/s (Willgoose pers. comm.) and a well defined storm duration. Storm events with discharge peaks less than approximately 1L/s, were considered to be non-significant events, when compared to events with discharge peaks ten times larger, for example the first event on 21st January with a peak of 0.4L/s, compared to the event on the 22nd February with a peak of 4L/s. The prediction of the discharge hydrograph, compared to that which was observed, for storm events with peak discharges less than 1L/s was generally much poorer than those storm events with peak discharges in excess of 1L/s. Comparisons between storm events can be made by consulting Appendix 3.A.

Figure 3.6.2 illustrates the storm event occurring on the 23-24th January, which was considered to be an example of a storm event with an ill-defined duration.

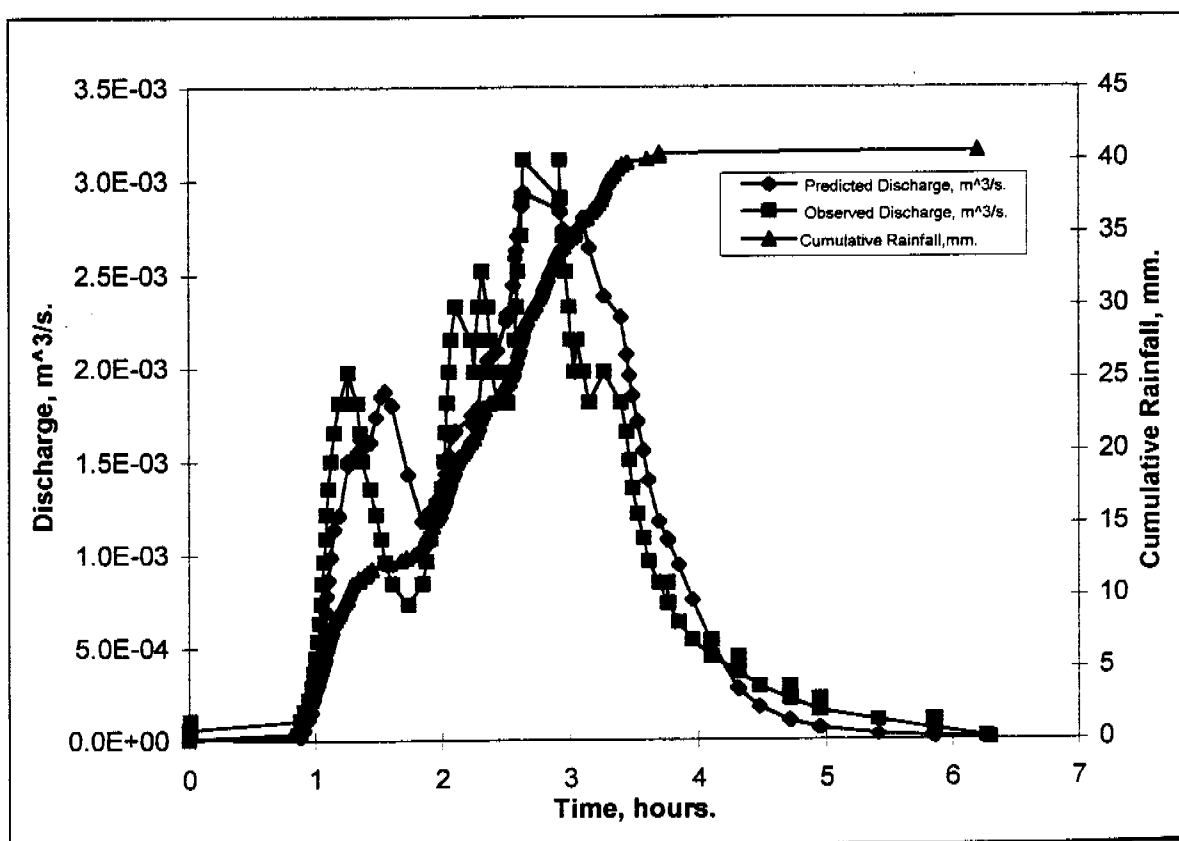


Figure 3.6.2: The ill-defined duration of the overnight storm event occurring over the 23rd-24th January, resulted in the considerable differences between the observed and predicted hydrographs.

The overnight storm event (Figure 3.6.2), involved only mild, drizzle-like rainfall for approximately four hours which resulted in considerable variation in the observed hydrograph, and hence was omitted from further analysis. Similar drizzle-like rainfall was prevalent for the overnight storm event occurring on the 11th-12th of January and was also omitted from further analysis.

Also featured in Table 3.6.2, is the error model utilised to obtain the best prediction of the runoff hydrograph compared to that observed. The utilisation of the auto-regressive model is summarised as 'AR', and the Box-Cox transformation model is summarised as 'BC'.

Table 3.6.2: Summary of infiltration and kinematic wave parameter values for all storm events that had a peak discharge in excess of 1L/s, and a definite storm duration.

Storm Event	Error Model	Kinematic Wave Parameters	Mean (Standard Deviation)	Infiltration Parameters	Mean (Standard Deviation)
1/1/97	1 AR BC=0.1	C_r	1.529(0.176)	S_p (mm/hr ^{1/2})	7.825(0.715)
		e_m	1.631(0.091)	ϕ (mm/hr)	0.001
3/1/97	BC=0.1	C_r	4.001(0.668)	S_p (mm/hr ^{1/2})	0.001
		e_m	1.554(0.081)	ϕ (mm/hr)	9.031(0.281)
4/1/97	Least Squares	C_r	6.775(0.152)	S_p (mm/hr ^{1/2})	0.001
		e_m	1.291(0.096)	ϕ (mm/hr)	3.783(0.458)
21/1/97 nd	BC=0.5	C_r	2.161(0.534)	S_p (mm/hr ^{1/2})	14.997(8.211)
		e_m	1.513(0.153)	ϕ (mm/hr)	7.544(29.642)
23/1/97	Least Squares	C_r	2.257(0.109)	S_p (mm/hr ^{1/2})	0.001
		e_m	1.596(0.051)	ϕ (mm/hr)	51.591(1.119)
28/1/97	Least Squares	C_r	9.168(1.083)	S_p (mm/hr ^{1/2})	0.001
		e_m	2.697(0.083)	ϕ (mm/hr)	25.52(0.464)
19/2/97	Least Squares	C_r	0.631(0.097)	S_p (mm/hr ^{1/2})	11.7(0.385)
		e_m	4.517(0.350)	ϕ (mm/hr)	0.001
20/2/97	Least Squares	C_r	3.211(0.505)	S_p (mm/hr ^{1/2})	2.2578(1.913)
		e_m	2.093(0.189)	ϕ (mm/hr)	22.743(4.03)
22/2/97	Least Squares	C_r	4.312(0.537)	S_p (mm/hr ^{1/2})	0.001
		e_m	2.104(0.085)	ϕ (mm/hr)	15.579(0.489)
22/2/97 ^{pm}	Least Squares	C_r	11.62(2.005)	S_p (mm/hr ^{1/2})	3.233(0.165)
		e_m	2.237(0.096)	ϕ (mm/hr)	0.001
23/2/97	Least Squares	C_r	6.110(0.788)	S_p (mm/hr ^{1/2})	0.001
		e_m	2.077(0.103)	ϕ (mm/hr)	13.701(2.768)

The notation '1 AR', (Table 3.6.2), refers to the utilisation of a single auto-regressive factor, and the notation 'BC=0.5', refers to the use of a Box-Cox Lambda factor of magnitude 0.5. It should be noted that infiltrative parameters with a mean value of 0.001 with no standard deviation value in closed brackets in Table 3.6.2, refer to the scenario where the parameter was determined to be redundant by the NLFIT model. Large changes in a redundant parameter results in only minuscule changes in the objective function, and hence the magnitude of this parameter is irrelevant.

It can be observed from Table 3.6.2, that the magnitude of the kinematic wave parameters C_r , and e_m , for a few storm events are quite large. The relative magnitudes of the power term, e_m , of the conveyance function can be related to the various cross-sectional hillslope geometries discussed in Section 3.2.3. Several cross sectional areas were considered, with e_m values ranging from 1.67 to 1.21, for the constant depth over the entire width of the hillslope, case 'A', to the irregular natural surface, case 'D', respectively (Figure 3.2.5).

Willgoose (pers. comm.) noted that fitted storm events with e_m values well in excess of approximately 2.0 should be neglected, as e_m is a function of the geometric cross-sectional area and cannot realistically have such magnitudes. Two storm events were considered to have excessively high e_m values, 28th January (2.697) and 19th February (4.517), (Table 3.6.2). Examination of the observed versus predicted discharge output from the DISTFW model for the storm event on the 19th February, illustrates the unpredictable nature of the observed hydrograph which is believed to have resulted in the extraneous e_m value being obtained (Figure 3.6.3).

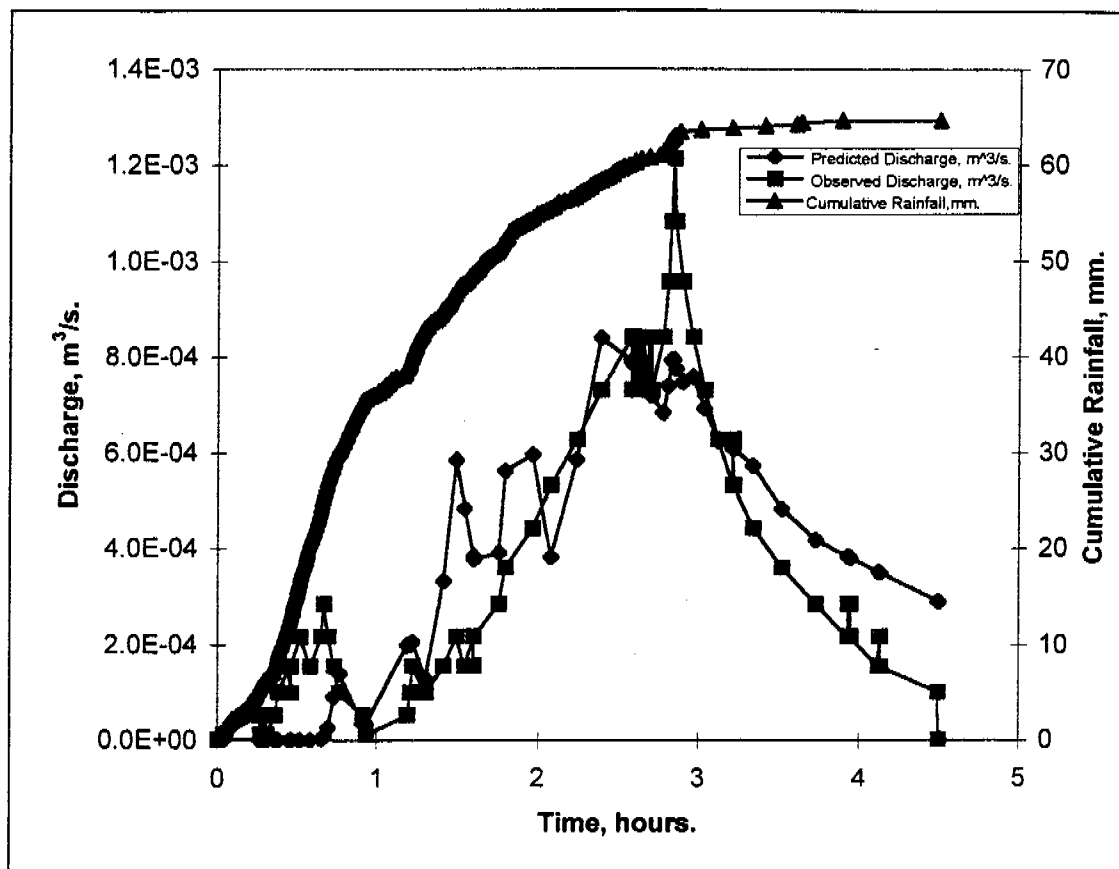


Figure 3.6.3: The predicted hydrograph of the storm event occurring on the 19th February, does not compare well with the observed hydrograph. Considerable fluctuation in the observed hydrograph over an extended period of time virtually negates the possibility of a smooth predicted response curve.

It can be observed from Figure 3.6.3, that the inclination and recession limbs, and the peak of the predicted hydrograph do not correspond well to the observed hydrograph. The considerable degree of fluctuation in the observed hydrograph is believed to be caused by fluctuating rainfall intensity.

The storm event occurring on the 28th January, although well fitted, Figure 3.6.4, has considerable fluctuation in the recession limb.

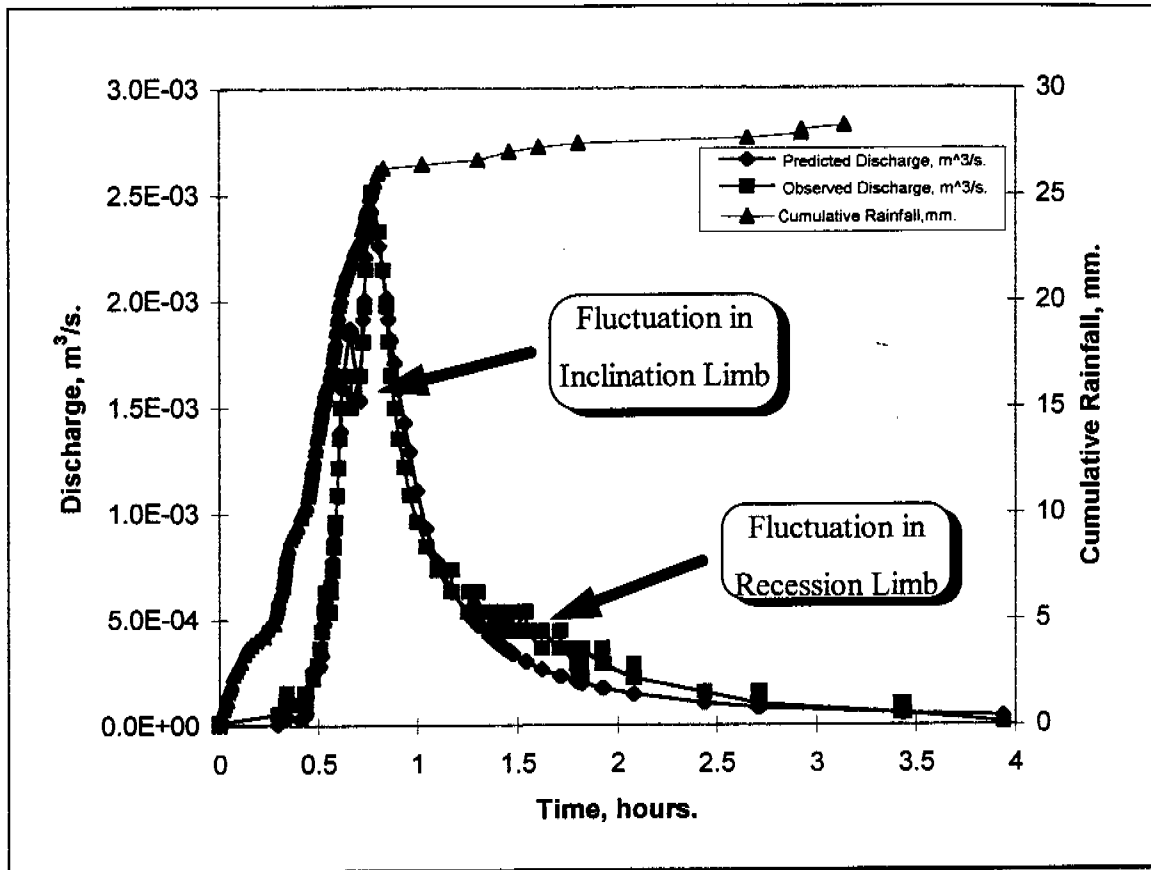


Figure 3.6.4: The inclination limb of the storm event occurring on the 28th January, is well estimated, with a slight drop in discharge resulting from a fluctuation in rainfall, highlighted by an arrow. The recession limb is dominated by fluctuations in the observed hydrograph, highlighted by an arrow, resulting from intermittent rainfall occurring at the 1.5 hour mark.

The arrows in Figure 3.6.4 highlight considerable fluctuation in the incline and recession limbs of the observed hydrograph which was surmised to have resulted in the extraneous c_m value of 2.667 being obtained from the DISTFW model.

The prediction of the runoff hydrograph for the second storm event occurring on the 21st January was considerably different from that which were observed. Figure 3.6.5 illustrates the plot of the cumulative rainfall, and the observed and predicted hydrographs for that storm event which was fitted with a Box-Cox error model.

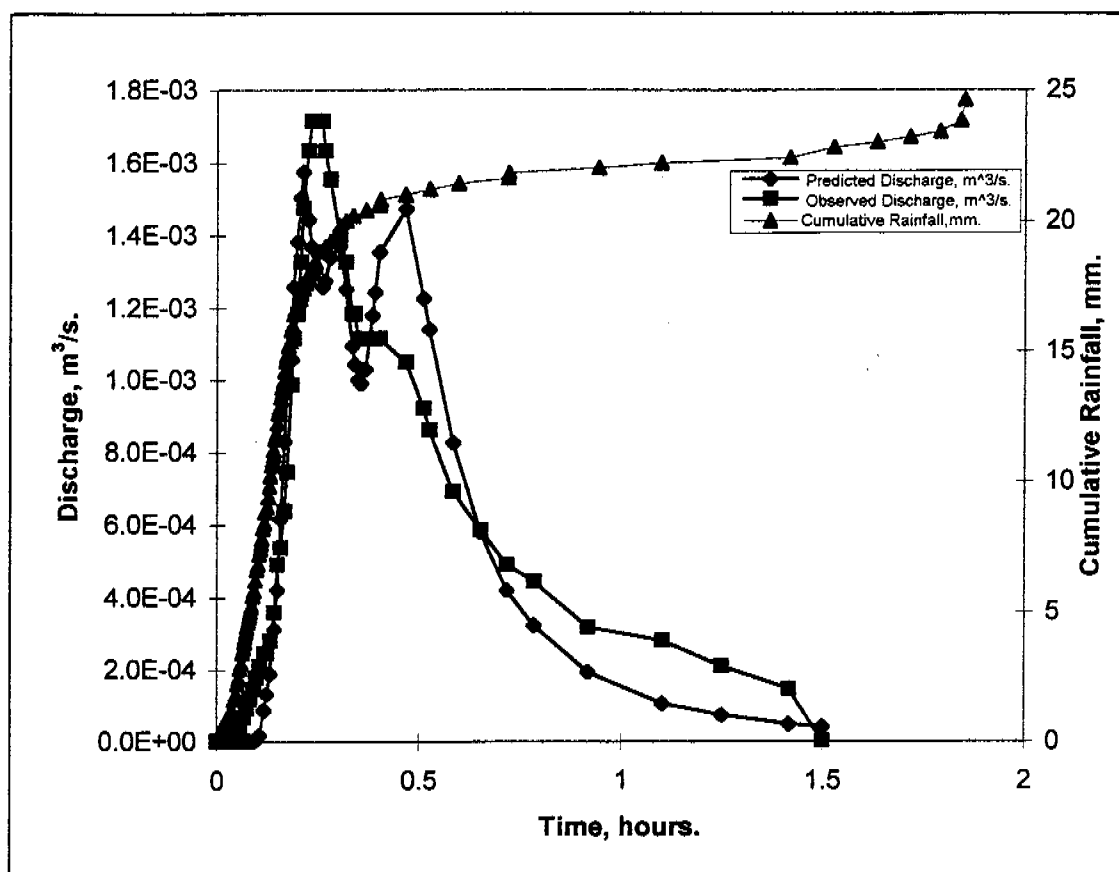


Figure 3.6.4: The inclination limb of the second storm event of the 21st January is adequately fitted, however the peak and the recession limb is poorly approximated. A large second discharge peak is predicted at the 0.5 hour mark and considerable under-prediction is evident beyond the 0.75 hour mark.

The predicted hydrograph for the second storm event occurring on the 21st January at the half and three-quarter hour marks, over-predicts and under-predicts respectively. This storm event was omitted from further analysis due to the poor predicted hydrograph compared to the prediction of hydrographs from other storm events.

3.7 Parameter Comparison

The DISTFW-NLFIT package has the ability to estimate parameters for a single rainfall event for a single site, or estimate one set of parameters to a number of events simultaneously at a single site (Saynor *et al*, 1995).

The surface storage parameters C_s and γ in the current study, were fixed permanently at 0.003 and 0.375 respectively, effectively disabling the surface storage component of the DISTFW model. In the analysis of the Tin Camp Creek data (Moliere *et al*, 1996), the same surface storage parameters values were chosen.

Moliere *et al* (1996) considered all the storm events that were fitted from data from the Tin Camp Creek study, and concluded the single fitted storm event(s), on the 30th December adequately represented all storm activity from both the Quartz and Mica sites. A module of the NLFIT program suite, PREDICT, enables the prediction of discharge for a sequence of storm events using the parameters fitted from a single event. The chosen parameters (in this case those estimated for the storm event(s) occurring on the 30th December), are considered adequate if more than 90% of the observed hydrograph data falls within the 90% prediction limits, plotted by the PREDICT module (Kuczera, 1994). This was the rationale utilised for the selection of the 30th December storm event as being representative.

Table 3.7.1 illustrates a comparison between the infiltrative and kinematic wave parameters from the current study for all the storm events listed in Table 3.6.2, (negating the three storm events referred to in Section 3.6) and the Tin Camp Creek study (Moliere *et al*, 1996).

Table 3.7.1: Mean and standard deviations for the kinematic wave and infiltrative loss DISTFW parameters for all the storm events from the current study listed in Table 3.6.2 (neglecting 22/1/97^{and}, 23-24/1/97, and 28/1/97) and the Tin Camp Creek study (Moliere *et al*, 1996).

	Natural Site Pit No.1 ERARM	Tin Camp Creek			
		Representative Storm Quartz Site	Multiple Fitted Storm Quartz Site	Representative Storm Mica Site	Multiple Fitted Storm Mica Site
Parameter	Mean (Std.Dev.)	Mean (Std.Dev.)	Mean (Std.Dev.)	Mean (Std.Dev.)	Mean (Std.Dev.)
C_r	4.98 (3.22)	7.44 (1.12)	6.48 (0.56)	28.48 (35.12)	2.06 (0.32)
e_m	1.82 (0.34)	1.31 (0.05)	1.24 (0.03)	1.75 (0.32)	1.24 (0.04)
S_p (mm/hr^{1/2})	1.67 (2.79)	17.81 (0.78)	8.65 (0.12)	3.35 (1.50)	0.97 (0.39)
ϕ (mm/hr)	14.55 (16.95)	4.73 (0.50)	5.24 (0.26)	65.29 (5.24)	47.22 (1.98)

The multiple storms from the Quartz and Mica sites, referred to in Table 3.7.1, occurred on the 25th, 27th, 29th, and 30th of December 1993, are found in Moliere *et al*, (1996).

The representative storms referred to in Table 3.7.1 for the Quartz and Mica sites, are event(s) that occurred on the 30th December 1993, and can also be found in Moliere *et al*, (1996). Two storm events were monitored on the Quartz site on the 30th December, approximately two hours apart, whilst only one event was monitored on the Mica site. The relatively large standard deviations of both the kinematic wave and infiltrative loss parameters exhibited by the representative Mica site storm was due to the relatively poor fit of the observed hydrograph with respect to the peak and the volume of flow (Moliere *et al*, 1996).

The mean and standard deviations listed in Table 3.7.1 for the Tin Camp Creek study were produced from the DISTFW-NLFIT model. The mean and standard deviations reported in Table 3.7.1 for the current study, were produced from simple descriptive statistics of the estimated parameter values from eight individually calibrated storm events.

The standard deviation of the infiltrative loss parameters listed in Table 3.7.1 for the natural site are considerable, 2.79, and 16.95, for S_ϕ and ϕ , respectively. However, a large number of storm events, (five of the eight individually calibrated storm events) had redundant S_ϕ values, which were fixed at a value of 0.001. The standard deviation of ϕ for the natural site, although having fewer redundant values, (two of the eight individually calibrated storm events), was large with values ranging from 0.001 (redundant) to 51.59 mm/hr.

Considerable effort was taken to attempt to estimate a single set of parameters for a number of combinations of four storm events from the current study, to emulate what was undertaken in the Tin Camp Creek study. Large standard deviations, many orders of magnitude beyond the mean, were consistently obtained.

The inability to achieve reasonable estimations of a single set of parameters describing four storm events was believed to result from;

- Large differences in initial soil moisture conditions,
- Differences in rainfall intensities and durations, leading to different hydrological responses with respect to both hydrograph peaks and volumes, and
- Small uncertainties in the estimation of parameter values for individual events interacting to yield larger uncertainties in multiple storm parameter estimation.

Comparison of the hillslope routing and infiltrative properties of the natural site and the Mica and Quartz sites was undertaken utilising the COMPAT module of the NLFIT program suite.

The DISTFW-NLFIT program produces a posterior moments file (termed PMF files), which contains the mean and standard deviations of the parameters estimated in a correlation matrix. As a function of the COMPAT program, the Tin Camp Creek PMF's for the two sets of multiple storm events from the Mica and Quartz sites (Table 3.7.1), were not compatible with the single storm event PMF's produced from the current study. The number of parameters in the correlation matrix from the multiple storm sets from the Mica and Quartz sites totalled fifteen each, the seven parameters directly associated with the DISTFW model; C_r , e_m , C_s , γ , S_ϕ , ϕ , C_g , and a further eight parameters, (four lots of '*timing*' and '*initial wetness*' parameters for each storm event). As a set of multiple storm events could not be estimated for the current study, the single storm event PMF's (containing the seven parameters from the DISTFW model, and one set of '*timing*' and '*initial wetness*' parameters) were altered to include three extra sets of '*timing*' and '*initial wetness*' parameters to emulate a four storm set. The incorporation of the three 'dummy' storm events did not compromise the quality of the estimation of parameter values.

95% posterior probability plots from the module COMPAT, for the kinematic wave parameters, C_r and e_m , and the infiltrative loss parameters, S_ϕ , and ϕ , for the natural site and the Tin Camp Creek study were produced to evaluate the similarities between the data sets.

Two parameters are involved in each posterior probability plot, which are assumed for clarity of explanation to have a normal 'bell' shaped distribution with a certain mean and standard deviation. The combination of these two normal distributions, in three dimensional space, results in the formation of a mountain of posterior probability. The 95% probability ellipse is merely a plan view of the 95% slice of the three dimensional posterior probability mountain.

Any set of parameter values chosen from the data set under consideration has a 5% chance of falling outside the 95% probability ellipse. Each ellipse is thus an approximation to the actual region, which is increasingly accurate as the coefficient of variation of the parameters declines.

If the 95% probability ellipses for different data sets intersect, then the parameters in the data sets are considered not to be statistically different at the 5% level, implying compatibility. If a 95% ellipse of a single data set of two parameters is horizontal or vertical then it can be argued that the parameters are statistically independent of each other. A detailed evaluation of the statistical theory behind the COMPAT module of the NLFIT suite can be found in Kuczera, (1994).

The standard deviations for the redundant parameters reported in Table 3.7.2, were not obtained from the calibration procedure employed to obtain the results listed in Table 3.6.2. To adequately compare the infiltrative loss and kinematic wave parameters from the current study and the Tin Camp Creek study, the standard deviations of these redundant parameters were determined in a separate calibration series. Table 3.7.2 also lists the storm events that correspond to the numbered labels in Figure 3.7.1, which is a 95% posterior probability plot of the kinematic wave parameters, C_r and e_m .

Table 3.7.2: Summary of infiltration and kinematic wave parameter values for eight representative storm events from the natural site and from the Tin Camp Creek study.

Label Number	Storm Event	Error Model	Kinematic Wave Parameters	Mean (Standard Deviation)	Infiltration Parameters	Mean (Standard Deviation)
1	1/1/97	Least Squares	C_r	1.684 (0.081)	S_p (mm/hr ^{1/2})	7.948 (1.525)
			e_m	1.675 (0.083)	ϕ (mm/hr)	0.280 (2.247)
2	3/1/97	Least Squares	C_r	4.480 (1.574)	S_p (mm/hr ^{1/2})	0.245 (1.839)
			e_m	1.544 (0.199)	ϕ (mm/hr)	13.64 (2.071)
3	4/1/97	Least Squares	C_r	0.775 (0.137)	S_p (mm/hr ^{1/2})	0.001 (214.54)
			e_m	1.291 (0.108)	ϕ (mm/hr)	3.783 (88.194)
4	23/1/97	Least Squares	C_r	2.258 (0.106)	S_p (mm/hr ^{1/2})	0.001 (1867.6)
			e_m	1.596 (0.068)	ϕ (mm/hr)	51.58 (246.60)
5	20/2/97	Least Squares	C_r	3.211 (0.505)	S_p (mm/hr ^{1/2})	2.258 (1.913)
			e_m	2.093 (0.189)	ϕ (mm/hr)	22.743 (4.03)
6	22/2/97	Least Squares	C_r	4.336 (0.506)	S_p (mm/hr ^{1/2})	0.001 (124.55)
			e_m	2.108 (0.080)	ϕ (mm/hr)	15.541 (3.47)
7	22/2/97pm	1 AR BC=0.5	C_r	11.58 (2.402)	S_p (mm/hr ^{1/2})	3.236 (0.689)
			e_m	2.236 (0.135)	ϕ (mm/hr)	0.001 (1.049)
8	23/2/97	Least Squares	C_r	6.110 (1.591)	S_p (mm/hr ^{1/2})	0.001 (839.87)
			e_m	2.077 (0.246)	ϕ (mm/hr)	13.70 (593.17)
9	Mica	Least Squares	C_r	2.064 (0.321)	S_p (mm/hr ^{1/2})	0.968 (0.393)
			e_m	1.242 (0.039)	ϕ (mm/hr)	47.225 (1.982)
10	Quartz	Least Squares	C_r	6.475 (0.562)	S_p (mm/hr ^{1/2})	8.645 (0.122)
			e_m	1.242 (0.027)	ϕ (mm/hr)	5.238 (0.260)

It can be observed in Figure 3.7.1, that there is a well defined relationship between the kinematic wave parameters from the natural site, ellipses 1 to 8, Table 3.7.2. The Mica and Quartz sites, labelled explicitly in Figure 3.7.1, are quite similar in behaviour compared to the natural site. The Quartz site appears to be an outlier, however, differences in the geometry of the cross-sectional areas of flow were expected between the three different sites.

Storm events occurring towards the end of February generally had e_m values noticeably higher than events occurring at the beginning of the wet season. Figure 3.7.1, illustrates this trend with storm events labelled, 5 to 8, (20/2/97, 22/2/97, 22/2/97 pm, and 23/2/97) having a mean e_m value clearly above storm events 1 to 4 (1/1/97, 3/1/97, 4/1/97, and 23/1/97). Detailed consideration of the effect of vegetation growth across the field site is presented in Section 5.0.

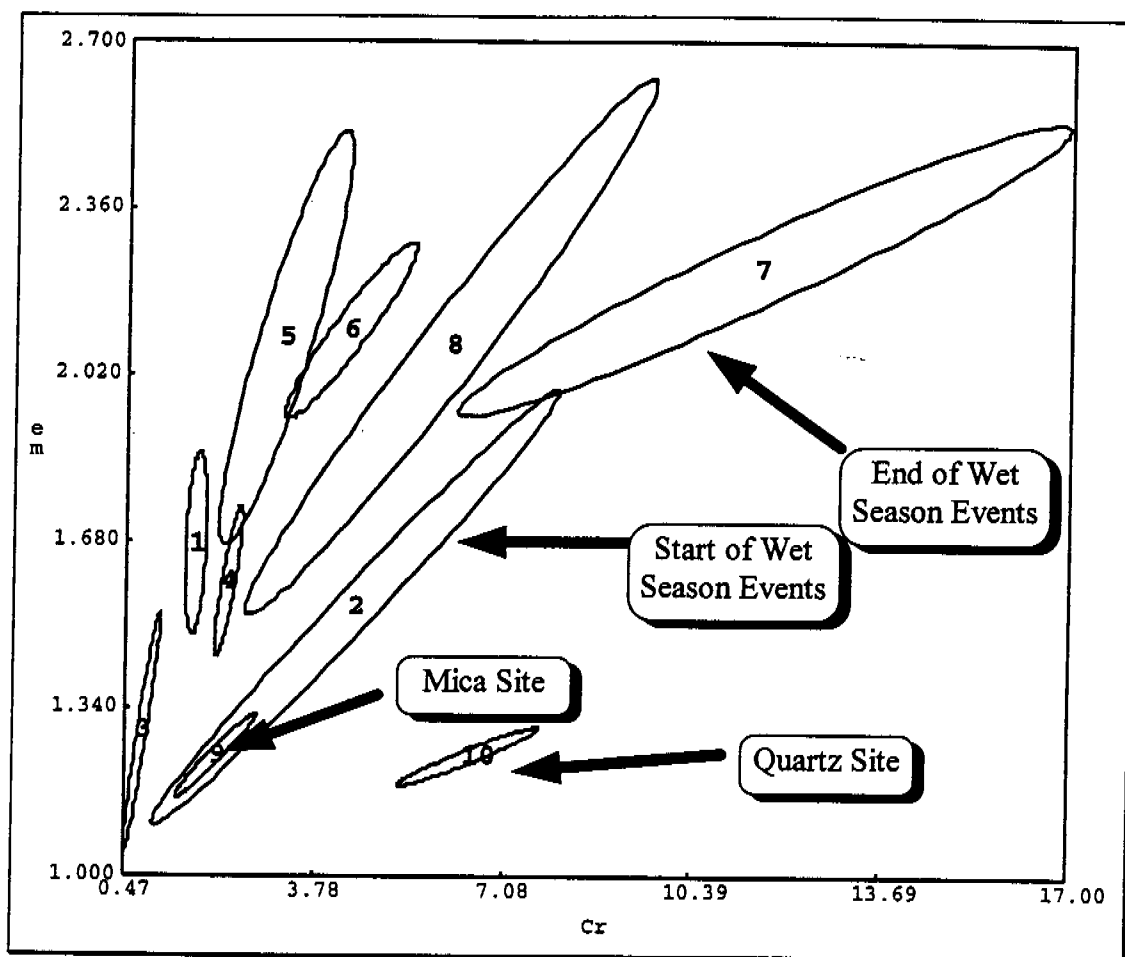


Figure 3.7.1: 95% posterior probability plot of the kinematic wave parameters, C_r and e_m , for the ten storm events listed from the current study and two parameter sets from the Mica and Quartz sites (Table 3.7.1).

The comparison of infiltrative parameters between the current study and the Mica and Quartz sites, utilising the same set of storms listed in Table 3.7.2, and displayed in Figure 3.7.1, was not conducted due to their considerable standard deviations. The DISTFW model, by producing large standard deviations for infiltrative parameters, is essentially stating that the volume of the hydrograph is very difficult to determine.

Storm events occurring on the 4th and 22nd of January and the 22nd and 23rd of February (listed in Table 3.7.2), had considerable standard deviations for infiltrative loss parameters and were examined individually, but omitted from further analysis. Figure 3.7.2, illustrates the predicted hydrograph from the storm event occurring on the 4th January.

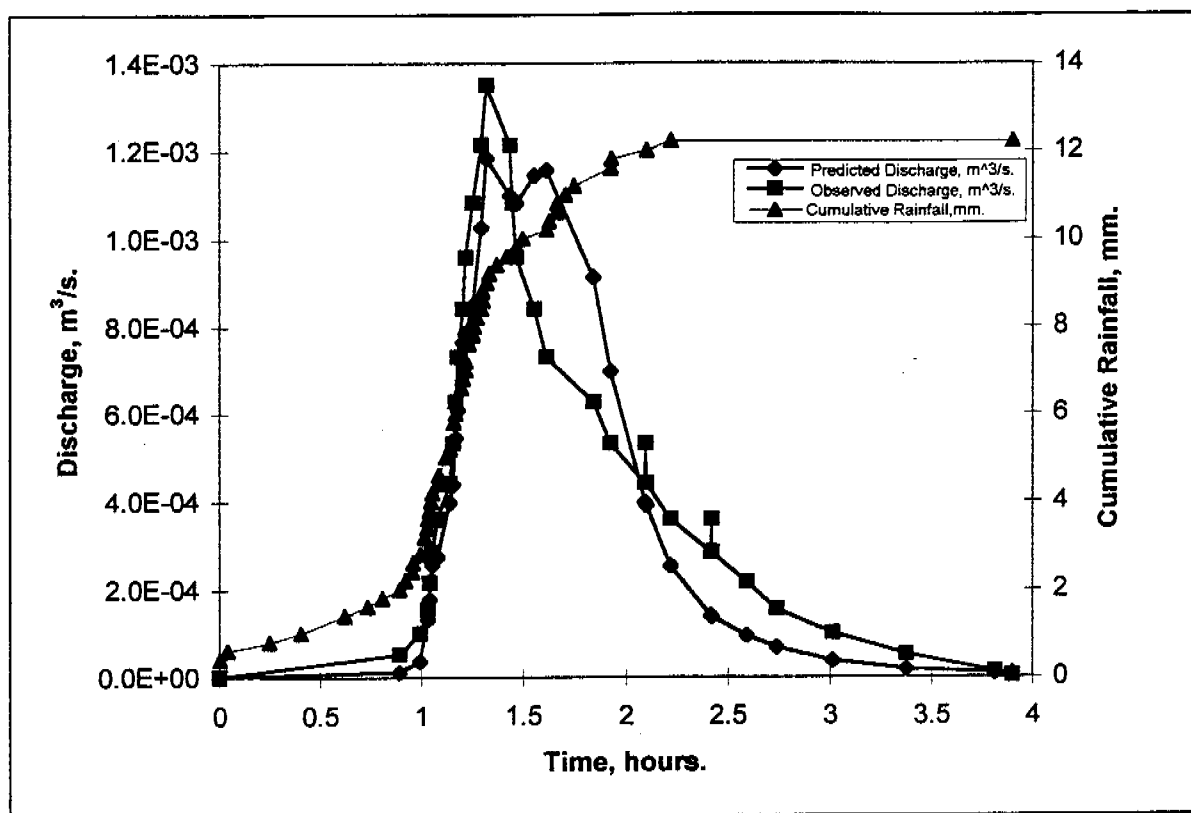


Figure 3.7.2: The predicted hydrograph for the storm event occurring on the 4th January, exhibits considerable deviation from the observed hydrograph in both the peak and the recession limb. Differences in the volume of the predicted hydrograph compared to that which was observed is believed to have been the origin of the large standard deviations of the infiltrative loss parameters listed in Table 3.7.2 for this event.

The storm event occurring on the 4th January had a peak discharge of only 1.30 L/s, which was the smallest of all storm events listed in Table 3.7.2 by at least 50 percent. Figure 3.7.2 highlights a poorly predicted hydrograph recession limb, which is believed to have resulted in the large standard deviations for the infiltrative loss parameters S_{ϕ} and ϕ , of 214.54, and 88.194, respectively (Table 3.7.2).

The peak discharge for the storm event occurring on the 23rd January was approximately 12 L/s, with a rainfall intensity of over 80mm/hour. The initial modelling attempt with DISTFW yielded a close fit between the predicted and observed hydrographs with a redundant initial loss (S_ϕ) parameter. A considerable amount of storm activity had occurred in the two days previous to this event, with two rainfall events occurring on the 21st January, and one ill-defined event occurring on the 22nd January which consisted of intermittent rainfall for a period of over eight hours. The large standard deviation of the S_ϕ parameter of 1867.6 (Table 3.7.2), illustrated the considerable uncertainty in the estimation of this parameter, which was believed to be a function of the unusually saturated soil conditions as a result of storm activity from the previous two days.

Figure 3.7.3 features the first storm event that occurred on the 22nd February. The cessation of the observed hydrograph is at approximately 3.25 hours, yet it has a non-zero discharge. The lack of hydrograph completion was caused by an error in the definition of the number of data lines in the DISTFW runoff file which prematurely cut off the end of the hydrograph. The non-zero end of the hydrograph caused problems as DISTFW attempted to estimate a virtually infinite hydrograph volume, which was translated into the relative large standard deviations for the parameters S_ϕ and ϕ , of 214.54, and 88.194, respectively (Table 3.7.2).

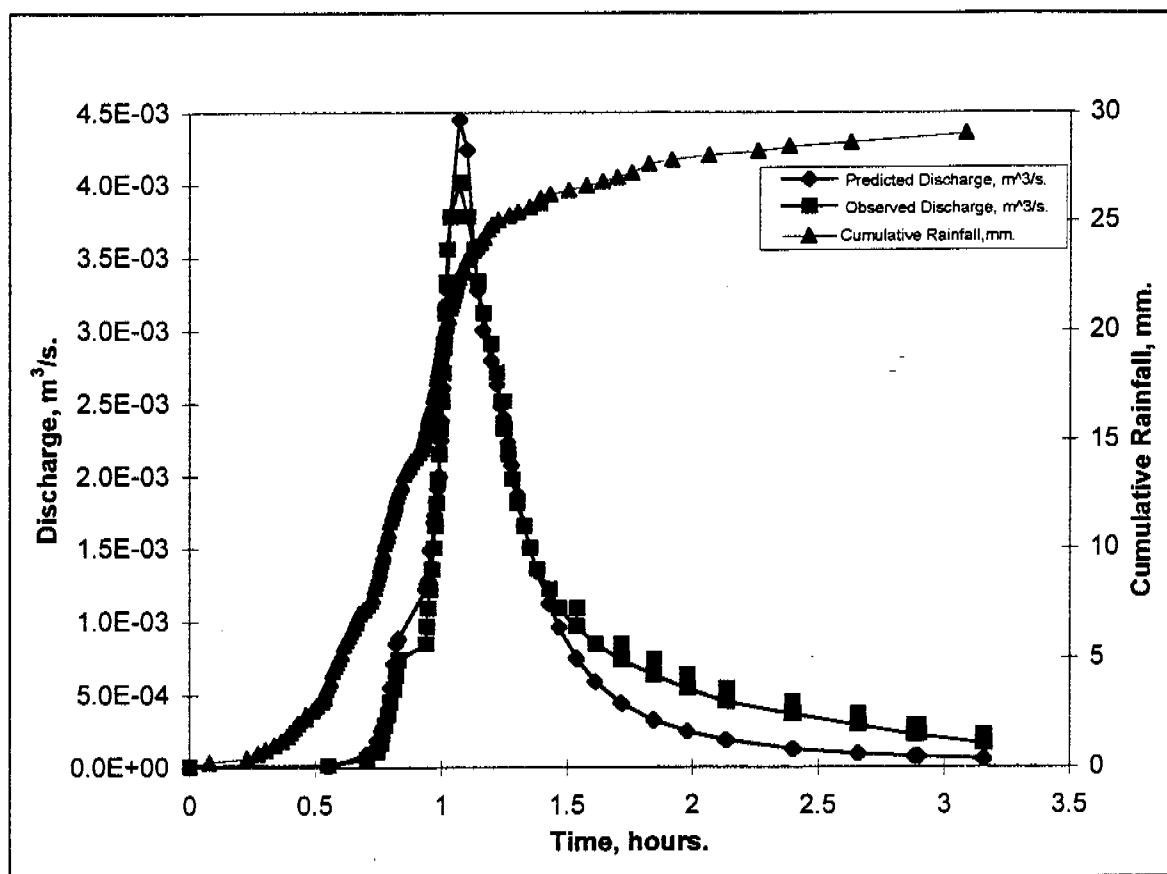


Figure 3.7.3: The end of predicted hydrograph for the storm event occurring on the 22nd February was non-zero, due to an error in the DISTFW runoff input file. This was believed to have resulted in difficulties in the estimation of the volume of the hydrograph which was translated into large standard deviations for the infiltrative loss parameters, S_ϕ and ϕ .

The storm event that occurred on the 23rd February (Figure 3.7.4), exhibited considerable fluctuation in rainfall intensity resulting in considerable corresponding fluctuation in the observed hydrograph. Large differences were noted between the predicted and observed hydrographs which was believed to be the origin of the large standard deviations for the infiltrative loss parameters, S_ϕ and ϕ , of 839.87, and 593.17, respectively (Table 3.7.2).

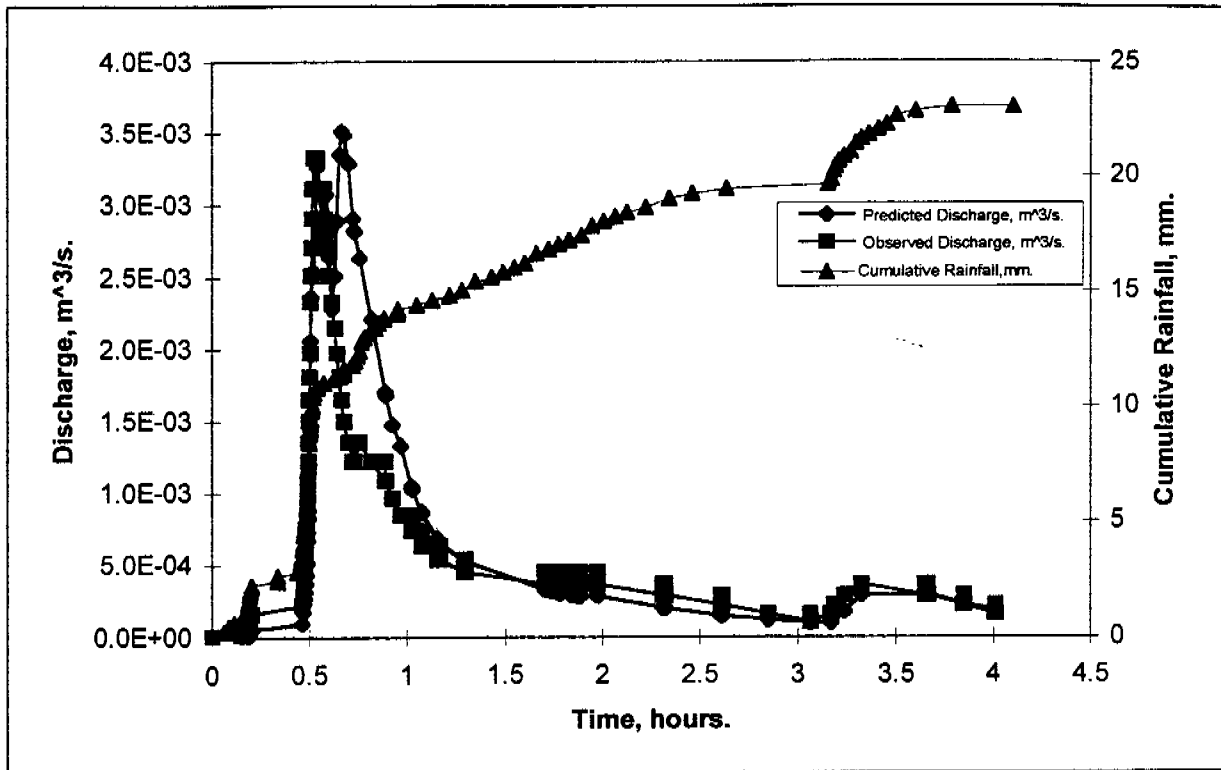


Figure 3.7.4: The predicted hydrograph for the storm event occurring on the 23rd February, exhibits considerable deviation from the observed hydrograph in both the peak and in the recession limb. Differences in the volume of the predicted hydrograph compared to that which was observed is believed to be the origin of the large deviations of the infiltrative loss parameters, S_ϕ and ϕ .

The 95% posterior probability plot of the infiltrative loss parameters, S_ϕ and ϕ , for the current study (neglecting storm events occurring on the 4th, and 23rd January, and 22nd and 23rd February), and the Mica and Quartz sites is presented as Figure 3.7.5.

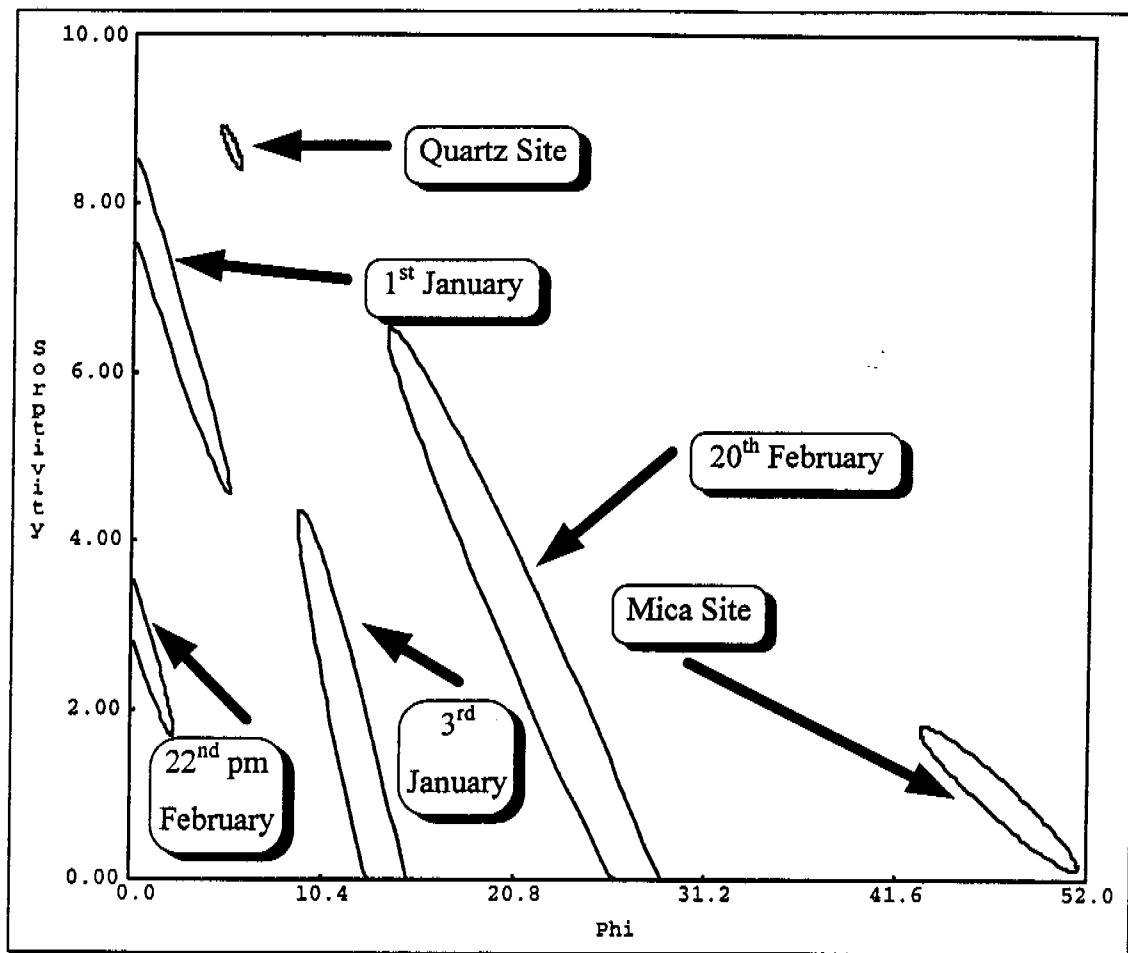


Figure 3.7.5: 95% posterior probability plot of the infiltrative parameters, S_{ϕ} and ϕ , for four storm events from the natural site, 1st and 3rd January, 20th and 22nd pm February, and the Quartz and Mica sites from Tin Camp Creek.

It can be observed in Figure 3.7.5, that the Mica site appears to not conform to the general trend exhibited by the remainder of the storm events from the natural site, and the Quartz site.

In conclusion, the Quartz site was not considered to be significantly different from the C_r and e_m parameter values, (Figure 3.7.1), from the current study and the Mica site. The Mica site however, was considered to be significantly different from the S_{ϕ} and ϕ parameter values, (Figure 3.7.5), from the current study and the Quartz site.

4.0 Sediment Transport Model Parameter Fitting

4.1 Introduction

Gerrard (1991) noted that materials on hillslopes can be moved by a number of mechanisms including; rainsplash, surface wash, solution and mass movement. The processes of solution and mass movement are not of relevance to the current study, however rainsplash and surface wash erosion were observed on the field plot. Suspended and bedload sediment data collected from observed storm events enabled the parameterisation of a number of models that can be used to predict rates of erosion.

The potential effect of fluvial erosion of the above-ground landform on the surrounding environment of Magela Creek, was reported in Section 1.0, and emphasises the importance of erosion rate prediction.

Willgoose and Loch (1996) noted that considerable research had occurred in the Tin Camp Creek area and that the processing of this data would be cost effective. Moliere *et al* (1996) focused upon the two field sites from Tin Camp Creek research, termed the Mica and Quartz sites. The Tin Camp Creek site was chosen in a desktop study by Uren (1992; cited in Moliere *et al*, 1996), as having chemical and physical soil properties that most likely reflected the rehabilitated structure at ERARM after long term weathering.

The ability to quantifiably reduce the erosion rate over time, from the parameterisation of erosion models from data collected from these three studies, will enable more accurate estimation by SIBERIA of the structural state of the rehabilitated landform in the long term.

4.2 Sediment Transportation Models

Willgoose and Riley (1993) described the overland flow erosion model (Equation 4.2.1), as one which is in common use by soil scientists and geomorphologists.

$$Q_s = \beta_1 W^{(1-m_1)} Q^{m_1} S^{n_1} \quad (4.2.1)$$

where

Q_s = Sediment discharge, (g/s),

Q = Discharge, (L/s),

S = Local slope, (m/m), and

W = Width of hillslope, (m).

Willgoose and Riley continued that the parameters, β_1 , m_1 and n_1 are fixed by flow geometry and erosion physics.

Equation (4.2.1) is one of the erosion models that is utilised in this study and has been used in previous work on the Northern Waste Rock Dump (Willgoose and Riley, 1993; and Saynor *et al*, 1995), and in the Tin Camp Creek area (Moliere *et al*, 1996).

The width of hillslope referred to in Equation (4.2.1), ' W ', (m), for the current study, is the width of the field plot which was 20 metres. The sediment discharge, ' Q_s ', (g/s), is a function of discharge, ' Q ', (L), and the suspended sediment concentration ' C ', (g/L), (Equation 4.2.2).

$$Q_s = Q C \quad (4.2.2)$$

where

C = Suspended sediment concentration, (g/L).

The overland flow erosion model is parameterised utilising only the suspended sediment concentration data.

The rearrangement of the overland flow erosion model (Equation 4.2.1), gives the total sediment loss model for an entire rainfall event which has also been utilised in previous studies on the Northern Waste Rock Dump and in the Tin Camp Creek area.

The total sediment loss, 'T', (g), over an entire rainfall event, Equation (4.2.3), is based on the work of Evans et al, (1995).

$$T = \beta_1 W^{(1-m_1)} S^{n_1} \int Q^{m_1} dt \quad (4.2.3)$$

where

T = Total sediment loss, (g), and

$\int Q^{m_1} dt$ = Function of cumulative runoff over event duration, (L^{m_1})

The total sediment loss 'T', (g), (Equation 4.2.3), comprises both suspended and bedload sediment. The differences between the data sets utilised in the overland flow erosion model and the total sediment loss model, enables a comparison between the magnitudes of the parameters β_1 and m_1 .

4.3 Data

Complete sets of bedload and suspended sediment data were collected from eight storm events over the 96/97 wet season (Appendix 4.A). Table 4.3.1 lists the date of the occurrence of these storm events and their respective rainfall and runoff characteristics.

Table 4.3.1: Storm events and respective rainfall and runoff characteristics for eight monitored storm events from the natural site.

Storm Event.	Total Rainfall, (mm).	Peak Discharge, (L/s).
1197	70.2	11.00
12197	5.0 ^a	0.25
12197pm	16.5 ^a	0.55
17197	29.6	0.35
211971 st	11.8	0.40
211972 nd	22.4	1.70
23197	43.8	12.00
28197	28.2	2.50

^a Electronic raingauge failure.

The suspended sediment samples were collected in 600mL Buzl flasks and processed as described in Appendix 4.A.

Suspended sediment concentrations were plotted against time for all storm events listed in Table 4.3.1, and are featured in Appendix 4.A. Figure 4.3.1 illustrates the suspended sediment concentration, (g/L), plot against time, (hours) for the storm event occurring on the 1st January.

It can be observed from Figure 4.3.1, that the sediograph plotted has a sharp initial incline, two peaks, which are similar to that observed with the hydrograph, and a gradual but considerably fluctuating decline.

All the suspended sediment samples from the eight storm events listed in Table 4.3.1 were utilised to parameterise the overland flow erosion model (Equation 4.2.1).

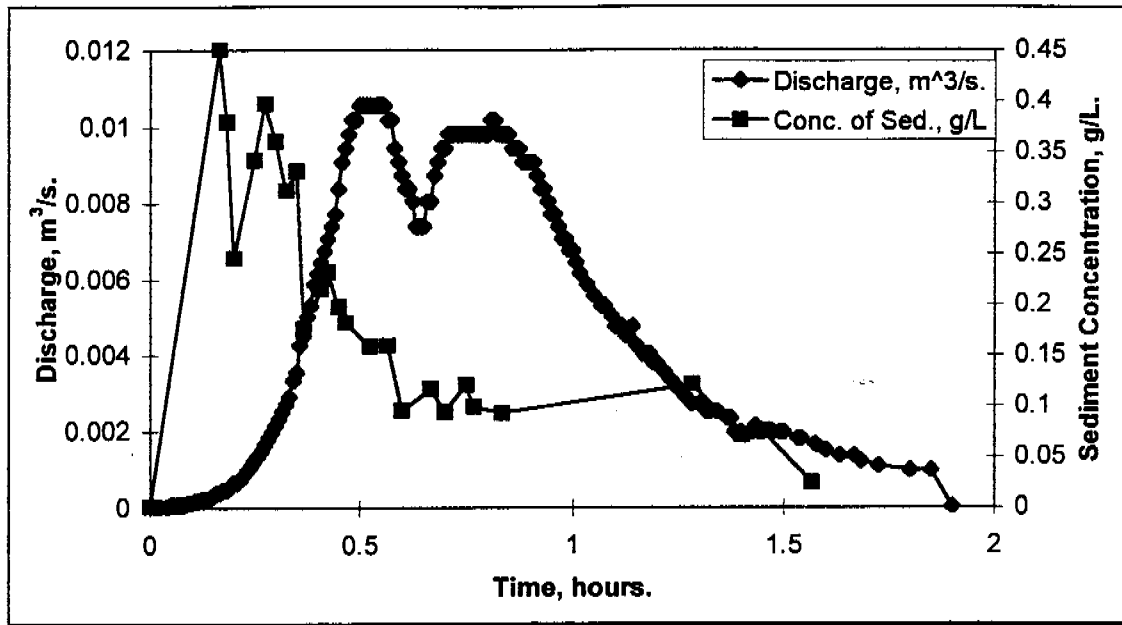


Figure 4.3.1: Plot of the suspended sediment concentration, (g/L), and discharge, (m^3/s), versus time, (hours), for a storm event occurring on the 1st January 1997.

The overland flow erosion model, Equation (4.2.1), was simplified as Equation (4.3.1).

$$Q_s = \beta_1 w^{(1-m_1)} Q^{m_1} S^{n_1} \quad (4.2.1)$$

$$Q_s = K Q^{m_1} \quad (4.3.1)$$

where

$$K = \beta_1 w^{(1-m_1)} S^{n_1}$$

A logarithmic transformation of Equation (4.3.1), was performed (Equation 4.3.2).

$$\log_{10}(Q_s) = \log_{10}(K) + m_1 \log_{10}(Q) \quad (4.3.2)$$

Equation (4.3.2) was fitted with sediment discharge data from all monitored storm events, and is illustrated in Figure 4.3.2.

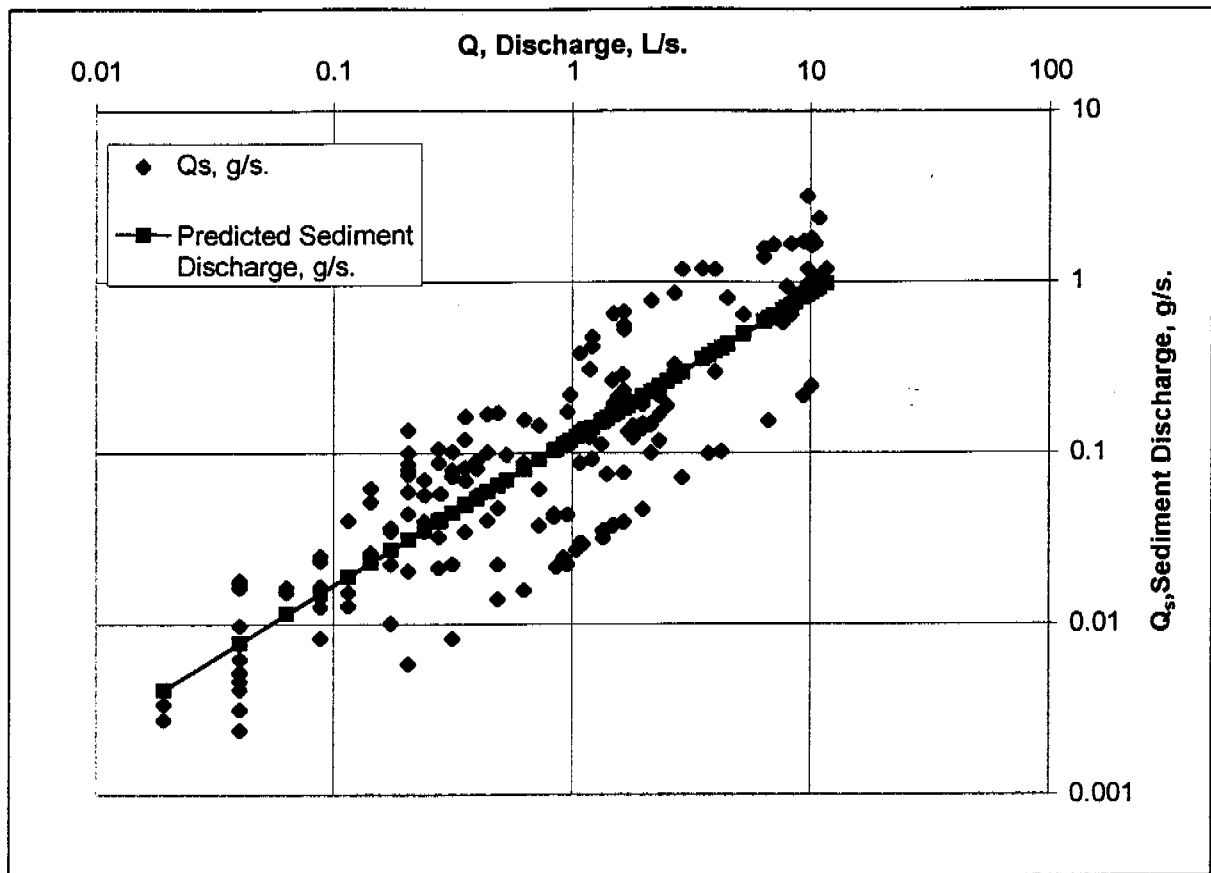


Figure 4.3.2: A log-log regression analysis of 'Q', discharge, (L/s), versus 'Q_s', sediment discharge, (g/s), Equation (4.3.2), was performed utilising all the suspended sediment samples from eight storm events (Table 4.3.1).

The slope of the field plot, determined from a topographic survey reported in Section 3.3, was an average of 0.027 (m/m). The exponent on the slope term of Equation (4.2.1), 'n₁', was assumed to equal 0.69, from previous work, Willgoose and Riley (1993) and Evans *et al* (1995).

Evans *et al* (1995) noted that the parameter 'n₁', originated from Equation (4.3.3).

$$Q_s \propto \frac{1}{(d_{50})^{1.5}} \quad (4.3.3)$$

where

d₅₀ = Median sediment grain diameter, (mm).

Evans *et al* continued that this relationship was derived from the Brown function, Einsteins bed-load function, and Shields formula for bedload. The relationship developed by Evans *et al* (1995), involving the d_{50} values for the cap and batter sites (0.54 and 1.39 mm respectively), yielded a ' n_1 ' value of 0.71, which was similar to that derived by Willgoose and Riley (1993). A random number of particle size samples were collected and processed from the natural site (Appendix 4.B). The d_{50} for the natural site was determined to be approximately 0.8 mm, (Smith, 1997), which is comparable to that reported for the cap and batter sites.

Equation (4.3.4) highlights the parameter values obtained from the fitting of the overland flow erosion model (Figure 4.3.2).

$$Q_s = 0.917 W^{(1-0.854)} Q^{0.854} S^{0.69} \quad (r^2=0.74, df=169, p<0.001) \quad (4.3.4)$$

The parameters β_1 and m_1 , have mean and standard errors of 0.917 +/- 0.03, and 0.854 +/- 0.04, respectively. The raw output from the regression analysis is listed in Appendix 4.C.

The determination of the total quantity of bedload sediment is an integral component of the total sediment loss model, Equation (4.2.3). The bedload sediment samples collected were processed following the procedure listed in Appendix 4.A.

The total sediment loss model (Equation 4.2.3), was simplified (Equation 4.3.5).

$$T = \beta_1 W^{(1-m_1)} S^{n_1} \int Q^{m_1} dt \quad (4.2.3)$$

$$T = K \int Q^{m_1} dt \quad (4.3.5)$$

where

$$K = \beta_1 W^{(1-m_1)} S^{n_1}$$

Equation (4.3.5) was transformed with logarithms into Equation (4.3.6).

$$\log_{10}(T) = \log_{10}(K) + x \log_{10}\left(\int Q^{m_1} dt\right) \quad (4.3.6)$$

where

x = Transformation parameter.

An initial ' m_1 ' value was selected and through a trial and error procedure and regression analysis, the magnitude of the parameter ' x ' was iterated to unity. The values of the parameters β_1 and m_1 , that were associated with the magnitude of the parameter ' x ' being equal to 1, were chosen as the fitted parameter values.

The integration of ' Q^{m_1} ' with respect to time, from the total sediment loss model (Equation 4.2.3), for a entire rainfall event was determined using a backward difference numerical integration approximation (Equation 4.3.7).

$$\int Q^{m_1} dt = \sum_{i=0}^n \left[\left(\frac{Q_i^{m_1} + Q_{i-1}^{m_1}}{2} \right) \times (t_i - t_{i-1}) \right] \quad (4.3.7)$$

where

t_i = Time at the current time step ' i ', (s), and

$Q_i^{m_1}$ = Discharge to the exponent m_1 at the current time step ' i ', $((L/s)^{m_1})$.

The total sediment loss 'T', (g), from the total sediment loss model, comprised both suspended and bedload sediment. The determination of the total suspended sediment loss, (g), for the entire event, ' $\int Q_s dt$ ', involved the numerical integration of the suspended sediment discharge (Equation 4.3.8).

$$\int Q_s dt = \sum_{i=0}^n \left[\left(\frac{Q_{s_i} + Q_{s_{i-1}}}{2} \right) \times (t_i - t_{i-1}) \right] \quad (4.3.8)$$

where

Q_{s_i} = Sediment discharge at the current time step 'i', (g/s).

Table 4.3.2 lists the total runoff, (L), and total suspended and bedload sediment loss, (g), for all events listed in Table 4.3.1.

Table 4.3.2: Eight observed storm events from the natural site and their respective total runoff, (L), total suspended and bedload sediment, (g).

Storm Event.	Total Runoff, (L).	Total Suspended Sediment Loss, (g).	Total Bedload Sediment Loss, (g).	Total Sediment Loss, (g).
1197	29445.7	3699.6	3367.8	7067.3
12197	47.1	12.9	771.1	784.0
12197pm	984.3	61.1	65.3	126.4
17197	434.4	224.2	302.7	526.9
211971 st	258.3	81.1	430.4	511.4
211972 nd	2867.2	229.2	172.3	401.5
23197	16843.8	1621.0	1145.5	2766.5
28197	5178.1	352.9	368.5	721.5

It can be observed from Table 4.3.2, that the total runoff, (L), from the first storm event occurring on the 12th January of 47.1L, is three orders of magnitude smaller than the total runoff from the storm event occurring on the 1st January. The storm events occurring on the 17th January and the first event on the 21st January, have comparable small total runoff magnitudes to the first event on the 12th January, 434.4 and 258.3 L, respectively. These three storm events were not fitted to the total sediment loss equation because of their small quantity of total runoff compared to the other storm events listed in Table 4.3.2.

Equation (4.3.6) was fitted by regression analysis and the results are illustrated in Figure 4.3.3.

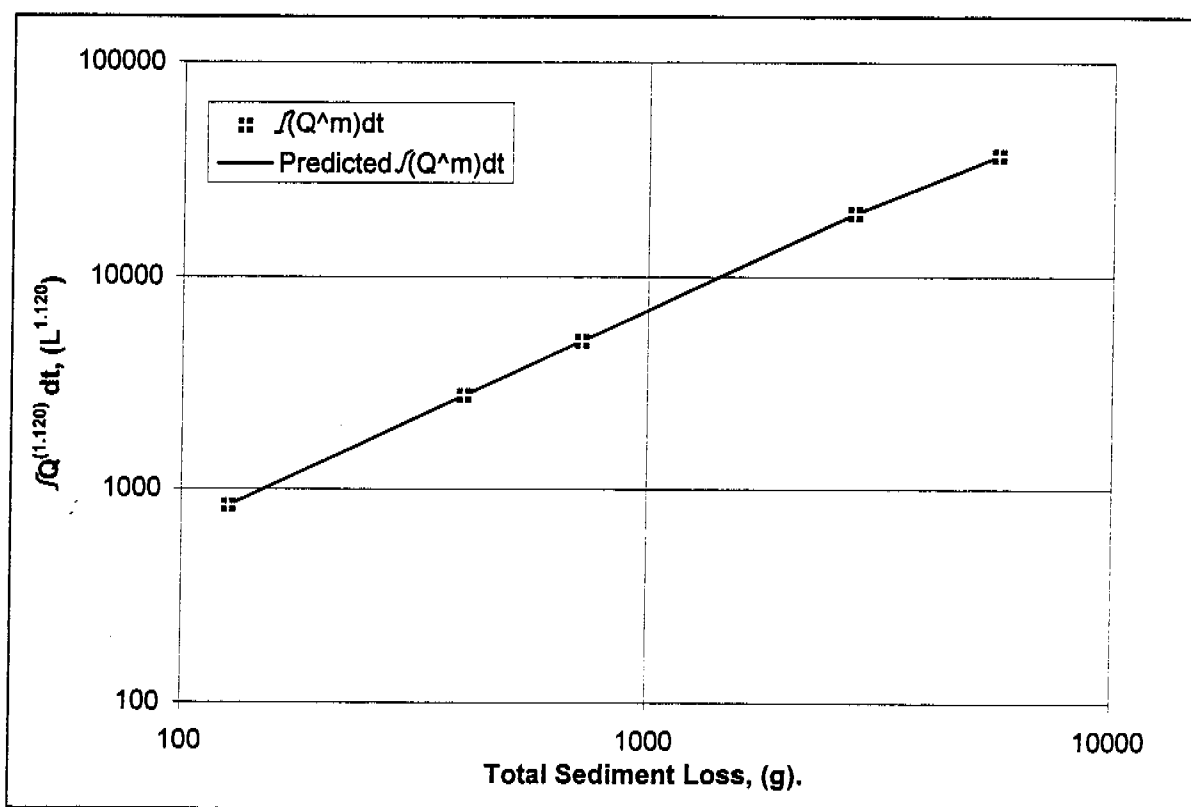


Figure 4.3.3: A log-log regression analysis of the integration of $Q^{m1} dt, (L^{m1})$, against the total sediment loss, 'T', (g), was performed utilising the five storm events listed in Table 4.3.2.

Equation (4.3.9), highlights the parameter values obtained from the fitting of the total sediment loss model.

$$T = 1.171 W^{(1 - 1.120)} S^{0.69} \int Q^{1.120} dt \quad (r^2=0.99, df=4, p<0.001) \quad (4.3.9)$$

It can be observed from Equation (4.3.9), that the parameters β_1 and m_1 , have mean and standard errors of 1.171 +/- 0.05, and 1.120, respectively. The exponent on the slope term, ' n_1 ' was assumed to have a magnitude of 0.69, which was similarly adopted for the fitting of the overland flow erosion model. The output from the regression analysis is listed in Appendix 4.C.

4.4 Parameter Comparison

The two sets of erosion parameters, β_1 and m_1 , derived from the overland flow erosion model (Equation 4.3.4), and the total sediment loss model (Equation 4.3.9), that were fitted from experimental data from the natural site, are of comparable magnitude (Table 4.4.1).

Table 4.4.1: Comparison between the fitted erosion parameters β_1 and m_1 , from the overland flow erosion and the total sediment loss model.

Parameter	Overland Flow Erosion Model	Total Sediment Loss Model
β_1	0.917	1.171
m_1	0.854	1.120

A comparison between the parameter values obtained from the overland flow erosion model, from the Tin Camp Creek study (Moliere *et al*, 1996), and the current study was necessitated because of insufficient data from the Tin Camp Creek study. Willgoose and Riley (1993) determined erosion parameters from the overland flow erosion model in their study at ERARM, for landform evolution modelling with the program SIBERIA. Table 4.4.2 lists the magnitudes of the β_1 and m_1 parameters obtained from the two studies.

Table 4.4.2: Comparison between the fitted erosion parameters β_1 and m_1 , from the overland flow erosion model for the Tin Camp Creek, utilising the complete data set, and data with discharge values less than 10L/s, and the natural site study.

Parameter	Tin Camp Creek ^a		Natural Site
	Complete Data Set	Data set, Q <10 L/s	
β_1	0.626	0.410	0.917
m_1	1.480	1.371	0.854

^a Moliere *et al* (1996).

Moliere *et al* (1996) reported that an erosion threshold at approximately 10L/s, appeared to exist in the suspended sediment data set from the Tin Camp Creek study.

It can be observed from Table 4.4.2 that there is considerable difference between the magnitude of the m_1 parameter (the exponent on discharge in Equation 4.2.1), between the Tin Camp Creek Site and the natural site.

A comparison between the parameter values obtained from the total sediment loss model from the current study and previous work from the Northern Waste Rock Dump (Saynor *et al*, 1995), and in the Tin Camp Creek (Moliere *et al*, 1996) is summarised in Table 4.4.3.

Table 4.4.3: Comparison between the fitted erosion parameters β_1 and m_1 , from the total sediment loss model for studies conducted on the Northern Waste Rock Dump, in the Tin Camp Creek area, and the current study.

Parameter	Northern Waste Rock Dump ^a			Tin Camp Creek	Natural Site
	Cap Site	Batter Site	Soil Site	Mica and Quartz Site ^b	
β_1	12.76	3.08	23.29	2.86	1.171
m_1	1.67	1.67	1.67	1.33	1.120

^a Saynor *et al* (1995)

^b Moliere *et al* (1996), $n_1 = 1.19$

The parameters reported in Table 4.4.3 for Northern Waste Rock Dump (Saynor *et al*, 1995), are from data sets collected in 1993 (cap and batter sites) and in 1995 (soil site). In all cases the ' n_1 ' exponent on the slope term of the total sediment loss model was fixed at a constant 0.71 (Equations 4.4.1 to 4.4.3).

$$T(\text{cap}) = 12.76 W^{(-0.67)} S^{0.71} \int Q^{1.67} dt \quad (r^2 = 0.90, df=30) \quad (4.4.1)$$

$$T(\text{batter}) = 3.08 W^{(-0.67)} S^{0.71} \int Q^{1.67} dt \quad (r^2 = 0.90, df=30) \quad (4.4.2)$$

$$T(\text{soil}) = 23.29 W^{(-0.67)} S^{0.71} \int Q^{1.67} dt \quad (r^2 = 0.90, df=30) \quad (4.4.3)$$

Due to data shortages in the Tin Camp Creek study, a modification of the total sediment loss model (Equation 4.4.4), was fitted to the experimental data (Moliere *et al*, 1996).

$$\frac{T}{S^{n_1}} = \beta_1 \int Q^{m_1} dt \quad (4.4.4)$$

The results listed in Table 4.4.3, for the Mica and Quartz sites are derived from Equation (4.4.5), with the 'n₁' exponent, fixed at a constant 1.19.

$$\frac{T}{S^{1.19 \pm 0.03}} = 2.857^{+0.91}_{-0.69} \int Q^{1.33 \pm 0.503} dt \quad (4.4.5)$$

The constant 'n₁' term was derived from regression analysis of suspended sediment concentration reported in Moliere *et al* (1996).

The two erosion models in this study, utilised different data sets; suspended sediment for the overland flow erosion model; and bedload and suspended sediment for the total sediment loss model. The two models independently achieved erosion parameter values for β_1 and m_1 , that were similar in magnitude. A comparison between the results from the Tin Camp Creek and the current study (Table 4.4.2), highlighted that a general trend existed, that is the rate of sediment transport is predicted to be higher in the Tin Camp Creek area than on the natural site. This comparison is based on the values for the parameter m_1 , which is the exponent of Equation (4.2.1). This exponent on discharge, tends to govern the overland flow erosion model.

Table 4.4.3 highlights a more conclusive trend with respect to the erosion parameter values derived from the total sediment loss model for the NWRD, Tin Camp Creek and the current study. As previously reported (Section 1.0), the NWRD is considered to represent the weathered state of waste rock material after 10 years of exposure, the Tin Camp Creek site is assumed to represent waste rock material after at least 100 years of exposure. Finally the current study is assumed to represent waste rock material after at least 100,000 years of exposure. The natural site had the lowest magnitude of β_1 and m_1 , of 1.170 and 1.120, respectively, which implies that the sediment transportation rate is lowest for the current study. The β_1 and m_1 values from the Tin Camp Creek study were in between the results obtained from the current study and those obtained from studies on the NWRD, suggesting that the assumption that the Tin Camp Creek site represents medianly weathered waste rock material is not inconsistent with the data.

The exponent m_1 , from the cap, batter and soil sites from the NWRD, were of similar magnitudes but noticeably higher than those values reported for the other studies. The β_1 parameter values from the NWRD were consistently higher than those values reported from other studies, except for the batter site where the value of 3.08 obtained is only marginally higher than the value of 2.86, from the Tin Camp Creek study.

5.0 Evaluation of the Effect of Vegetation Growth Over Wet Season

The vegetation present on the field site was non-uniform in both ground cover and leaf surface area. Numerous species of trees and low shrubs were present on the site as well as a large quantity of developing spear grass. The evaluation of vegetation growth throughout the 1996/1997 wet season was not quantified, however Figures 5.1, 5.2, and 5.3, are photographs from the site on the 5th, and 30th December, and the 29th January, and serve to illustrate the development of vegetation, especially spear grass.

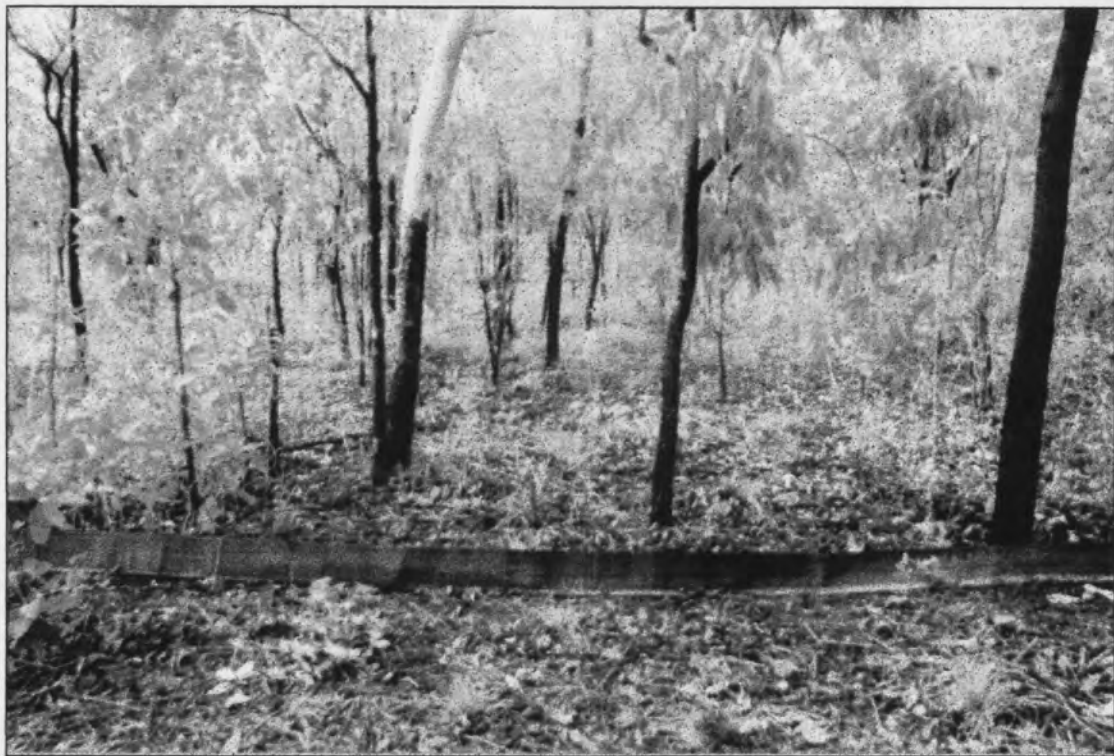


Figure 5.1: Natural field plot, 5th December 1996.



Figure 5.2: Natural field plot, 30th December 1996.

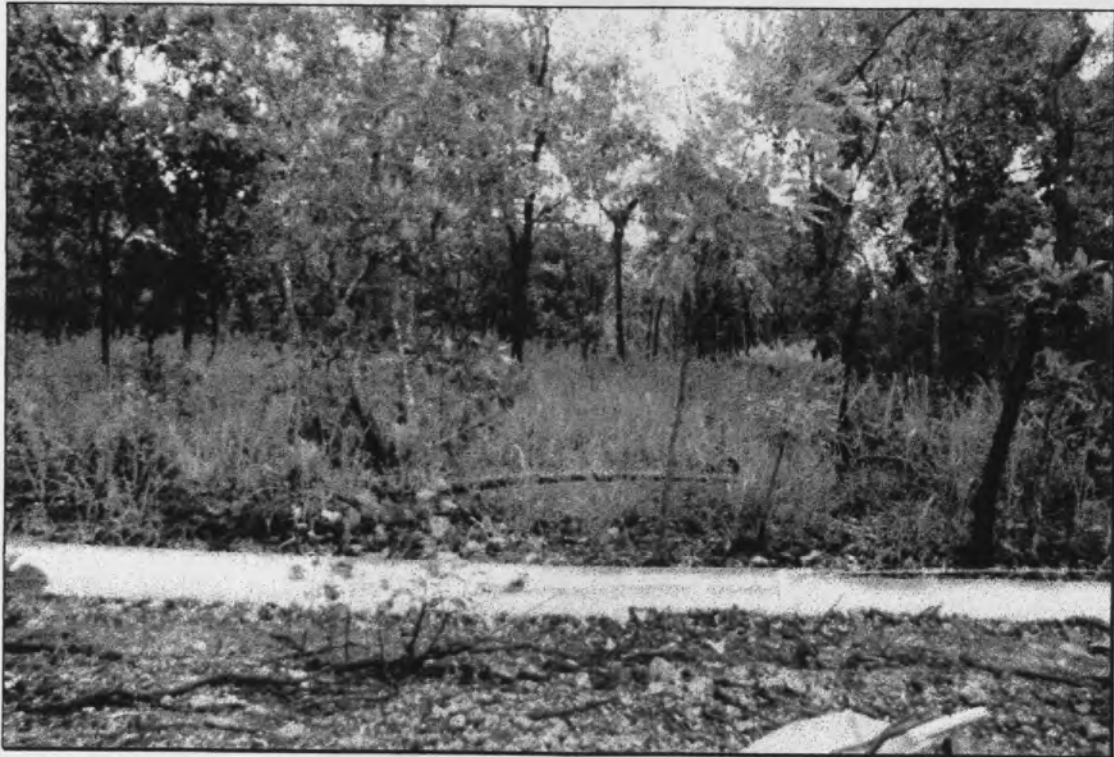


Figure 5.3: Natural field plot, 29th January 1997.

The main trunk and rooting system of the spear grass occupies only a relatively small area at the ground level in comparison to other larger shrub and tree plant species. As the spear grass can grow to considerable height, some metres during the wet season, the change in the leaf interception area of this species was hypothesised to have an effect on the quantity of rainfall hitting the soil.

The large amount of decomposing leaf litter (Figure 5.4), built up over the dry season, provides a shield for the soil underneath.



Figure 5.4: Decomposing leaf litter from the previous wet season slowly breaks down during the course of the year and provides considerable coverage of the soil surface.

The kinetic energy of rainfall impacting the soil will be reduced by this leaf litter. Exposed sections, devoid of leaf litter near the PVC pipe, due to construction were affected by splash erosion. The impact of exposed soil on the transport of sediment during the experiment was considered negligible as the 300 millimetre diameter PVC pipe was completely installed by late November, and monitoring did not commence until late December. The area of soil subjected to increased splash erosion was only a very small fraction of the 600 square metre site.

A considerable degree of storm activity occurred towards the end of February which exhibited different behaviour with respect to kinematic wave parameter values to those storm events that occurred towards the start of the wet season. Table 5.1 is a summary of the kinematic wave and infiltrative loss parameter values from Table 3.7.2, to highlight the differences between events occurring at the start of the wet season and those events occurring at the end of wet season.

Table 5.1: Summary of kinematic wave parameter values for eight storm events from the current study that occurred at the start of January and the end of February.

Storm Event	Peak Runoff, L/s.	Kinematic Wave Parameters	Mean (Standard Deviation)	Infiltration Parameters	Mean (Standard Deviation)
1/1/97	11.00	C_r	1.684(0.081)	S_p (mm/hr ^{1/2})	7.948(1.525)
		e_m	1.675(0.083)	ϕ (mm/hr)	0.280(2.247)
3/1/97	6.00	C_r	4.480(1.574)	S_p (mm/hr ^{1/2})	0.245 (1.839)
		e_m	1.544(0.199)	ϕ (mm/hr)	13.64(2.071)
4/1/97	1.30	C_r	0.775 (0.137)	S_p (mm/hr ^{1/2})	0.001 (214.54)
		e_m	1.291 (0.108)	ϕ (mm/hr)	3.783 (88.194)
23/1/97	12.00	C_r	2.258 (0.106)	S_p (mm/hr ^{1/2})	0.001 (1867.6)
		e_m	1.596 (0.068)	ϕ (mm/hr)	51.58 (246.60)
20/2/97	4.00	C_r	3.211(0.505)	S_p (mm/hr ^{1/2})	2.2578(1.913)
		e_m	2.093(0.189)	ϕ (mm/hr)	22.743(4.03)
22/2/97	4.00	C_r	4.336 (0.506)	S_p (mm/hr ^{1/2})	0.001 (124.55)
		e_m	2.108 (0.080)	ϕ (mm/hr)	15.541 (3.47)
22/2/97pm	3.70	C_r	11.58 (2.402)	S_p (mm/hr ^{1/2})	3.236 (0.689)
		e_m	2.236 (0.135)	ϕ (mm/hr)	0.001 (1.049)
23/2/97	3.30	C_r	6.110 (1.591)	S_p (mm/hr ^{1/2})	3.235 (0.689)
		e_m	2.077 (0.246)	ϕ (mm/hr)	0.001 (1.049)

Storm events occurring towards the end of February generally had e_m values noticeably higher than events occurring at the beginning of the wet season. Figure 5.1 illustrates this trend with storm events; 20th, 22nd, 22nd pm, and 23rd of February having a mean e_m value well above storm events; 1st, 3rd, 4th, and the 23rd of January.

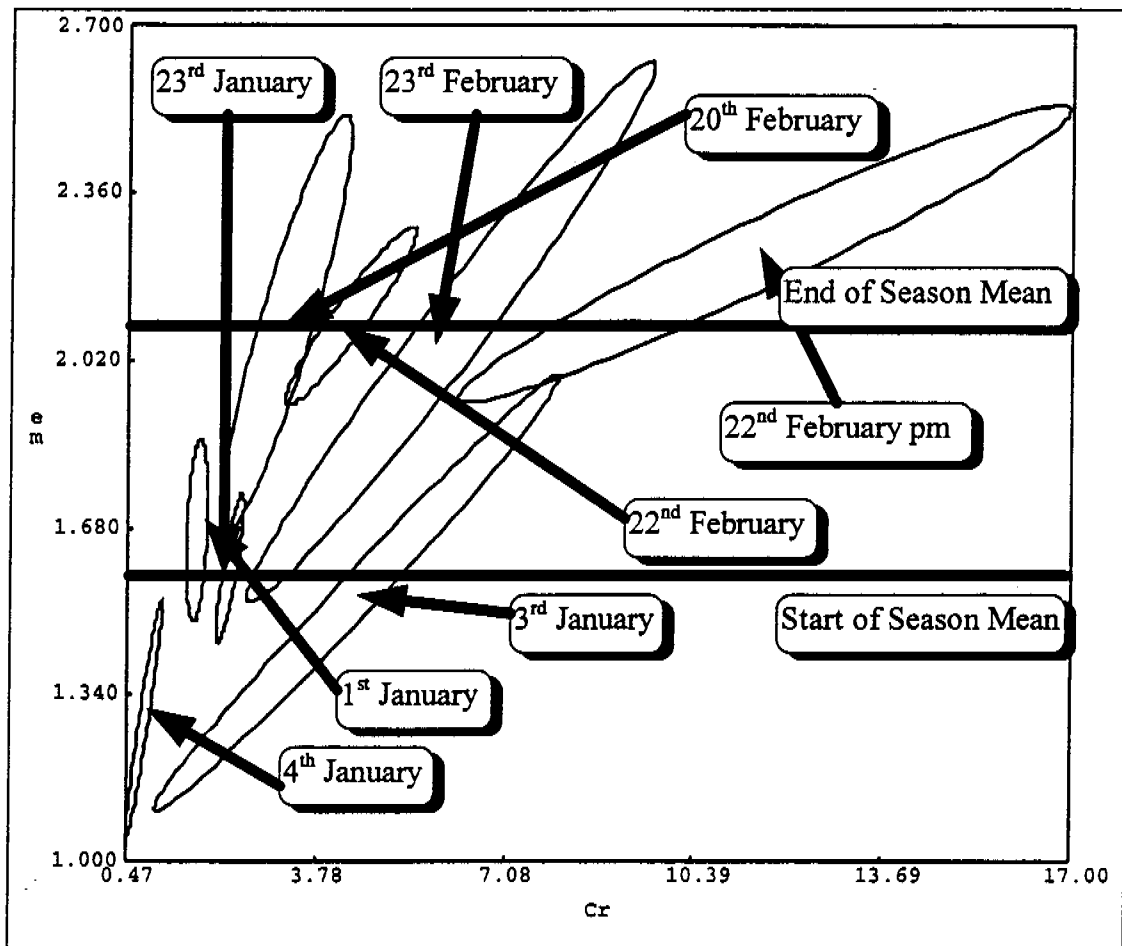


Figure 5.1: 95% posterior probability plot of the kinematic wave parameters C_r and e_m , for the eight storm events listed in Table 5.1. The eight storm events were divided into two groups, those occurring at the start and at the end of the wet season, each with their on defined mean.

The mean e_m value at the start of the wet season, highlighted by the lower large line in Figure 5.1, for the storm events occurring on the 1st, 3rd, 4th, and the 23rd of January, was determined to be 1.53. The mean e_m value at the end of the wet season, highlighted by the upper large line in Figure 5.1, for the storm events occurring on the 20th, 22nd, 22nd pm, and 23rd of February, was determined to be 2.13.

Figure 3.2.5 illustrates four different hillslope geometries that are governed by the exponent of the power law function, e_m . Comparison of the mean e_m values of 1.53 and 2.13 with the e_m values of the different hillslope geometries from Figure 3.2.5, tends to indicate that the hillslope surface became less hydraulically rough throughout the wet season.

The peak recorded discharges for eight storm events (Table 5.1), were fairly uniform, hence the possible influence of differences between discharge peaks was ignored.

As the wet season progressed, more of the hillslope was behaving as constant depth sheet flow (Geometry A, Figure 3.2.5), which may be a function of the saturated hydraulic conductivity of the soil. It is hypothesised that no major changes in the hillslope cross sectional area occurred during the course of the wet season as a result of erosion.

A plot of the values of sorptivity over the wet season from Table 5.1, does not highlight any conclusive trends.

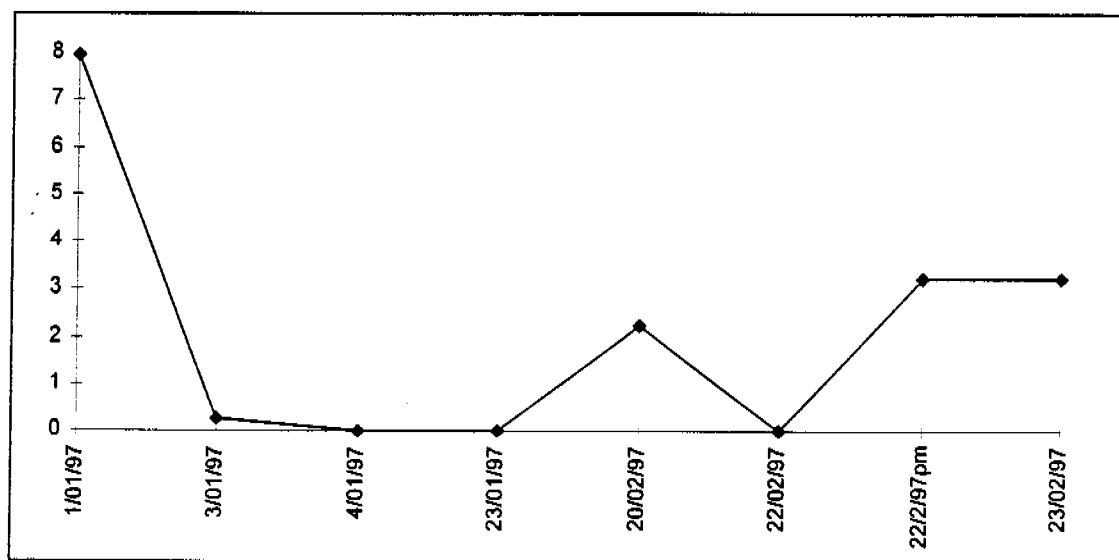


Figure 5.2: Plot of the S_s values fitted from DISTFW-NLFIT, for eight storm events that occurred over the wet season that are listed in Table 5.1.

A similar plot of the values of the continuing loss parameter, ϕ , for the eight storm events listed in Table 5.1, does reflect a possible trend.

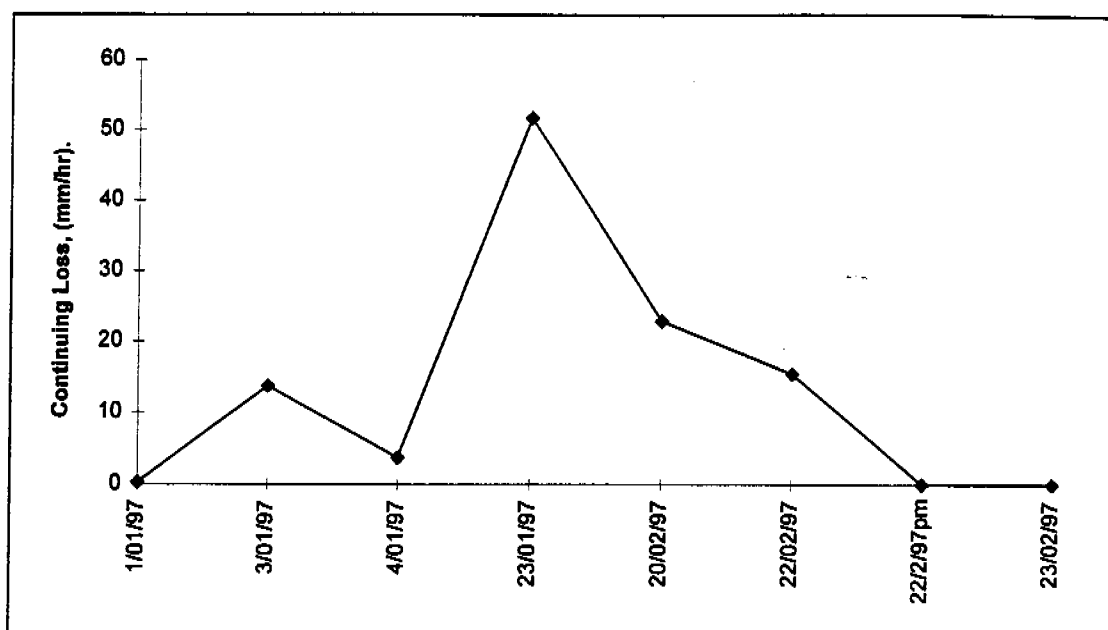


Figure 5.3: Plot of the ϕ values fitted from DISTFW-NLFIT, for eight storm events that occurred over the wet season that are listed in Table 5.1.

The storm event that occurred on the 4th January had a small peak discharge (1.3 L/s), when compared to 6 and 12 L/s for storm events occurring on the 3rd and 23rd January, respectively. By the omission of the 4th January storm event, a trend of increasing then decreasing continuing loss rates throughout the wet season is evident.

It is hypothesised that the effect of leaf interception area would not be as great as the effect of the withdrawal of water from the upper portions of the soil matrix by the extremely fast growing spear grass and other vegetation. Due to the distinct short wet season, it is believed that the vegetation would have a tendency to increase water uptake during this period due to water availability. Increased and then decreased water removal couple with the previously hypothesised decrease in hydraulic conductivity of the soil matrix over the wet season due to saturation goes a part of the way to attempt to explain the behaviour of the plot of continuing loss against time (Figure 5.3)

6.0 Further Work

Further natural storm event monitoring on the field for the purpose of sediment transportation parameter estimation is not considered by the author as necessary because of the significant results obtained and reported.

For reasons stated previously, one set of DISTFW parameters could not be fitted to a number of combinations of four storm events, similar to that conducted in the Tin Camp Creek study. Although this limitation was overcome, multiple storm event calibration should be theoretically possible and may warrant further investigation for confirmation of results.

A brief evaluation of the possible effect of vegetation growth over the wet season on the field plot was conducted, however, further work needs to be conducted to quantify the hydrologic effect of this growth. Two small natural field plots could be constructed and monitored during the wet season, with one acting as the control, by allowing vegetation to grow (especially spear grass), and one where the spear grass was carefully removed.

7.0 References

Chaudhry M.H., (1993), *Open-Channel Flow*, Prentice-Hall Incorporated, Englewood Cliffs, New Jersey.

Evans K.G., Willgoose G.R., and Riley S.J., (1995), *Preliminary Report of Sediment Transport Model Parameters Using Large Scale Rainfall Simulator Data from Ranger Mine*, Environmental Research Institute for the Supervising Scientist, Canberra, Internal Report 182, Unpublished Paper.

Evans K.G., Saynor M.J., and Riley S.J., (1996), *Ranger Uranium Mine Waste Rock Dump Rainfall Simulation Experiments 1993: Large Scale Plots-Data*, Environmental Research Institute for the Supervising Scientist, Canberra, Internal Report 209, Unpublished Paper.

Evans K.G. and Riley S.J., (1993), *Regression Equations for the Determination of Discharge Through RBC Flumes*. Supervising Scientist for the Alligator Rivers Region, Canberra, Internal report 104, Unpublished paper.

Fetter C.W., (1994), *Applied Hydrogeology*, 3rd Edition, Prentice-Hall Incorporated, Englewood Cliffs, New Jersey.

Field, W.H., and Williams, B.J., (1987), *A Generalised Kinematic Catchment Model*, Water Resources Research, 23(8), p 1693-1696.

Finnegan L.G., (1993), *Hydraulic characteristics of deep ripping under simulated rainfall at Ranger Uranium Mine*, Supervising Scientist for the Alligator Rivers Region, Canberra, Internal Report 134 (Thesis), Unpublished Paper.

George E.M., (1996), *Hydrology of ripped surfaces under rainfall simulation: RUM 1993 data and vegetation, sediment and hydrology studies of the fire and soil sites: WRD, RUM 1995-96 Wet season monitoring*, Environmental Research Institute for the Supervising Scientist, Canberra, Internal Report 201, Unpublished Paper.

Gerrard A.J., (1981), *Soils and Landforms, An Integration of Geomorphology and Pedology*, George Allen and Unwin (Publishers) Ltd, London.

Johnston P.R., and Pilgram D.H., (1976), *Parameter Optimisation for Watershed Models*, Water Resources Research, 12(3):477-486.

Johnston A., (1995), *ERISS, A Brief Description*, Environmental Research Institute for the Supervising Scientist, Canberra, Unpublished Paper.

Kirby M.J., and Morgan R.P.C., (1980), *Soil Erosion*, John Wiley and Sons, New York.

Kuczera G.A., (1989), *An Application of Bayesian Nonlinear Regression To Hydrologic Models*, Advanced Engineering Software, Vol. 11, 3, p149-154.

Kuczera G.A., (1994), *NLFIT A Bayesian Nonlinear Regression Program Suite, Version 1.00g*, Department of Civil Engineering and Surveying, University of Newcastle, Newcastle.

Kuczera G.A., (1996), *Civil 342 Hydrology Lecture Notes*, Department of Civil, Surveying and Environmental Engineering, University of Newcastle, Newcastle.

Moliere D.R., Evans K.G., Riley S.J., and Willgoose G.R., (1996), *Erosion and DISTFW Hydrology model Parameters for Tin Camp Creek Catchments, Arnhem Land, Northern Territory*, Environmental Research Institute for the Supervising Scientist, Canberra, Internal Report 237, Registry File JR -05-138, Unpublished Paper.

Saynor M.J, Evans K.G., Smith B.L, and Willgoose G.R., (1995), *Experimental Study on the Effect of Vegetation on Erosion of the Ranger Uranium Mine Waste Rock Dump*, Environmental Research Institute for the Supervising Scientist, Canberra, Internal Report 200, Unpublished Paper.

Smith B.L, (1997), *Particle Size Analysis for Natural Site Adjacent to Pit No.1 ERA Ranger Mine*, Environmental Research Institute for the Supervising Scientist, Canberra, Unprinted Data.

Willgoose G.R., and Kuczera G.A, (1995), *Estimation of Subgrid Scale Kinematic Wave Parameters for Hillslopes*, Hydrological Processes, 9, pp 469-482.

Willgoose G.R., and Loch R., (1996), *An Assessment of the Nabarlek Rehabilitation, Tin Camp Creek and Other Mine Sites in the Alligator Rivers Region as Test Sites for Examining Long Term Erosion Processes and the Validation of the SIBERIA Model*, Environmental Research Institute for the Supervising Scientist Internal Report 229, TUNRA, The University of Newcastle, Newcastle.

Willgoose G.R., and Riley S., (1993), *The Assessment of the Long-term Erosional Stability of Engineering Structured of a Proposed Mine Rehabilitation*, Hydrological Processes, pp 667-673.

Willgoose G.R., Bras R.L, and Rodriguez-Iturbe I., (1989), *A Physically Based Channel Network and Catchment Evolution Model*, TR 322, Ralph M. Parsons Laboratory, Department of Civil Engineering, MIT, Boston, MA.

Willgoose G.R., Kuczera G.A., and Williams B.J., (1995), *DISTFW-NLFIT: Rainfall-Runoff and Erosion Model Calibration and Model Uncertainty Assessment Suite User Manual*, Research Report No. 108.03.1995, The University of Newcastle, Department of Civil, Surveying and Environmental Engineering, Newcastle.

Appendix 3.A

**DISTFW Rainfall and Runoff Input Files and Predicted
versus Observed Output Hydrographs and
Accompanying Statistics.**

1st January

RUM 96-97 Monitoring

pit 1 site

Rainfall 1/1/97 1550hrs

168

0	0	0.1833	9.2	0.35	21	0.5167	35.2	0.6833	44.6	0.85	55.4	1.0167	62	1.2667	66	1.6	69.2
0.0167	0.2	0.1917	9.6	0.3583	21.4	0.525	36	0.6917	45.4	0.8583	56	1.0333	62.2	1.2833	66.2	1.6333	69.2
0.025	0.4	0.2	9.8	0.3667	22.2	0.5333	36.4	0.7	45.8	0.8667	56.4	1.05	62.8	1.3	66.6	1.6667	69.6
0.0417	0.8	0.2083	10.2	0.375	22.8	0.5417	36.8	0.7083	46.6	0.875	56.8	1.0667	63	1.3167	66.6	1.6833	69.6
0.05	1	0.2167	11	0.3833	23.4	0.55	37.2	0.7167	47	0.8833	57.2	1.075	63.2	1.325	66.8	1.725	69.8
0.0583	1.2	0.225	11.4	0.3917	24.2	0.5583	37.6	0.725	47.4	0.8917	57.8	1.0917	63.4	1.3417	67	1.8	70
0.0667	1.6	0.2333	11.8	0.4	24.8	0.5667	38.2	0.7333	48	0.9	58	1.1	63.6	1.3667	67.2	1.85	70.2
0.075	2.2	0.2417	12.2	0.4083	25.4	0.575	38.4	0.7417	48.6	0.9083	58.4	1.1083	63.8	1.375	67.2	1.9	70.2
0.0833	2.4	0.25	13	0.4167	26	0.5833	38.8	0.75	49	0.9167	58.8	1.1167	64	1.3833	67.6		
0.0917	3	0.2583	13.4	0.425	27	0.5917	39	0.7583	49.6	0.925	59	1.125	64.2	1.4	67.8		
0.1	3.6	0.2667	14.2	0.4333	27.6	0.6	39.2	0.7667	50.2	0.9333	59.2	1.1417	64.6	1.425	68		
0.1083	4.2	0.275	14.8	0.4417	28.6	0.6083	39.6	0.775	50.8	0.9417	59.6	1.15	64.8	1.4333	68		
0.1167	4.8	0.2833	15.6	0.45	29.4	0.6167	39.8	0.7833	51.4	0.95	59.8	1.1667	65	1.4417	68		
0.125	5.4	0.2917	16.2	0.4583	30	0.625	40	0.7917	51.8	0.9583	60.2	1.175	65	1.45	68.2		
0.1333	6	0.3	16.8	0.4667	31.2	0.6333	40.6	0.8	52.4	0.9667	60.4	1.1833	65.2	1.475	68.6		
0.1417	6.6	0.3083	17.4	0.475	31.6	0.6417	41.2	0.8083	53.2	0.975	60.6	1.1917	65.2	1.4917	68.6		
0.15	7.2	0.3167	18	0.4833	32.2	0.65	41.8	0.8167	53.8	0.9833	60.8	1.2	65.6	1.5	68.8		
0.1583	7.8	0.325	18.8	0.4917	33.2	0.6583	42.8	0.825	54	0.9917	61.2	1.2167	65.6	1.5333	68.8		
0.1667	8.2	0.3333	19.4	0.5	33.8	0.6667	43.4	0.8333	54.6	1	61.4	1.2333	65.8	1.5417	69		
0.175	8.6	0.3417	20	0.5083	34.4	0.675	44	0.8417	54.8	1.0083	61.6	1.25	65.8	1.575	69		

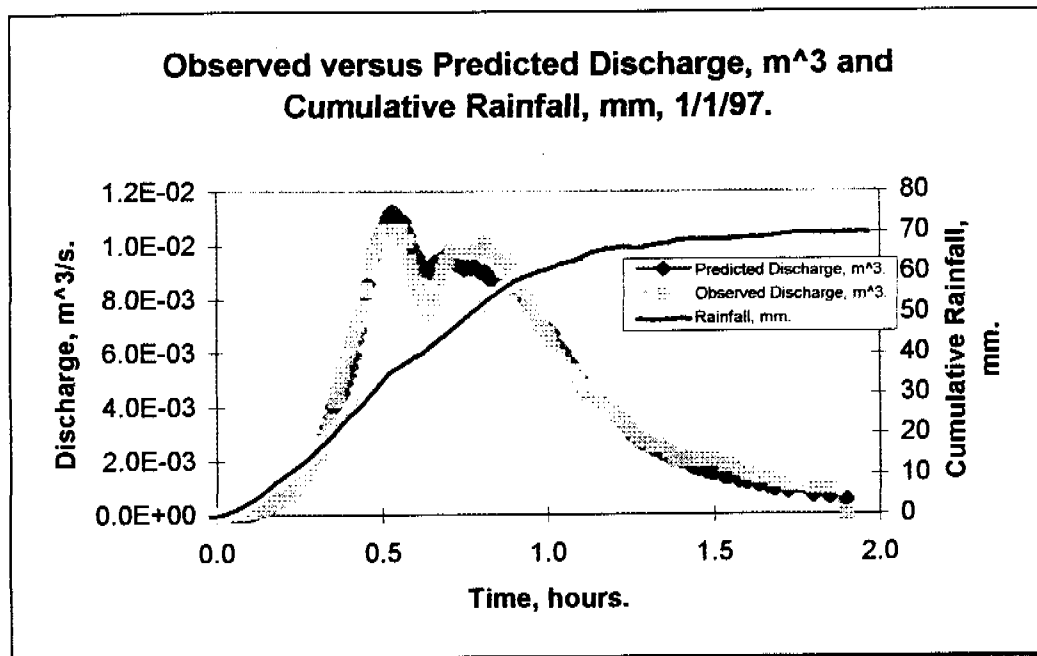
RUM 96-97 Monitoring

pit 1 site

Runoff 1/1/97 1550hrs

168

0	0	0.183	0.00044	0.35	0.00354	0.517	0.01054	0.683	0.00906	0.85	0.00979	1.017	0.00614	1.267	0.0029	1.6	0.00149
0.017	0.00001	0.192	0.00053	0.358	0.00425	0.525	0.01054	0.692	0.00942	0.858	0.00942	1.033	0.00585	1.283	0.0027	1.633	0.00135
0.025	0.00001	0.2	0.00063	0.367	0.0045	0.533	0.01054	0.7	0.00942	0.867	0.00942	1.05	0.00556	1.3	0.0027	1.667	0.00135
0.042	0.00001	0.208	0.00063	0.375	0.00502	0.542	0.01054	0.708	0.00979	0.875	0.00942	1.067	0.00529	1.317	0.00251	1.683	0.00121
0.05	0.00005	0.217	0.00073	0.383	0.00529	0.55	0.01054	0.717	0.00979	0.883	0.00906	1.075	0.00529	1.325	0.00251	1.725	0.00108
0.058	0.00005	0.225	0.00084	0.392	0.00585	0.558	0.01054	0.725	0.00979	0.892	0.00906	1.092	0.00502	1.342	0.00251	1.8	0.00096
0.067	0.00005	0.233	0.00096	0.4	0.00614	0.567	0.01016	0.733	0.00979	0.9	0.00906	1.1	0.00475	1.367	0.00232	1.85	0.00096
0.075	0.00005	0.242	0.00108	0.408	0.00643	0.575	0.01016	0.742	0.00979	0.908	0.00906	1.108	0.00475	1.375	0.00232	1.900	0.000
0.083	0.00005	0.25	0.00121	0.417	0.00674	0.583	0.00942	0.75	0.00979	0.917	0.00871	1.117	0.00475	1.383	0.00197		
0.092	0.0001	0.258	0.00135	0.425	0.00705	0.592	0.00906	0.758	0.00979	0.925	0.00836	1.125	0.0045	1.4	0.00197		
0.1	0.0001	0.267	0.00149	0.433	0.00737	0.6	0.00871	0.767	0.00979	0.933	0.00836	1.142	0.00475	1.425	0.00197		
0.108	0.00015	0.275	0.00165	0.442	0.00769	0.608	0.00836	0.775	0.00979	0.942	0.00803	1.15	0.00425	1.433	0.00214		
0.117	0.00015	0.283	0.0018	0.45	0.00836	0.617	0.00836	0.783	0.00979	0.95	0.00769	1.167	0.00401	1.442	0.00197		
0.125	0.00021	0.292	0.00197	0.458	0.00906	0.625	0.00803	0.792	0.00979	0.958	0.00769	1.175	0.00401	1.45	0.00197		
0.133	0.00021	0.3	0.00214	0.467	0.00942	0.633	0.00737	0.8	0.00979	0.967	0.00737	1.183	0.00401	1.475	0.00197		
0.142	0.00021	0.308	0.00232	0.475	0.00979	0.642	0.00737	0.808	0.01016	0.975	0.00705	1.192	0.00377	1.492	0.00197		
0.15	0.00028	0.317	0.00251	0.483	0.01016	0.65	0.00737	0.817	0.01016	0.983	0.00705	1.2	0.00377	1.5	0.00197		
0.158	0.00036	0.325	0.0027	0.492	0.01016	0.658	0.00803	0.825	0.00979	0.992	0.00674	1.217	0.00354	1.533	0.0018		
0.167	0.00036	0.333	0.0029	0.5	0.01054	0.667	0.00803	0.833	0.00979	1	0.00674	1.233	0.00332	1.542	0.0018		
0.175	0.00044	0.342	0.00332	0.508	0.01054	0.675	0.00871	0.842	0.00979	1.008	0.00643	1.25	0.00311	1.575	0.00165		



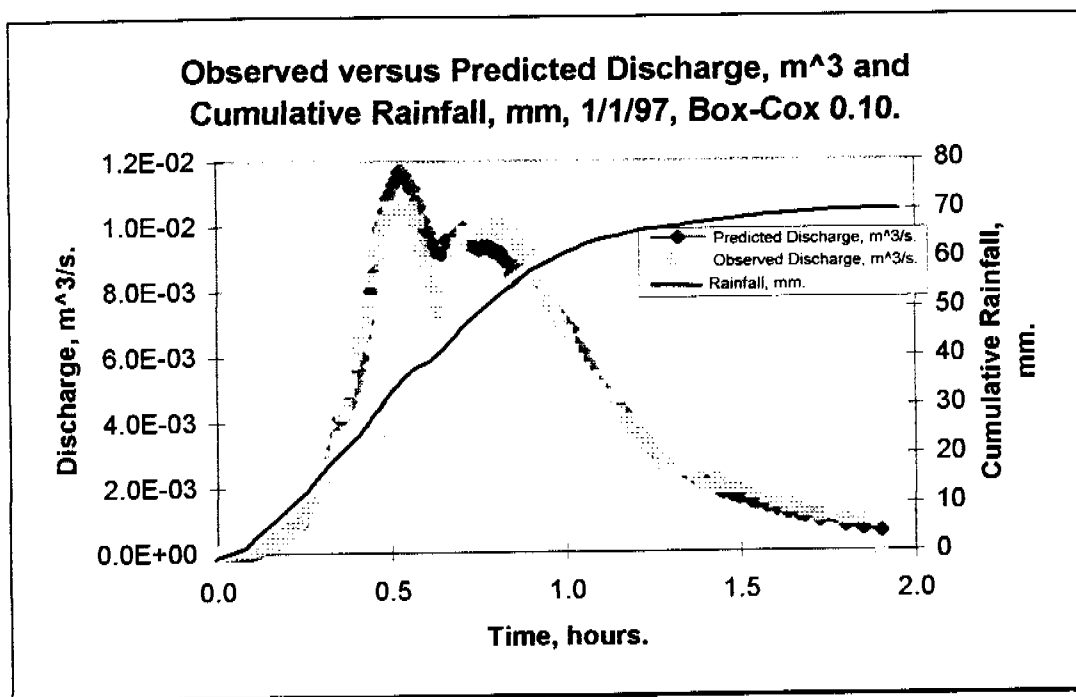
NLFIT Input files: 1197.fw, 1197.ro/rf.

NLFIT Output files: 1197L.prt/pmf/plr.

Parameter.	Mean.	Standard Deviation.	Parameter.	Mean.	Standard Deviation.
C_T	1.68372	0.0811	$S\phi$	7.94852	1.52483
e_m	1.67457	0.0833	ϕ	0.2795	2.24711

Convergence Monitor	R^2 , %	Cumulative Periodogram.		Standardised Residual Versus Time.	Standardised Residual Versus N(0,1) Variate.		Auto Correlation Plot.	Partial Auto Correlation Plot.
		Test Statistic.	5%.	Z.	Test Statistic.	5%	Exceedances.	Exceedances.
2.73959	97.9	0.7986	0.1493	-9.497	0.1091	0.069	11	3

Storm Specific Comment: The convergence monitor is not adequate, below 0.1, the R^2 is adequate at 97.9%, the cumulative periodogram does not pass the test statistic. The standardised residual versus time plot exceeds the Z statistic limit of $|2|$, the standardised residual versus N(0,1) variate does not pass the test statistic. The auto-correlation plot is exceeded 11 times, and the partial auto-correlation plot is exceeded 3 times.



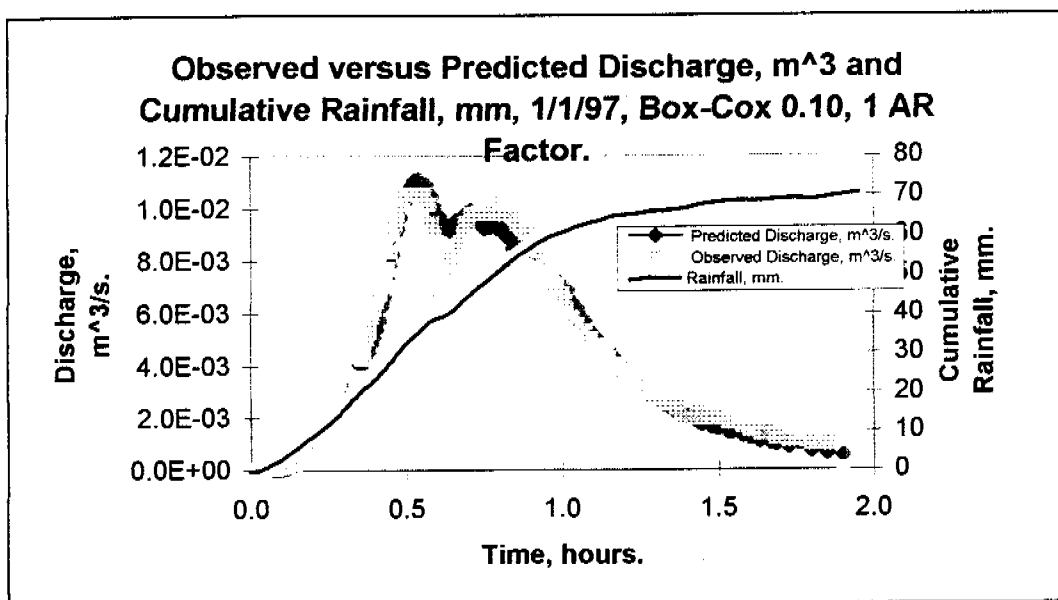
NLFIT Input files: 1197.fw, 1197.ro/rf.

NLFIT Output files: 1197WG10.prt/pmf/plt.

Parameter.	Mean.	Standard Deviation.	Parameter.	Mean.	Standard Deviation.
C_r	1.80267	0.07523	$S\phi$	7.25475	0.2133
e_m	1.79591	0.04182	ϕ	0.001	

		Cumulative Periodogram.		Standardised Residual Versus Time.	Standardised Residual Versus N(0,1) Variate.		Auto Correlation Plot.	Partial Auto Correlation Plot.
		Test Statistic.	5%.	Z.	Test Statistic.	5%.	Exceedances.	Exceedances.
Convergence Monitor.	R^2 , %.							
0.01059	97.9	0.7234	0.1493	-9.699	0.0687	0.069	11	3

Storm Specific Comment: The convergence monitor is adequate, below 0.1, the R^2 is adequate at 97.9%, the cumulative periodogram does not pass the test statistic. The standardised residual versus time plot exceeds the Z statistic limit of |2|, the standardised residual versus N(0,1) variate does pass the test statistic. The auto-correlation plot is exceeded 11 times, and the partial auto-correlation plot is exceeded 3 times.



NLFIT Input files: 1197.fw, 1197.ro/rf.

NLFIT Output files: 1197WAR1.prt/pmf/plt.

Parameter.	Mean.	Standard Deviation.	Parameter.	Mean.	Standard Deviation.
C _r	1.5285	0.176085	S ϕ	7.8249	0.71538
e _m	1.63087	0.09052	ϕ	0.001	

		Cumulative Periodogram.		Standardised Residual Versus Time.	Standardised Residual Versus N(0,1) Variate.		Auto Correlation Plot.	Partial Auto Correlation Plot.
Convergence Monitor.	R ² , %.	Test Statistic.	5%.	Z.	Test Statistic.	5%.	Exceedances.	Exceedances.
0.02893	97.9	0.0765	0.1493	-0.719	0.1563	0.069	0	0

Storm Specific Comment: The convergence monitor is adequate, below 0.1, the R² is adequate at 97.9%, the cumulative periodogram does pass the test statistic. The standardised residual versus time plot does not exceed the Z statistic limit of |2|, the standardised residual versus N(0,1) variate does not pass the test statistic. The auto-correlation plot is exceeded 0 times, and the partial auto-correlation plot is exceeded 0 times.

General Comment: There is little difference between the three plots, a Box-Cox of 0.10 was evaluated to give the best fit, the Box-Cox plot seemed to over-predict the first peak, yet the inclusion of an auto-regressive factor addressed this issue. Thus the best plot is 1197war1.*.

3rd January

RUM 96-97 Monitoring

pit 1 site

Rainfall 3/1/97 0400hrs

254

0	0	0.724	4.2	1.09	9	1.442	13.6	1.793	18.4	1.89	23.4	1.993	28.4	2.103	33	2.254	37.6	2.463	42.4	2.726	47	3.024	51.4	3.881	55.8
0.05	0.2	0.761	4.4	1.113	9.2	1.46	13.8	1.794	18.6	1.896	23.6	1.997	28.6	2.114	33.4	2.265	37.8	2.481	42.8	2.735	47.2	3.063	51.6	3.947	56
0.1	0.4	0.79	4.6	1.132	9.4	1.475	14.2	1.806	18.8	1.901	24	1.999	28.8	2.125	33.6	2.275	38.2	2.49	43	2.744	47.4	3.096	51.8	4.024	56.2
0.142	0.6	0.817	5	1.133	9.6	1.497	14.4	1.815	19	1.908	24.2	2.003	29	2.133	33.8	2.282	38.4	2.497	43.2	2.746	47.6	3.097	52	4.096	56.4
0.186	1	0.843	5.2	1.15	9.8	1.515	14.6	1.825	19.4	1.914	24.4	2.01	29.2	2.14	34.2	2.292	38.6	2.506	43.4	2.756	47.8	3.129	52.2	4.276	56.8
0.232	1.2	0.857	5.4	1.167	10	1.538	14.8	1.831	19.6	1.919	24.8	2.014	29.4	2.15	34.4	2.303	39	2.517	43.8	2.765	48	3.169	52.4	4.5	57
0.271	1.4	0.871	5.6	1.182	10.2	1.556	15.2	1.835	19.8	1.925	25	2.015	29.6	2.163	34.6	2.317	39.2	2.531	44	2.776	48.2	3.221	52.6	4.601	57.2
0.311	1.6	0.883	6	1.183	10.4	1.576	15.4	1.84	20.2	1.932	25.4	2.021	29.8	2.172	34.8	2.329	39.4	2.551	44.2	2.789	48.6	3.29	52.8	4.713	57.4
0.361	1.8	0.903	6.2	1.197	10.6	1.594	15.6	1.846	20.4	1.938	25.6	2.026	30	2.174	35	2.342	39.6	2.557	44.4	2.803	48.8	3.353	53.2	4.75	57.6
0.363	2	0.922	6.4	1.217	10.8	1.611	15.8	1.85	20.6	1.943	25.8	2.032	30.4	2.182	35.2	2.356	40	2.558	44.6	2.824	49	3.393	53.4	4.768	57.8
0.404	2.2	0.933	6.8	1.243	11	1.628	16.2	1.851	20.8	1.949	26.2	2.039	30.6	2.188	35.4	2.368	40.2	2.564	44.8	2.84	49.2	3.439	53.6	4.769	58
0.439	2.4	0.944	7	1.274	11.4	1.65	16.4	1.856	21	1.954	26.4	2.044	30.8	2.192	35.6	2.379	40.4	2.571	45	2.856	49.4	3.489	53.8	4.785	58.2
0.485	2.6	0.958	7.2	1.293	11.6	1.681	16.6	1.86	21.4	1.96	26.6	2.05	31.2	2.193	35.8	2.392	40.6	2.582	45.4	2.869	49.8	3.542	54	4.821	58.4
0.531	2.8	0.975	7.4	1.308	11.8	1.706	16.8	1.864	21.6	1.961	26.8	2.056	31.4	2.197	36	2.399	40.8	2.596	45.6	2.882	50	3.568	54.2	4.9	58.4
0.532	3	0.994	7.6	1.326	12	1.707	17	1.868	22	1.965	27	2.061	31.6	2.204	36.2	2.4	41	2.618	45.8	2.894	50.2	3.569	54.4		
0.583	3.2	0.996	7.8	1.346	12.4	1.729	17.2	1.872	22.2	1.971	27.2	2.063	31.8	2.214	36.6	2.407	41.2	2.644	46	2.911	50.4	3.606	54.6		
0.624	3.4	1.015	8	1.367	12.6	1.747	17.4	1.876	22.6	1.976	27.4	2.069	32	2.224	36.8	2.414	41.4	2.679	46.2	2.932	50.6	3.646	54.8		
0.658	3.6	1.035	8.2	1.389	12.8	1.758	17.8	1.881	22.8	1.978	27.6	2.076	32.2	2.233	37	2.421	41.8	2.701	46.4	2.933	50.8	3.701	55		
0.694	3.8	1.05	8.6	1.411	13	1.768	18	1.885	23	1.982	27.8	2.085	32.6	2.243	37.2	2.429	42	2.703	46.6	2.964	51	3.765	55.2		
0.696	4	1.067	8.8	1.426	13.4	1.781	18.2	1.886	23.2	1.988	28.2	2.093	32.8	2.244	37.4	2.446	42.2	2.715	46.8	2.992	51.2	3.822	55.6		

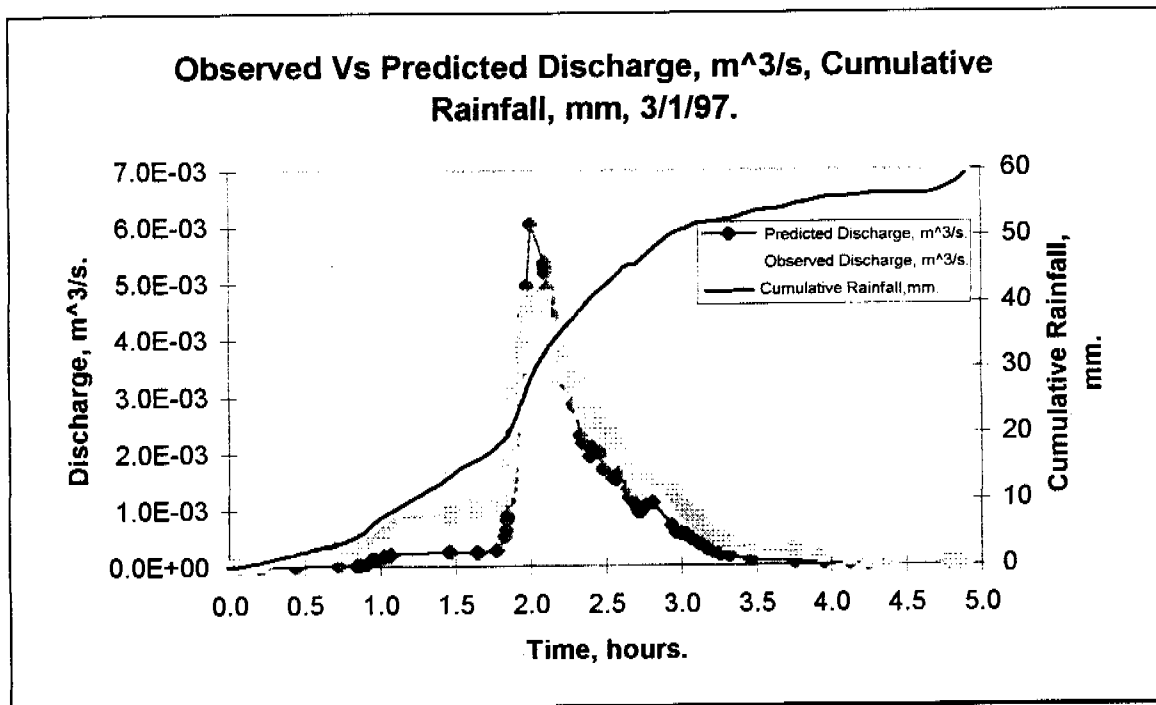
RUM 96-97 Monitoring

pit 1 site

Runoff 3/1/97 0400hrs

131

0	0	1.024	7.29E-04	1.865	2.14E-03	2.122	4.25E-03	2.388	2.51E-03	2.814	1.49E-03	3.76	2.14E-04
0.067	5.07E-05	1.063	8.39E-04	1.868	2.32E-03	2.124	4.01E-03	2.406	2.70E-03	2.936	1.35E-03	3.761	2.83E-04
0.068	9.97E-06	1.064	7.29E-04	1.876	2.51E-03	2.131	3.77E-03	2.453	2.51E-03	2.967	1.21E-03	3.763	2.14E-04
0.093	5.07E-05	1.075	8.39E-04	1.882	2.70E-03	2.132	4.01E-03	2.454	2.70E-03	3.004	1.08E-03	3.946	1.53E-04
0.094	9.97E-06	1.458	9.57E-04	1.889	2.90E-03	2.135	3.77E-03	2.456	2.51E-03	3.036	9.57E-04	4.122	9.84E-05
0.096	5.07E-05	1.463	8.39E-04	1.894	3.11E-03	2.139	4.01E-03	2.479	2.32E-03	3.068	8.39E-04	4.251	5.07E-05
0.207	9.84E-05	1.464	9.57E-04	1.903	3.32E-03	2.144	3.77E-03	2.543	2.14E-03	3.121	7.29E-04	4.351	9.97E-06
0.208	5.07E-05	1.639	1.08E-03	1.924	3.54E-03	2.165	3.54E-03	2.565	2.32E-03	3.122	8.39E-04	4.779	5.07E-05
0.222	9.84E-05	1.642	9.57E-04	1.939	3.77E-03	2.178	3.32E-03	2.604	2.14E-03	3.124	7.29E-04	4.858	9.84E-05
0.442	1.53E-04	1.647	1.08E-03	1.95	4.01E-03	2.192	3.54E-03	2.626	1.97E-03	3.172	6.26E-04	4.86	5.07E-05
0.724	2.14E-04	1.649	9.57E-04	1.965	4.25E-03	2.199	3.77E-03	2.643	1.80E-03	3.213	5.30E-04	4.9	0
0.846	2.83E-04	1.65	1.08E-03	1.978	4.50E-03	2.224	3.54E-03	2.66	1.65E-03	3.26	4.41E-04		
0.875	3.58E-04	1.651	9.57E-04	2.004	4.75E-03	2.239	3.32E-03	2.678	1.49E-03	3.261	5.30E-04		
0.911	4.41E-04	1.776	1.08E-03	2.093	4.50E-03	2.244	3.54E-03	2.708	1.35E-03	3.263	4.41E-04		
0.94	5.30E-04	1.825	1.21E-03	2.094	4.75E-03	2.246	3.32E-03	2.715	1.49E-03	3.324	3.58E-04		
0.967	6.26E-04	1.835	1.35E-03	2.096	4.50E-03	2.281	3.11E-03	2.717	1.35E-03	3.325	4.41E-04		
1.017	7.29E-04	1.84	1.49E-03	2.097	4.75E-03	2.285	3.32E-03	2.718	1.49E-03	3.326	3.58E-04		
1.019	6.26E-04	1.846	1.65E-03	2.099	4.50E-03	2.29	3.11E-03	2.719	1.35E-03	3.463	2.83E-04		
1.021	7.29E-04	1.854	1.80E-03	2.11	4.25E-03	2.328	2.90E-03	2.728	1.49E-03	3.756	2.14E-04		
1.022	6.26E-04	1.86	1.97E-03	2.121	4.01E-03	2.34	2.70E-03	2.761	1.65E-03	3.757	2.83E-04		



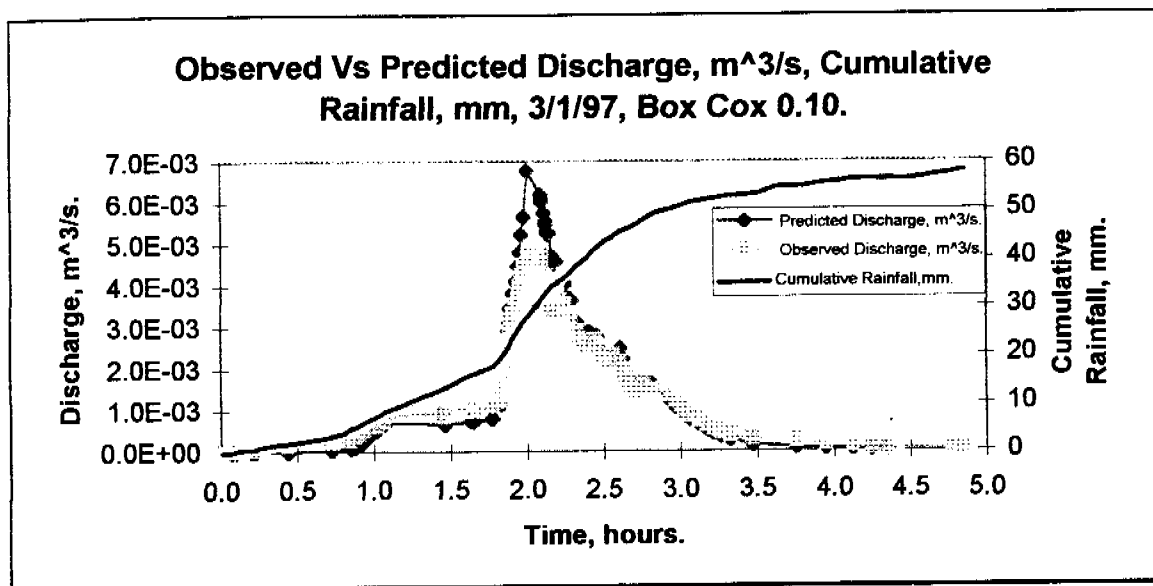
NLFIT Input files: 3197.fw, 3197.ro/rf.

NLFIT Output files: 3197.prt/pmf/plf.

Parameter.	Mean.	Standard Deviation.	Parameter.	Mean.	Standard Deviation.
C_r	4.47971	1.57423	$S\phi$	0.245176	1.86864
e_m	1.54443	0.198571	ϕ	13.6394	2.0712

		Cumulative Periodogram.		Standardised Residual Versus Time.	Standardised Residual Versus N(0,1) Variate.		Auto Correlation Plot.	Partial Auto Correlation Plot.
Convergence Monitor.	R^2 , %.	Test Statistic.	5%.	Z.	Test Statistic.	5%.	Exceedances.	Exceedances.
4.14001	95.4	0.8526	0.17	-9.383	0.1171	0.078	13	8

Storm Specific Comment: The convergence monitor is not adequate, below 0.1, the R^2 is adequate at 95.4%, the cumulative periodogram does not pass the test statistic. The standardised residual versus time plot exceeds the Z statistic limit of |2|, the standardised residual versus N(0,1) variate does not pass the test statistic. The auto-correlation plot is exceeded 13 times, and the partial auto-correlation plot is exceeded 8 times.



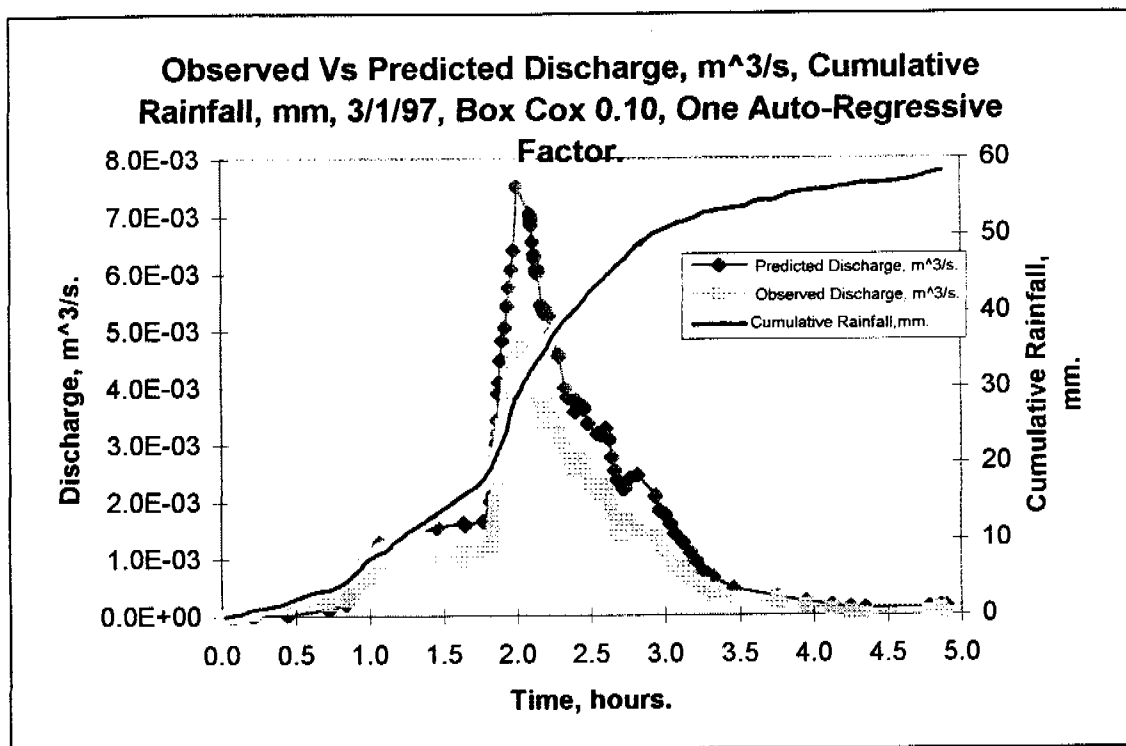
NLFIT Input files: 3197.fw, 3197.ro/rf.

NLFIT Output files: 3197WG10.prt/pmf/plf.

Parameter.	Mean.	Standard Deviation.	Parameter.	Mean.	Standard Deviation.
C_r	4.00082	0.66808	$S\phi$	0.001	
e_m	1.55394	0.081335	ϕ	9.03137	0.280544

		Cumulative Periodogram.		Standardised Residual Versus Time.	Standardised Residual Versus N(0,1) Variate.		Auto Correlation Plot.	Partial Auto Correlation Plot.
Convergence Monitor.	R^2 , %.	Test Statistic.	5%.	Z.	Test Statistic.	5%.	Exceedances.	Exceedances.
0.25	98.2	0.866	0.17	-9.144	0.1089	0.0781	15	6

Storm Specific Comment: The convergence monitor is not adequate, below 0.1, the R^2 is adequate and improved at 98.2%, the cumulative periodogram does not pass the test statistic. The standardised residual versus time plot exceeds the Z statistic limit of $|2|$, the standardised residual versus N(0,1) variate does not pass the test statistic. The auto-correlation plot is exceeded 15 times, and the partial auto-correlation plot is exceeded 6 times.



NLFIT Input files: 3197.fw, 3197.ro/rf.

NLFIT Output files: 3197WAR1.prt/pmf/plf.

Parameter.	Mean.	Standard Deviation.	Parameter.	Mean.	Standard Deviation.
C_r	4.00082	0.66808	$S\phi$	0.001	
e_m	1.55394	0.081335	ϕ	9.03137	0.280544

		Cumulative Periodogram.		Standardised Residual Versus Time.	Standardised Residual Versus N(0,1) Variate.		Auto Correlation Plot.	Partial Auto Correlation Plot.
Convergence Monitor.	R^2 , %.	Test Statistic.	5%.	Z.	Test Statistic.	5%.	Exceedances.	Exceedances.
0.1053	99.3	0.3261	0.17	3.611	0.086	0.0781	1	1

Storm Specific Comment: The convergence monitor is adequate, 0.1, the R^2 is adequate at 99.3%, the cumulative periodogram does not pass the test statistic. The standardised residual versus time plot exceeds the Z statistic limit of $|2|$, the standardised residual versus N(0,1) variate does pass the test statistic. The auto-correlation plot is exceeded 1 times, and the partial auto-correlation plot is exceeded 1 times.

General Comment: The first plot is an adequate fit in the centre, the inclination and recession limbs are fitted badly, the centre section is over-predicted only slightly. When a more general error model is adopted, a Box-Cox of 0.10, a better fit is obtained in the inclination and recession limbs. The addition of an auto-regressive factor results in a model which over-predicts everywhere except at the beginning and at the end.

3rd pm January

RUM 96-97 Monitoring

pit 1 site

Rainfall 3/1/97 1139hrs

63

0	0	1.35	4.6	2.156	9.6	2.982	14.2
0.082	0.4	1.375	5	2.182	9.8	3.215	14.4
0.264	0.6	1.392	5.2	2.183	10	4.1	14.4
0.599	0.8	1.406	5.4	2.201	10.2		
0.676	1	1.417	5.6	2.215	10.4		
0.749	1.2	1.432	6	2.236	10.6		
0.819	1.4	1.456	6.2	2.261	10.8		
0.821	1.6	1.485	6.4	2.263	11		
0.89	1.8	1.558	6.6	2.308	11.2		
0.944	2	1.679	7	2.329	11.4		
0.985	2.2	1.724	7.2	2.353	11.6		
1.019	2.4	1.764	7.4	2.378	12		
1.058	2.8	1.831	7.6	2.394	12.2		
1.092	3	1.856	8	2.413	12.4		
1.128	3.2	1.879	8.2	2.46	12.6		
1.178	3.4	1.925	8.4	2.518	13		
1.214	3.6	1.971	8.6	2.571	13.2		
1.249	4	2.038	9	2.579	13.4		
1.297	4.2	2.101	9.2	2.593	13.6		
1.322	4.4	2.132	9.4	2.653	14		

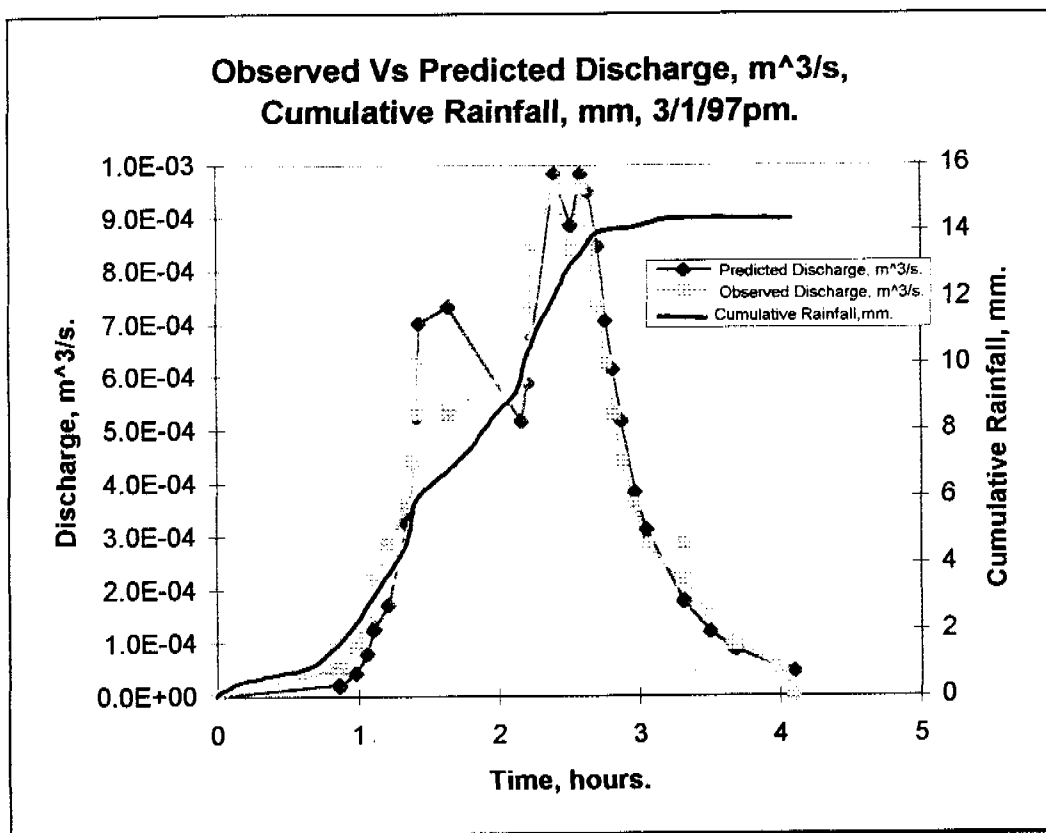
RUM 96-97 Monitoring

pit 1 site

Runoff 3/1/97 1139hrs

49

0	0	2.206	7.29E-04	3.661	9.84E-05
0.858	5.07E-05	2.242	8.39E-04	3.663	1.53E-04
0.867	9.97E-06	2.399	9.57E-04	3.664	9.84E-05
0.869	5.07E-05	2.51	8.39E-04	3.665	1.53E-04
0.982	9.84E-05	2.59	9.57E-04	3.667	9.84E-05
1.06	1.53E-04	2.636	8.39E-04	3.675	1.53E-04
1.107	2.14E-04	2.639	9.57E-04	3.676	9.84E-05
1.11	1.53E-04	2.64	8.39E-04	4.013	5.07E-05
1.111	2.14E-04	2.704	7.29E-04	4.1	0
1.214	2.83E-04	2.764	6.26E-04		
1.349	3.58E-04	2.819	5.30E-04		
1.35	2.83E-04	2.875	4.41E-04		
1.351	3.58E-04	2.967	3.58E-04		
1.389	4.41E-04	3.05	2.83E-04		
1.413	5.30E-04	3.31	2.14E-04		
1.438	6.26E-04	3.311	2.83E-04		
1.642	5.30E-04	3.314	2.14E-04		
2.157	6.26E-04	3.5	1.53E-04		
2.158	5.30E-04	3.501	2.14E-04		
2.161	6.26E-04	3.503	1.53E-04		



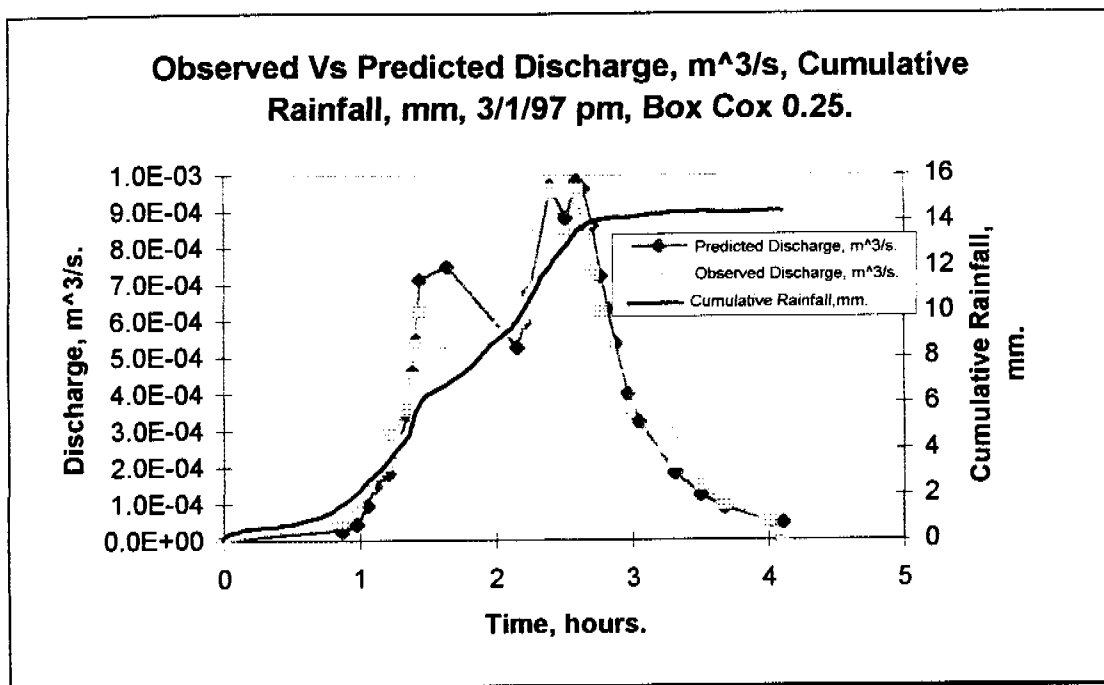
NLFIT Input files: 3197pm.fw, 3197pm.ro/rf.

NLFIT Output files: 3197pmn.prt/pmf/plt.

Parameter.	Mean.	Standard Deviation.	Parameter.	Mean.	Standard Deviation.
C_r	5.15159	1.82944	$S\phi$	0.001	
c_m	1.91751	0.138991	ϕ	2.27864	0.135633

		Cumulative Periodogram.		Standardised Residual Versus Time.	Standardised Residual Versus N(0,1) Variate.		Auto Correlation Plot.	Partial Auto Correlation Plot.
Convergence Monitor.	R^2 , %.	Test Statistic.	5%.	Z.	Test Statistic.	5%.	Exceedances.	Exceedances.
0.0159	93.9	0.4443	0.3206	-4.405	0.0859	0.1441	2	2

Storm Specific Comment: The convergence monitor is adequate, below 0.1, the R^2 is adequate 93.9%, the cumulative periodogram does not pass the test statistic. The standardised residual versus time plot exceeds the Z statistic limit of $|2|$, the standardised residual versus N(0,1) variate does pass the test statistic. The auto-correlation plot is exceeded 2 times, and the partial auto-correlation plot is exceeded 2 times.



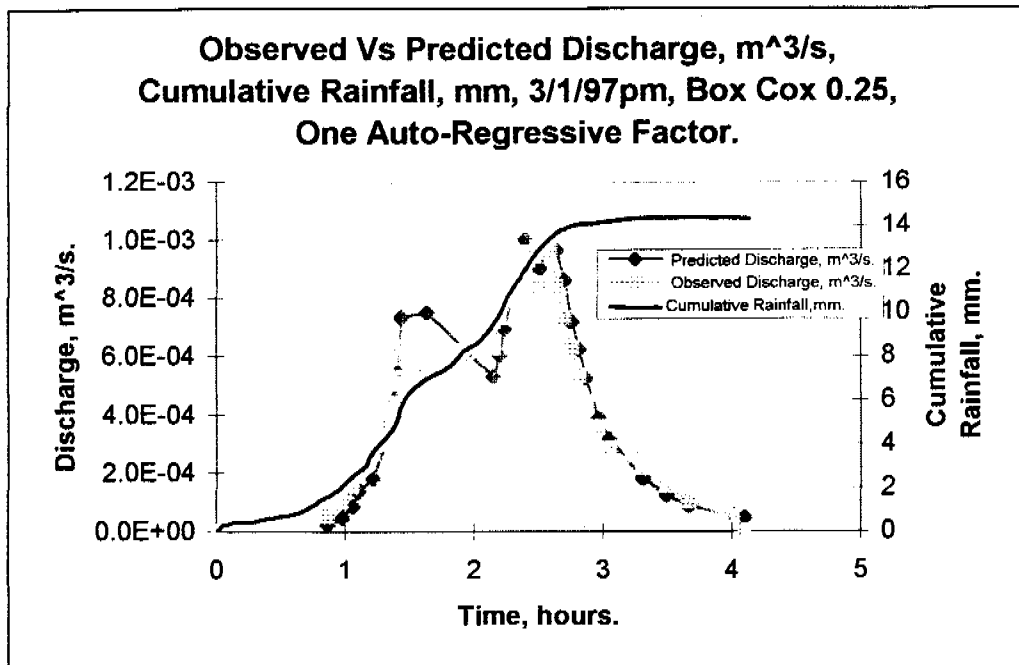
NLFIT Input files: 3197pm.fw, 3197pm.ro/rf.

NLFIT Output files: 31pmn25.prt/pmf/plt.

Parameter.	Mean.	Standard Deviation.	Parameter.	Mean.	Standard Deviation.
C_r	4.08908	1.39135	$S\phi$	0.001	
e_m	1.83423	0.132293	ϕ	2.23393	0.143048

		Cumulative Periodogram.		Standardised Residual Versus Time.	Standardised Residual Versus N(0,1) Variate.		Auto Correlation Plot.	Partial Auto Correlation Plot.
Convergence Monitor.	R^2 , %.	Test Statistic.	5%.	Z.	Test Statistic.	5%.	Exceedances.	Exceedances.
0.017768	93.7	0.4666	0.3206	-4.473	0.0779	0.1441	5	2

Storm Specific Comment: The convergence monitor is adequate, below 0.1, the R^2 is adequate 93.7%, the cumulative periodogram does not pass the test statistic. The standardised residual versus time plot exceeds the Z statistic limit of $|2|$, the standardised residual versus N(0,1) variate does pass the test statistic. The auto-correlation plot is exceeded 5 times, and the partial auto-correlation plot is exceeded 2 times.



NLFIT Input files: 3197pm.fw, 3197pm.ro/rf.

NLFIT Output files: 31pmn25.prt/pmf/plt.

Parameter.	Mean.	Standard Deviation.	Parameter.	Mean.	Standard Deviation.
C_r	4.08908	1.39135	$S\phi$	0.001	
e_m	1.83423	0.132293	ϕ	2.23393	0.143048

		Cumulative Periodogram.		Standardised Residual Versus Time.	Standardised Residual Versus N(0,1) Variate.		Auto Correlation Plot.	Partial Auto Correlation Plot.
Convergence Monitor.	R^2 , %.	Test Statistic.	5%.	Z.	Test Statistic.	5%.	Exceedances.	Exceedances.
0.017768	93.7	0.4666	0.3206	-4.473	0.0779	0.1441	5	2

Storm Specific Comment: The convergence monitor is adequate, below 0.1, the R^2 is adequate 93.7%, the cumulative periodogram does not pass the test statistic. The standardised residual versus time plot exceeds the Z statistic limit of $|2|$, the standardised residual versus N(0,1) variate does pass the test statistic. The auto-correlation plot is exceeded 5 times, and the partial auto-correlation plot is exceeded 2 times.

General Comment: The initial plot is adequate with respect to fit in the inclination and recession limbs, however there is over-prediction between 1.5 and 2.5 hours. It should be noted that this storm is only very small, 14.4mm over four hours. The inclusion of a more general error model with a Box-Cox factor of 0.25, improves the general fit, especially in the inclining limb. The inclusion of an auto-regressive factor made little impact on the quality of the model prediction.

4th January

RUM 96-97 Monitoring

pit 1 site

Rainfall 4/1/97 2324hrs

54

0	0	1.122	4.6	1.418	9.4
0.042	0.4	1.14	5	1.419	9.6
0.247	0.6	1.151	5.2	1.496	9.8
0.403	0.8	1.16	5.4	1.526	10
0.621	1	1.168	5.8	1.626	10.2
0.733	1.4	1.178	6	1.663	10.4
0.806	1.6	1.193	6.2	1.664	10.6
0.872	1.8	1.201	6.6	1.707	10.8
0.922	2	1.21	6.8	1.747	11
0.957	2.2	1.218	7	1.801	11.2
0.958	2.4	1.232	7.2	1.928	11.6
0.99	2.6	1.246	7.6	2.004	11.8
1.015	2.8	1.26	7.8	2.143	12
1.026	3.2	1.271	8	2.325	12.2
1.032	3.4	1.286	8.2	3.900	12.2
1.039	3.6	1.299	8.4		
1.049	3.8	1.3	8.6		
1.05	4	1.315	8.8		
1.065	4.2	1.332	9		
1.086	4.4	1.365	9.2		

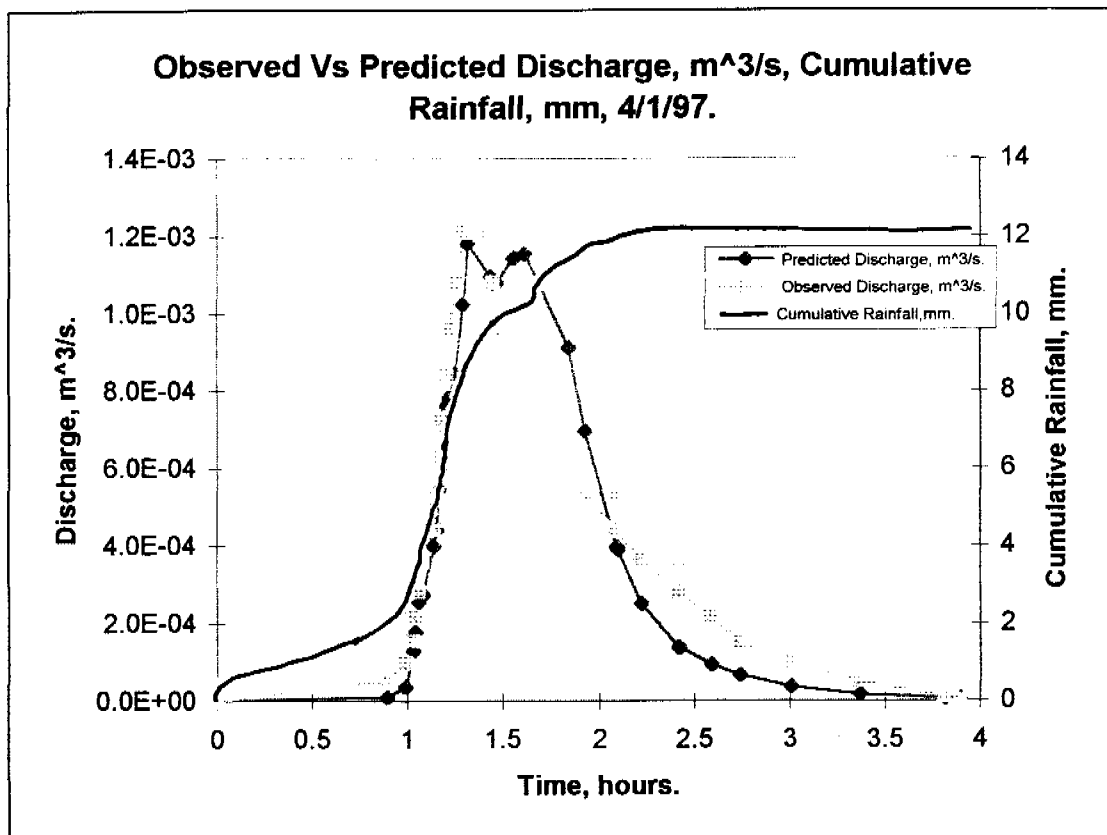
RUM 96-97 Monitoring

pit 1 site

Runoff 4/1/97 2324hrs

36

0	0	1.615	7.29E-04
0.893	5.07E-05	1.844	6.26E-04
0.994	9.84E-05	1.925	5.30E-04
1.031	1.53E-04	2.094	4.41E-04
1.042	2.14E-04	2.096	5.30E-04
1.056	2.83E-04	2.099	4.41E-04
1.081	3.58E-04	2.222	3.58E-04
1.142	4.41E-04	2.419	2.83E-04
1.156	5.30E-04	2.421	3.58E-04
1.168	6.26E-04	2.422	2.83E-04
1.178	7.29E-04	2.593	2.14E-04
1.204	8.39E-04	2.738	1.53E-04
1.217	9.57E-04	3.011	9.84E-05
1.251	1.08E-03	3.374	5.07E-05
1.294	1.21E-03	3.817	9.97E-06
1.318	1.35E-03	3.9	0
1.432	1.21E-03		
1.446	1.08E-03		
1.465	9.57E-04		
1.554	8.39E-04		



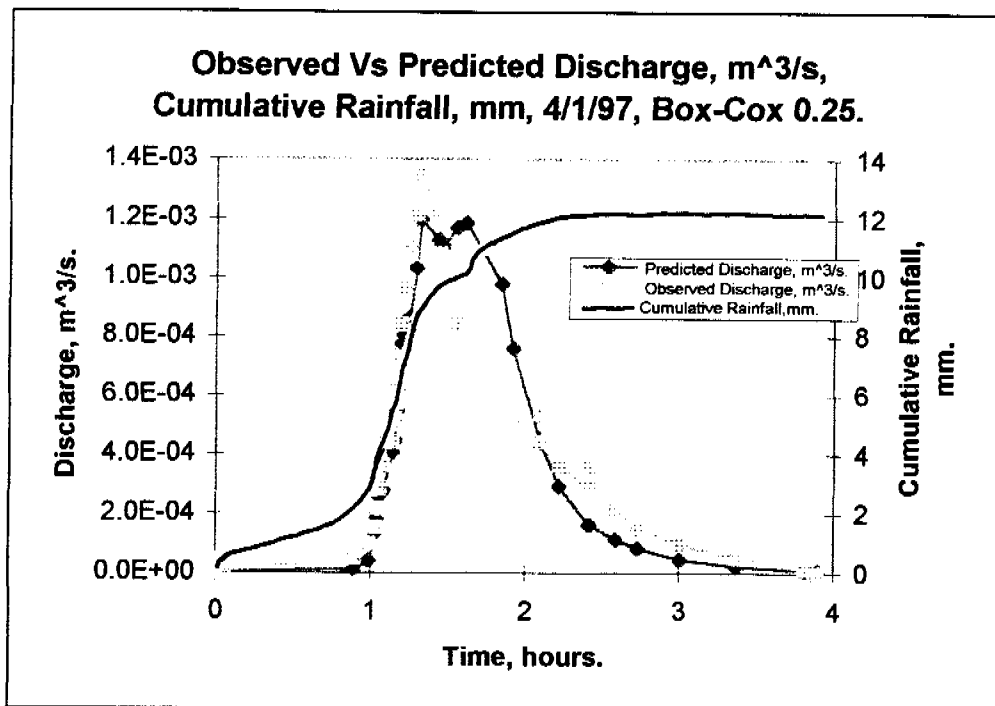
NLFIT Input files: 4197.fw, 4197.ro/rf.

NLFIT Output files: 4197.prt/pmf/plt.

Parameter.	Mean.	Standard Deviation.	Parameter.	Mean.	Standard Deviation.
C_r	6.775246	0.164583	$S\phi$	0.001	
e_m	1.29117	0.103352	ϕ	3.78292	0.458148

		Cumulative Periodogram.		Standardised Residual Versus Time.	Standardised Residual Versus N(0,1) Variate.		Auto Correlation Plot.	Partial Auto Correlation Plot.
Convergence Monitor.	R^2 , %.	Test Statistic.	5%.	Z.	Test Statistic.	5%.	Exceedances.	Exceedances.
0.213098	87.3	0.6704	0.3298	-4.293	0.2174	0.1479	7	4

Storm Specific Comment: The convergence monitor is not adequate, below 0.1, the R^2 is not adequate 87.3%, the cumulative periodogram does not pass the test statistic. The standardised residual versus time plot exceeds the Z statistic limit of $|2|$, the standardised residual versus N(0,1) variate does not pass the test statistic. The auto-correlation plot is exceeded 7 times, and the partial auto-correlation plot is exceeded 4 times.

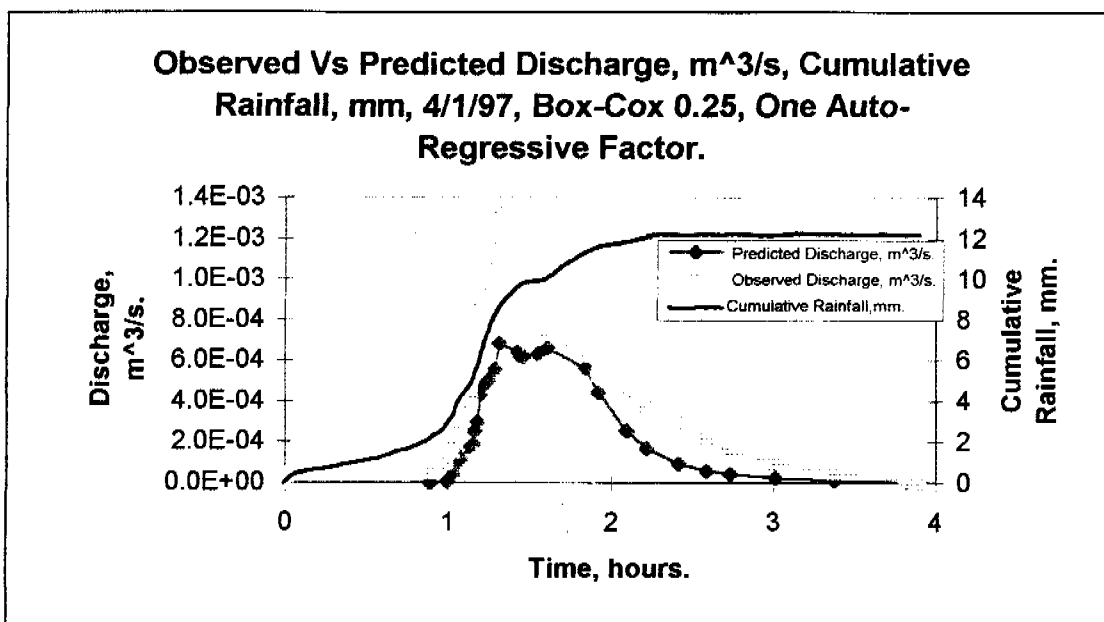


NLFIT Input files: 4197.fw, 4197.ro/rf.
NLFIT Output files: 4197G25.prt/pmf/plf.

Parameter.	Mean.	Standard Deviation.	Parameter.	Mean.	Standard Deviation.
C_r	0.77032	0.152273	$S\phi$	0.001	
e_m	1.31183	0.09616	ϕ	3.29316	0.405084

		Cumulative Periodogram.		Standardised Residual Versus Time.	Standardised Residual Versus N(0,1) Variate.		Auto Correlation Plot.	Partial Auto Correlation Plot.
Convergence Monitor.	R^2 , %.	Test Statistic.	5%.	Z.	Test Statistic.	5%.	Exceedances.	Exceedances.
0.196123	86.5	0.6981	0.3298	-4.604	0.2067	0.1479	6	4

Storm Specific Comment: The convergence monitor is not adequate, below 0.1, the R^2 is not adequate 86.5%, the cumulative periodogram does not pass the test statistic. The standardised residual versus time plot exceeds the Z statistic limit of |2|, the standardised residual versus N(0,1) variate does not pass the test statistic. The auto-correlation plot is exceeded 6 times, and the partial auto-correlation plot is exceeded 4 times.



NLFIT Input files: 4197.fw, 4197.ro/rf.

NLFIT Output files: 419725A.prt/pmf/plt.

Parameter.	Mean.	Standard Deviation.	Parameter.	Mean.	Standard Deviation.
C_r	0.931426	0.272287	$S\phi$	0.001	
e_m	1.33777	0.125770	ϕ	9.52134	2.54988

		Cumulative Periodogram.		Standardised Residual Versus Time.	Standardised Residual Versus N(0,1) Variate.		Auto Correlation Plot.	Partial Auto Correlation Plot.
		Test Statistic.	5%.	Z.	Test Statistic.	5%.	Exceedances.	Exceedances.
Convergence Monitor.	R^2 , %.	0.3442	0.3298	-3.586	0.0718	0.1479	1	1

Storm Specific Comment: The convergence monitor is not adequate, below 0.1, the R^2 is not adequate 84.6%, the cumulative periodogram does not pass the test statistic. The standardised residual versus time plot exceeds the Z statistic limit of $|2|$, the standardised residual versus N(0,1) variate does pass the test statistic. The auto-correlation plot is exceeded 1 times, and the partial auto-correlation plot is exceeded 1 times.

General Comments: The least squares prediction, 4197.*, was a relatively poor fit, however the inclining limb of the hydrograph was adequate. The peak is over-predicted and the recession limb changes from over-prediction to under-prediction. The recession limb, beyond 2 hours of the more general error model, Box-Cox 0.25, has a better shape when compared to the least squares fit, yet it suffers also from over prediction of the peak discharge and initial component of the recession limb. The inclusion of an auto-regressive factor was not advantageous as under-prediction was observed at every point.

11th-12th January

RUM 96-97 Monitoring

pit 1 site

Rainfall 11-12/1/97 2200hrs

149

0	0	1.34	5	1.382	10	1.421	15.6	1.478	21.6	1.654	26.2	1.743	31.6	1.878	35.8
1.263	0.4	1.343	5.2	1.383	10.2	1.424	16	1.485	21.8	1.66	26.4	1.749	31.8	1.922	36
1.275	0.6	1.344	5.4	1.385	10.4	1.426	16.4	1.499	22	1.665	26.8	1.753	32	2.365	36.4
1.285	0.8	1.347	5.6	1.386	10.6	1.429	16.8	1.524	22.2	1.671	27	1.754	32.2	2.525	36.6
1.29	1.2	1.35	6	1.388	11	1.432	17	1.543	22.6	1.675	27.2	1.757	32.4	2.664	36.8
1.296	1.4	1.353	6.4	1.39	11.2	1.433	17.2	1.553	22.8	1.679	27.6	1.763	32.6	2.824	37
1.301	1.6	1.356	6.6	1.393	11.6	1.435	17.4	1.56	23	1.685	27.8	1.764	32.8	3.042	37.2
1.307	2	1.358	7	1.396	12	1.438	17.8	1.565	23.2	1.689	28.2	1.769	33	3.043	37.4
1.311	2.2	1.361	7.4	1.399	12.4	1.44	18.2	1.567	23.4	1.693	28.4	1.775	33.2	3.29	37.6
1.314	2.4	1.364	7.6	1.4	12.6	1.443	18.4	1.572	23.6	1.697	28.6	1.779	33.4	4.1	37.6
1.315	2.6	1.365	7.8	1.403	13	1.446	18.8	1.579	23.8	1.699	28.8	1.781	33.6		
1.318	2.8	1.367	8	1.406	13.4	1.449	19.2	1.586	24	1.703	29	1.786	33.8		
1.322	3.2	1.369	8.4	1.408	13.8	1.451	19.4	1.588	24.2	1.707	29.4	1.794	34		
1.325	3.6	1.372	8.6	1.41	14	1.454	19.6	1.594	24.4	1.711	29.6	1.801	34.2		
1.328	3.8	1.374	8.8	1.411	14.2	1.456	19.8	1.604	24.6	1.715	30	1.803	34.4		
1.329	4	1.375	9	1.413	14.4	1.458	20	1.614	24.8	1.719	30.2	1.811	34.6		
1.331	4.2	1.376	9.2	1.414	14.6	1.461	20.4	1.624	25.2	1.724	30.4	1.822	34.8		
1.333	4.4	1.378	9.4	1.415	14.8	1.465	20.6	1.632	25.4	1.729	30.8	1.833	35		
1.336	4.6	1.379	9.6	1.417	15	1.468	21	1.64	25.6	1.733	31	1.846	35.4		
1.338	4.8	1.381	9.8	1.418	15.4	1.472	21.2	1.647	26	1.739	31.4	1.86	35.6		

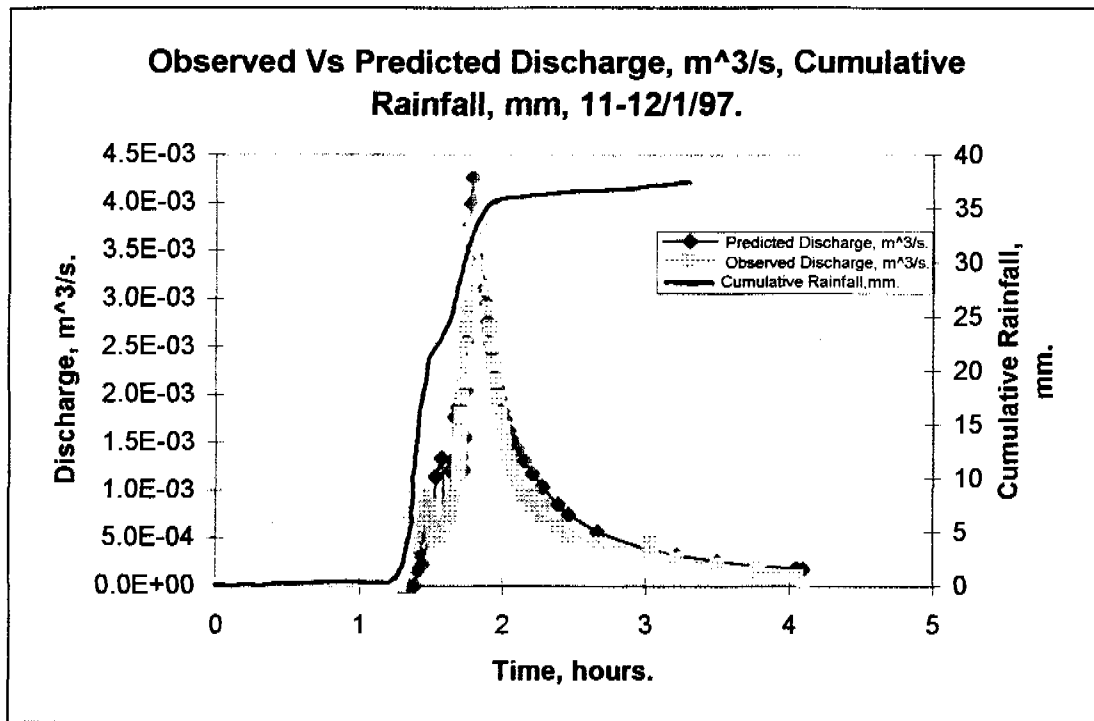
RUM 96-97 Monitoring

pit 1 site

Runoff 11-12/1/97 2200hrs

81

0	0	1.597	6.26E-04	1.776	3.54E-03	2.211	8.39E-04	4.1	0
1.281	9.97E-06	1.625	7.29E-04	1.788	3.77E-03	2.213	9.57E-04		
1.289	5.07E-05	1.643	8.39E-04	1.875	3.54E-03	2.214	8.39E-04		
1.297	9.84E-05	1.644	7.29E-04	1.876	3.77E-03	2.276	7.29E-04		
1.311	1.53E-04	1.646	8.39E-04	1.878	3.54E-03	2.278	8.39E-04		
1.326	2.14E-04	1.663	9.57E-04	1.886	3.32E-03	2.281	7.29E-04		
1.333	2.83E-04	1.686	1.08E-03	1.899	3.11E-03	2.388	6.26E-04		
1.344	3.58E-04	1.69	1.21E-03	1.906	2.90E-03	2.468	5.30E-04		
1.383	4.41E-04	1.696	1.35E-03	1.917	2.70E-03	2.663	4.41E-04		
1.392	5.30E-04	1.7	1.49E-03	1.925	2.51E-03	3.036	3.58E-04		
1.406	6.26E-04	1.704	1.65E-03	1.936	2.32E-03	3.039	4.41E-04		
1.414	7.29E-04	1.708	1.80E-03	1.951	2.14E-03	3.049	3.58E-04		
1.428	8.39E-04	1.715	1.97E-03	1.967	1.97E-03	3.218	2.83E-04		
1.442	9.57E-04	1.721	2.14E-03	1.982	1.80E-03	3.5	2.14E-04		
1.503	8.39E-04	1.726	2.32E-03	2.004	1.65E-03	3.782	1.53E-04		
1.51	7.29E-04	1.735	2.51E-03	2.017	1.49E-03	3.783	2.14E-04		
1.515	6.26E-04	1.743	2.70E-03	2.046	1.35E-03	3.785	1.53E-04		
1.521	5.30E-04	1.751	2.90E-03	2.069	1.21E-03	3.786	2.14E-04		
1.535	4.41E-04	1.761	3.11E-03	2.106	1.08E-03	3.788	1.53E-04		
1.574	5.30E-04	1.768	3.32E-03	2.153	9.57E-04	4.056	9.84E-05		



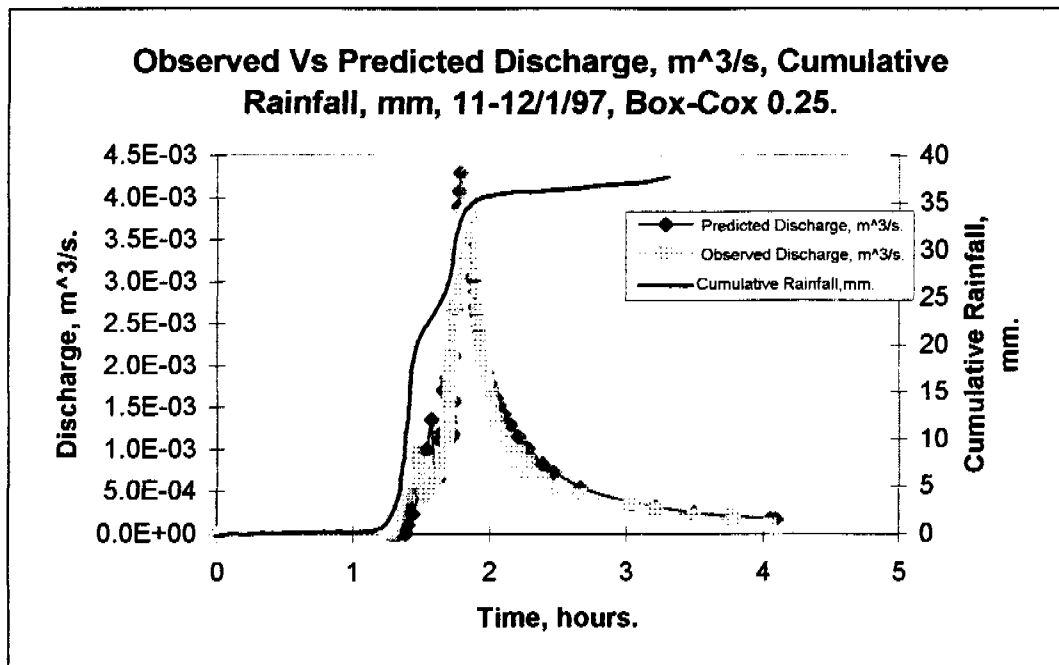
NLFIT Input files: 1112197.fw, 1112197.ro/rf.

NLFIT Output files: 1112197.prt/pmf/plt.

Parameter.	Mean.	Standard Deviation.	Parameter.	Mean.	Standard Deviation.
C_r	5.68622	0.950998	$S\phi$	0.001	
e_m	4.54421	0.221561	ϕ	22.6072	1.0667

		Cumulative Periodogram.		Standardised Residual Versus Time.	Standardised Residual Versus N(0,1) Variate.		Auto Correlation Plot.	Partial Auto Correlation Plot.
Convergence Monitor.	R^2 , %.	Test Statistic.	5%.	Z.	Test Statistic.	5%.	Exceedances.	Exceedances.
0.1495	86.3	0.6687	0.2178	-6.488	0.0908	0.0991	4	4

Storm Specific Comment: The convergence monitor is not adequate, below 0.1, the R^2 is not adequate 86.3%, the cumulative periodogram does not pass the test statistic. The standardised residual versus time plot exceeds the Z statistic limit of $|2|$, the standardised residual versus N(0,1) variate does pass the test statistic. The auto-correlation plot is exceeded 4 times, and the partial auto-correlation plot is exceeded 4 times.



NLFIT Input files: 1112197.fw, 1112197.ro/rf.

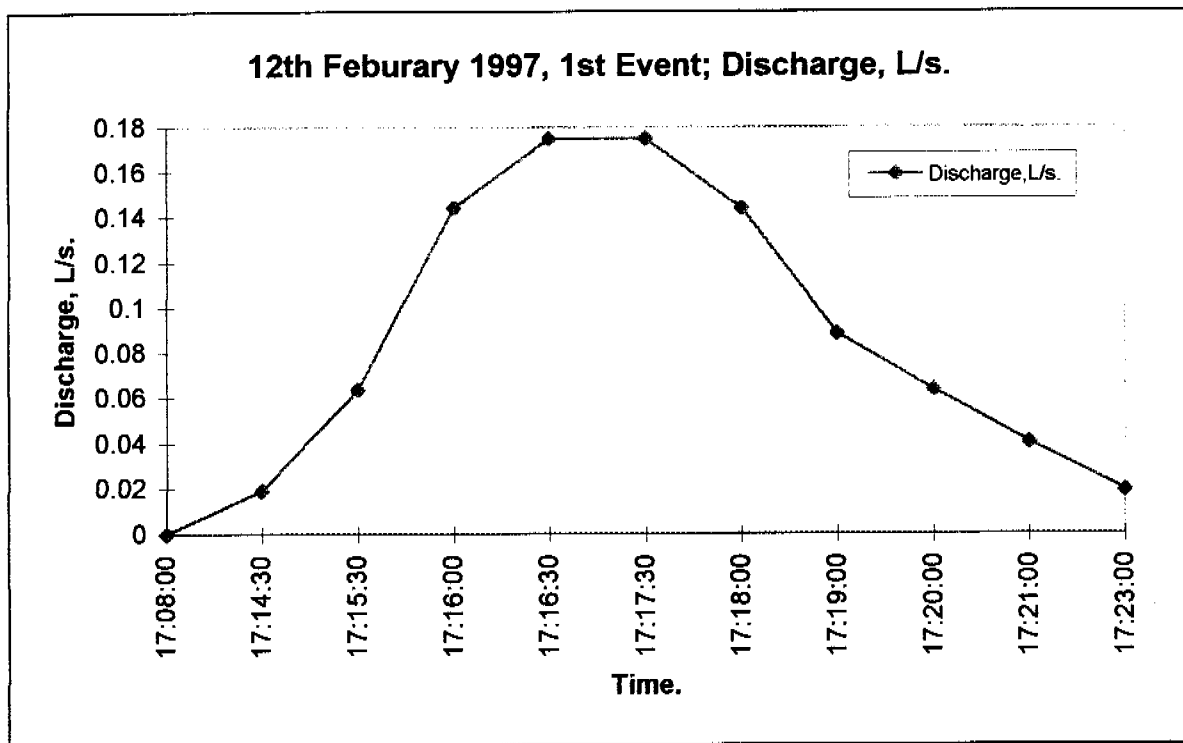
NLFIT Output files: 11197w25.prt/pmf/plt.

Parameter.	Mean.	Standard Deviation.	Parameter.	Mean.	Standard Deviation.
C_r	6.88617	1.34466	$S\phi$	0.001	
e_m	4.80447	0.248375	ϕ	22.2196	1.16230

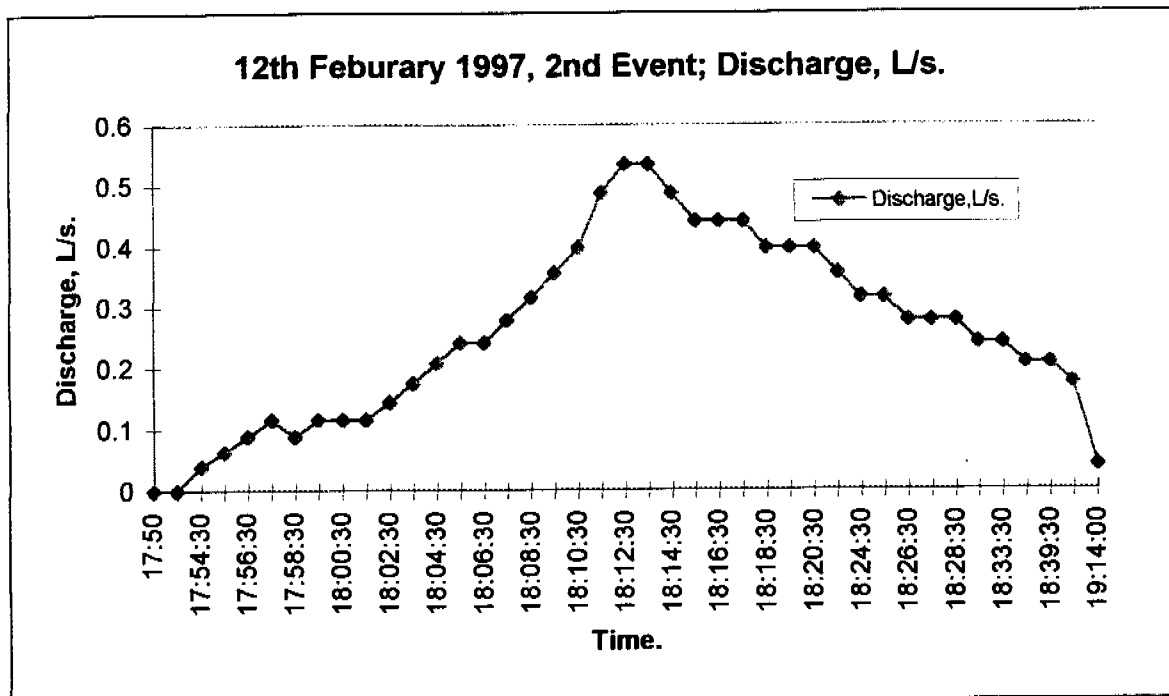
Convergence Monitor.	R^2 , %.	Cumulative Periodogram.		Standardised Residual Versus Time.	Standardised Residual Versus N(0,1) Variate.		Auto Correlation Plot.	Partial Auto Correlation Plot.
		Test Statistic.	5%.	Z.	Test Statistic.	5%.	Exceedances.	Exceedances.
0.04202	84.4	0.6722	0.2178	-6.06	0.0864	0.0991	8	4

Storm Specific Comment: The convergence monitor is adequate, below 0.1, the R^2 is not adequate 84.4%, the cumulative periodogram does not pass the test statistic. The standardised residual versus time plot exceeds the Z statistic limit of $|2|$, the standardised residual versus N(0,1) variate does pass the test statistic. The auto-correlation plot is exceeded 8 times, and the partial auto-correlation plot is exceeded 4 times.

General Comments: The original prediction, utilising a least squares error model was adequate, however, a more general error model, Box-Cox 0.25, produced the superior fit.



Storm Specific Comment: Due to failure of tipping bucket rainguage, cumulative rainfall was unavailable for this storm event.



Storm Specific Comment: Due to failure of tipping bucket rainguage, cumulative rainfall was unavailable for this storm event.

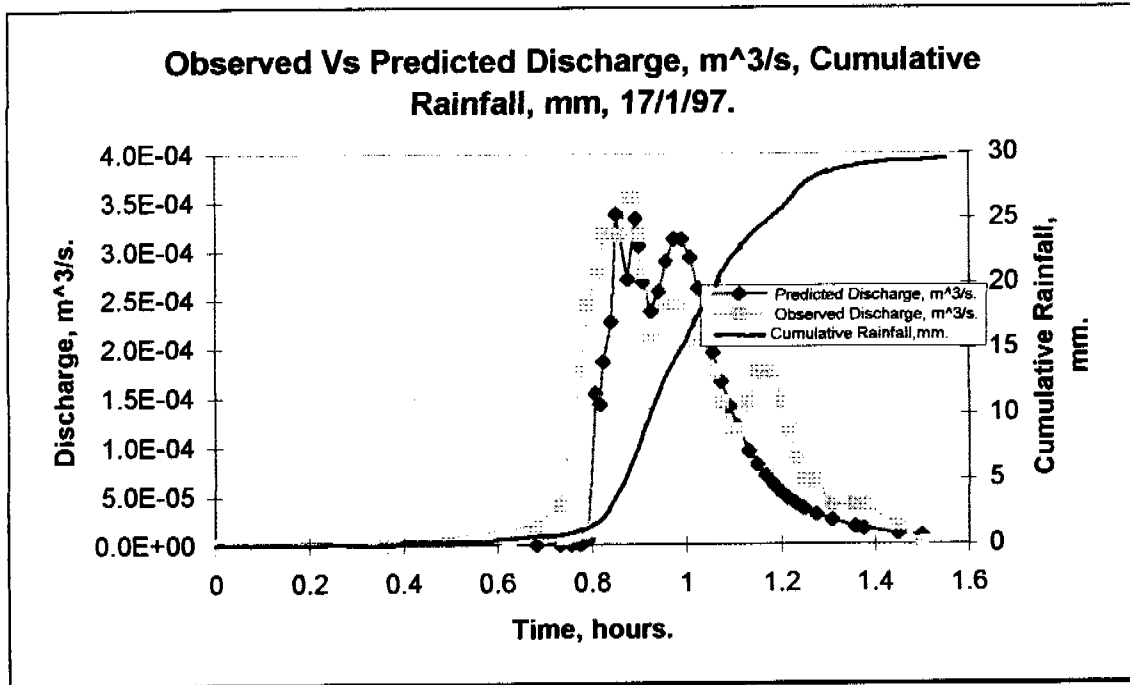
17th January

RUM 96-97 Monitoring
pit 1 site
Rainfall 17/1/97 1632hrs

0	0	0.942	18	1.45	29.6
0.367	0.2	0.958	19	1.5	29.6
0.683	0.8	0.975	20		
0.733	1.8	0.992	21		
0.758	3.4	1.008	22		
0.775	4.8	1.025	22.8		
0.783	5.6	1.042	23.4		
0.792	6	1.058	24.2		
0.8	6.8	1.075	24.4		
0.808	7.8	1.092	25.2		
0.817	8.4	1.108	25.8		
0.825	9	1.133	26.8		
0.842	10.6	1.15	27.4		
0.85	11.4	1.167	28		
0.858	12	1.183	28.2		
0.875	13.4	1.2	28.4		
0.892	14.6	1.217	28.6		
0.9	15.2	1.25	29		
0.908	15.8	1.308	29.2		
0.925	16.6	1.375	29.4		

RUM 96-97 Monitoring
pit 1 site
Runoff 17/1/97 1632hrs
43

0	0.00E+00	0.975	2.42E-04	1.375	4.06E-05
0.367	0.00E+00	0.992	2.42E-04	1.45	1.93E-05
0.683	1.93E-05	1.008	2.07E-04	1.5	0
0.733	4.06E-05	1.025	2.42E-04		
0.758	8.86E-05	1.042	2.07E-04		
0.775	1.75E-04	1.058	1.75E-04		
0.792	2.42E-04	1.075	1.44E-04		
0.808	2.78E-04	1.092	1.16E-04		
0.817	2.78E-04	1.108	1.16E-04		
0.825	3.16E-04	1.133	1.44E-04		
0.842	3.16E-04	1.15	1.75E-04		
0.85	3.16E-04	1.167	1.75E-04		
0.858	3.16E-04	1.183	1.75E-04		
0.875	3.56E-04	1.2	1.44E-04		
0.892	3.56E-04	1.217	1.16E-04		
0.9	3.16E-04	1.233	8.86E-05		
0.908	2.78E-04	1.25	6.37E-05		
0.925	2.07E-04	1.275	6.37E-05		
0.942	2.07E-04	1.308	4.06E-05		
0.958	2.42E-04	1.358	4.06E-05		



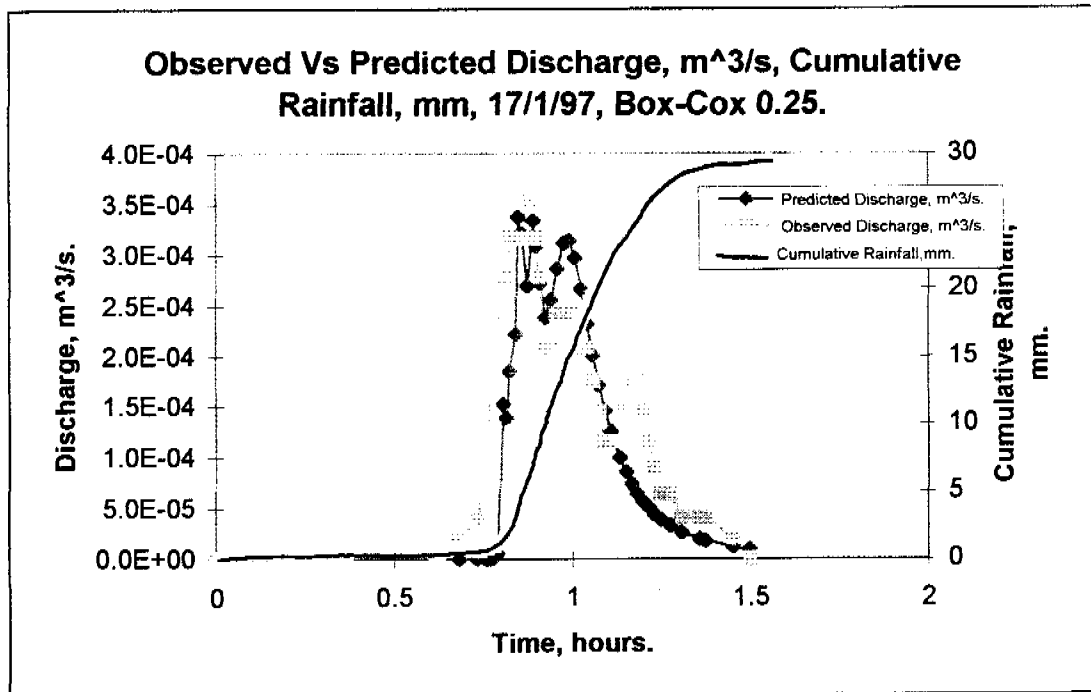
NLFIT Input files: 17197.fw, 17197.ro/rf.

NLFIT Output files: 17197w.prt/pmf/plf.

Parameter.	Mean.	Standard Deviation.	Parameter.	Mean.	Standard Deviation.
C_r	7.67941	7.31717	$S\phi$	0.001	
e_m	1.42309	0.234173	ϕ	85.5677	1.59935

		Cumulative Periodogram.		Standardised Residual Versus Time.	Standardised Residual Versus N(0,1) Variate.		Auto Correlation Plot.	Partial Auto Correlation Plot.
		Test Statistic.	5%.	Z.	Test Statistic.	5%.	Exceedances.	Exceedances.
Convergence Monitor.	R^2 , %.	0.6571	0.3041	-4.79	0.1061	0.1371	9	6

Storm Specific Comment: The convergence monitor is adequate, below 0.1, the R^2 is not adequate 66.4%, the cumulative periodogram does not pass the test statistic. The standardised residual versus time plot exceeds the Z statistic limit of $|2|$, the standardised residual versus N(0,1) variate does pass the test statistic. The auto-correlation plot is exceeded 9 times, and the partial auto-correlation plot is exceeded 6 times.



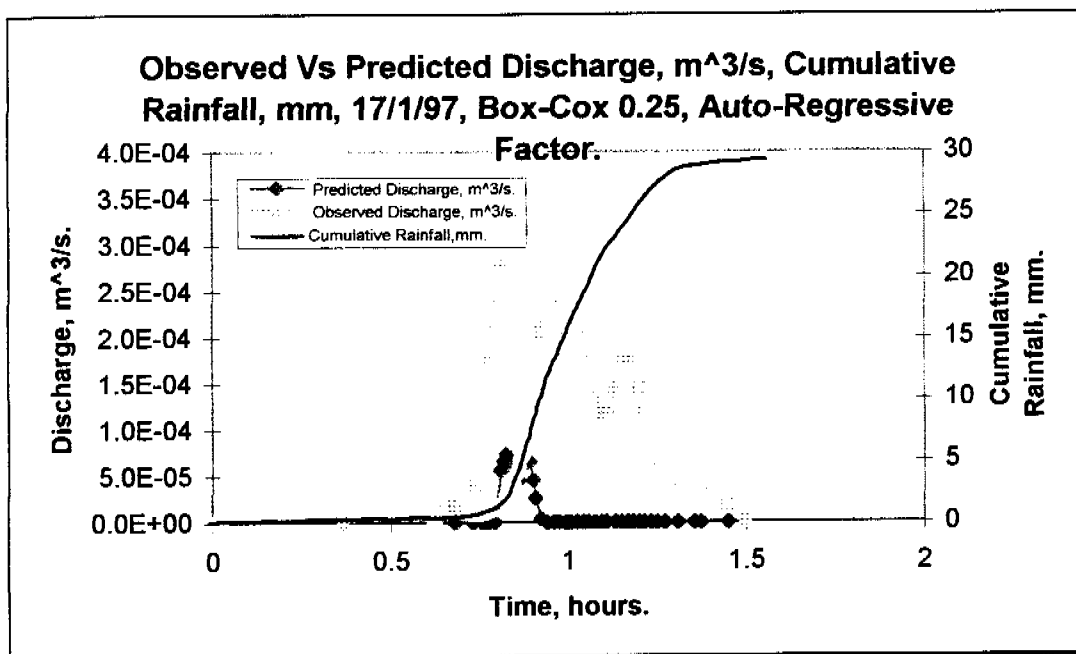
NLFIT Input files: 17197.fw, 17197.ro/rf.

NLFIT Output files: 17197w25.prt/pmf/plt.

Parameter.	Mean.	Standard Deviation.	Parameter.	Mean.	Standard Deviation.
C_r	8.1221	7.88141	$S\phi$	0.001	
e_m	1.44145	0.238411	ϕ	85.2681	1.6366

		Cumulative Periodogram.		Standardised Residual Versus Time.	Standardised Residual Versus N(0,1) Variate.		Auto Correlation Plot.	Partial Auto Correlation Plot.
Convergence Monitor.	R^2 , %.	Test Statistic.	5%.	Z.	Test Statistic.	5%.	Exceedances.	Exceedances.
0.02936	65.7	0.6578	0.3041	-4.79	0.1069	0.1371	9	5

Storm Specific Comment: The convergence monitor is adequate, below 0.1, the R^2 is not adequate 65.7%, the cumulative periodogram does not pass the test statistic. The standardised residual versus time plot exceeds the Z statistic limit of $|2|$, the standardised residual versus N(0,1) variate does pass the test statistic. The auto-correlation plot is exceeded 9 times, and the partial auto-correlation plot is exceeded 5 times.



NLFIT Input files: 17197.fw, 17197.ro/rf.

NLFIT Output files: 17197wa.prt/pmf/plt.

Parameter.	Mean.	Standard Deviation.	Parameter.	Mean.	Standard Deviation.
C_r	2.3178	2.8068	$S\phi$	0.001	
e_m	0.94507	0.1841	ϕ	107.87	3.6323

		Cumulative Periodogram.		Standardised Residual Versus Time.	Standardised Residual Versus N(0,1) Variate.		Auto Correlation Plot.	Partial Auto Correlation Plot.
		Test Statistic.	5%.	Z.	Test Statistic.	5%.	Exceedances.	Exceedances.
Convergence Monitor.	R^2 , %.							
0.01202	49.8	0.3647	0.3041	-2.251	0.1327	0.1371	1	1

Storm Specific Comment: The convergence monitor is adequate, below 0.1, the R^2 is not adequate 49.8%, the cumulative periodogram does not pass the test statistic. The standardised residual versus time plot exceeds the Z statistic limit of $|2|$, the standardised residual versus N(0,1) variate does pass the test statistic. The auto-correlation plot is exceeded 1 times, and the partial auto-correlation plot is exceeded 1 times.

General Comment: The utilisation of a more general error model with a Box Cox of 0.25, 17197w25.*, did not improve the predicted response over the general error model, 17197w. The addition of an auto-regressive factor, 17197wa.*, yielded a very poor predicted response.

19th January

RUM 96-97 Monitoring

pit 1 site

Rainfall 19/1/97 1642hrs

84

0	0	0.965	4.6	1.006	9.6	1.053	14.8	1.368	19.2
0.043	0.2	0.967	4.8	1.008	10	1.054	15	1.758	19.4
0.115	0.4	0.968	5	1.011	10.2	1.056	15.2	1.792	19.6
0.836	0.6	0.969	5.2	1.015	10.6	1.058	15.4	1.9	19.6
0.869	0.8	0.971	5.6	1.018	10.8	1.06	15.6		
0.871	1	0.974	6	1.022	11.2	1.061	15.8		
0.907	1.2	0.976	6.4	1.025	11.4	1.064	16.2		
0.933	1.4	0.979	6.6	1.028	11.8	1.067	16.4		
0.938	1.8	0.982	7	1.031	12	1.069	16.6		
0.942	2	0.985	7.4	1.032	12.2	1.071	16.8		
0.944	2.2	0.988	7.6	1.033	12.4	1.081	17		
0.946	2.4	0.99	7.8	1.036	12.8	1.088	17.2		
0.949	2.8	0.992	8	1.039	13	1.1	17.4		
0.951	3	0.993	8.2	1.04	13.2	1.114	17.8		
0.953	3.2	0.994	8.4	1.042	13.4	1.135	18		
0.954	3.4	0.997	8.6	1.043	13.6	1.165	18.2		
0.957	3.6	0.999	8.8	1.044	13.8	1.185	18.4		
0.958	3.8	1	9	1.047	14.2	1.219	18.6		
0.961	4.2	1.001	9.2	1.05	14.4	1.221	18.8		
0.964	4.4	1.003	9.4	1.051	14.6	1.251	19		

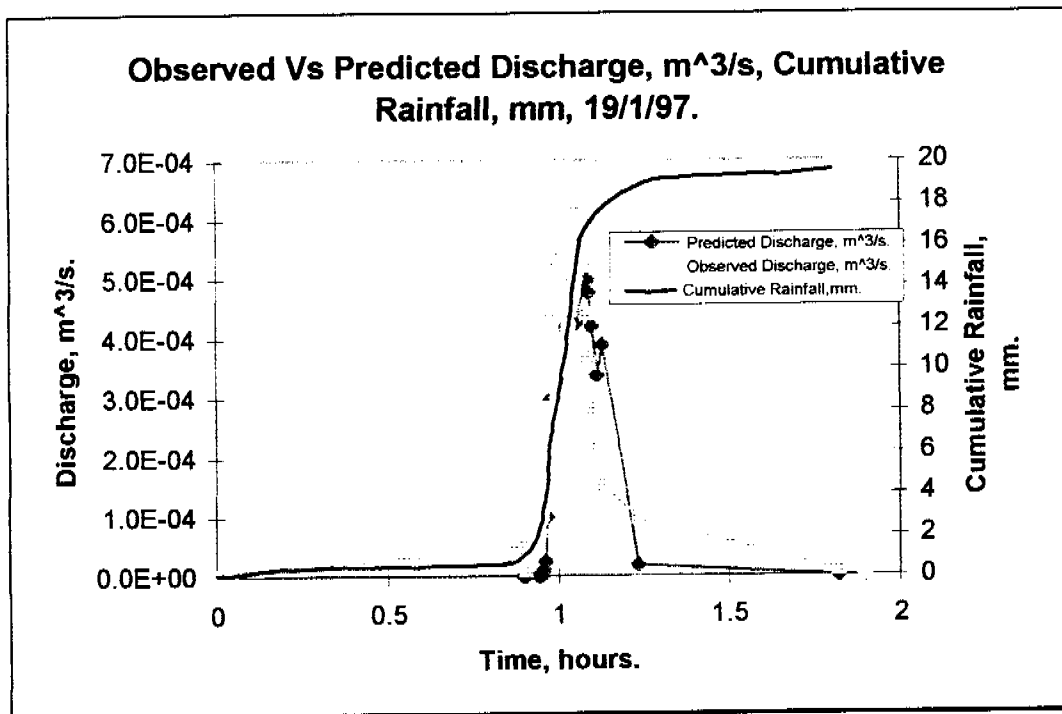
RUM 96-97 Monitoring

pit 1 site

Runoff 19/1/97 1642hrs

23

0	0	1.236	9.84E-05
0.899	5.07E-05	1.822	9.97E-06
0.906	9.97E-06	1.9	0
0.907	5.07E-05		
0.942	9.84E-05		
0.951	1.53E-04		
0.958	2.14E-04		
0.963	2.83E-04		
0.969	3.58E-04		
0.976	4.41E-04		
0.983	5.30E-04		
1.025	4.41E-04		
1.026	5.30E-04		
1.054	6.26E-04		
1.079	5.30E-04		
1.086	4.41E-04		
1.092	3.58E-04		
1.1	2.83E-04		
1.115	2.14E-04		
1.131	1.53E-04		



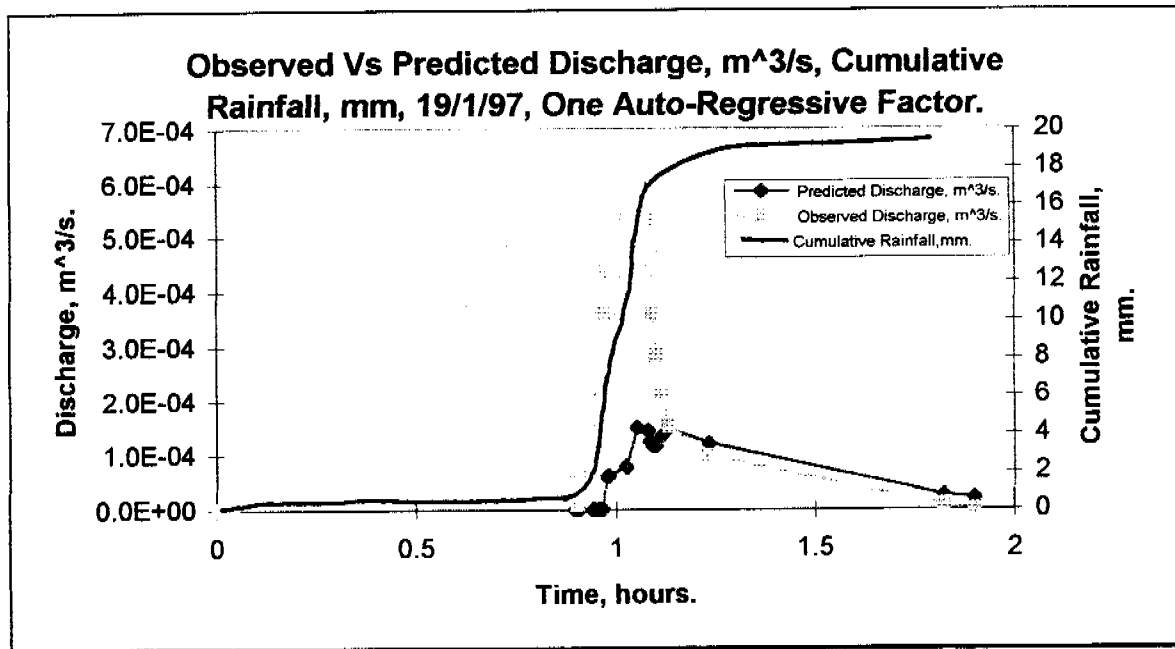
NLFIT Input files: 19197.fw, 19197.ro/rf.

NLFIT Output files: 19197.prt/pmf/plt.

Parameter.	Mean.	Standard Deviation.	Parameter.	Mean.	Standard Deviation.
C_r	0.46137	0.364846	$S\phi$	0.001	
e_m	0.72775	0.18173	ϕ	133.278	3.13251

		Cumulative Periodogram.		Standardised Residual Versus Time.	Standardised Residual Versus N(0,1) Variate.		Auto Correlation Plot.	Partial Auto Correlation Plot.
		Test Statistic.	5%.	Z.	Test Statistic.	5%.	Exceedances.	Exceedances.
Convergence Monitor.	R^2 , %.	0.6221	0.4301	-3.539	0.102	0.1881	4	2

Storm Specific Comment: The convergence monitor is adequate, below 0.1, the R^2 is not adequate 58.3%, the cumulative periodogram does not pass the test statistic. The standardised residual versus time plot exceeds the Z statistic limit of $|2|$, the standardised residual versus N(0,1) variate does pass the test statistic. The auto-correlation plot is exceeded 4 times, and the partial auto-correlation plot is exceeded 2 times.



NLFIT Input files: 19197.fw, 19197.ro/rf.

NLFIT Output files: 19197ar1.prt/pmf/plt.

Parameter.	Mean.	Standard Deviation.	Parameter.	Mean.	Standard Deviation.
C_r	20.3043	74.4625	$S\phi$	0.001	
e_m	1.8244	0.951322	ϕ	135.641	13.0241

		Cumulative Periodogram.		Standardised Residual Versus Time.	Standardised Residual Versus N(0,1) Variate.		Auto Correlation Plot.	Partial Auto Correlation Plot.
Convergence Monitor.	R^2 , %.	Test Statistic.	5%.	Z.	Test Statistic.	5%.	Exceedances.	Exceedances.
0.3388	15.2	0.4567	0.4301	-1.723	0.133	0.1841	3	3

Storm Specific Comment: The convergence monitor is adequate, below 0.1, the R^2 is not adequate 15.2%, the cumulative periodogram does not pass the test statistic. The standardised residual versus time plot does not exceed the Z statistic limit of $|2|$, the standardised residual versus N(0,1) variate does pass the test statistic. The auto-correlation plot is exceeded 3 times, and the partial auto-correlation plot is exceeded 3 times.

General Comments: 19197.* was a relatively poor fit as the inclination and recession limbs are under-predicted, the immediate addition of an auto-regressive factor worsened the predicted response considerably, 19197ar1.*.

21st January 1st Event

RUM 96-97 Monitoring

pit 1 site

Rainfall 21/1/97 1529hrs

51

0	0	0.267	4.6	0.333	9.6
0.063	0.2	0.271	4.8	0.339	9.8
0.088	0.4	0.275	5.2	0.349	10.2
0.089	0.6	0.279	5.4	0.354	10.4
0.131	0.8	0.283	5.6	0.36	10.8
0.199	1	0.285	5.8	0.364	11
0.215	1.2	0.288	6	0.372	11.2
0.221	1.4	0.292	6.4	0.382	11.6
0.222	1.6	0.294	6.6	0.4	11.8
0.228	1.8	0.297	7	0.431	12
0.233	2	0.3	7.2	0.77	12
0.235	2.2	0.304	7.6		
0.236	2.4	0.307	7.8		
0.24	2.8	0.311	8.2		
0.243	3	0.314	8.4		
0.247	3.2	0.318	8.6		
0.249	3.4	0.319	8.8		
0.253	3.6	0.324	9		
0.257	4	0.328	9.2		
0.263	4.2	0.329	9.4		

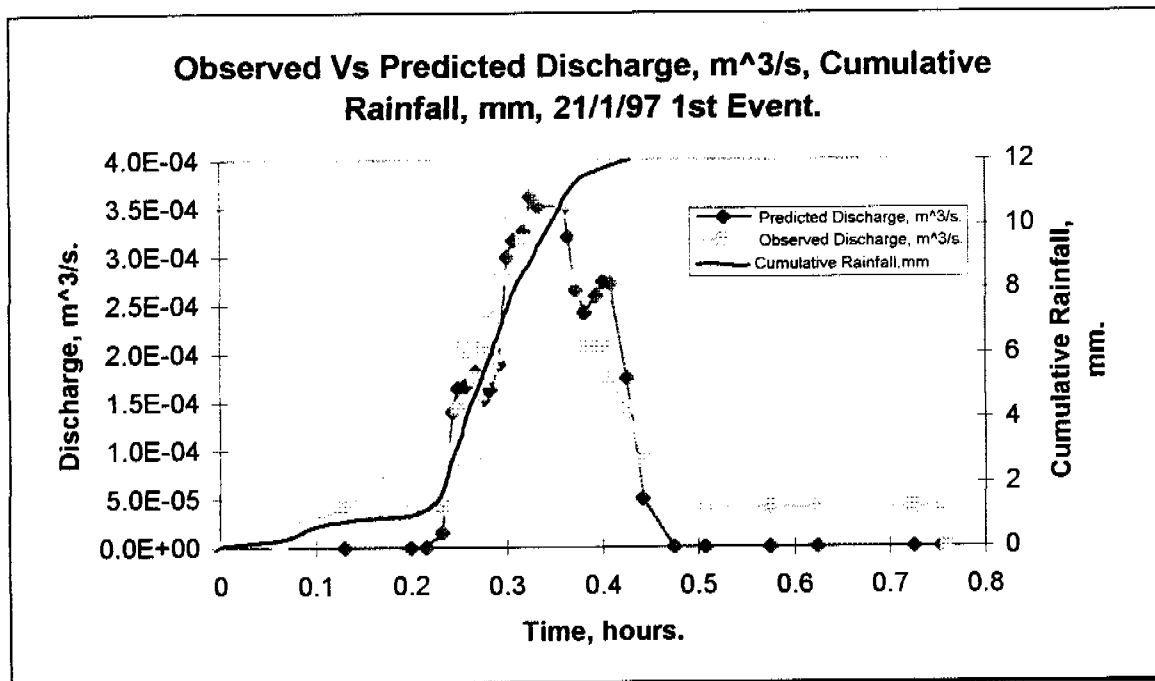
RUM 96-97 Monitoring

pit 1 site

Runoff 21/1/97 1529hrs

33

0	0.00E+00	0.382	2.07E-04
0.131	4.06E-05	0.393	2.07E-04
0.199	4.06E-05	0.4	2.07E-04
0.215	4.06E-05	0.408	1.75E-04
0.233	4.06E-05	0.425	1.44E-04
0.243	8.86E-05	0.442	8.86E-05
0.249	1.44E-04	0.475	6.37E-05
0.257	2.07E-04	0.508	4.06E-05
0.267	1.75E-04	0.575	4.06E-05
0.275	2.07E-04	0.625	4.06E-05
0.283	2.42E-04	0.725	4.06E-05
0.292	2.78E-04	0.754	4.06E-05
0.3	2.78E-04	0.76	0
0.307	2.78E-04		
0.318	3.16E-04		
0.325	3.98E-04		
0.333	3.98E-04		
0.36	3.98E-04		
0.364	3.56E-04		
0.372	2.78E-04		



NLFIT Input files: 211971ma.fw, 211971ma.ro/rf.

NLFIT Output files: 211971ma.prt/pmf/plt.

Parameter.	Mean.	Standard Deviation.	Parameter.	Mean.	Standard Deviation.
C_r	1.40487	0.43596	$S\phi$	0.001	
e_m	0.89214	0.05896	ϕ	86.88	0.8426

		Cumulative Periodogram.		Standardised Residual Versus Time.	Standardised Residual Versus N(0,1) Variate.		Auto Correlation Plot.	Partial Auto Correlation Plot.
		Test Statistic.	5%.	Z.	Test Statistic.	5%.	Exceedances.	Exceedances.
Convergence Monitor.	R^2 , %.	0.5371	0.3512	-2.479	0.2330	0.1567	4	2

Storm Specific Comment: The convergence monitor is adequate, below 0.1, the R^2 is not adequate 88.5%, the cumulative periodogram does not pass the test statistic. The standardised residual versus time plot exceeds the Z statistic limit of [2], the standardised residual versus N(0,1) variate does not pass the test statistic. The auto-correlation plot is exceeded 4 times, and the partial auto-correlation plot is exceeded 2 times.

General Comment: 211971ma.* has a predicted response that is adequate compared to that which is observed, major problems exist in the areas of the inclination and recession. The centre section is not precisely predicted by the model.

21st January 2nd Event

RUM 96-97 Monitoring

pit 1 site

Rainfall 21/1/97 1658hrs

94

0	0	0.083	5	0.14	11	0.2	16.8	0.525	21.2
0.007	0.2	0.086	5.2	0.142	11.2	0.207	17	0.596	21.4
0.015	0.4	0.09	5.6	0.144	11.6	0.208	17.2	0.719	21.6
0.024	0.8	0.093	5.8	0.147	11.8	0.214	17.4	0.721	21.8
0.031	1	0.096	6.2	0.15	12.2	0.221	17.6	0.942	22
0.038	1.2	0.1	6.6	0.153	12.6	0.228	17.8	1.099	22.2
0.043	1.6	0.103	6.8	0.156	12.8	0.229	18	1.417	22.4
0.049	1.8	0.106	7.2	0.158	13.2	0.236	18.2	1.526	22.8
0.051	2.2	0.108	7.4	0.161	13.4	0.244	18.4	1.632	23
0.054	2.4	0.11	7.6	0.163	13.6	0.256	18.8	1.714	23.2
0.058	2.8	0.113	7.8	0.165	13.8	0.269	19	1.789	23.4
0.061	3	0.115	8.2	0.168	14.2	0.282	19.2	1.84	23.8
0.064	3.4	0.118	8.4	0.171	14.6	0.294	19.4	1.85	24.6
0.067	3.6	0.121	8.8	0.174	14.8	0.306	19.8	1.9	24.6
0.068	3.8	0.125	9	0.178	15.2	0.321	20		
0.071	4	0.128	9.4	0.182	15.4	0.338	20.2		
0.074	4.2	0.131	9.8	0.185	15.8	0.369	20.4		
0.075	4.4	0.133	10.2	0.188	16	0.404	20.6		
0.079	4.6	0.136	10.6	0.19	16.4	0.406	20.8		
0.082	4.8	0.138	10.8	0.194	16.6	0.465	21		

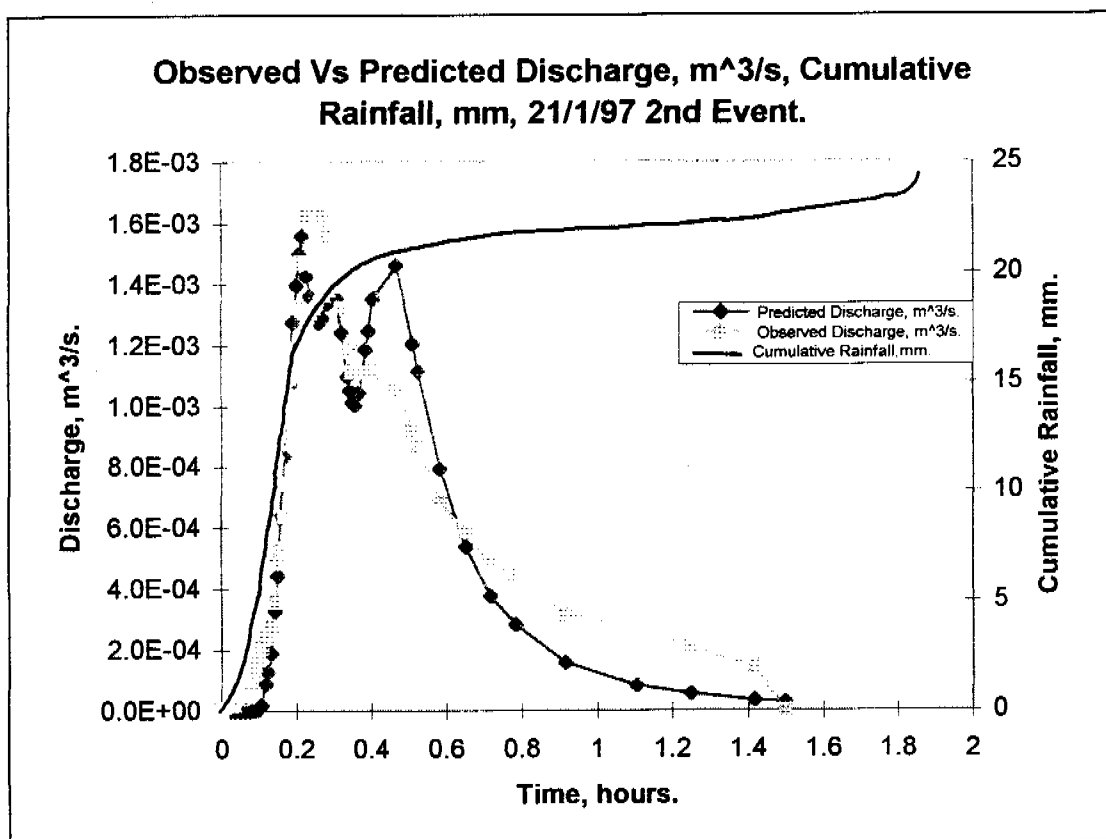
RUM 96-97 Monitoring

pit 1 site

Runoff 21/1/97 1658hrs

72

0	0.00E+00	0.294	1.08E-03	0.464	8.39E-04	0.908	2.83E-04
0.036	9.97E-06	0.336	9.57E-04	0.467	9.57E-04	0.91	3.58E-04
0.044	5.07E-05	0.338	1.08E-03	0.468	8.39E-04	0.911	2.83E-04
0.064	9.84E-05	0.339	9.57E-04	0.511	7.29E-04	0.915	3.58E-04
0.074	1.53E-04	0.342	1.08E-03	0.513	8.39E-04	0.917	2.83E-04
0.103	2.14E-04	0.343	9.57E-04	0.514	7.29E-04	1.103	2.14E-04
0.11	2.83E-04	0.344	1.08E-03	0.579	6.26E-04	1.25	1.53E-04
0.118	3.58E-04	0.346	9.57E-04	0.581	7.29E-04	1.256	2.14E-04
0.125	4.41E-04	0.347	1.08E-03	0.583	6.26E-04	1.257	1.53E-04
0.135	5.30E-04	0.349	9.57E-04	0.651	5.30E-04	1.842	2.14E-04
0.14	6.26E-04	0.35	1.08E-03	0.653	6.26E-04	1.856	1.53E-04
0.15	7.29E-04	0.351	9.57E-04	0.654	5.30E-04	1.9	0
0.154	8.39E-04	0.356	1.08E-03	0.656	6.26E-04		
0.161	9.57E-04	0.357	9.57E-04	0.657	5.30E-04		
0.172	1.08E-03	0.386	1.08E-03	0.658	6.26E-04		
0.178	1.21E-03	0.388	9.57E-04	0.66	5.30E-04		
0.19	1.35E-03	0.39	1.08E-03	0.714	4.41E-04		
0.196	1.49E-03	0.392	9.57E-04	0.715	5.30E-04		
0.243	1.35E-03	0.403	1.08E-03	0.717	4.41E-04		
0.263	1.21E-03	0.404	9.57E-04	0.785	3.58E-04		



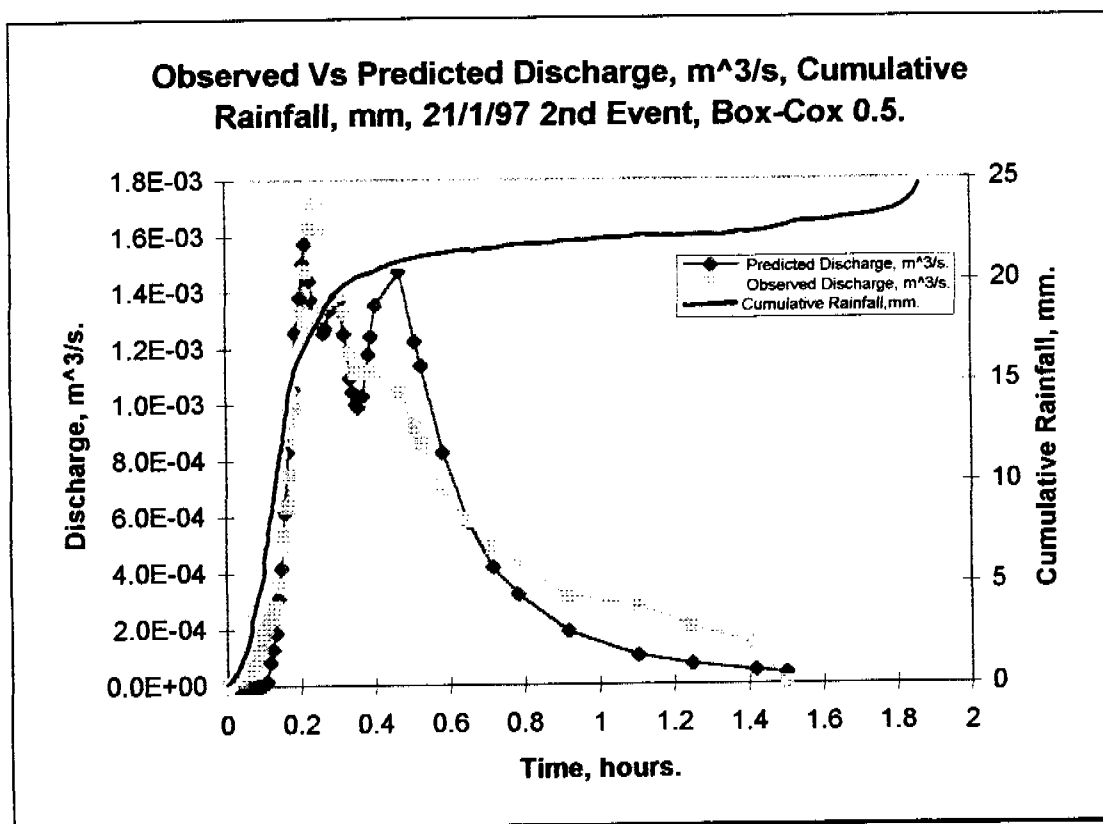
NLFIT Input files: 211972ma.fw, 211972ma.ro/rf

NLFIT Output files: 211972ma.prt/pmf/plt.

Parameter.	Mean.	Standard Deviation.	Parameter.	Mean.	Standard Deviation.
C_r	1.92171	0.4953	$S\phi$	15.1560	7.45779
e_m	1.4351	0.155761	ϕ	8.37335	26.733

		Cumulative Periodogram.		Standardised Residual Versus Time.	Standardised Residual Versus N(0,1) Variate.		Auto Correlation Plot.	Partial Auto Correlation Plot.
Convergence Monitor.	R^2 , %.	Test Statistic.	5%.	Z.	Test Statistic.	5%.	Exceedances.	Exceedances.
0.198951	90.3	0.7105	0.272	-5.659	0.1378	0.1223	13	6

Storm Specific Comment: The convergence monitor is not adequate, below 0.1, the R^2 is adequate 90.3%, the cumulative periodogram does not pass the test statistic. The standardised residual versus time plot exceeds the Z statistic limit of $|2|$, the standardised residual versus N(0,1) variate does not pass the test statistic. The auto-correlation plot is exceeded 13 times, and the partial auto-correlation plot is exceeded 6 times.

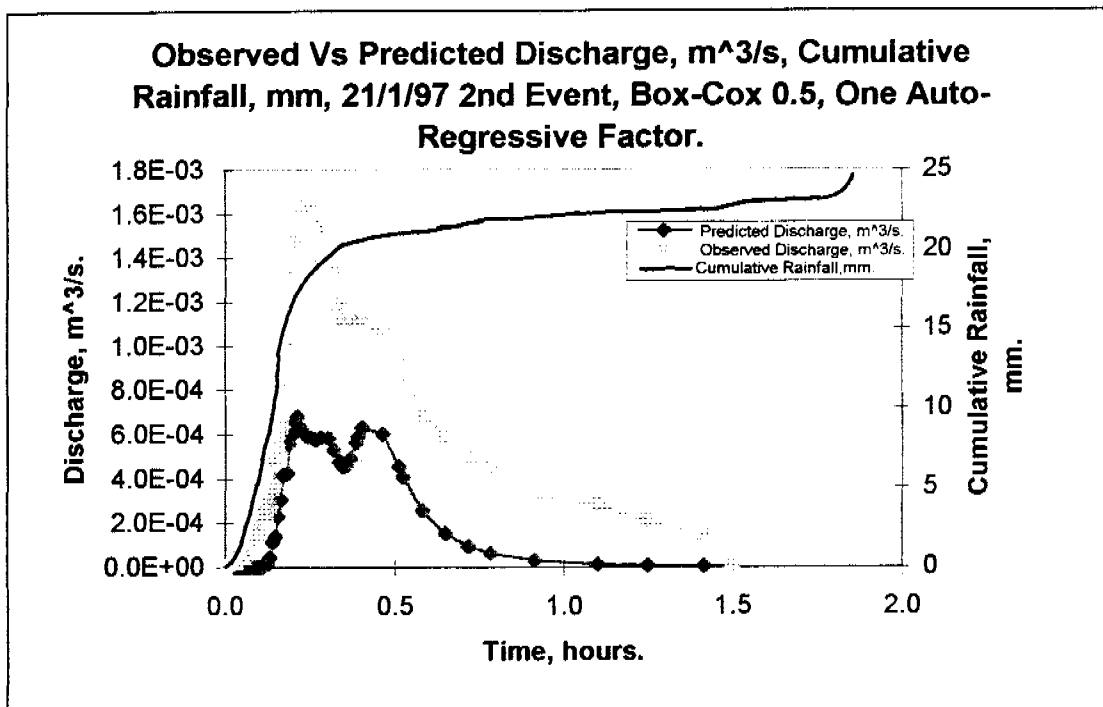


NLFIT Input files: 211972ma.fw, 211972ma.ro/rf
 NLFIT Output files: 211972m5.prt/pmf/plt.

Parameter.	Mean.	Standard Deviation.	Parameter.	Mean.	Standard Deviation.
C_r	2.16115	0.53374	$S\phi$	14.9971	8.21074
e_m	1.51277	0.1533003	ϕ	7.54384	29.6416

Convergence Monitor.	R^2 , %.	Cumulative Periodogram.		Standardised Residual Versus Time.	Standardised Residual Versus N(0,1) Variate.		Auto Correlation Plot.	Partial Auto Correlation Plot.
		Test Statistic.	5%.	Z.	Test Statistic.	5%.	Exceedances.	Exceedances.
0.140712	90.1	0.7019	0.272	-5.659	0.1249	0.1223	12	4

Storm Specific Comment: The convergence monitor is not adequate, below 0.1, the R^2 is adequate 90.1%, the cumulative periodogram does not pass the test statistic. The standardised residual versus time plot exceeds the Z statistic limit of |2|, the standardised residual versus N(0,1) variate does pass the test statistic. The auto-correlation plot is exceeded 12 times, and the partial auto-correlation plot is exceeded 4 times.



NLFIT Input files: 211972ma.fw, 211972ma.ro/rf

NLFIT Output files: 2119725a.prt/pmf/plf.

Parameter.	Mean.	Standard Deviation.	Parameter.	Mean.	Standard Deviation.
C_r	1.98791	0.80197	$S\phi$	17.8263	14.7934
e_m	1.26774	0.15133	ϕ	18.9524	52.6817

		Cumulative Periodogram.		Standardised Residual Versus Time.	Standardised Residual Versus N(0,1) Variate.		Auto Correlation Plot.	Partial Auto Correlation Plot.
Convergence Monitor.	R^2 , %.	Test Statistic.	5%.	Z.	Test Statistic.	5%.	Exceedances.	Exceedances.
0.647961	90.9	0.3036	0.272	-3.057	0.1606	0.1223	3	2

Storm Specific Comment: The convergence monitor is not adequate, below 0.1, the R^2 is adequate 90.9%, the cumulative periodogram does not pass the test statistic. The standardised residual versus time plot exceeds the Z statistic limit of $|2|$, the standardised residual versus N(0,1) variate does not pass the test statistic. The auto-correlation plot is exceeded 3 times, and the partial auto-correlation plot is exceeded 2 times.

General Comment: There is little improvement in the predicted response between the least squares error model, 211972ma.*, and 211972m5.*, ie with a Box-Cox factor of 0.5. The addition of an auto-regressive factor deteriorates the predicted response, 2119725a.*.

22nd January

RUM 96-97 Monitoring

pit 1 site

Rainfall 22/1/97 1441hrs

135

0	0	0.164	4.4	1.328	9	2.357	14	2.869	18.6	3.686	23.2	4.49	28
0.008	0.4	1.074	4.6	1.333	9.4	2.363	14.2	2.926	18.8	3.713	23.6	4.528	28.2
0.026	0.6	1.146	5	1.34	9.6	2.364	14.4	2.943	19	3.744	23.8	4.568	28.4
0.029	0.8	1.2	5.2	1.346	9.8	2.374	14.6	2.961	19.2	3.786	24	4.636	28.6
0.036	1	1.225	5.4	1.353	10.2	2.383	14.8	2.963	19.4	3.822	24.2	4.728	29
0.042	1.2	1.256	5.6	1.36	10.4	2.394	15	2.992	19.6	3.856	24.4	4.829	29.2
0.049	1.4	1.267	5.8	1.368	10.6	2.413	15.4	3.06	19.8	3.892	24.8	4.969	29.4
0.05	1.6	1.268	6	1.378	11	2.426	15.6	3.128	20	3.925	25	5.099	29.6
0.064	1.8	1.274	6.2	1.389	11.2	2.446	15.8	3.182	20.4	3.968	25.2	5.257	29.8
0.079	2	1.279	6.6	1.396	11.4	2.461	16	3.232	20.6	4.017	25.4	5.378	30
0.09	2.2	1.285	6.8	1.404	11.6	2.472	16.4	3.278	20.8	4.068	25.8	5.379	30.2
0.092	2.4	1.29	7	1.406	11.8	2.482	16.6	3.321	21	4.101	26	5.651	30.4
0.1	2.6	1.296	7.2	1.419	12	2.496	16.8	3.369	21.2	4.132	26.2	5.94	30.6
0.108	2.8	1.297	7.4	2.161	12.2	2.515	17	3.421	21.6	4.175	26.4	6.471	30.8
0.118	3	1.301	7.6	2.278	12.4	2.538	17.2	3.458	21.8	4.238	26.6	8.2	30.8
0.119	3.2	1.307	8	2.294	12.8	2.539	17.4	3.497	22	4.3	26.8		
0.131	3.4	1.313	8.2	2.315	13	2.554	17.6	3.538	22.2	4.301	27		
0.136	3.6	1.318	8.4	2.331	13.2	2.575	17.8	3.576	22.6	4.353	27.2		
0.142	4	1.322	8.6	2.339	13.6	2.625	18	3.615	22.8	4.396	27.4		
0.149	4.2	1.324	8.8	2.349	13.8	2.736	18.4	3.649	23	4.446	27.6		

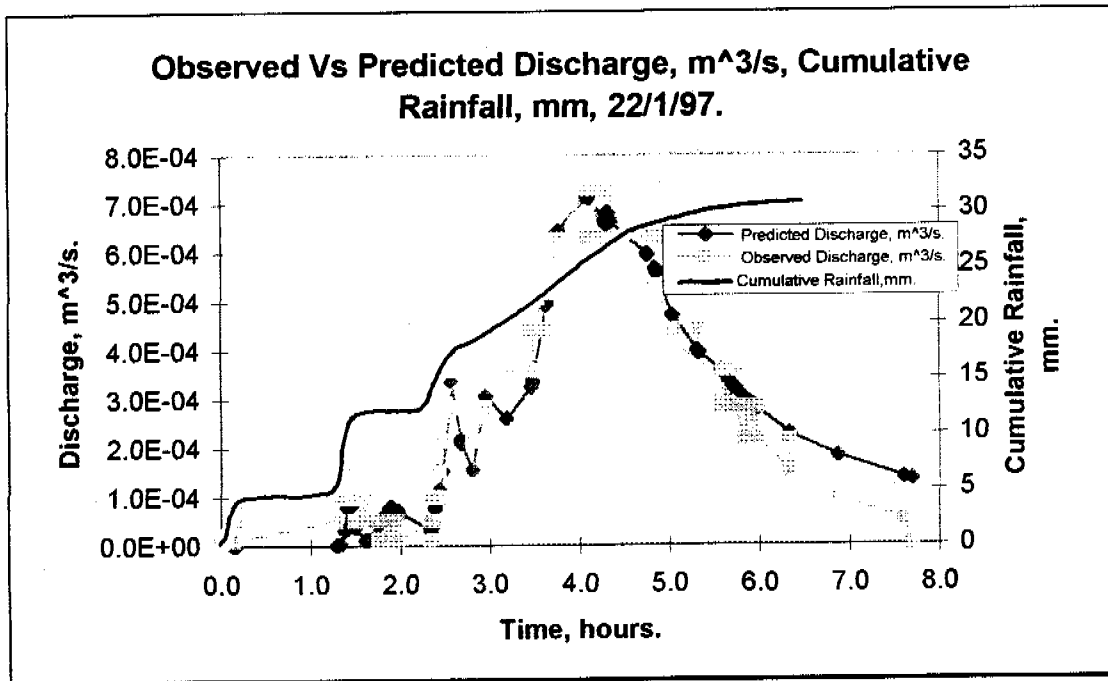
RUM 96-97 Monitoring

pit 1 site

Runoff 22/1/97 1441hrs

166

0	0.00E+00	1.618	9.84E-05	2.338	9.97E-06	2.679	3.58E-04	4.108	7.29E-04	4.34	7.29E-04	5.315	3.58E-04	5.735	3.58E-04	7.606	9.84E-05
0.039	9.97E-06	1.621	5.07E-05	2.342	5.07E-05	2.681	2.83E-04	4.11	6.26E-04	4.342	6.26E-04	5.317	4.41E-04	5.738	2.83E-04	7.608	5.07E-05
0.151	5.07E-05	1.625	9.84E-05	2.343	9.97E-06	2.807	2.14E-04	4.111	7.29E-04	4.343	7.29E-04	5.326	3.58E-04	5.833	2.14E-04	7.642	9.84E-05
0.158	9.97E-06	1.628	5.07E-05	2.351	5.07E-05	2.946	2.83E-04	4.283	6.26E-04	4.344	6.26E-04	5.328	4.41E-04	5.849	2.83E-04	7.643	5.07E-05
1.282	5.07E-05	1.76	9.97E-06	2.353	9.97E-06	3.19	3.58E-04	4.286	7.29E-04	4.35	7.29E-04	5.329	3.58E-04	5.85	2.14E-04	8.193	9.97E-06
1.301	9.84E-05	1.771	5.07E-05	2.354	5.07E-05	3.469	4.41E-04	4.29	6.26E-04	4.75	6.26E-04	5.332	4.41E-04	5.925	2.83E-04	8.2	0
1.332	1.53E-04	1.775	9.97E-06	2.356	9.97E-06	3.471	3.58E-04	4.292	7.29E-04	4.751	7.29E-04	5.333	3.58E-04	5.929	2.14E-04		
1.374	9.84E-05	1.783	5.07E-05	2.357	5.07E-05	3.486	4.41E-04	4.293	6.26E-04	4.76	6.26E-04	5.335	4.41E-04	5.931	2.83E-04		
1.407	1.53E-04	1.785	9.97E-06	2.364	9.84E-05	3.489	3.58E-04	4.297	7.29E-04	4.843	5.30E-04	5.338	3.58E-04	5.932	2.14E-04		
1.408	9.84E-05	1.789	5.07E-05	2.389	1.53E-04	3.49	4.41E-04	4.299	6.26E-04	4.844	6.26E-04	5.339	4.41E-04	5.954	2.83E-04		
1.457	9.84E-05	1.79	9.97E-06	2.392	9.84E-05	3.635	5.30E-04	4.3	7.29E-04	4.846	5.30E-04	5.34	3.58E-04	5.972	2.14E-04		
1.49	5.07E-05	1.799	5.07E-05	2.425	1.53E-04	3.638	4.41E-04	4.301	6.26E-04	4.847	6.26E-04	5.583	2.83E-04	5.974	2.83E-04		
1.492	9.84E-05	1.8	9.97E-06	2.428	9.84E-05	3.639	5.30E-04	4.306	7.29E-04	4.857	5.30E-04	5.589	3.58E-04	5.975	2.14E-04		
1.493	5.07E-05	1.878	5.07E-05	2.431	1.53E-04	3.64	4.41E-04	4.307	6.26E-04	4.86	6.26E-04	5.59	2.83E-04	6.338	1.53E-04		
1.494	9.84E-05	1.889	9.97E-06	2.476	2.14E-04	3.661	5.30E-04	4.311	7.29E-04	4.865	5.30E-04	5.628	3.58E-04	6.339	2.14E-04		
1.5	5.07E-05	1.907	5.07E-05	2.544	2.83E-04	3.747	6.26E-04	4.314	6.26E-04	5.046	4.41E-04	5.629	2.83E-04	6.343	1.53E-04		
1.503	9.84E-05	1.908	9.97E-06	2.569	3.58E-04	3.75	5.30E-04	4.315	7.29E-04	5.047	5.30E-04	5.632	3.58E-04	6.871	9.84E-05		
1.504	5.07E-05	1.972	5.07E-05	2.675	2.83E-04	3.765	6.26E-04	4.317	6.26E-04	5.049	4.41E-04	5.669	2.83E-04	6.872	1.53E-04		
1.615	9.84E-05	1.974	9.97E-06	2.676	3.58E-04	4.089	7.29E-04	4.325	7.29E-04	5.05	5.30E-04	5.707	3.58E-04	6.875	9.84E-05		
1.617	5.07E-05	2.336	5.07E-05	2.678	2.83E-04	4.09	6.26E-04	4.326	6.26E-04	5.051	4.41E-04	5.733	2.83E-04	7.604	5.07E-05		



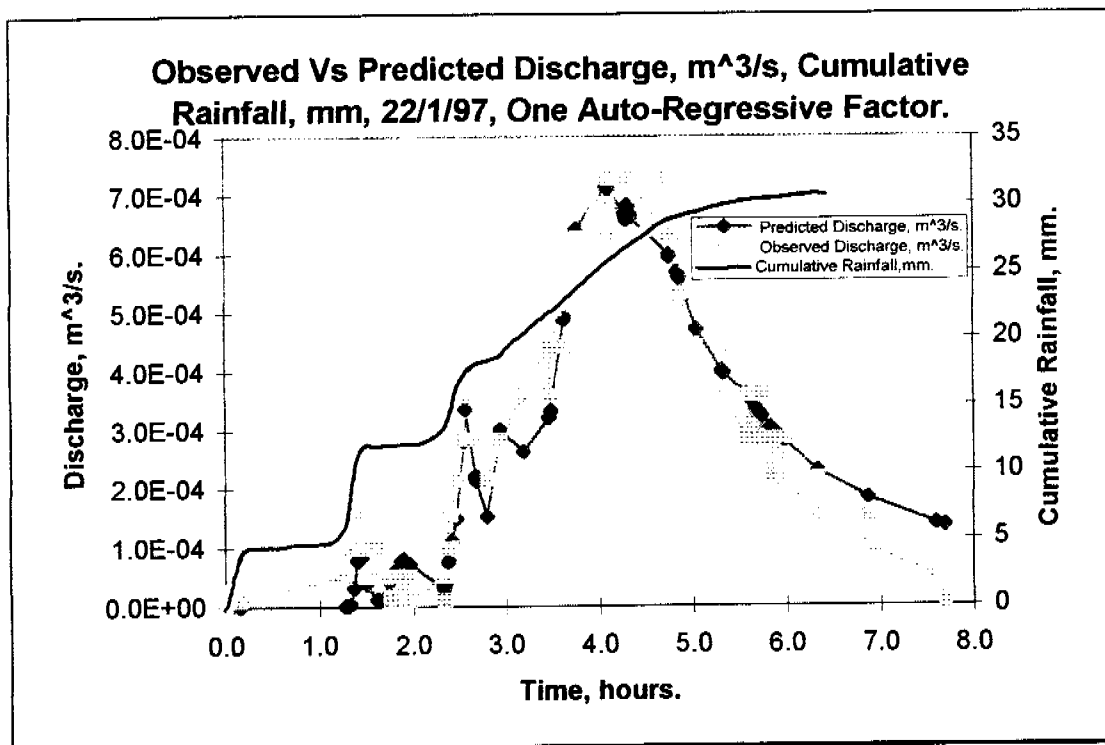
NLFIT Input files: 22197.fw, 22197.ro/rf

NLFIT Output files: 22197.prt/pmf/plr.

Parameter.	Mean.	Standard Deviation.	Parameter.	Mean.	Standard Deviation.
C_r	2.16115	0.53374	$S\phi$	14.9971	8.21074
e_m	1.51277	0.1533003	ϕ	0.001	

		Cumulative Periodogram.		Standardised Residual Versus Time.	Standardised Residual Versus N(0,1) Variate.		Auto Correlation Plot.	Partial Auto Correlation Plot.
Convergence Monitor.	R^2 , %.	Test Statistic.	5%.	Z.	Test Statistic.	5%.	Exceedances.	Exceedances.
0.04104	94.5	0.3356	0.153	0.509	0.0881	0.0704	6	2

Storm Specific Comment: The convergence monitor is adequate, below 0.1, the R^2 is adequate 94.5%, the cumulative periodogram does not pass the test statistic. The standardised residual versus time plot does not exceed the Z statistic limit of $|2|$, the standardised residual versus N(0,1) variate does pass the test statistic. The auto-correlation plot is exceeded 6 times, and the partial auto-correlation plot is exceeded 2 times.



NLFIT Input files: 22197.fw, 22197.ro/rf

NLFIT Output files: 22197a.prt/pmf/plt.

Parameter.	Mean.	Standard Deviation.	Parameter.	Mean.	Standard Deviation.
C_r	1.8182	0.2208	$S\phi$	2.5737	0.0699
e_m	3.8905	0.1019	ϕ	0.001	

		Cumulative Periodogram.		Standardised Residual Versus Time.	Standardised Residual Versus N(0,1) Variate.		Auto Correlation Plot.	Partial Auto Correlation Plot.
Convergence Monitor.	R^2 , %.	Test Statistic.	5%.	Z.	Test Statistic.	5%.	Exceedances.	Exceedances.
0.0560	94.4	0.2586	0.153	3.493	0.1064	0.0704	5	2

Storm Specific Comment: The convergence monitor is adequate, below 0.1, the R^2 is adequate 94.4%, the cumulative periodogram does not pass the test statistic. The standardised residual versus time plot exceeds the Z statistic limit of $|2|$, the standardised residual versus N(0,1) variate does not pass the test statistic. The auto-correlation plot is exceeded 5 times, and the partial auto-correlation plot is exceeded 2 times.

General Comment: The addition of an auto-regressive factor, 22197a.*, to 22197.*, did not improve the predicted response over the least squares model. The statistical tests indicate that the addition of the auto-regressive factor has worsened the normality of the predicted response.

23rd January

RUM 96-97 Monitoring

pit 1 site

Rainfall 23/1/97 1617hrs

154

0	0	0.085	4.8	0.157	10.4	0.207	15.8	0.257	22.8	0.307	29.8	0.351	35.6	0.426	40.6
0.01	0.2	0.089	5	0.16	10.8	0.21	16.2	0.26	23.2	0.31	30	0.353	35.8	0.431	40.8
0.017	0.4	0.096	5.4	0.163	11	0.213	16.6	0.263	23.6	0.311	30.2	0.354	36	0.438	41.2
0.019	0.6	0.103	5.6	0.165	11.4	0.215	17	0.265	23.8	0.313	30.6	0.357	36.4	0.44	41.6
0.021	0.8	0.11	5.8	0.168	11.6	0.218	17.4	0.268	24	0.314	31	0.36	36.6	0.444	41.8
0.024	1	0.115	6	0.171	11.8	0.221	17.6	0.269	24.2	0.315	31.4	0.361	36.8	0.454	42
0.026	1.2	0.117	6.2	0.172	12	0.224	18	0.271	24.4	0.318	31.6	0.363	37	0.465	42.4
0.028	1.4	0.121	6.4	0.174	12.2	0.226	18.2	0.272	24.6	0.321	32	0.364	37.2	0.483	42.6
0.032	1.6	0.125	6.8	0.175	12.4	0.228	18.4	0.275	25.4	0.324	32.4	0.365	37.4	0.549	42.8
0.036	1.8	0.128	7	0.176	12.6	0.229	18.6	0.276	25.8	0.326	32.6	0.367	37.6	0.6	43
0.04	2.2	0.131	7.2	0.181	13	0.232	19	0.279	26.2	0.329	32.8	0.369	37.8	0.703	43.4
0.044	2.4	0.132	7.4	0.183	13.4	0.235	19.4	0.282	26.6	0.331	33	0.375	38.4	0.892	43.6
0.049	2.8	0.135	7.8	0.186	13.6	0.238	20.6	0.285	27	0.333	33.2	0.383	38.6	1.438	43.8
0.054	3	0.138	8	0.189	13.8	0.24	20.8	0.288	27.2	0.336	33.4	0.392	38.8	2.6	43.8
0.058	3.4	0.14	8.4	0.19	14	0.243	21.2	0.29	27.6	0.338	33.6	0.397	39		
0.064	3.6	0.143	8.8	0.193	14.2	0.246	21.6	0.293	28	0.34	33.8	0.399	39.2		
0.071	3.8	0.146	9	0.196	14.6	0.249	21.8	0.296	28.4	0.343	34.2	0.404	39.6		
0.072	4	0.149	9.4	0.199	14.8	0.251	22.2	0.299	28.6	0.346	34.4	0.411	39.8		
0.075	4.2	0.151	9.8	0.201	15.2	0.254	22.4	0.301	29	0.349	34.6	0.417	40.2		
0.079	4.6	0.154	10	0.204	15.6	0.256	22.6	0.304	29.4	0.35	35.4	0.424	40.4		

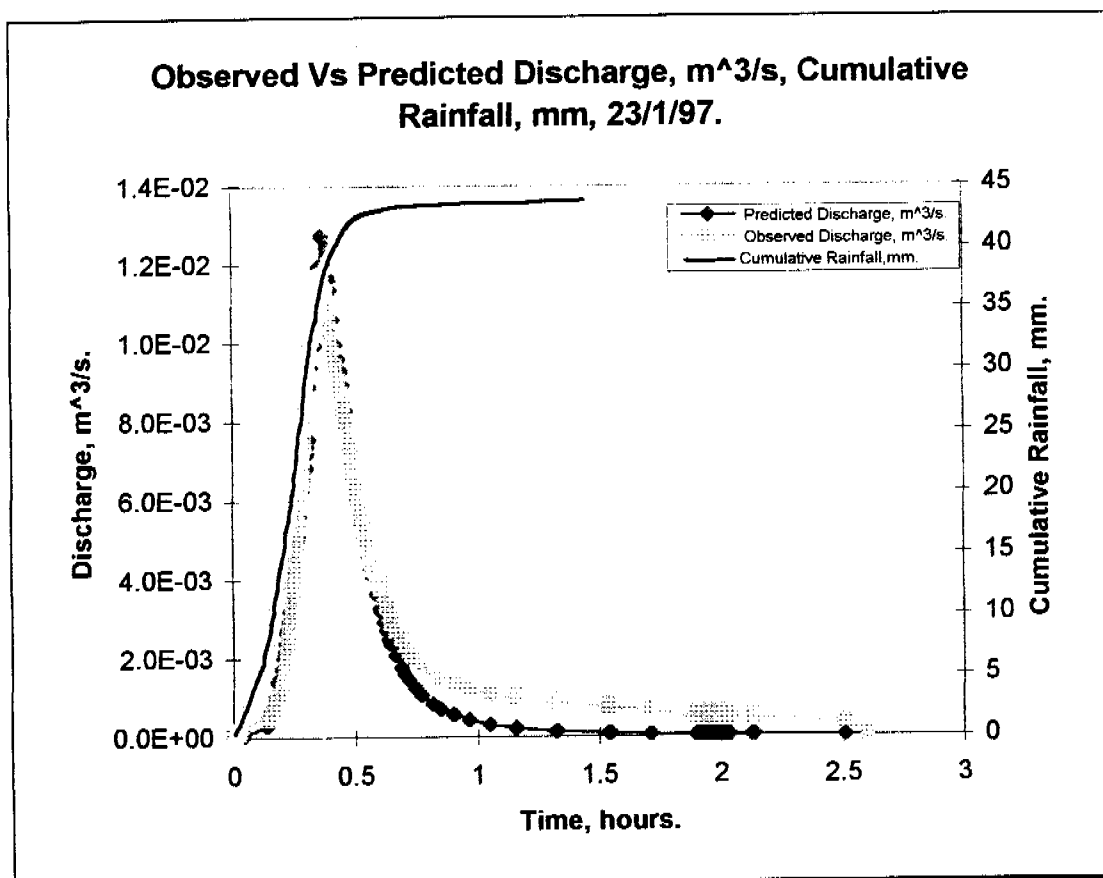
RUM 96-97 Monitoring

pit 1 site

Runoff 23/1/97 1617hrs

156

0	0.00E+00	0.219	2.14E-03	0.289	7.05E-03	0.435	9.06E-03	0.603	3.77E-03	1.16	9.57E-04	1.919	5.30E-04	1.99	4.41E-04
0.014	5.07E-05	0.224	2.32E-03	0.292	7.37E-03	0.447	8.71E-03	0.615	3.54E-03	1.164	1.08E-03	1.921	6.26E-04	1.992	5.30E-04
0.024	9.84E-05	0.225	2.51E-03	0.293	7.69E-03	0.454	8.36E-03	0.625	3.32E-03	1.165	9.57E-04	1.926	5.30E-04	1.994	6.26E-04
0.029	1.53E-04	0.228	2.70E-03	0.296	8.03E-03	0.465	8.03E-03	0.636	3.11E-03	1.324	8.39E-04	1.929	6.26E-04	1.996	5.30E-04
0.035	2.14E-04	0.233	2.90E-03	0.3	8.36E-03	0.474	7.69E-03	0.638	3.32E-03	1.325	9.57E-04	1.932	5.30E-04	2.008	4.41E-04
0.036	2.83E-04	0.238	3.11E-03	0.304	8.71E-03	0.481	7.37E-03	0.639	3.11E-03	1.329	8.39E-04	1.933	6.26E-04	2.01	5.30E-04
0.039	3.58E-04	0.239	3.32E-03	0.307	9.06E-03	0.486	7.05E-03	0.644	2.90E-03	1.538	7.29E-04	1.936	4.41E-04	2.028	6.26E-04
0.138	4.41E-04	0.242	3.54E-03	0.311	9.42E-03	0.492	6.74E-03	0.663	2.70E-03	1.539	8.39E-04	1.939	6.26E-04	2.029	4.41E-04
0.15	5.30E-04	0.243	3.77E-03	0.318	9.79E-03	0.499	6.43E-03	0.686	2.51E-03	1.542	7.29E-04	1.94	4.41E-04	2.032	5.30E-04
0.157	6.26E-04	0.25	4.01E-03	0.325	1.02E-02	0.507	6.14E-03	0.701	2.32E-03	1.547	8.39E-04	1.942	6.26E-04	2.036	4.41E-04
0.164	7.29E-04	0.253	4.25E-03	0.34	1.05E-02	0.513	5.85E-03	0.717	2.14E-03	1.549	7.29E-04	1.951	5.30E-04	2.038	5.30E-04
0.171	8.39E-04	0.257	4.50E-03	0.353	1.09E-02	0.522	5.56E-03	0.744	1.97E-03	1.713	6.26E-04	1.953	6.26E-04	2.129	4.41E-04
0.179	9.57E-04	0.26	4.75E-03	0.358	1.13E-02	0.535	5.29E-03	0.771	1.80E-03	1.714	7.29E-04	1.956	5.30E-04	2.131	5.30E-04
0.188	1.08E-03	0.263	5.02E-03	0.367	1.17E-02	0.538	5.02E-03	0.815	1.65E-03	1.718	6.26E-04	1.968	6.26E-04	2.138	4.41E-04
0.199	1.21E-03	0.267	5.29E-03	0.385	1.13E-02	0.551	4.75E-03	0.849	1.49E-03	1.9	4.41E-04	1.969	5.30E-04	2.51	3.58E-04
0.204	1.35E-03	0.269	5.56E-03	0.39	1.09E-02	0.563	4.50E-03	0.901	1.35E-03	1.901	6.26E-04	1.971	4.41E-04	2.6	0
0.208	1.49E-03	0.274	5.85E-03	0.399	1.05E-02	0.569	4.25E-03	0.903	1.49E-03	1.903	5.30E-04	1.972	5.30E-04		
0.211	1.65E-03	0.278	6.14E-03	0.404	1.02E-02	0.586	4.01E-03	0.904	1.35E-03	1.906	6.26E-04	1.979	6.26E-04		
0.214	1.80E-03	0.282	6.43E-03	0.414	9.79E-03	0.6	3.77E-03	0.967	1.21E-03	1.91	4.41E-04	1.981	5.30E-04		
0.217	1.97E-03	0.285	6.74E-03	0.426	9.42E-03	0.601	4.01E-03	1.051	1.08E-03	1.911	6.26E-04	1.989	6.26E-04		



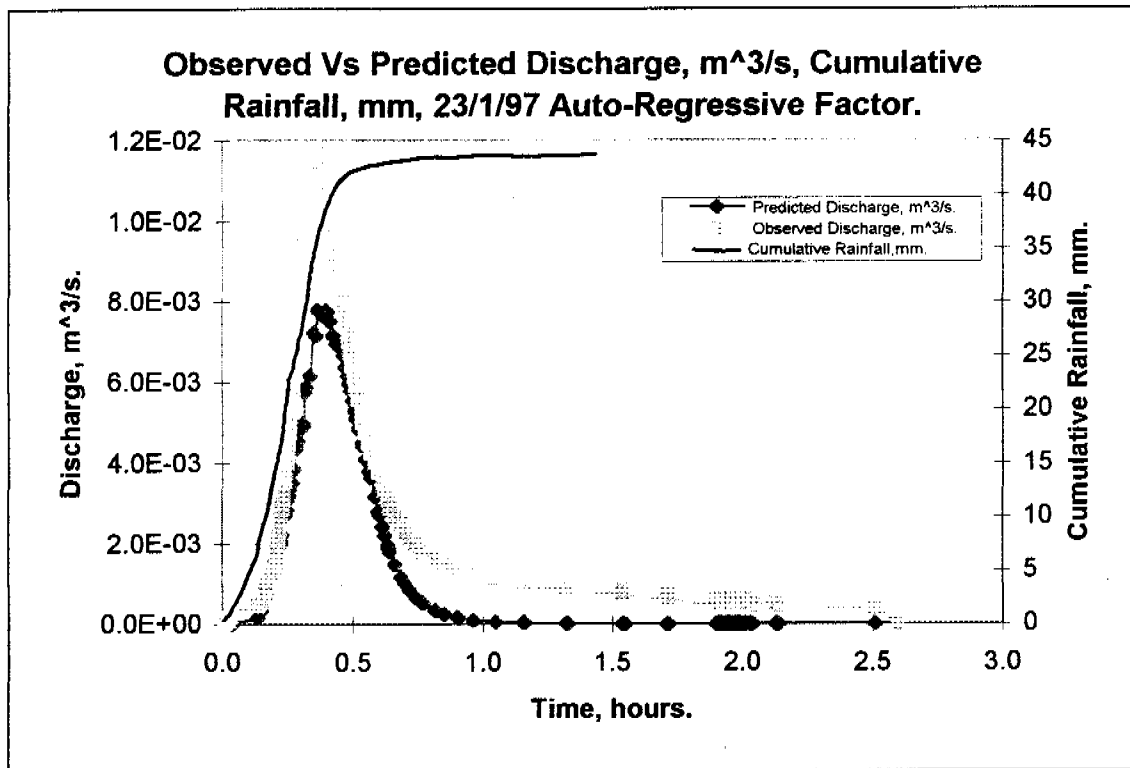
NLFIT Input files: 23197.fw, 23197.ro/rf

NLFIT Output files: 23197.prt/pmf/plt.

Parameter.	Mean.	Standard Deviation.	Parameter.	Mean.	Standard Deviation.
C_r	2.257	0.1087	$S\phi$	0.001	
e_m	1.5957	0.0506	ϕ	51.591	1.119

Convergence Monitor.	R^2 , %.	Cumulative Periodogram.		Standardised Residual Versus Time.	Standardised Residual Versus N(0,1) Variate.		Auto Correlation Plot.	Partial Auto Correlation Plot.
		Test Statistic.	5%.	Z.	Test Statistic.	5%.	Exceedances.	Exceedances.
0.0986	97.7	0.7857	0.155	-9.894	0.1581	0.0716	9	5

Storm Specific Comment: The convergence monitor is adequate, below 0.1, the R^2 is adequate 97.7%, the cumulative periodogram does not pass the test statistic. The standardised residual versus time plot exceeds the Z statistic limit of $|2|$, the standardised residual versus N(0,1) variate does not pass the test statistic. The auto-correlation plot is exceeded 9 times, and the partial auto-correlation plot is exceeded 5 times.



NLFIT Input files: 23197.fw, 23197.ro/rf

NLFIT Output files: 23197a.prt/pmf/plt.

Parameter.	Mean.	Standard Deviation.	Parameter.	Mean.	Standard Deviation.
C_r	1.554	0.137	$S\phi$	0.001	
e_m	1.226	0.070	ϕ	74.0854	5.717

		Cumulative Periodogram.		Standardised Residual Versus Time.	Standardised Residual Versus N(0,1) Variate.		Auto Correlation Plot.	Partial Auto Correlation Plot.
Convergence Monitor.	R^2 , %.	Test Statistic.	5%.	Z.	Test Statistic.	5%.	Exceedances.	Exceedances.
0.1347	95.1	0.2022	0.155	-0.076	0.0681	0.0716	5	4

Storm Specific Comment: The convergence monitor is not adequate, below 0.1, the R^2 is adequate 95.1%, the cumulative periodogram does not pass the test statistic. The standardised residual versus time plot does not exceed the Z statistic limit of $|2|$, the standardised residual versus N(0,1) variate does pass the test statistic. The auto-correlation plot is exceeded 5 times, and the partial auto-correlation plot is exceeded 4 times.

General Comment: The inclusion of an auto-regressive factor, although improving the statistical compliance, the overall quality of the predicted versus observed discharge deteriorated compared to the least squares fitting regime.

23-24th January

RUM 96-97 Monitoring

pit 1 site

Rainfall 23-24/1/97 1919hrs

177

0	0	1.025	4.4	1.192	8.8	1.846	13.4	2.067	18	2.319	22.6	2.625	27.8	2.846	32.4	3.246	37.2
0.811	0.4	1.033	4.6	1.204	9	1.86	13.6	2.068	18.2	2.333	22.8	2.631	28	2.857	32.6	3.247	37.4
0.836	0.6	1.042	4.8	1.206	9.2	1.874	13.8	2.079	18.4	2.375	23.2	2.636	28.2	2.867	32.8	3.257	37.6
0.853	0.8	1.05	5	1.221	9.4	1.885	14	2.092	18.6	2.431	23.4	2.638	28.4	2.882	33	3.268	37.8
0.867	1	1.057	5.2	1.24	9.6	1.886	14.2	2.103	18.8	2.453	23.6	2.646	28.6	2.896	33.4	3.279	38
0.882	1.2	1.058	5.4	1.256	9.8	1.897	14.4	2.114	19.2	2.467	23.8	2.658	28.8	2.91	33.6	3.292	38.4
0.883	1.4	1.067	5.6	1.265	10.2	1.91	14.6	2.126	19.4	2.481	24.2	2.671	29	2.928	33.8	3.306	38.6
0.896	1.6	1.075	5.8	1.274	10.4	1.928	14.8	2.143	19.6	2.497	24.4	2.692	29.4	2.954	34	3.326	38.8
0.91	1.8	1.081	6	1.283	10.6	1.946	15.2	2.163	19.8	2.517	24.6	2.706	29.6	2.982	34.4	3.349	39
0.924	2	1.088	6.4	1.3	10.8	1.958	15.4	2.183	20	2.535	24.8	2.719	29.8	3.011	34.6	3.374	39.4
0.938	2.2	1.096	6.6	1.349	11	1.972	15.6	2.185	20.2	2.55	25.2	2.736	30	3.039	34.8	3.407	39.6
0.939	2.4	1.101	6.8	1.35	11.2	1.989	15.8	2.2	20.4	2.561	25.4	2.751	30.4	3.053	35	3.451	39.8
0.956	2.6	1.108	7	1.394	11.4	1.999	16.2	2.226	20.6	2.568	25.6	2.765	30.6	3.064	35.4	3.608	40
0.968	2.8	1.11	7.2	1.414	11.6	2.008	16.4	2.254	20.8	2.574	26	2.779	30.8	3.078	35.6	3.7	40.2
0.979	3	1.118	7.4	1.447	11.8	2.018	16.6	2.265	21.2	2.582	26.2	2.789	31	3.099	35.8	3.701	40.4
0.988	3.4	1.126	7.6	1.593	12.2	2.028	16.8	2.275	21.4	2.589	26.4	2.797	31.2	3.138	36	6.203	40.6
0.997	3.6	1.135	7.8	1.681	12.4	2.036	17.2	2.283	21.6	2.597	26.8	2.799	31.4	3.168	36.4	6.3	40.6
1.007	3.8	1.146	8.2	1.722	12.6	2.044	17.4	2.293	21.8	2.606	27	2.808	31.6	3.188	36.6		
1.017	4	1.16	8.4	1.783	12.8	2.053	17.6	2.301	22.2	2.611	27.2	2.819	31.8	3.208	36.8		
1.024	4.2	1.178	8.6	1.829	13.2	2.06	17.8	2.308	22.4	2.618	27.6	2.832	32	3.229	37		

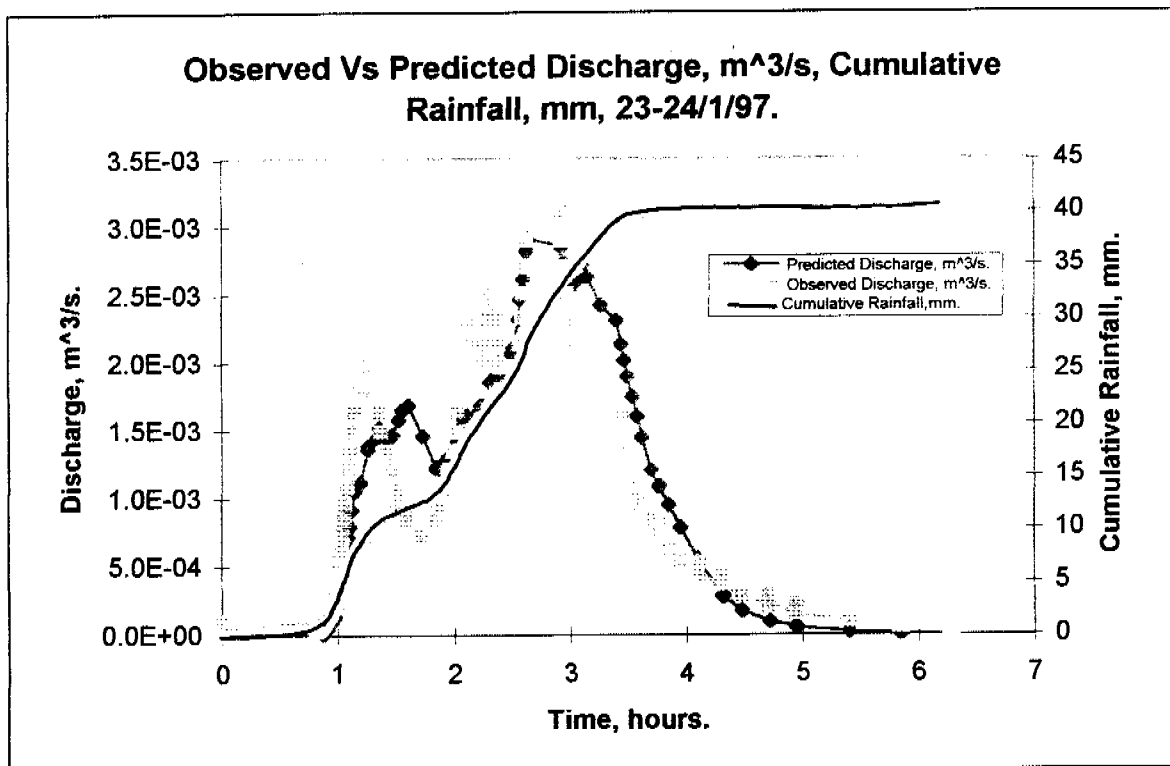
RUM 96-97 Monitoring

pit 1 site

Runoff 23-24/1/97 1919hrs

132

0	0.00E+00	1.193	1.80E-03	2.042	1.80E-03	2.575	2.14E-03	3.401	1.80E-03	4.314	3.58E-04	5.843	9.84E-05				
0.001	5.07E-05	1.263	1.97E-03	2.054	1.97E-03	2.588	2.32E-03	3.443	1.65E-03	4.317	4.41E-04	5.846	5.07E-05				
0.01	9.84E-05	1.264	1.80E-03	2.072	2.14E-03	2.596	2.51E-03	3.465	1.49E-03	4.318	3.58E-04	5.847	9.84E-05				
0.011	5.07E-05	1.265	1.97E-03	2.106	2.32E-03	2.621	2.70E-03	3.492	1.35E-03	4.478	2.83E-04	5.849	5.07E-05				
0.882	9.84E-05	1.34	1.80E-03	2.231	2.14E-03	2.631	2.90E-03	3.532	1.21E-03	4.713	2.14E-04	5.85	9.84E-05				
0.914	1.53E-04	1.358	1.65E-03	2.251	1.97E-03	2.643	3.11E-03	3.575	1.08E-03	4.714	2.83E-04	5.854	5.07E-05				
0.951	2.14E-04	1.374	1.49E-03	2.253	2.14E-03	2.924	2.90E-03	3.618	9.57E-04	4.715	2.14E-04	5.857	9.84E-05				
0.974	2.83E-04	1.438	1.35E-03	2.258	1.97E-03	2.926	3.11E-03	3.696	8.39E-04	4.717	2.83E-04	5.858	5.07E-05				
0.988	3.58E-04	1.483	1.21E-03	2.261	2.14E-03	2.928	2.90E-03	3.763	7.29E-04	4.718	2.14E-04	5.864	9.84E-05				
1.004	4.41E-04	1.525	1.08E-03	2.29	2.32E-03	2.951	2.70E-03	3.764	8.39E-04	4.721	2.83E-04	5.865	5.07E-05				
1.021	5.30E-04	1.556	9.57E-04	2.311	2.51E-03	2.968	2.51E-03	3.768	7.29E-04	4.722	2.14E-04	6.267	9.97E-06				
1.036	6.26E-04	1.611	8.39E-04	2.361	2.32E-03	2.993	2.32E-03	3.847	6.26E-04	4.944	1.53E-04	6.3	0				
1.05	7.29E-04	1.735	7.29E-04	2.378	2.14E-03	3.01	2.14E-03	3.954	5.30E-04	4.946	2.14E-04						
1.058	8.39E-04	1.847	8.39E-04	2.394	1.97E-03	3.033	1.97E-03	4.1	4.41E-04	4.949	1.53E-04						
1.072	9.57E-04	1.878	9.57E-04	2.432	1.80E-03	3.035	2.14E-03	4.101	5.30E-04	4.95	2.14E-04						
1.085	1.08E-03	1.911	1.08E-03	2.503	1.97E-03	3.036	1.97E-03	4.104	4.41E-04	4.951	1.53E-04						
1.093	1.21E-03	1.953	1.21E-03	2.504	1.80E-03	3.056	2.14E-03	4.106	5.30E-04	4.954	2.14E-04						
1.108	1.35E-03	1.999	1.35E-03	2.511	1.97E-03	3.107	1.97E-03	4.107	4.41E-04	4.956	1.53E-04						
1.126	1.49E-03	2.018	1.49E-03	2.513	1.80E-03	3.149	1.80E-03	4.31	3.58E-04	5.41	9.84E-05						
1.151	1.65E-03	2.032	1.65E-03	2.56	1.97E-03	3.268	1.97E-03	4.311	4.41E-04	5.842	5.07E-05						



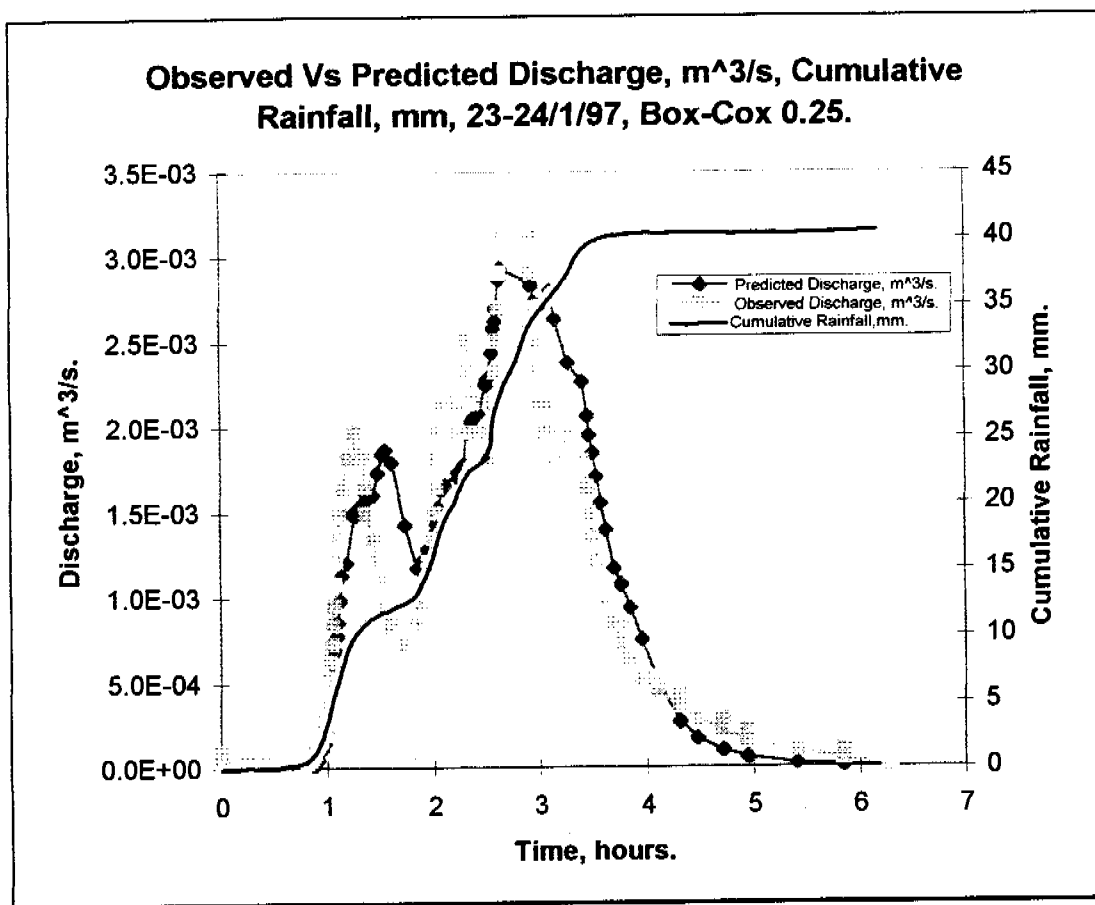
NLFIT Input files: 2324197.fw, 2324197.ro/rf

NLFIT Output files: 2324197.prt/pmf/plt.

Parameter.	Mean.	Standard Deviation.	Parameter.	Mean.	Standard Deviation.
C_r	0.625	0.081	$S\phi$	1.9503	0.2352
e_m	1.2664	0.087	ϕ	0.001	

		Cumulative Periodogram.		Standardised Residual Versus Time.	Standardised Residual Versus N(0,1) Variate.		Auto Correlation Plot.	Partial Auto Correlation Plot.
Convergence Monitor.	R^2 , %.	Test Statistic.	5%.	Z.	Test Statistic.	5%.	Exceedances.	Exceedances.
0.02048	86.8	0.8054	0.1687	-10.203	0.1258	0.0778	8	5

Storm Specific Comment: The convergence monitor is adequate, below 0.1, the R^2 is not adequate 86.8%, the cumulative periodogram does not pass the test statistic. The standardised residual versus time plot exceeds the Z statistic limit of $|2|$, the standardised residual versus N(0,1) variate does not pass the test statistic. The auto-correlation plot is exceeded 8 times, and the partial auto-correlation plot is exceeded 5 times.

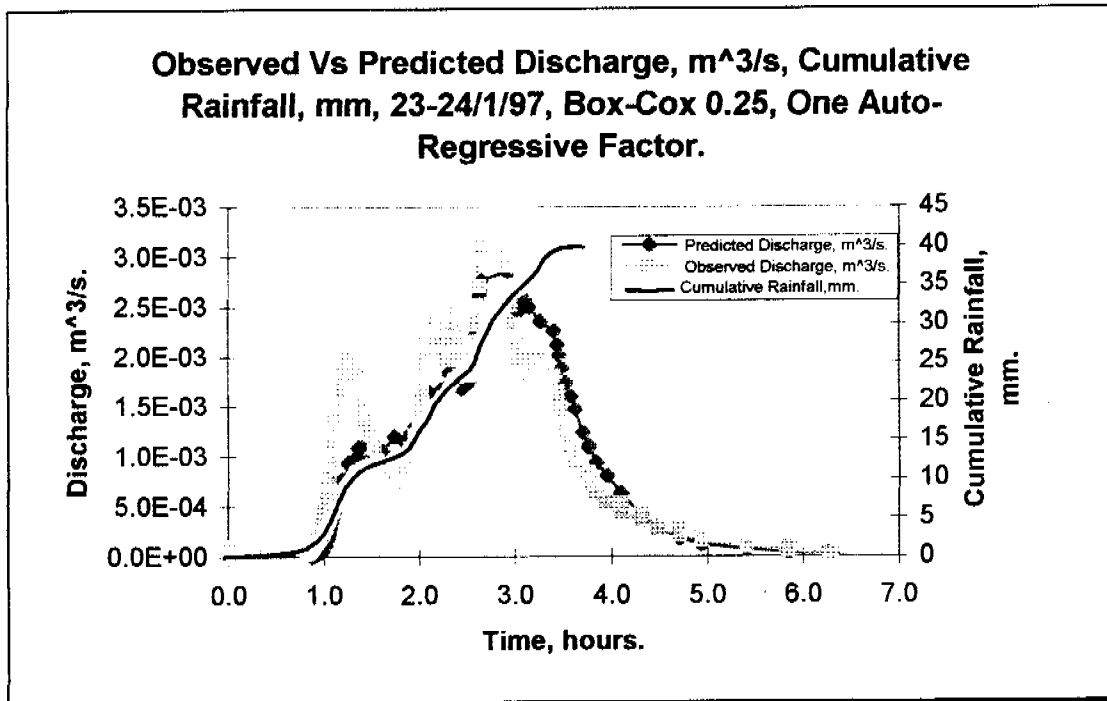


NLFIT Input files: 2324197.fw, 2324197.ro/rf
 NLFIT Output files: 23241g25.prt/pmf/plt.

Parameter.	Mean.	Standard Deviation.	Parameter.	Mean.	Standard Deviation.
C_r	0.7170	0.095	$S\phi$	1.746	0.233
e_m	1.316	0.0807	ϕ	0.001	

		Cumulative Periodogram.		Standardised Residual Versus Time.	Standardised Residual Versus N(0,1) Variate.		Auto Correlation Plot.	Partial Auto Correlation Plot.
Convergence Monitor.	R^2 , %.	Test Statistic.	5%.	Z.	Test Statistic.	5%.	Exceedances.	Exceedances.
0.07687	87.2	0.8021	0.1687	-9.465	0.129	0.0778	8	3

Storm Specific Comment: The convergence monitor is adequate, below 0.1, the R^2 is not adequate 87.2%, the cumulative periodogram does not pass the test statistic. The standardised residual versus time plot exceeds the Z statistic limit of $|2|$, the standardised residual versus N(0,1) variate does not pass the test statistic. The auto-correlation plot is exceeded 8 times, and the partial auto-correlation plot is exceeded 3 times.



NLFIT Input files: 2324197.fw, 2324197.ro/rf

NLFIT Output files: 23241a25.prt/pmf/plt.

Parameter.	Mean.	Standard Deviation.	Parameter.	Mean.	Standard Deviation.
C_r	0.7052	0.127	$S\phi$	2.541	1.160
e_m	1.463	0.183	ϕ	0.001	

Convergence Monitor.	R^2 , %.	Cumulative Periodogram.		Standardised Residual Versus Time.	Standardised Residual Versus N(0,1) Variate.		Auto Correlation Plot.	Partial Auto Correlation Plot.
		Test Statistic.	5%.	Z.	Test Statistic.	5%.	Exceedances.	Exceedances.
0.21812	82.6	0.1466	0.1687	0.026	0.1579	0.0778	2	2

Storm Specific Comment: The convergence monitor is not adequate, below 0.1, the R^2 is not adequate 82.6%, the cumulative periodogram does pass the test statistic. The standardised residual versus time plot does not exceed the Z statistic limit of |2|, the standardised residual versus N(0,1) variate does not pass the test statistic. The auto-correlation plot is exceeded 2 times, and the partial auto-correlation plot is exceeded 2 times.

General Comment: The inclusion of an auto-regressive factor to a more general error model, 23241a25.*, has yielded a better fit than a least squares model fit, 2324197.*, and the inclusion of only a more general error model, 23241g25.*.

28th January

RUM 96-97 Monitoring

pit 1 site

Rainfall 28/1/97 1246hrs

121

0	0	0.281	4.8	0.386	9.2	0.507	14	0.59	18.2	0.725	23.4	3.144	28.2
0.006	0.2	0.286	5.2	0.399	9.4	0.511	14.2	0.594	18.6	0.731	23.6	4	28.2
0.014	0.4	0.292	5.4	0.417	9.8	0.513	14.4	0.597	18.8	0.738	23.8		
0.022	0.8	0.297	5.6	0.418	10	0.517	14.6	0.601	19.2	0.744	24.2		
0.029	1	0.3	5.8	0.432	10.2	0.521	14.8	0.604	19.4	0.751	24.4		
0.038	1.2	0.301	6	0.444	10.4	0.522	15	0.608	19.8	0.758	24.6		
0.044	1.6	0.311	6.2	0.451	10.8	0.528	15.2	0.613	20	0.764	25		
0.056	1.8	0.318	6.4	0.456	11	0.532	15.4	0.617	20.2	0.771	25.2		
0.063	2	0.325	6.6	0.46	11.2	0.536	15.6	0.621	20.6	0.781	25.4		
0.072	2.4	0.326	6.8	0.464	11.4	0.538	15.8	0.626	20.8	0.789	25.6		
0.083	2.6	0.331	7	0.465	11.6	0.543	16	0.633	21	0.806	26		
0.094	2.8	0.333	7.2	0.468	11.8	0.553	16.2	0.644	21.2	0.832	26.2		
0.108	3	0.335	7.4	0.472	12	0.563	16.4	0.646	21.4	1.024	26.4		
0.125	3.4	0.338	7.6	0.474	12.2	0.564	16.6	0.656	21.6	1.299	26.6		
0.142	3.6	0.34	7.8	0.478	12.4	0.568	16.8	0.667	21.8	1.46	27		
0.163	3.8	0.342	8	0.482	12.6	0.574	17	0.674	22	1.607	27.2		
0.192	4	0.344	8.2	0.488	13	0.578	17.4	0.685	22.4	1.803	27.4		
0.225	4.2	0.353	8.4	0.493	13.2	0.582	17.6	0.697	22.6	2.654	27.6		
0.226	4.4	0.363	8.8	0.497	13.6	0.586	17.8	0.711	22.8	2.926	27.8		
0.246	4.6	0.376	9	0.501	13.8	0.588	18	0.718	23	2.928	28		

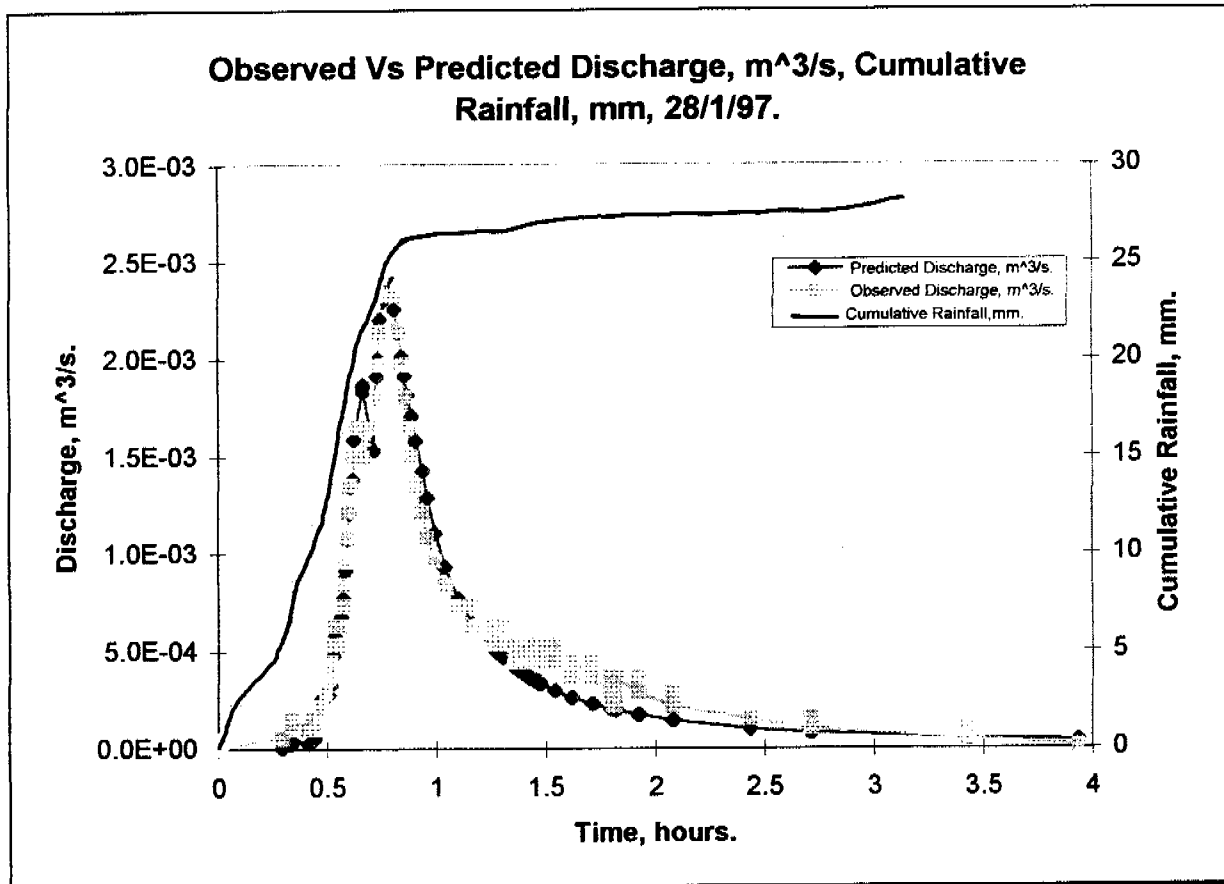
RUM 96-97 Monitoring

pit 1 site

Runoff 28/1/97 1246hrs

133

0	0	0.597	1.08E-03	0.91	1.35E-03	1.301	6.26E-04	1.433	4.41E-04	1.717	4.41E-04	2.085	2.14E-04
0.001	9.97E-06	0.604	1.21E-03	0.938	1.21E-03	1.303	5.30E-04	1.435	5.30E-04	1.719	3.58E-04	2.438	1.53E-04
0.297	5.07E-05	0.61	1.35E-03	0.963	1.08E-03	1.356	4.41E-04	1.436	4.41E-04	1.797	2.83E-04	2.708	9.84E-05
0.335	9.84E-05	0.618	1.49E-03	0.999	9.57E-04	1.357	5.30E-04	1.439	5.30E-04	1.799	3.58E-04	2.71	1.53E-04
0.342	1.53E-04	0.625	1.65E-03	1.044	8.39E-04	1.381	4.41E-04	1.453	4.41E-04	1.804	2.83E-04	2.713	9.84E-05
0.414	9.84E-05	0.667	1.49E-03	1.1	7.29E-04	1.383	5.30E-04	1.456	5.30E-04	1.808	2.14E-04	2.715	1.53E-04
0.438	1.53E-04	0.668	1.65E-03	1.168	6.26E-04	1.39	4.41E-04	1.464	4.41E-04	1.81	3.58E-04	2.717	9.84E-05
0.439	9.84E-05	0.669	1.49E-03	1.169	7.29E-04	1.392	5.30E-04	1.467	5.30E-04	1.811	2.83E-04	3.425	5.07E-05
0.444	1.53E-04	0.715	1.65E-03	1.171	6.26E-04	1.393	4.41E-04	1.471	4.41E-04	1.814	3.58E-04	3.426	9.84E-05
0.476	2.14E-04	0.731	1.80E-03	1.253	5.30E-04	1.396	5.30E-04	1.472	5.30E-04	1.815	2.14E-04	3.431	5.07E-05
0.497	2.83E-04	0.738	1.97E-03	1.257	6.26E-04	1.404	4.41E-04	1.474	4.41E-04	1.817	2.83E-04	3.436	9.84E-05
0.511	3.58E-04	0.744	2.14E-03	1.26	5.30E-04	1.406	5.30E-04	1.475	5.30E-04	1.818	2.14E-04	3.44	5.07E-05
0.519	4.41E-04	0.758	2.32E-03	1.264	6.26E-04	1.41	4.41E-04	1.479	4.41E-04	1.821	3.58E-04	3.939	9.97E-06
0.533	5.30E-04	0.774	2.51E-03	1.265	5.30E-04	1.411	5.30E-04	1.544	5.30E-04	1.822	2.14E-04	4	0
0.54	6.26E-04	0.813	2.32E-03	1.269	6.26E-04	1.414	4.41E-04	1.546	4.41E-04	1.824	3.58E-04		
0.563	5.30E-04	0.831	2.14E-03	1.271	5.30E-04	1.418	5.30E-04	1.622	3.58E-04	1.924	2.83E-04		
0.565	6.26E-04	0.846	1.97E-03	1.274	6.26E-04	1.419	4.41E-04	1.624	4.41E-04	1.925	3.58E-04		
0.576	7.29E-04	0.858	1.80E-03	1.275	5.30E-04	1.425	5.30E-04	1.713	3.58E-04	1.932	2.83E-04		
0.583	8.39E-04	0.871	1.65E-03	1.278	6.26E-04	1.428	4.41E-04	1.714	4.41E-04	2.079	2.14E-04		
0.59	9.57E-04	0.888	1.49E-03	1.279	5.30E-04	1.431	5.30E-04	1.715	3.58E-04	2.081	2.83E-04		



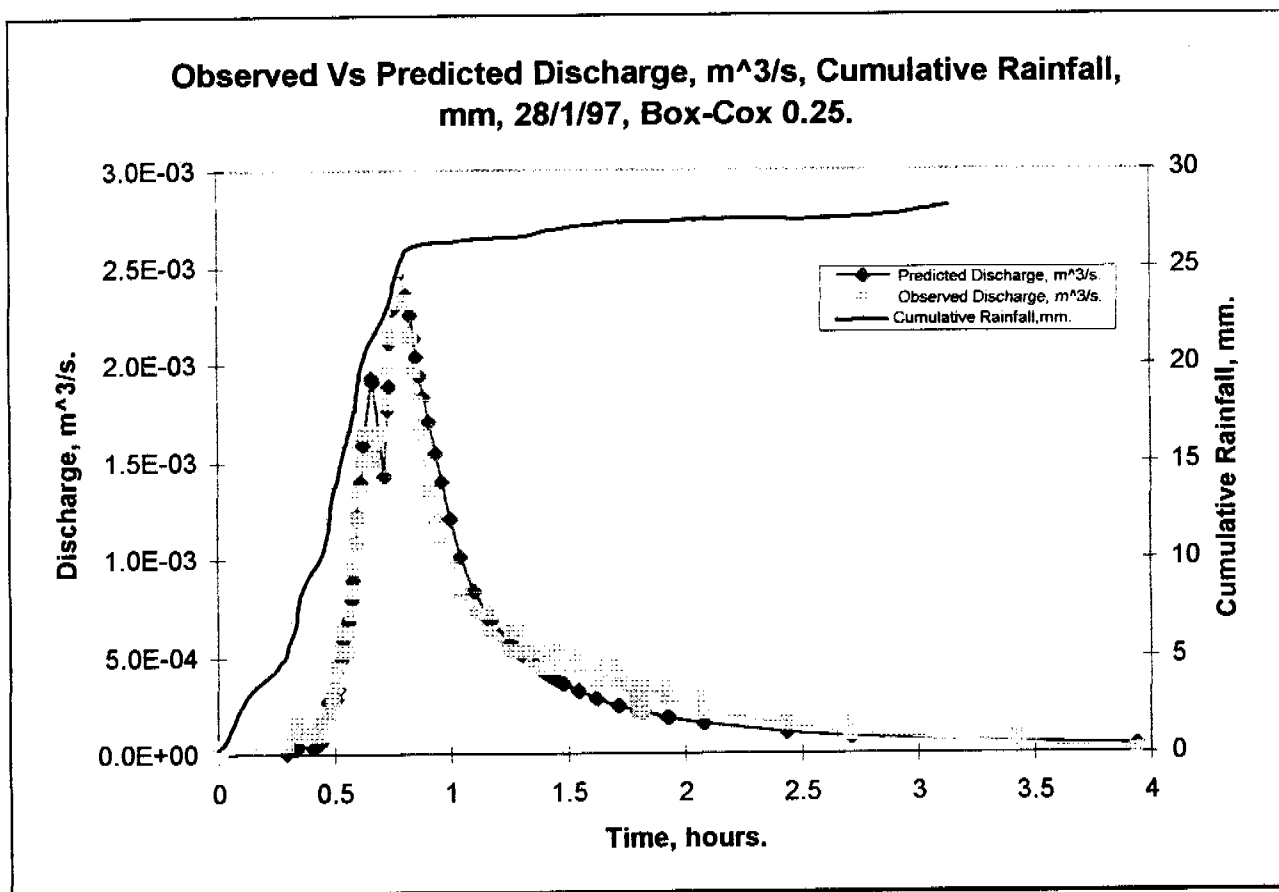
NLFIT Input files: 28197.fw, 28197.ro/rf

NLFIT Output files: 28197.prt/pmf/plt.

Parameter.	Mean.	Standard Deviation.	Parameter.	Mean.	Standard Deviation.
C_r	9.168	1.083	$S\phi$	0.001	
e_m	2.697	0.083	ϕ	25.520	0.464

		Cumulative Periodogram.		Standardised Residual Versus Time.	Standardised Residual Versus N(0,1) Variate.		Auto Correlation Plot.	Partial Auto Correlation Plot.
Convergence Monitor.	R^2 , %.	Test Statistic.	5%.	Z.	Test Statistic.	5%.	Exceedances.	Exceedances.
0.0846	97.4	0.5158	0.1687	-6.998	0.1214	0.0775	15	7

Storm Specific Comment: The convergence monitor is adequate, below 0.1, the R^2 is adequate 97.4%, the cumulative periodogram does not pass the test statistic. The standardised residual versus time plot exceeds the Z statistic limit of $|2|$, the standardised residual versus N(0,1) variate does not pass the test statistic. The auto-correlation plot is exceeded 15 times, and the partial auto-correlation plot is exceeded 7 times.

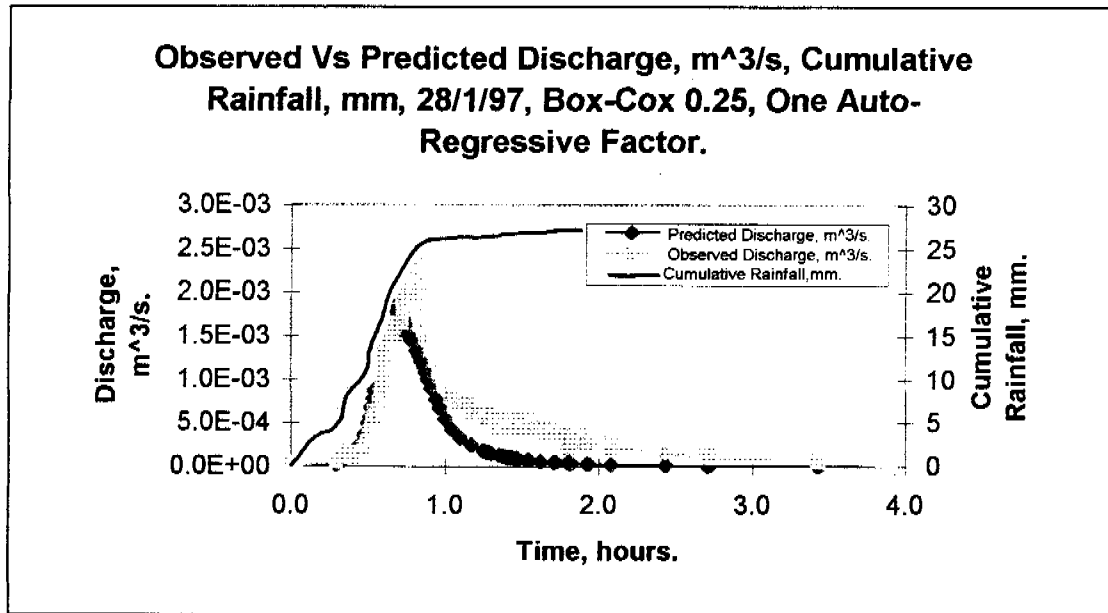


NLFIT Input files: 28197.fw, 28197.ro/rf
 NLFIT Output files: 28197g25.prt/pmf/plt.

Parameter.	Mean.	Standard Deviation.	Parameter.	Mean.	Standard Deviation.
C_r	7.574	0.8921	$S\phi$	0.001	
e_m	2.666	0.0855	ϕ	24.239	0.561

		Cumulative Periodogram.		Standardised Residual Versus Time.	Standardised Residual Versus N(0,1) Variate.		Auto Correlation Plot.	Partial Auto Correlation Plot.
Convergence Monitor.	R^2 , %.	Test Statistic.	5%.	Z.	Test Statistic.	5%.	Exceedances.	Exceedances.
0.1178	96.6	0.5244	0.1687	-4.300	0.1035	0.0775	15	4

Storm Specific Comment: The convergence monitor is adequate, below 0.1, the R^2 is adequate 96.6%, the cumulative periodogram does not pass the test statistic. The standardised residual versus time plot exceeds the Z statistic limit of $|2|$, the standardised residual versus N(0,1) variate does not pass the test statistic. The auto-correlation plot is exceeded 15 times, and the partial auto-correlation plot is exceeded 4 times.



NLFIT Input files: 28197.fw, 28197.ro/rf

NLFIT Output files: 2819725a.prt/pmf/plt.

Parameter.	Mean.	Standard Deviation.	Parameter.	Mean.	Standard Deviation.
C_r	3.75278	0.9382	$S\phi$	0.001	
e_m	1.627	0.121	ϕ	39.990	3.968

		Cumulative Periodogram.		Standardised Residual Versus Time.	Standardised Residual Versus N(0,1) Variate.		Auto Correlation Plot.	Partial Auto Correlation Plot.
Convergence Monitor.	R^2 , %.	Test Statistic.	5%.	Z.	Test Statistic.	5%.	Exceedances.	Exceedances.
0.00041	78.2	0.435	0.1687	4.733	0.1680	0.0775	7	3

Storm Specific Comment: The convergence monitor is adequate, below 0.1, the R^2 is adequate 78.2%, the cumulative periodogram does not pass the test statistic. The standardised residual versus time plot exceeds the Z statistic limit of $|2|$, the standardised residual versus N(0,1) variate does not pass the test statistic. The auto-correlation plot is exceeded 7 times, and the partial auto-correlation plot is exceeded 3 times.

General Comment: 28197.* was a good predicted response, 97.4%, with near perfect inclination and recession limbs of the hydrograph. The utilisation of a more general error model deteriorated the fit in the recession portion of the hydrograph, 28197g25.*, the addition of an auto-regressive factor worsened the predicted response even further, 2819725a.*.

19th February

RUM 96-97 Monitoring

pit 1 site

Rainfall 19/2/97 1921hrs

285

0	0	0.24	4.6	0.379	9	0.474	14	0.543	18.6	0.642	23.8	0.722	28.6	0.843	33.2	1.074	37.2	1.269	42.2	1.465	46.4	1.746	51	2.068	55.4	2.51	59.6	3.406	64
0.017	0.2	0.246	4.8	0.383	9.2	0.478	14.4	0.547	18.8	0.646	24	0.724	28.8	0.847	33.4	1.092	37.6	1.276	42.4	1.475	46.6	1.756	51.2	2.093	55.6	2.531	59.8	3.603	64.2
0.028	0.6	0.247	5	0.388	9.4	0.482	14.6	0.551	19	0.649	24.2	0.729	29	0.854	33.6	1.117	37.8	1.278	42.6	1.486	47	1.757	51.4	2.118	56	2.564	60	3.633	64.4
0.036	0.8	0.254	5.2	0.393	9.8	0.486	14.8	0.556	19.4	0.65	24.4	0.736	29.2	0.863	33.8	1.156	38	1.286	42.8	1.496	47.2	1.764	51.6	2.153	56.2	2.6	60.2	3.886	64.6
0.044	1	0.263	5.4	0.399	10	0.49	15	0.56	19.6	0.653	24.6	0.74	29.6	0.871	34	1.167	38.2	1.296	43	1.51	47.4	1.771	51.8	2.196	56.4	2.601	60.4	4.5	64.6
0.053	1.2	0.272	5.6	0.404	10	0.492	15.2	0.564	19.8	0.657	25	0.747	29.8	0.872	34.2	1.175	38.4	1.31	43.2	1.528	47.6	1.779	52	2.219	56.6	2.638	60.6		
0.058	1.4	0.282	5.8	0.41	10	0.496	15.4	0.565	20	0.66	25.2	0.756	30	0.879	34.4	1.182	38.8	1.328	43.6	1.543	47.8	1.789	52.2	2.236	56.8	2.69	60.8		
0.067	1.6	0.296	6.2	0.417	10	0.499	15.6	0.569	20.2	0.664	25.4	0.765	30.2	0.888	34.6	1.189	39	1.35	43.8	1.557	48	1.797	52.4	2.251	57	2.753	61		
0.078	1.8	0.308	6.4	0.422	11	0.5	15.8	0.575	20.4	0.668	25.8	0.772	30.4	0.896	34.8	1.196	39.2	1.365	44	1.571	48.4	1.806	52.6	2.271	57.2	2.775	61.2		
0.096	2.2	0.322	6.6	0.426	11	0.503	16	0.581	20.8	0.672	26	0.774	30.6	0.903	35	1.201	39.4	1.376	44.2	1.586	48.6	1.818	53	2.294	57.4	2.776	61.4		
0.118	2.4	0.333	6.8	0.431	11	0.507	16.2	0.586	21	0.675	26.2	0.781	30.8	0.904	35.2	1.207	39.8	1.386	44.4	1.6	48.8	1.831	53.2	2.317	57.6	2.786	61.6		
0.139	2.6	0.343	7	0.438	11	0.51	16.4	0.592	21.2	0.676	26.4	0.788	31	0.914	35.4	1.213	40	1.396	44.6	1.614	49	1.849	53.4	2.318	57.8	2.797	61.8		
0.156	2.8	0.35	7.2	0.443	12	0.511	16.6	0.599	21.6	0.681	26.6	0.794	31.2	0.932	35.6	1.217	40.2	1.397	44.8	1.625	49.2	1.869	53.6	2.34	58	2.806	62		
0.169	3	0.351	7.4	0.447	12	0.515	16.8	0.604	21.8	0.686	26.8	0.801	31.6	0.954	35.8	1.221	40.6	1.407	45	1.638	49.6	1.896	53.8	2.364	58.2	2.814	62.4		
0.182	3.2	0.357	7.6	0.453	12	0.519	17.2	0.611	22	0.692	27.2	0.807	31.8	0.978	36	1.226	40.8	1.418	45.2	1.65	49.8	1.918	54	2.386	58.4	2.822	62.6		
0.193	3.4	0.363	7.8	0.457	12	0.524	17.4	0.617	22.4	0.696	27.4	0.814	32	1.007	36.2	1.232	41	1.428	45.4	1.663	50	1.939	54.2	2.41	58.6	2.832	62.8		
0.206	3.8	0.367	8	0.461	13	0.528	17.8	0.622	22.6	0.701	27.6	0.821	32.4	1.008	36.4	1.239	41.2	1.438	45.6	1.676	50.2	1.961	54.4	2.433	58.8	2.846	63		
0.217	4	0.368	8.2	0.465	13	0.532	18	0.628	23	0.707	28	0.828	32.6	1.031	36.6	1.246	41.6	1.447	45.8	1.694	50.4	1.988	54.8	2.457	59	2.878	63.4		
0.226	4.2	0.372	8.4	0.469	13	0.538	18.2	0.632	23.2	0.711	28.2	0.836	32.8	1.044	36.8	1.253	41.8	1.449	46	1.715	50.6	2.015	55	2.458	59.2	3.007	63.6		
0.233	4.4	0.375	8.6	0.471	13	0.542	18.4	0.636	23.4	0.717	28.4	0.842	33	1.058	37	1.26	42	1.457	46.2	1.733	50.8	2.042	55.2	2.483	59.4	3.203	63.8		

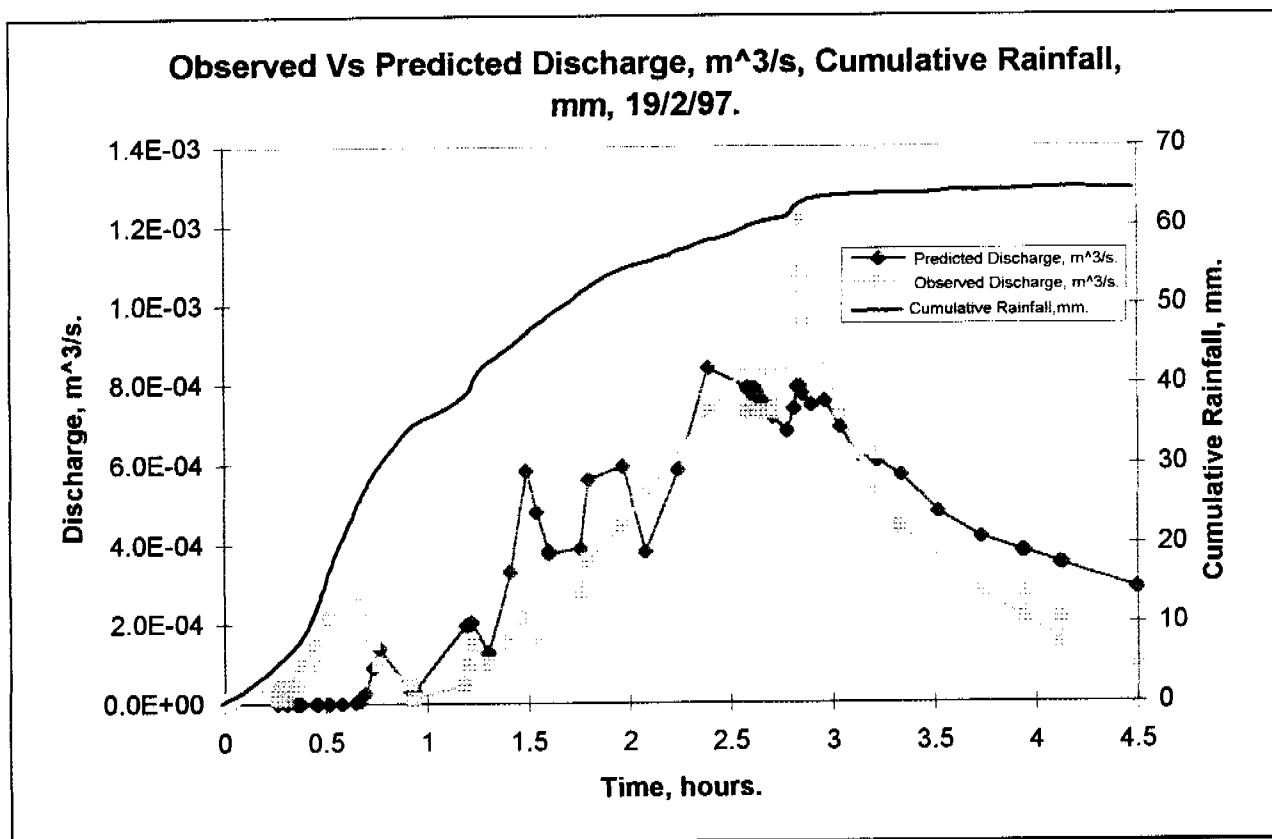
RUM 96-97 Monitoring

pit 1 site

Runoff 19/2/97 1921hrs

91

0	0	0.732	1.53E-04	2.581	8.39E-04	2.703	8.39E-04	3.933	2.83E-04
0.036	9.97E-06	0.765	9.84E-05	2.583	7.29E-04	2.704	7.29E-04	3.935	2.14E-04
0.263	5.07E-05	0.913	5.07E-05	2.585	8.39E-04	2.706	8.39E-04	3.946	2.83E-04
0.264	9.97E-06	0.935	9.97E-06	2.586	7.29E-04	2.707	7.29E-04	3.947	2.14E-04
0.265	5.07E-05	1.188	5.07E-05	2.588	8.39E-04	2.778	8.39E-04	4.121	1.53E-04
0.308	9.97E-06	1.207	9.84E-05	2.59	7.29E-04	2.811	9.57E-04	4.126	2.14E-04
0.31	5.07E-05	1.219	1.53E-04	2.592	8.39E-04	2.828	1.08E-03	4.131	1.53E-04
0.311	9.97E-06	1.3	9.84E-05	2.6	7.29E-04	2.842	1.21E-03	4.132	2.14E-04
0.36	5.07E-05	1.411	1.53E-04	2.601	8.39E-04	2.856	1.08E-03	4.133	1.53E-04
0.381	9.84E-05	1.488	2.14E-04	2.606	7.29E-04	2.9	9.57E-04	4.494	9.84E-05
0.454	1.53E-04	1.542	1.53E-04	2.608	8.39E-04	2.963	8.39E-04	4.5	0
0.458	9.84E-05	1.597	2.14E-04	2.618	7.29E-04	3.035	7.29E-04		
0.46	1.53E-04	1.599	1.53E-04	2.621	8.39E-04	3.122	6.26E-04		
0.461	9.84E-05	1.6	2.14E-04	2.625	7.29E-04	3.214	5.30E-04		
0.463	1.53E-04	1.757	2.83E-04	2.628	8.39E-04	3.215	6.26E-04		
0.517	2.14E-04	1.794	3.58E-04	2.65	7.29E-04	3.218	5.30E-04		
0.583	1.53E-04	1.967	4.41E-04	2.651	8.39E-04	3.339	4.41E-04		
0.653	2.14E-04	2.079	5.30E-04	2.689	7.29E-04	3.519	3.58E-04		
0.669	2.83E-04	2.238	6.26E-04	2.69	8.39E-04	3.731	2.83E-04		
0.694	2.14E-04	2.389	7.29E-04	2.701	7.29E-04	3.931	2.14E-04		



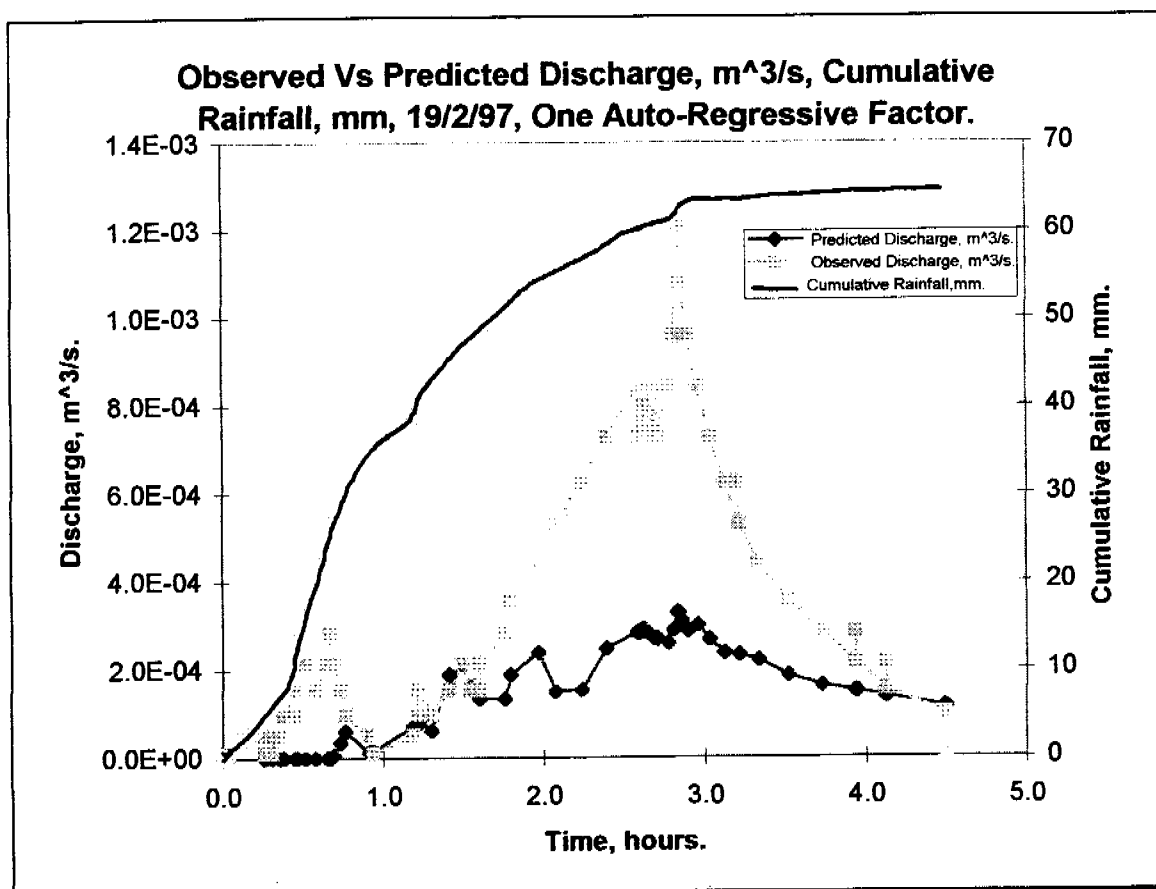
NLFIT Input files: 19297.fw, 19297.ro/rf

NLFIT Output files: 19297.prt/pmf/plt.

Parameter.	Mean.	Standard Deviation.	Parameter.	Mean.	Standard Deviation.
C_r	0.6307	0.097	$S\phi$	11.700	0.385
e_m	4.5174	0.3497	ϕ	0.001	

		Cumulative Periodogram.		Standardised Residual Versus Time.	Standardised Residual Versus N(0,1) Variate.		Auto Correlation Plot.	Partial Auto Correlation Plot.
Convergence Monitor.	R^2 , %.	Test Statistic.	5%.	Z.	Test Statistic.	5%.	Exceedances.	Exceedances.
0.01597	81.2	0.6697	0.2050	-4.198	0.0566	0.0936	10	4

Storm Specific Comment: The convergence monitor is adequate, below 0.1, the R^2 is not adequate 81.2%, the cumulative periodogram does not pass the test statistic. The standardised residual versus time plot exceeds the Z statistic limit of $|2|$, the standardised residual versus N(0,1) variate does pass the test statistic. The auto-correlation plot is exceeded 10 times, and the partial auto-correlation plot is exceeded 4 times.



NLFIT Input files: 19297.fw, 192197.ro/rf

NLFIT Output files: 19297a.prt/pmf/plt.

Parameter.	Mean.	Standard Deviation.	Parameter.	Mean.	Standard Deviation.
C_r	10.2689	13.8353	$S\phi$	20.0872	2.2290
e_m	4.0003	0.5531	ϕ	0.001	

		Cumulative Periodogram.		Standardised Residual Versus Time.	Standardised Residual Versus N(0,1) Variate.		Auto Correlation Plot.	Partial Auto Correlation Plot.
Convergence Monitor.	R^2 , %.	Test Statistic.	5%.	Z.	Test Statistic.	5%.	Exceedances.	Exceedances.
0.3485	80.5	0.398	0.205	2.544	0.1569	0.0936	10	3

Storm Specific Comment: The convergence monitor is not adequate, below 0.1, the R^2 is not adequate 80.5%, the cumulative periodogram does not pass the test statistic. The standardised residual versus time plot exceeds the Z statistic limit of $|2|$, the standardised residual versus N(0,1) variate does not pass the test statistic. The auto-correlation plot is exceeded 10 times, and the partial auto-correlation plot is exceeded 3 times.

General Comment: The inclusion of an auto-regressive factor has dramatically degraded the predicted versus observed response, 19297a.*. The least squares model provides the best alternative for a poorly fitted event.

20th February

RUM 96-97 Monitoring

pit 1 site

Rainfall 20/2/97 1514hrs

138

0	0	0.119	4.8	0.19	9.8	0.278	14.6	0.343	20	0.436	24.4	0.582	29
0.01	0.2	0.121	5	0.193	10	0.279	14.8	0.344	20.2	0.438	24.6	0.59	29.2
0.017	0.4	0.125	5.2	0.197	10.2	0.283	15	0.349	20.4	0.444	24.8	0.604	29.4
0.022	0.6	0.129	5.4	0.201	10.6	0.288	15.4	0.353	20.6	0.453	25	0.669	29.6
0.029	1	0.133	5.8	0.206	10.8	0.292	15.6	0.358	21	0.463	25.2	0.671	29.8
0.04	1.2	0.138	6	0.21	11.2	0.294	16	0.364	21.2	0.471	25.4	0.713	30
0.054	1.4	0.142	6.4	0.214	11.4	0.299	16.2	0.368	21.4	0.472	25.6	0.728	30.2
0.06	1.6	0.146	6.6	0.222	11.6	0.301	16.4	0.369	21.6	0.479	25.8	0.739	30.4
0.065	2	0.15	6.8	0.231	11.8	0.303	16.6	0.375	21.8	0.485	26	0.751	30.6
0.071	2.2	0.154	7.2	0.232	12	0.306	16.8	0.381	22	0.49	26.4	0.764	30.8
0.072	2.4	0.158	7.4	0.238	12.2	0.308	17.2	0.386	22.2	0.494	26.6	0.765	31
0.076	2.8	0.163	7.8	0.24	12.4	0.313	17.4	0.388	22.4	0.5	27	0.778	31.2
0.082	3	0.167	8	0.242	12.6	0.315	17.8	0.393	22.6	0.506	27.2	0.794	31.4
0.093	3.2	0.169	8.2	0.246	12.8	0.318	18	0.399	23	0.51	27.4	0.817	31.6
0.097	3.6	0.172	8.4	0.249	13	0.322	18.4	0.403	23.2	0.515	27.8	0.84	31.8
0.1	3.8	0.174	8.6	0.254	13.4	0.325	18.6	0.408	23.4	0.521	28	0.921	32.2
0.107	4	0.176	8.8	0.26	13.6	0.329	19	0.414	23.6	0.531	28.2	0.968	32.4
0.111	4.2	0.181	9.2	0.265	13.8	0.332	19.2	0.415	23.8	0.54	28.4	2.2	32.4
0.113	4.4	0.185	9.4	0.269	14.2	0.336	19.6	0.421	24	0.572	28.6		
0.117	4.6	0.189	9.6	0.274	14.4	0.34	19.8	0.429	24.2	0.574	28.8		

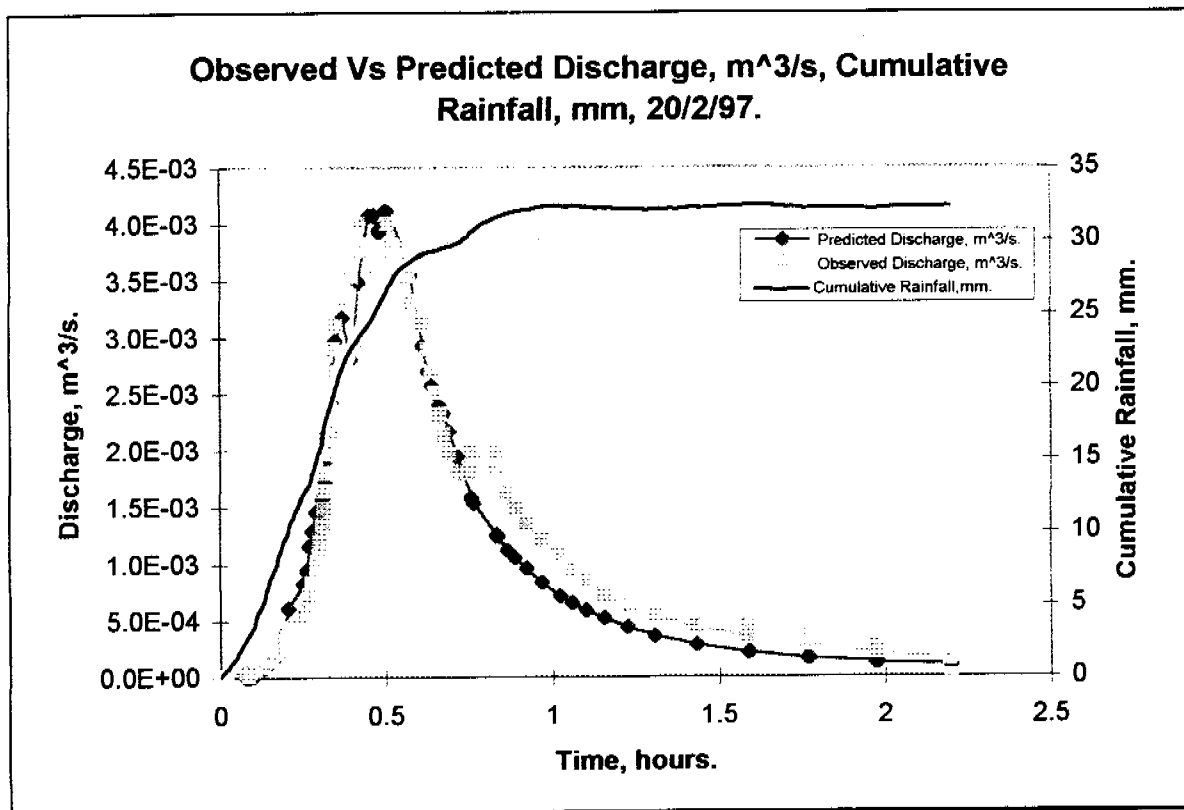
RUM 96-97 Monitoring

pit 1 site

Runoff 20/2/97 1514hrs

83

0	0.00E+00	0.318	1.65E-03	0.575	3.32E-03	1.058	9.57E-04	1.981	2.14E-04		
0.014	9.97E-06	0.322	1.80E-03	0.611	3.11E-03	1.1	8.39E-04	2.196	1.53E-04		
0.078	5.07E-05	0.326	1.97E-03	0.628	2.90E-03	1.154	7.29E-04	2.2	0		
0.085	9.97E-06	0.331	2.14E-03	0.64	2.70E-03	1.224	6.26E-04				
0.099	5.07E-05	0.336	2.51E-03	0.649	2.51E-03	1.308	5.30E-04				
0.133	9.84E-05	0.338	2.70E-03	0.661	2.32E-03	1.433	4.41E-04				
0.157	1.53E-04	0.343	2.90E-03	0.671	2.14E-03	1.588	3.58E-04				
0.175	2.14E-04	0.35	3.11E-03	0.689	1.97E-03	1.589	4.41E-04				
0.185	2.83E-04	0.372	3.32E-03	0.714	1.80E-03	1.593	3.58E-04				
0.192	3.58E-04	0.397	3.54E-03	0.757	1.97E-03	1.765	2.83E-04				
0.208	4.41E-04	0.406	3.77E-03	0.758	1.80E-03	1.767	3.58E-04				
0.251	5.30E-04	0.419	4.01E-03	0.764	1.97E-03	1.768	2.83E-04				
0.263	6.26E-04	0.45	3.77E-03	0.833	1.80E-03	1.771	3.58E-04				
0.272	7.29E-04	0.464	3.54E-03	0.835	1.97E-03	1.774	2.83E-04				
0.279	8.39E-04	0.481	3.32E-03	0.836	1.80E-03	1.972	2.14E-04				
0.293	9.57E-04	0.483	3.54E-03	0.865	1.65E-03	1.974	2.83E-04				
0.3	1.08E-03	0.5	3.77E-03	0.888	1.49E-03	1.975	2.14E-04				
0.304	1.21E-03	0.507	4.01E-03	0.922	1.35E-03	1.976	2.83E-04				
0.311	1.35E-03	0.56	3.77E-03	0.968	1.21E-03	1.978	2.14E-04				
0.315	1.49E-03	0.568	3.54E-03	1.022	1.08E-03	1.979	2.83E-04				



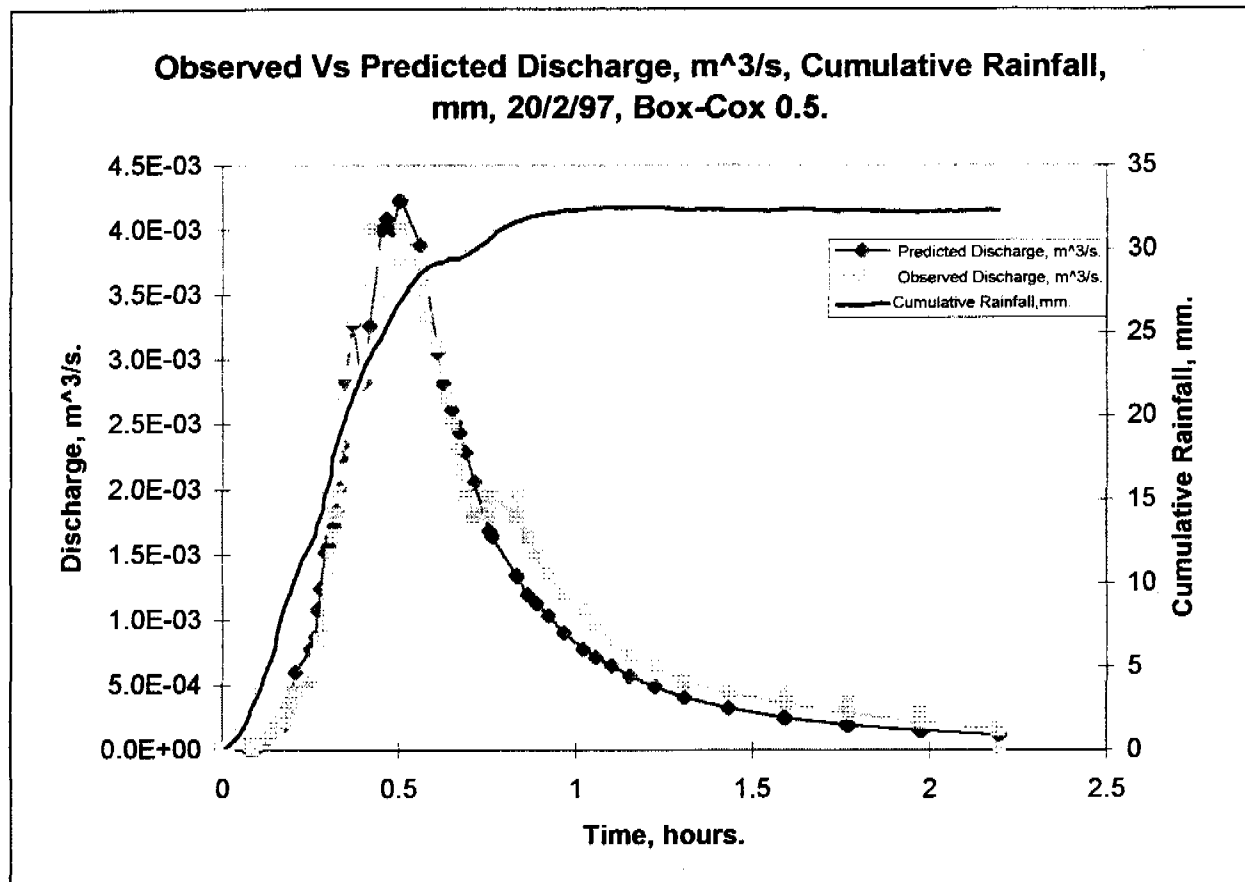
NLFIT Input files: 20297.fw, 202197.ro/rf

NLFIT Output files: 20297.prt/pmf/plt.

Parameter.	Mean.	Standard Deviation.	Parameter.	Mean.	Standard Deviation.
C_r	3.2113	0.5047	$S\phi$	2.2578	1.9129
e_m	2.0933	0.1891	ϕ	22.7432	4.0251

Convergence Monitor.	R^2 , %.	Cumulative Periodogram.		Standardised Residual Versus Time.	Standardised Residual Versus N(0,1) Variate.		Auto Correlation Plot.	Partial Auto Correlation Plot.
		Test Statistic.	5%.	Z.	Test Statistic.	5%.	Exceedances.	Exceedances.
0.1216	94.9	0.6263	0.215	-6.403	0.0992	0.0979	4	4

Storm Specific Comment: The convergence monitor is adequate, below 0.1, the R^2 is adequate 94.9%, the cumulative periodogram does not pass the test statistic. The standardised residual versus time plot exceeds the Z statistic limit of |2|, the standardised residual versus N(0,1) variate does pass the test statistic. The auto-correlation plot is exceeded 4 times, and the partial auto-correlation plot is exceeded 4 times.

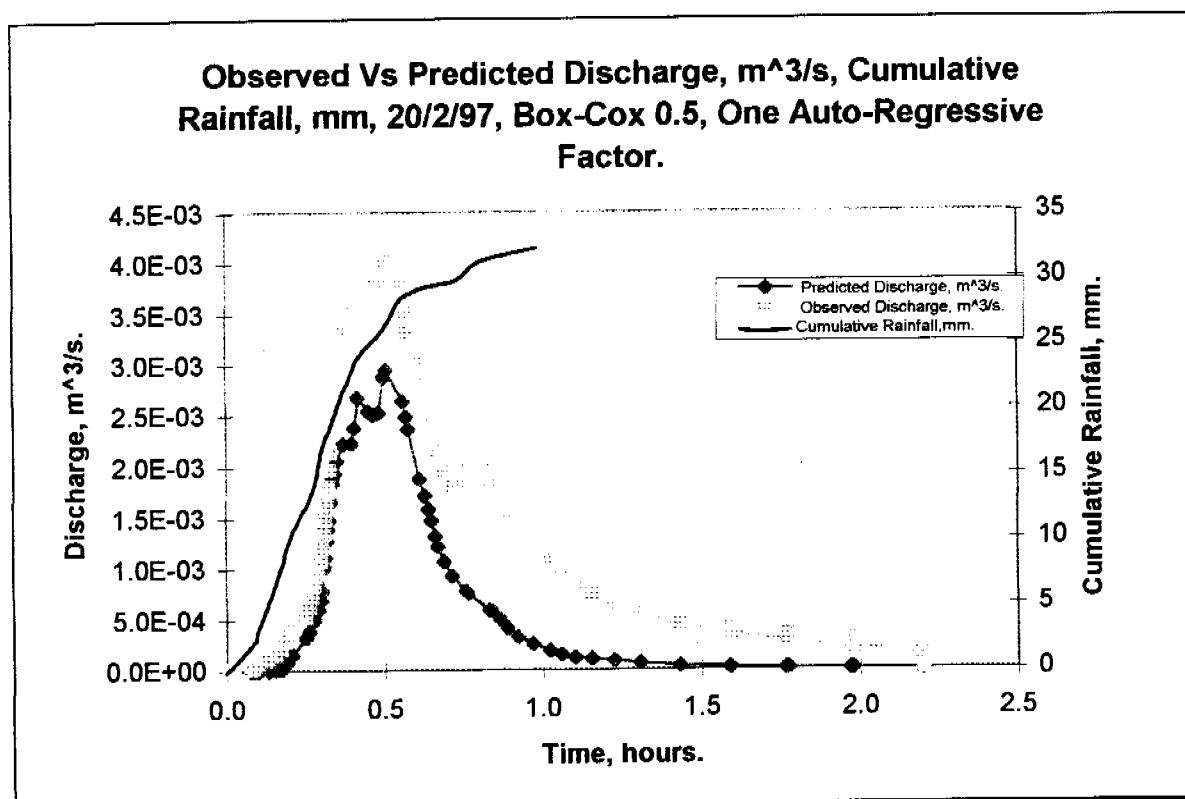


NLFIT Input files: 20297.fw, 20297.ro/rf
 NLFIT Output files: 20297g5.prt/pmf/plt.

Parameter.	Mean.	Standard Deviation.	Parameter.	Mean.	Standard Deviation.
C_r	3.2100	0.4872	$S\phi$	1.5585	1.7330
e_m	7.18971	0.1854	ϕ	22.9835	3.6822

		Cumulative Periodogram.		Standardised Residual Versus Time.	Standardised Residual Versus N(0,1) Variate.		Auto Correlation Plot.	Partial Auto Correlation Plot.
Convergence Monitor.	R^2 , %.	Test Statistic.	5%.	Z.	Test Statistic.	5%.	Exceedances.	Exceedances.
0.1484	94.5	0.6464	0.215	-7.33	0.1064	0.0979	7	3

Storm Specific Comment: The convergence monitor is not adequate, below 0.1, the R^2 is adequate 94.5%, the cumulative periodogram does not pass the test statistic. The standardised residual versus time plot exceeds the Z statistic limit of $|2|$, the standardised residual versus N(0,1) variate does pass the test statistic. The auto-correlation plot is exceeded 7 times, and the partial auto-correlation plot is exceeded 3 times.



NLFIT Input files: 20297.fw, 20297.ro/rf

NLFIT Output files: 202975a.prt/pmf/plt.

Parameter.	Mean.	Standard Deviation.	Parameter.	Mean.	Standard Deviation.
C_r	2.1864	0.3240	$S\phi$	13.6427	2.3932
e_m	1.32504	0.0818	ϕ	8.6438	6.6151

		Cumulative Periodogram.		Standardised Residual Versus Time.	Standardised Residual Versus N(0,1) Variate.		Auto Correlation Plot.	Partial Auto Correlation Plot.
Convergence Monitor.	R^2 , %.	Test Statistic.	5%.	Z.	Test Statistic.	5%.	Exceedances.	Exceedances.
0.5307	93.8	0.1279	0.215	-0.889	0.0652	0.0979	1	1

Storm Specific Comment: The convergence monitor is not adequate, below 0.1, the R^2 is adequate 93.8%, the cumulative periodogram does pass the test statistic. The standardised residual versus time plot does not exceed the Z statistic limit of |2|, the standardised residual versus N(0,1) variate does pass the test statistic. The auto-correlation plot is exceeded 1 times, and the partial auto-correlation plot is exceeded 1 times.

General Comment: The least squares predicted response, 20297.*, is superior to all other error models. The inclusion of a Box-Cox of 0.5, 20297g5.*, did not have a dramatic impact upon the predicted response, however there was a slight deterioration in the recession limb of the hydrograph. The inclusion of an auto-regressive factor, 202975a.*, further deteriorated the quality of the predicted response.

22nd February

RUM 96-97 Monitoring

pit 1 site

Rainfall 22/2/97 0514hrs

133

0	0	0.561	4	0.749	8.6	0.846	13	0.978	17.4	1.056	21.8	1.431	26.2
0.081	0.2	0.569	4.4	0.754	8.8	0.854	13.4	0.982	17.8	1.057	22	1.506	26.4
0.231	0.4	0.578	4.6	0.758	9	0.864	13.6	0.986	18	1.063	22.2	1.575	26.6
0.274	0.6	0.586	4.8	0.76	9.2	0.875	13.8	0.989	18.2	1.069	22.4	1.639	26.8
0.304	0.8	0.594	5	0.764	9.4	0.886	14	0.993	18.4	1.078	22.6	1.697	27
0.339	1	0.604	5.2	0.768	9.6	0.9	14.2	0.994	18.6	1.086	22.8	1.754	27.2
0.368	1.2	0.614	5.6	0.772	9.8	0.913	14.4	0.997	18.8	1.099	23.2	1.822	27.6
0.39	1.4	0.625	5.8	0.778	10.2	0.924	14.6	1.001	19	1.113	23.4	1.915	27.8
0.404	1.6	0.635	6	0.783	10.4	0.931	14.8	1.004	19.2	1.126	23.6	2.063	28
0.419	1.8	0.643	6.2	0.789	10.6	0.932	15	1.006	19.4	1.14	23.8	2.26	28.2
0.433	2	0.653	6.4	0.793	10.8	0.936	15.2	1.008	19.6	1.154	24	2.383	28.4
0.463	2.2	0.664	6.6	0.799	11.2	0.94	15.4	1.013	19.8	1.167	24.2	2.628	28.6
0.464	2.4	0.665	6.8	0.804	11.4	0.944	15.6	1.014	20	1.182	24.6	3.085	29
0.492	2.6	0.678	7	0.81	11.6	0.949	15.8	1.018	20.2	1.199	24.8	3.5	29
0.508	2.8	0.697	7.2	0.815	11.8	0.95	16	1.022	20.4	1.224	25		
0.526	3	0.711	7.4	0.819	12	0.954	16.2	1.028	20.6	1.268	25.2		
0.538	3.2	0.722	7.6	0.821	12.2	0.96	16.4	1.033	21	1.303	25.4		
0.539	3.4	0.731	7.8	0.825	12.4	0.965	16.6	1.039	21.2	1.35	25.6		
0.546	3.6	0.738	8.2	0.832	12.6	0.971	17	1.044	21.4	1.39	25.8		
0.554	3.8	0.743	8.4	0.839	12.8	0.975	17.2	1.05	21.6	1.392	26		

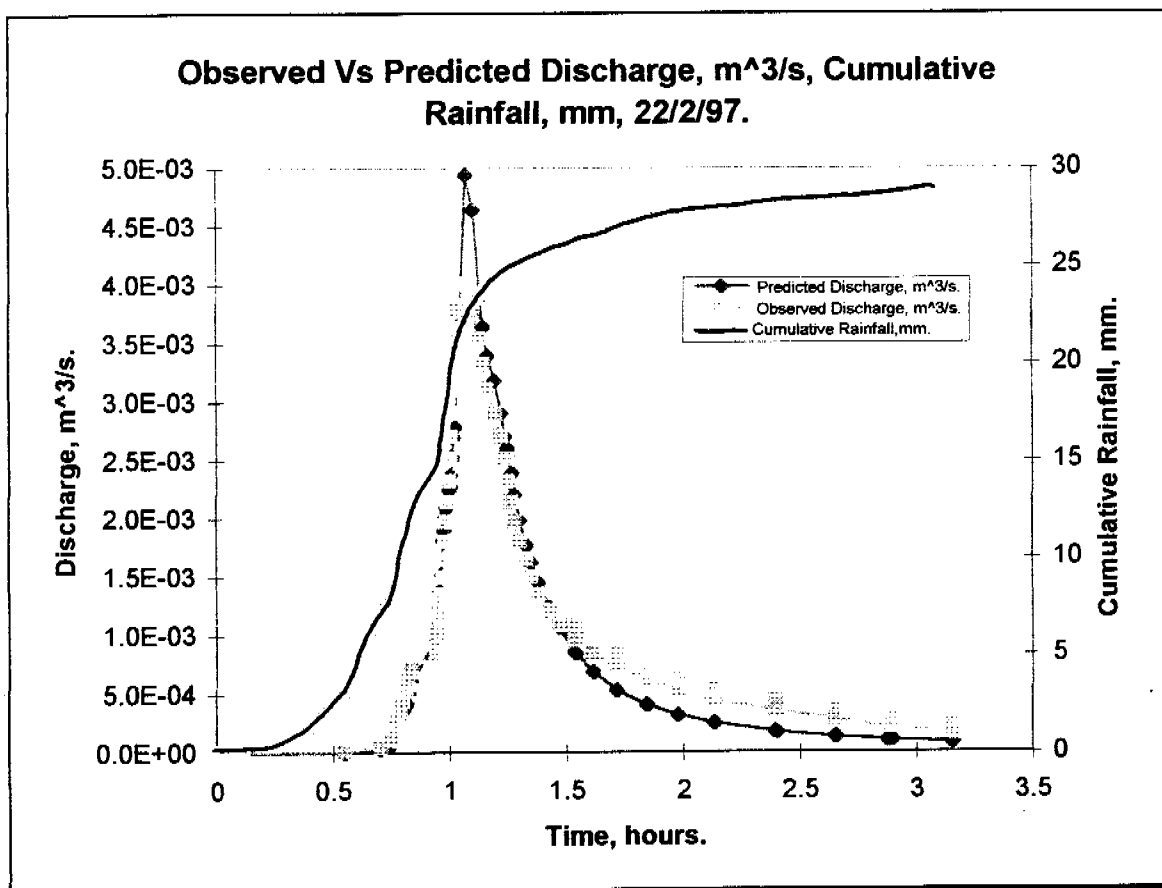
RUM 96-97 Monitoring

pit 1 site

Runoff 22/2/97 0514hrs

87

0	0	0.986	1.97E-03	1.249	2.32E-03	1.979	6.26E-04	2.897	2.83E-04				
0.553	9.97E-06	0.992	2.14E-03	1.263	2.14E-03	1.981	5.30E-04	2.899	2.14E-04				
0.707	5.07E-05	0.997	2.32E-03	1.279	1.97E-03	2.133	4.41E-04	3.154	1.53E-04				
0.747	9.84E-05	1.001	2.51E-03	1.301	1.80E-03	2.135	5.30E-04	3.156	2.14E-04				
0.763	1.53E-04	1.006	2.70E-03	1.328	1.65E-03	2.136	4.41E-04	3.157	1.53E-04				
0.769	2.14E-04	1.01	2.90E-03	1.351	1.49E-03	2.138	5.30E-04	3.158	2.14E-04				
0.779	2.83E-04	1.014	3.11E-03	1.379	1.35E-03	2.139	4.41E-04	3.161	1.53E-04				
0.79	3.58E-04	1.019	3.32E-03	1.428	1.21E-03	2.396	3.58E-04	3.447	9.84E-05				
0.8	4.41E-04	1.022	3.54E-03	1.468	1.08E-03	2.397	4.41E-04	3.5	0				
0.813	5.30E-04	1.035	3.77E-03	1.536	9.57E-04	2.403	3.58E-04						
0.822	6.26E-04	1.072	4.01E-03	1.538	1.08E-03	2.656	2.83E-04						
0.833	7.29E-04	1.101	3.77E-03	1.539	9.57E-04	2.657	3.58E-04						
0.94	8.39E-04	1.129	3.54E-03	1.611	8.39E-04	2.661	2.83E-04						
0.944	9.57E-04	1.143	3.32E-03	1.713	7.29E-04	2.879	2.14E-04						
0.949	1.08E-03	1.163	3.11E-03	1.715	8.39E-04	2.881	2.83E-04						
0.956	1.21E-03	1.196	2.90E-03	1.717	7.29E-04	2.885	2.14E-04						
0.964	1.35E-03	1.219	2.70E-03	1.843	6.26E-04	2.888	2.83E-04						
0.972	1.49E-03	1.235	2.51E-03	1.844	7.29E-04	2.89	2.14E-04						
0.976	1.65E-03	1.244	2.32E-03	1.846	6.26E-04	2.894	2.83E-04						
0.981	1.80E-03	1.246	2.51E-03	1.978	5.30E-04	2.896	2.14E-04						



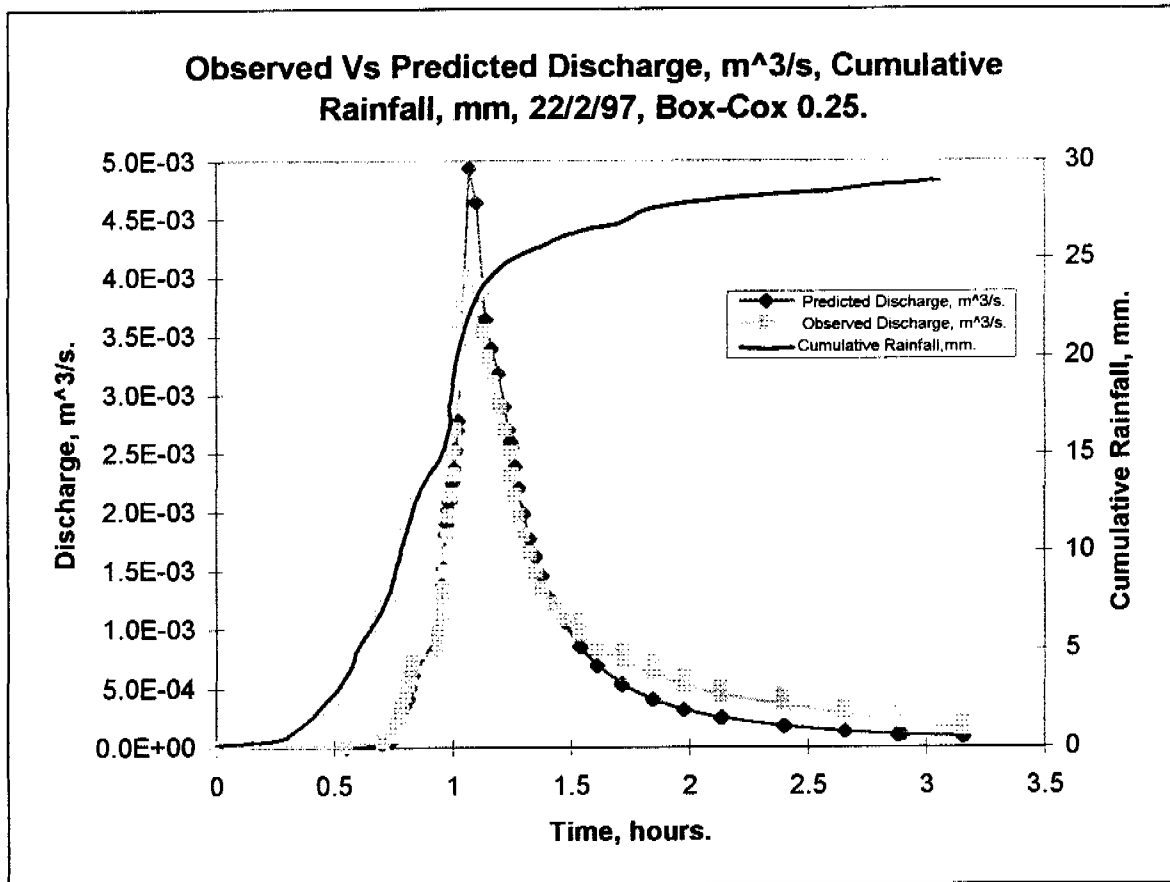
NLFIT Input files: 22297.fw, 22297.ro/rf

NLFIT Output files: 22297.prt/pmf/plt.

Parameter.	Mean.	Standard Deviation.	Parameter.	Mean.	Standard Deviation.
C_r	4.3148	0.5367	$S\phi$	0.001	
e_m	2.1037	0.0851	ϕ	15.579	0.4887

		Cumulative Periodogram.		Standardised Residual Versus Time.	Standardised Residual Versus N(0,1) Variate.		Auto Correlation Plot.	Partial Auto Correlation Plot.
Convergence Monitor.	R^2 , %.	Test Statistic.	5%.	Z.	Test Statistic.	5%.	Exceedances.	Exceedances.
0.07416	97.6	0.6581	0.2099	-7.398	0.0859	0.0957	16	1

Storm Specific Comment: The convergence monitor is adequate, below 0.1, the R^2 is adequate 97.6%, the cumulative periodogram does not pass the test statistic. The standardised residual versus time plot exceeds the Z statistic limit of $|2|$, the standardised residual versus N(0,1) variate does pass the test statistic. The auto-correlation plot is exceeded 16 times, and the partial auto-correlation plot is exceeded 1 times.



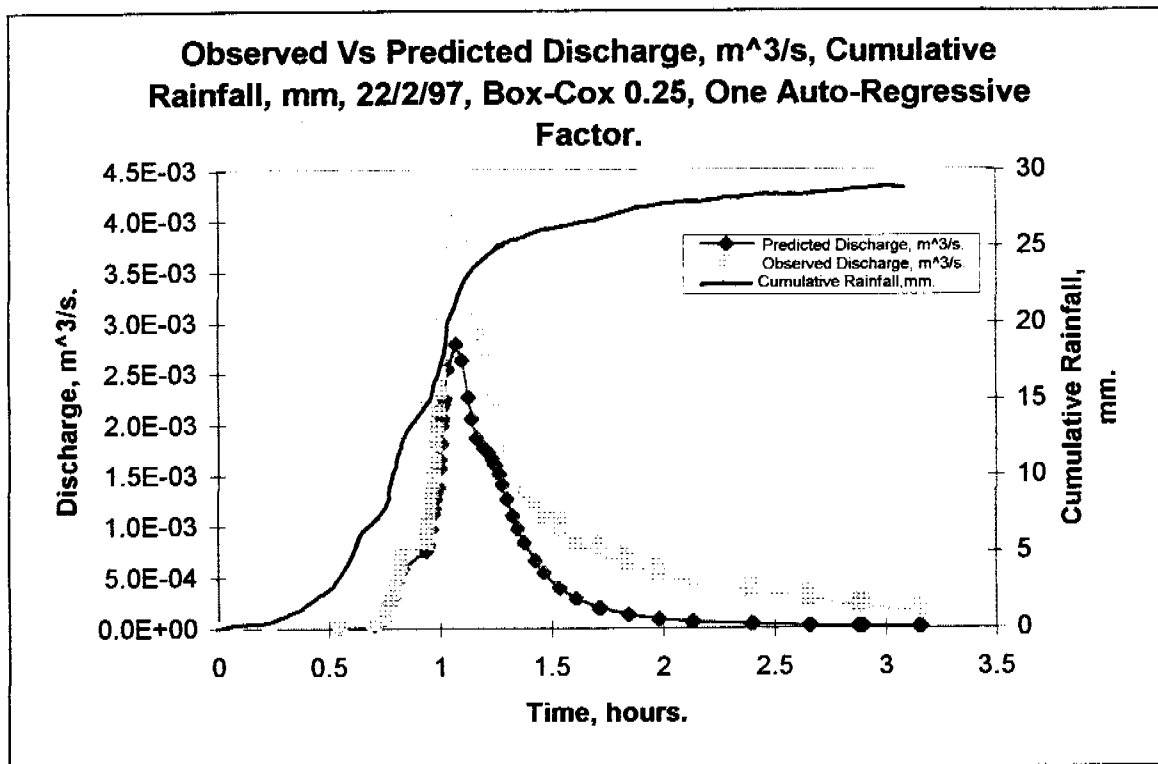
NLFIT Input files: 22297.fw, 22297.ro/rf

NLFIT Output files: 22297g25.prt/pmf/plf.

Parameter.	Mean.	Standard Deviation.	Parameter.	Mean.	Standard Deviation.
C_r	6.6952	1.0757	$S\phi$	0.001	
e_m	2.6072	0.1186	ϕ	12.6769	0.6236

		Cumulative Periodogram.		Standardised Residual Versus Time.	Standardised Residual Versus N(0,1) Variate.		Auto Correlation Plot.	Partial Auto Correlation Plot.
Convergence Monitor.	R^2 , %.	Test Statistic.	5%.	Z.	Test Statistic.	5%.	Exceedances.	Exceedances.
0.13191	96.0	0.6662	0.2099	-7.906	0.935	0.0957	12	1

Storm Specific Comment: The convergence monitor is not adequate, below 0.1, the R^2 is adequate 96.0%, the cumulative periodogram does not pass the test statistic. The standardised residual versus time plot exceeds the Z statistic limit of $|2|$, the standardised residual versus N(0,1) variate does pass the test statistic. The auto-correlation plot is exceeded 12 times, and the partial auto-correlation plot is exceeded 1 times.



NLFIT Input files: 22297.fw, 22297.ro/rf

NLFIT Output files: 2229725a.prt/pmf/plf.

Parameter.	Mean.	Standard Deviation.	Parameter.	Mean.	Standard Deviation.
C_r	0.9314	0.2723	$S\phi$	0.001	
e_m	1.3378	0.1258	ϕ	9.5213	2.5950

		Cumulative Periodogram.		Standardised Residual Versus Time.	Standardised Residual Versus N(0,1) Variate.		Auto Correlation Plot.	Partial Auto Correlation Plot.
Convergence Monitor.	R^2 , %.	Test Statistic.	5%.	Z.	Test Statistic.	5%.	Exceedances.	Exceedances.
0.1046	96.8	0.3041	0.2099	0.957	0.0977	0.0957	2	3

Storm Specific Comment: The convergence monitor is adequate, 0.1, the R^2 is adequate 96.8%, the cumulative periodogram does not pass the test statistic. The standardised residual versus time plot does not exceed the Z statistic limit of $|2|$, the standardised residual versus N(0,1) variate does pass the test statistic. The auto-correlation plot is exceeded 2 times, and the partial auto-correlation plot is exceeded 3 times.

General Comment: The predicted response of 22297.* is adequate compared to the observed hydrograph. The peak, however is over-predicted, and the recession limb is under-predicted slightly. 22297g25.*, the utilisation of a more general error model had little visual impact upon the quality of the predicted response, compared to 22297.*. The addition of an auto-regressive parameter, 2229725a.*, degraded the predicted response considerably.

22nd February pm Event

RUM 96-97 Monitoring

pit 1 site

Rainfall 22/2/97 1141hrs

123

0	0	0.214	4.4	0.335	8.8	0.617	13	0.81	17.2	0.972	22.2	1.549	26.4
0.119	0.2	0.218	4.6	0.342	9	0.643	13.2	0.818	17.4	0.981	22.4	2.282	26.6
0.132	0.4	0.225	4.8	0.347	9.2	0.675	13.4	0.828	17.8	0.99	22.6	3.225	26.8
0.139	0.6	0.231	5.2	0.353	9.4	0.689	13.6	0.836	18	0.999	22.8	4.2	26.8
0.14	0.8	0.235	5.4	0.363	9.6	0.697	13.8	0.844	18.2	1.008	23.2		
0.146	1	0.24	5.6	0.372	9.8	0.699	14	0.851	18.4	1.018	23.4		
0.151	1.2	0.247	5.8	0.374	10	0.708	14.2	0.86	18.8	1.029	23.6		
0.157	1.4	0.253	6	0.383	10.2	0.717	14.4	0.868	19	1.04	23.8		
0.158	1.6	0.26	6.4	0.396	10.4	0.725	14.6	0.875	19.2	1.054	24		
0.164	1.8	0.268	6.6	0.41	10.6	0.733	14.8	0.882	19.4	1.069	24.2		
0.169	2	0.279	6.8	0.424	10.8	0.742	15	0.89	19.6	1.085	24.4		
0.175	2.4	0.288	7	0.435	11.2	0.75	15.2	0.899	20	1.086	24.6		
0.179	2.6	0.292	7.2	0.444	11.4	0.751	15.4	0.907	20.2	1.1	24.8		
0.183	2.8	0.296	7.4	0.46	11.6	0.76	15.6	0.917	20.4	1.122	25		
0.189	3.2	0.297	7.6	0.511	11.8	0.767	15.8	0.926	20.6	1.189	25.2		
0.196	3.4	0.301	7.8	0.536	12	0.775	16	0.936	20.8	1.326	25.4		
0.201	3.6	0.307	8	0.551	12.2	0.781	16.2	0.943	21.2	1.388	25.6		
0.206	3.8	0.317	8.2	0.574	12.4	0.788	16.6	0.95	21.4	1.442	25.8		
0.21	4	0.326	8.4	0.575	12.6	0.793	16.8	0.957	21.6	1.443	26		
0.211	4.2	0.333	8.6	0.601	12.8	0.801	17	0.964	21.8	1.492	26.2		

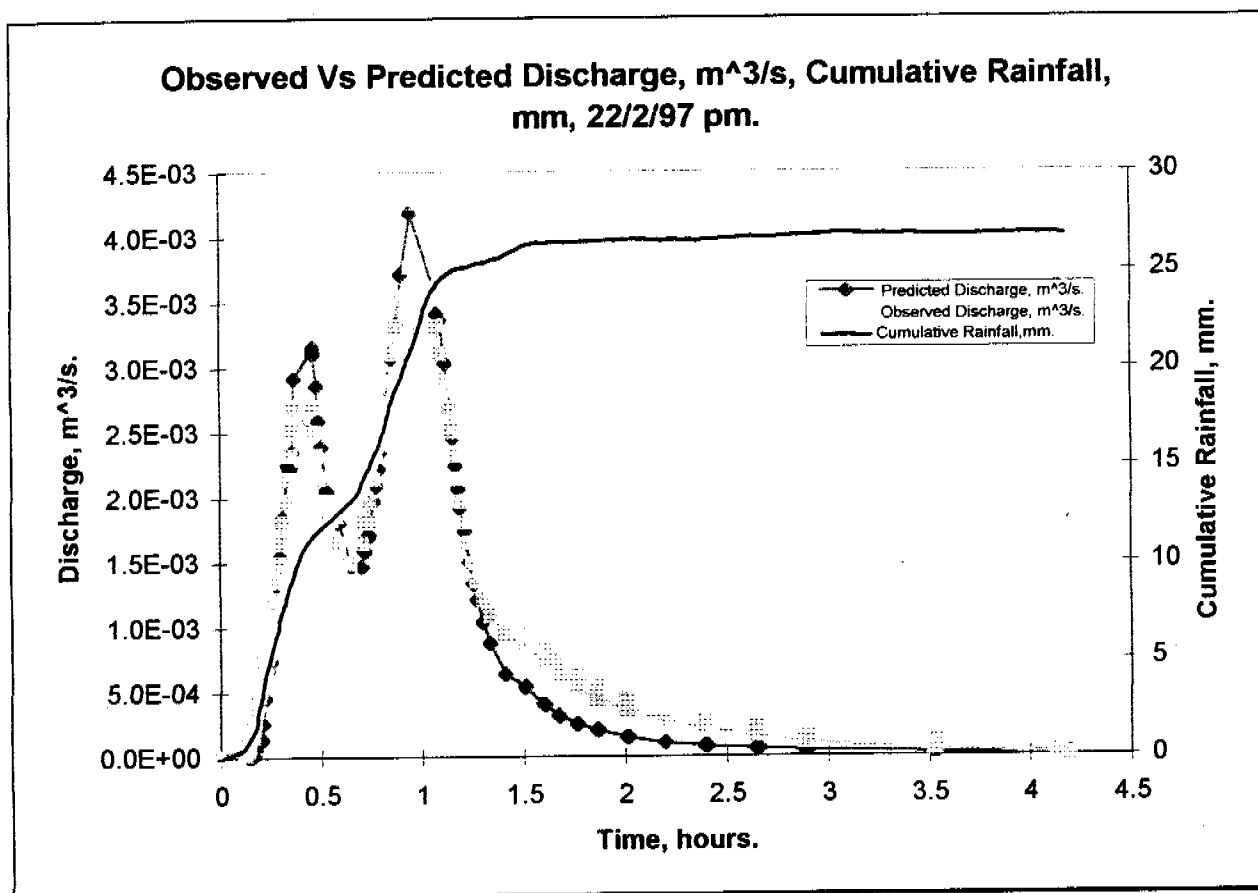
RUM 96-97 Monitoring

pit 1 site

Runoff 22/2/97 1141hrs

119

0	0.00E+00	0.351	2.32E-03	0.774	2.32E-03	1.271	1.35E-03	1.868	4.41E-04	2.657	1.53E-04		
0.144	9.84E-05	0.36	2.51E-03	0.786	2.51E-03	1.3	1.21E-03	1.871	5.30E-04	2.66	2.14E-04		
0.163	1.53E-04	0.371	2.70E-03	0.794	2.70E-03	1.335	1.08E-03	1.872	4.41E-04	2.661	1.53E-04		
0.169	2.14E-04	0.465	2.51E-03	0.835	2.90E-03	1.413	9.57E-04	2.008	3.58E-04	2.664	2.14E-04		
0.176	2.83E-04	0.467	2.70E-03	0.857	3.11E-03	1.508	8.39E-04	2.01	4.41E-04	2.665	1.53E-04		
0.182	3.58E-04	0.468	2.51E-03	0.879	3.32E-03	1.51	9.57E-04	2.013	3.58E-04	2.882	9.84E-05		
0.188	4.41E-04	0.481	2.32E-03	0.901	3.54E-03	1.511	8.39E-04	2.014	4.41E-04	2.883	1.53E-04		
0.196	5.30E-04	0.493	2.14E-03	0.95	3.77E-03	1.601	7.29E-04	2.018	3.58E-04	2.893	9.84E-05		
0.206	6.26E-04	0.504	1.97E-03	1.065	3.54E-03	1.603	8.39E-04	2.196	2.83E-04	2.899	1.53E-04		
0.213	7.29E-04	0.531	1.80E-03	1.078	3.32E-03	1.608	7.29E-04	2.392	2.14E-04	2.901	9.84E-05		
0.221	8.39E-04	0.532	1.97E-03	1.094	3.11E-03	1.674	6.26E-04	2.393	2.83E-04	3.521	5.07E-05		
0.238	9.57E-04	0.533	1.80E-03	1.119	2.90E-03	1.675	7.29E-04	2.4	2.14E-04	3.522	9.84E-05		
0.25	1.08E-03	0.594	1.65E-03	1.14	2.70E-03	1.678	6.26E-04	2.401	2.83E-04	3.525	5.07E-05		
0.263	1.21E-03	0.65	1.49E-03	1.153	2.51E-03	1.763	5.30E-04	2.403	2.14E-04	3.528	9.84E-05		
0.293	1.35E-03	0.707	1.65E-03	1.167	2.32E-03	1.765	6.26E-04	2.406	2.83E-04	3.529	5.07E-05		
0.297	1.49E-03	0.719	1.80E-03	1.181	2.14E-03	1.767	5.30E-04	2.407	2.14E-04	3.535	9.84E-05		
0.303	1.65E-03	0.739	1.97E-03	1.194	1.97E-03	1.861	4.41E-04	2.642	1.53E-04	3.536	5.07E-05		
0.31	1.80E-03	0.74	1.80E-03	1.211	1.80E-03	1.863	5.30E-04	2.643	2.14E-04	4.124	9.97E-06		
0.336	1.97E-03	0.742	1.97E-03	1.235	1.65E-03	1.865	4.41E-04	2.649	1.53E-04	4.2	0		
0.347	2.14E-03	0.763	2.14E-03	1.254	1.49E-03	1.867	5.30E-04	2.65	2.14E-04				



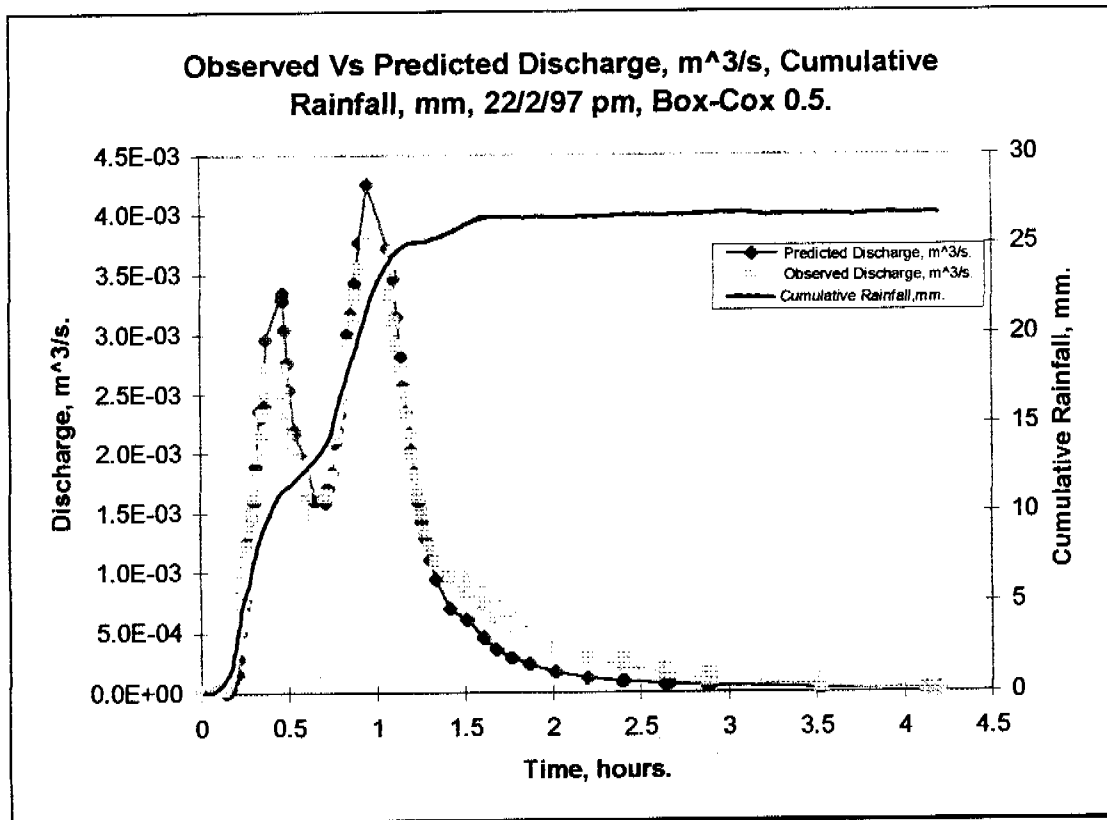
NLFIT Input files: 22297pm.fw, 22297pm.ro/rf

NLFIT Output files: 22297pm.prt/pmf/plt.

Parameter.	Mean.	Standard Deviation.	Parameter.	Mean.	Standard Deviation.
C_r	11.6162	2.0045	$S\phi$	3.2335	0.1646
e_m	2.2374	0.0957	ϕ	0.001	

		Cumulative Periodogram.		Standardised Residual Versus Time.	Standardised Residual Versus N(0,1) Variate.		Auto Correlation Plot.	Partial Auto Correlation Plot.
Convergence Monitor.	R^2 , %.	Test Statistic.	5%.	Z.	Test Statistic.	5%.	Exceedances.	Exceedances.
0.1471	97.2	0.7130	0.1786	-8.454	0.1210	0.0819	9	1

Storm Specific Comment: The convergence monitor is not adequate, below 0.1, the R^2 is adequate 97.2%, the cumulative periodogram does not pass the test statistic. The standardised residual versus time plot exceeds the Z statistic limit of $|2|$, the standardised residual versus N(0,1) variate does not pass the test statistic. The auto-correlation plot is exceeded 9 times, and the partial auto-correlation plot is exceeded 1 times.

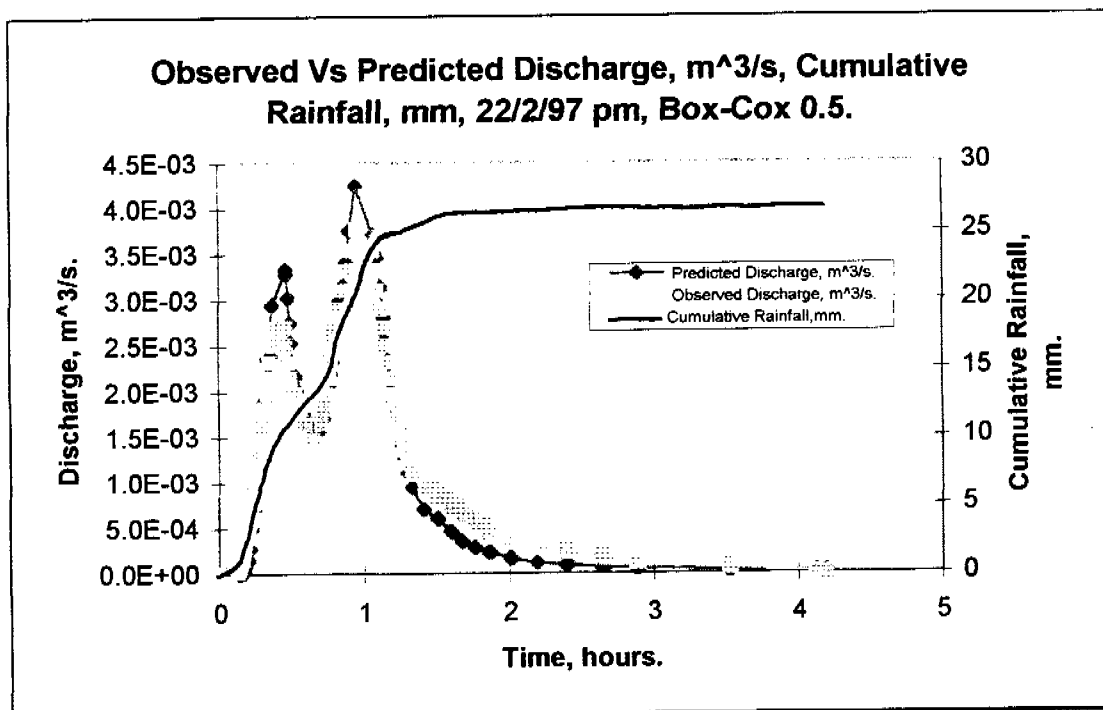


NLFIT Input files: 22297pm.fw, 22297pm.ro/rf
 NLFIT Output files: 22297pm5.prt/pmf/plt.

Parameter.	Mean.	Standard Deviation.	Parameter.	Mean.	Standard Deviation.
C_r	11.0298	2.2028	$S\phi$	2.7654	0.2017
e_m	2.2681	0.1115	ϕ	0.001	

Convergence Monitor.	R^2 , %.	Cumulative Periodogram.		Standardised Residual Versus Time.	Standardised Residual Versus N(0,1) Variate.		Auto Correlation Plot.	Partial Auto Correlation Plot.
		Test Statistic.	5%.	Z.	Test Statistic.	5%.	Exceedances.	Exceedances.
0.3285	97.1	0.7689	0.1786	-8.446	0.0911	0.0819	10	2

Storm Specific Comment: The convergence monitor is not adequate, below 0.1, the R^2 is adequate 97.1%, the cumulative periodogram does not pass the test statistic. The standardised residual versus time plot exceeds the Z statistic limit of $|2|$, the standardised residual versus N(0,1) variate does not pass the test statistic. The auto-correlation plot is exceeded 10 times, and the partial auto-correlation plot is exceeded 2 times.



NLFIT Input files: 22297pm.fw, 22297pm.ro/rf
 NLFIT Output files: 222pm5a.prt/pmf/plf.

Parameter.	Mean.	Standard Deviation.	Parameter.	Mean.	Standard Deviation.
C_r	6.1110	0.6369	$S\phi$	3.1698	0.6111
e_m	1.8741	0.0803	ϕ	0.001	

		Cumulative Periodogram.		Standardised Residual Versus Time.	Standardised Residual Versus N(0,1) Variate.		Auto Correlation Plot.	Partial Auto Correlation Plot.
Convergence Monitor.	R^2 , %.	Test Statistic.	5%.	Z.	Test Statistic.	5%.	Exceedances.	Exceedances.
0.0655	95.9	0.1618	0.1786	1.483	0.0808	0.0819	1	2

Storm Specific Comment: The convergence monitor is adequate, below 0.1, the R^2 is adequate 95.9%, the cumulative periodogram does pass the test statistic. The standardised residual versus time plot does not exceed the Z statistic limit of $|2|$, the standardised residual versus N(0,1) variate does pass the test statistic. The auto-correlation plot is exceeded 1 times, and the partial auto-correlation plot is exceeded 2 times.

General Comment: Although there is obvious problems with the least squares model, 22297pm.*, with respect to test statistics, the predicted response is slightly superior to 22297pm5.*, and 222pm5a*. The model including a Box-Cox factor of 0.5, and an auto-regressive factor, statistically is the best fit, however the visual exactness of the predicted response is indeterminately worse or better than that of 22297pm.*.

23rd February

RUM 96-97 Monitoring

pit 1 site

Rainfall 23/2/97 0016hrs

97

0	0	0.475	4.6	0.519	10.4	1.131	14.6	2.635	19.4
0.065	0.2	0.478	4.8	0.525	10.6	1.219	14.8	3.154	19.6
0.089	0.4	0.479	5	0.542	10.8	1.281	15	3.172	19.8
0.117	0.6	0.482	5.2	0.574	11	1.349	15.4	3.183	20.2
0.172	1	0.485	5.6	0.628	11.2	1.431	15.6	3.192	20.4
0.183	1.2	0.488	6	0.676	11.4	1.489	15.8	3.211	20.6
0.189	1.4	0.489	6.2	0.678	11.6	1.547	16	3.236	20.8
0.193	1.6	0.492	6.6	0.719	11.8	1.601	16.2	3.268	21
0.194	1.8	0.493	6.8	0.733	12	1.66	16.6	3.296	21.4
0.199	2	0.494	7	0.747	12.2	1.724	16.8	3.325	21.6
0.204	2.2	0.496	7.2	0.757	12.4	1.776	17	3.363	21.8
0.336	2.4	0.497	7.4	0.767	12.8	1.829	17.2	3.41	22
0.338	2.6	0.499	7.8	0.783	13	1.892	17.4	3.454	22.2
0.44	2.8	0.501	8.4	0.808	13.2	1.946	17.8	3.503	22.6
0.45	3	0.504	8.8	0.835	13.4	2.006	18	3.6	22.8
0.456	3.2	0.506	9	0.853	13.6	2.064	18.2	3.786	23
0.46	3.4	0.507	9.2	0.883	13.8	2.124	18.4	4.1	23
0.465	3.8	0.508	9.4	0.953	14	2.221	18.6		
0.469	4	0.513	9.8	0.954	14.2	2.343	19		
0.472	4.4	0.517	10	1.051	14.4	2.458	19.2		

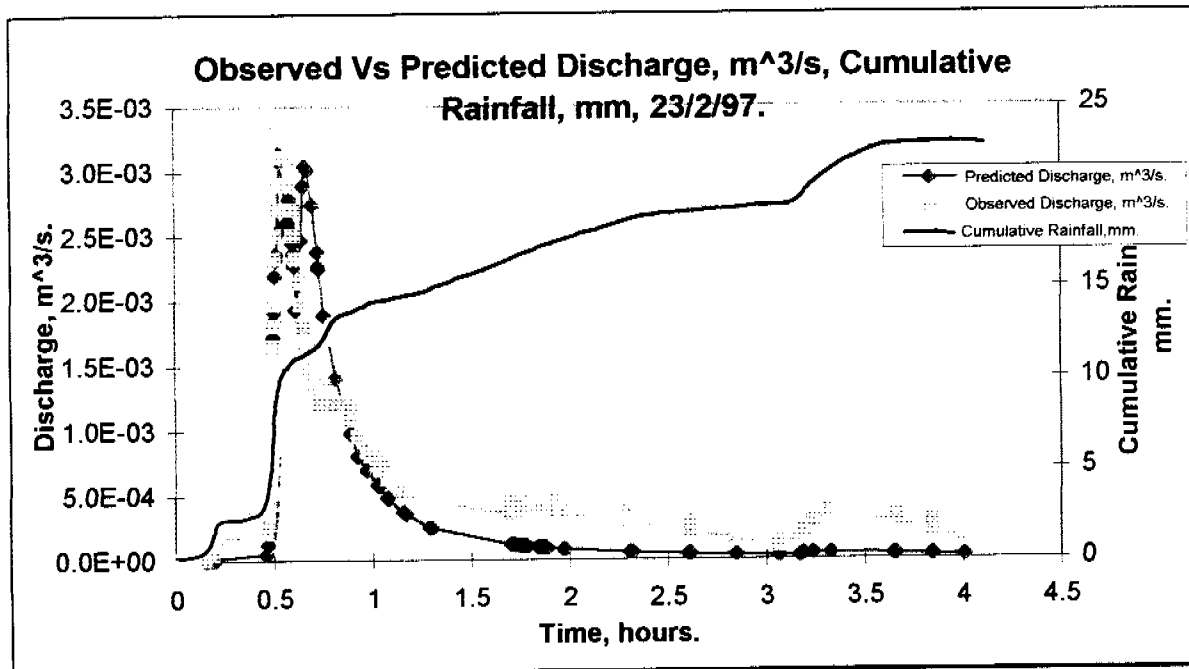
RUM 96-97 Monitoring

pit 1 site

Runoff 23/2/97 0016hrs

154

0	0	0.506	1.97E-03	0.653	1.80E-03	1.078	7.29E-04	1.724	3.58E-04	1.847	3.58E-04	1.976	3.58E-04	3.326	3.58E-04
0.153	9.97E-06	0.507	2.32E-03	0.664	1.65E-03	1.079	6.26E-04	1.725	4.41E-04	1.849	4.41E-04	2.307	2.83E-04	3.649	2.83E-04
0.189	5.07E-05	0.51	2.51E-03	0.676	1.49E-03	1.157	5.30E-04	1.726	3.58E-04	1.851	3.58E-04	2.308	3.58E-04	3.65	3.58E-04
0.196	9.84E-05	0.513	2.70E-03	0.7	1.35E-03	1.16	6.26E-04	1.74	4.41E-04	1.854	4.41E-04	2.311	2.83E-04	3.651	2.83E-04
0.204	1.53E-04	0.515	2.90E-03	0.721	1.21E-03	1.161	5.30E-04	1.743	3.58E-04	1.86	3.58E-04	2.313	3.58E-04	3.653	3.58E-04
0.464	2.14E-04	0.517	3.11E-03	0.728	1.35E-03	1.163	6.26E-04	1.744	4.41E-04	1.863	4.41E-04	2.318	2.83E-04	3.656	2.83E-04
0.471	2.83E-04	0.524	3.32E-03	0.729	1.21E-03	1.164	5.30E-04	1.746	3.58E-04	1.864	3.58E-04	2.322	3.58E-04	3.663	3.58E-04
0.474	3.58E-04	0.536	3.11E-03	0.757	1.35E-03	1.169	6.26E-04	1.747	4.41E-04	1.867	4.41E-04	2.324	2.83E-04	3.664	2.83E-04
0.476	4.41E-04	0.538	3.32E-03	0.818	1.21E-03	1.171	5.30E-04	1.749	3.58E-04	1.868	3.58E-04	2.607	2.14E-04	3.844	2.14E-04
0.479	5.30E-04	0.539	3.11E-03	0.889	1.08E-03	1.292	4.41E-04	1.753	4.41E-04	1.869	4.41E-04	2.608	2.83E-04	3.846	2.83E-04
0.483	6.26E-04	0.575	2.90E-03	0.89	1.21E-03	1.294	5.30E-04	1.754	3.58E-04	1.871	3.58E-04	2.613	2.14E-04	3.85	2.14E-04
0.486	7.29E-04	0.576	3.11E-03	0.892	1.08E-03	1.296	4.41E-04	1.771	4.41E-04	1.872	4.41E-04	2.615	2.83E-04	4.006	1.53E-04
0.489	8.39E-04	0.578	2.90E-03	0.926	9.57E-04	1.297	5.30E-04	1.772	3.58E-04	1.875	3.58E-04	2.617	2.14E-04	4.008	2.14E-04
0.493	9.57E-04	0.586	2.70E-03	0.969	8.39E-04	1.299	4.41E-04	1.779	4.41E-04	1.879	4.41E-04	2.849	1.53E-04	4.011	1.53E-04
0.494	1.08E-03	0.599	2.51E-03	1.024	7.29E-04	1.704	3.58E-04	1.782	3.58E-04	1.881	3.58E-04	3.064	9.84E-05	4.1	0
0.496	1.21E-03	0.601	2.70E-03	1.025	8.39E-04	1.706	4.41E-04	1.783	4.41E-04	1.882	4.41E-04	3.065	1.53E-04		
0.497	1.35E-03	0.603	2.51E-03	1.026	7.29E-04	1.711	3.58E-04	1.785	3.58E-04	1.885	3.58E-04	3.068	9.84E-05		
0.5	1.49E-03	0.614	2.32E-03	1.028	8.39E-04	1.715	4.41E-04	1.786	4.41E-04	1.886	4.41E-04	3.171	1.53E-04		
0.501	1.65E-03	0.631	2.14E-03	1.029	7.29E-04	1.717	3.58E-04	1.843	3.58E-04	1.888	3.58E-04	3.188	2.14E-04		
0.504	1.80E-03	0.64	1.97E-03	1.076	6.26E-04	1.718	4.41E-04	1.844	4.41E-04	1.975	4.41E-04	3.238	2.83E-04		



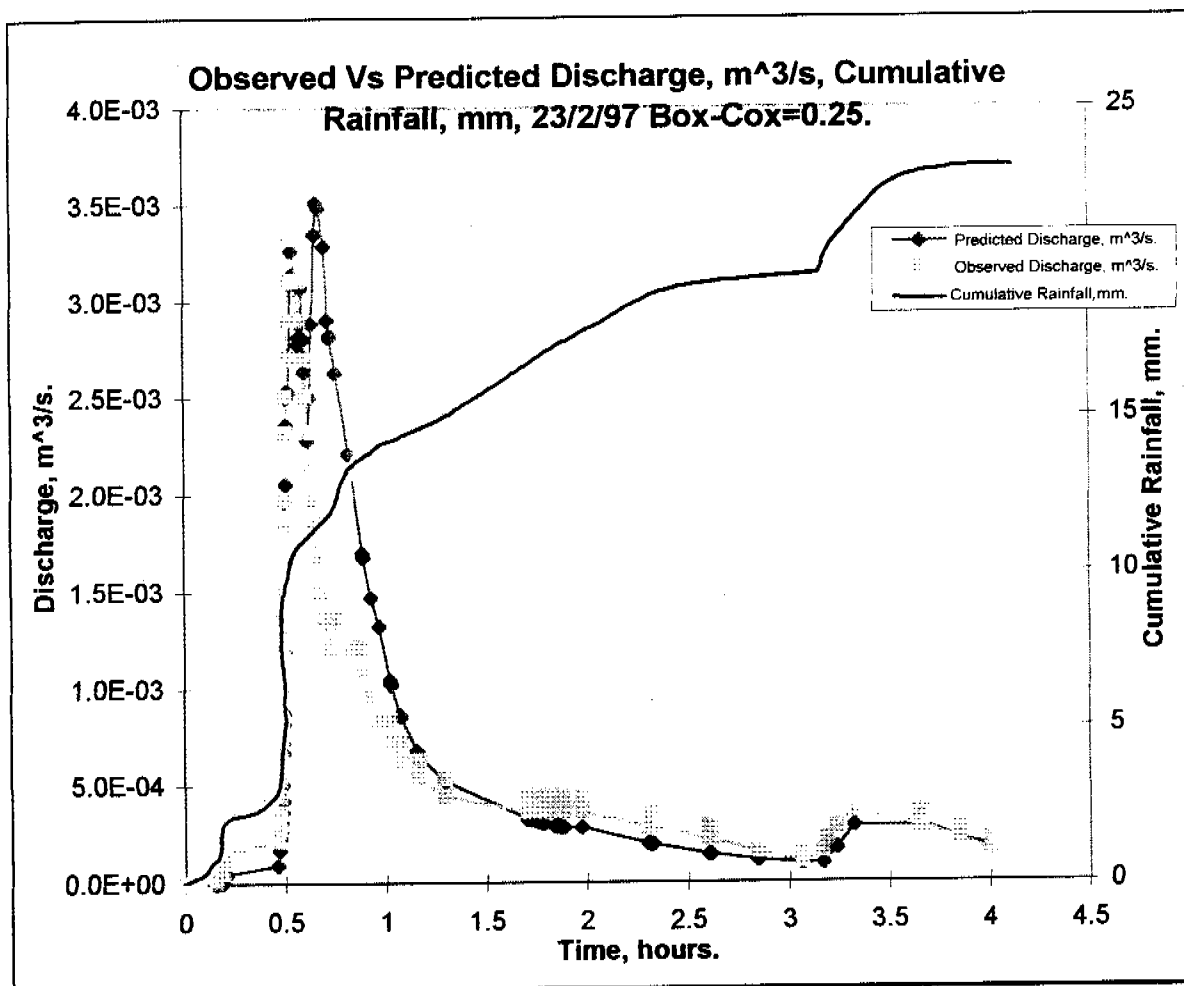
NLFIT Input files: 23297.fw, 23297.ro/rf

NLFIT Output files: 23297.prt/pmf/plt.

Parameter.	Mean.	Standard Deviation.	Parameter.	Mean.	Standard Deviation.
C_r	6.1101	0.7883	$S\phi$	0.001	
e_m	2.0768	0.10278	ϕ	13.7007	2.768

		Cumulative Periodogram.		Standardised Residual Versus Time.	Standardised Residual Versus N(0,1) Variate.		Auto Correlation Plot.	Partial Auto Correlation Plot.
Convergence Monitor.	R^2 , %.	Test Statistic.	5%.	Z.	Test Statistic.	5%.	Exceedances.	Exceedances.
0.170127	86.4	0.7269	0.156	-9.195	0.2854	0.072	7	5

Storm Specific Comment: The convergence monitor is adequate, below 0.1, the R^2 is not adequate 86.4%, the cumulative periodogram does not pass the test statistic. The standardised residual versus time plot does exceed the Z statistic limit of $|2|$, the standardised residual versus N(0,1) variate does not pass the test statistic. The auto-correlation plot is exceeded 7 times, and the partial auto-correlation plot is exceeded 5 times.

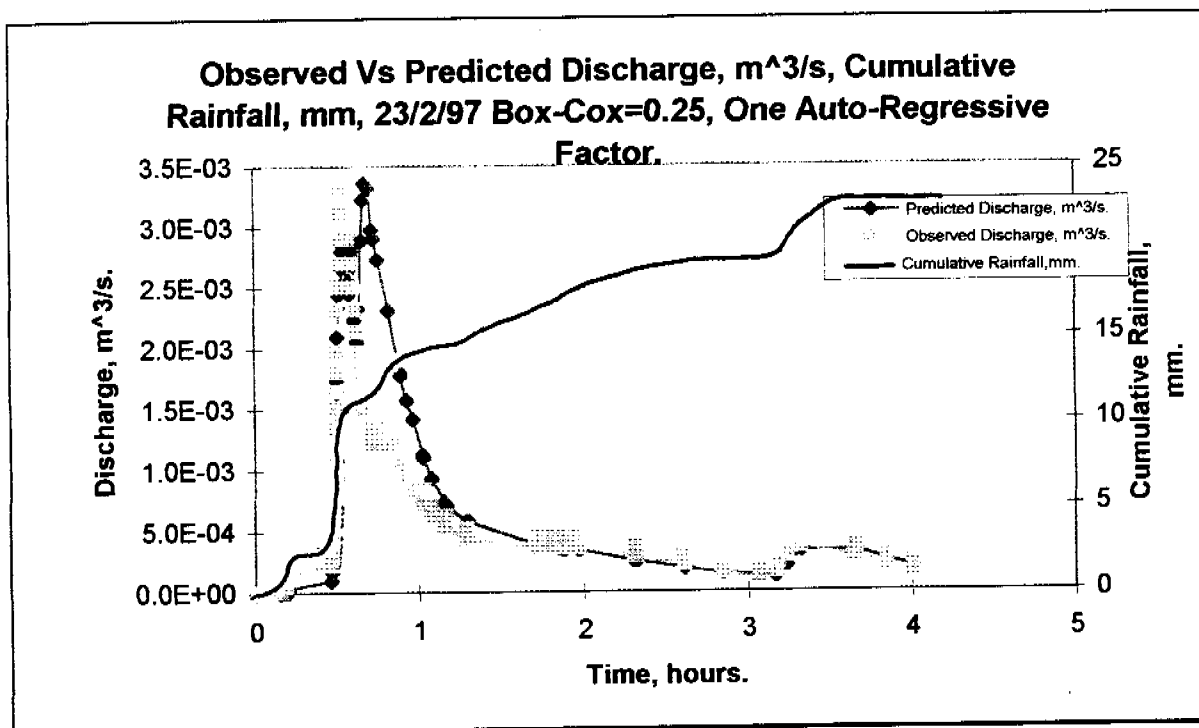


NLFIT Input files: 23297.fw, 23297.ro/rf
 NLFIT Output files: 23297g25.prt/pmf/plt.

Parameter.	Mean.	Standard Deviation.	Parameter.	Mean.	Standard Deviation.
C_r	7.094	0.756	$S\phi$	0.001	
e_m	2.425	0.0692	ϕ	2.728	0.266

		Cumulative Periodogram.		Standardised Residual Versus Time.	Standardised Residual Versus N(0,1) Variate.		Auto Correlation Plot.	Partial Auto Correlation Plot.
Convergence Monitor.	R^2 , %.	Test Statistic.	5%.	Z.	Test Statistic.	5%.	Exceedances.	Exceedances.
0.111218	80.6	0.7912	0.156	-7.76	0.23	0.072	16	10

Storm Specific Comment: The convergence monitor is adequate, below 0.1, the R^2 is not adequate 80.6%, the cumulative periodogram does not pass the test statistic. The standardised residual versus time plot does exceed the Z statistic limit of $|2|$, the standardised residual versus N(0,1) variate does not pass the test statistic. The auto-correlation plot is exceeded 16 times, and the partial auto-correlation plot is exceeded 10 times.



NLFIT Input files: 23297.fw, 23297.ro/rf

NLFIT Output files: 2329725a.prt/pmf/plt.

Parameter.	Mean.	Standard Deviation.	Parameter.	Mean.	Standard Deviation.
C_r	7.237	0.6988	$S\phi$	0.001	
e_m	2.5183	0.0887	ϕ	2.20263	0.708

		Cumulative Periodogram.		Standardised Residual Versus Time.	Standardised Residual Versus N(0,1) Variate.		Auto Correlation Plot.	Partial Auto Correlation Plot.
Convergence Monitor.	R^2 , %.	Test Statistic.	5%.	Z.	Test Statistic.	5%.	Exceedances.	Exceedances.
0.1597	75.0	0.2282	0.156	5.77	0.153	0.072	8	5

Storm Specific Comment: The convergence monitor is adequate, below 0.1, the R^2 is not adequate 75.0%, the cumulative periodogram does not pass the test statistic. The standardised residual versus time plot does exceed the Z statistic limit of [2], the standardised residual versus N(0,1) variate does not pass the test statistic. The auto-correlation plot is exceeded 8 times, and the partial auto-correlation plot is exceeded 5 times.

General Comment: The least squares model, even though statistically poor with respect to the diagnostic plots, has the most accurate predicted hydrograph compared to 2329725a (Box-Cox = 0.25, and an Auto-regressive parameter), and 23297g25(Box-Cox = 0.25).

Appendix 4.A

Suspended and Bedload Sediment Data and Sample Processing Procedure.

Suspended and Bedload Sediment Sampling Procedure

Suspended sediment samples were collected at various time intervals throughout a storm event in 600mL Bunzl plastic flasks. Figure 4.A.1, lists the procedure that was followed for suspended sediment sample processing.

- Record initial weight of an aluminium tray, after heating to 105°C for 4 hours to burn off plastic coating on the tray.
- The initial weight, sample number and details of the storm date were etched onto the tray and recorded onto a data sheet to yield tray weight reading.
- Suspended sediment sample was stirred, shaken, and the screw top lid removed to allow the measurement of conductivity with a conductivity probe.
- The sample was then poured into the aluminium tray and weighed again, to yield tray + water + sediment weight reading. The tray was then heated at 105°C for a period of 24 hours to evaporate water.
- The heated tray was then re-weighed to yield tray + sediment weight reading.

Figure 4.A.1: Suspended sediment sample processing procedure.

Bedload sediment samples were collected from within the large PVC pipe, and within the concrete reservoir utilising a hand-held aluminium shovel and placed in large plastic bags. Figure 4.A.2, lists the bedload sediment sample processing procedure.

- Initial weight of an aluminium tray was recorded, after heating to 105°C for 4 hours to burn off the plastic coating.
- The initial weight, sample number and details of the storm date were etched onto the tray and recorded, to yield a tray only weight reading.
- The sediment was dislodged with distilled water from the storage bag, and collected in trays. The tray was then heated at 105°C for a period of at least 24 hours to evaporate any water present in the sample.
- The heated tray was then re-weighed, to yield tray + sediment weight reading.

Figure 4.A.2: Suspended sediment sample processing procedure.

Suspended Sediment Analysis

1st January

Table 4.A.1: Suspended sediment analysis for the storm event occurring on the 1st January.

Site	Pir 1					Base level	2 uS/cm			
Date	1 JAN 97									
TIME		TIME	SAMPLE	CONT WGT	CONT+SED +H2O	water	CONDUCT	OD sed + cont. WT	Sed dried WT	Concentration
				g	g	g	uS/cm	g	g	g/l
hrs	min	sec								
16	0		16:00:00 18	12.97	391.22	378.08	42.9	13.14	0.17	0.449640288
16	1		16:01:00 19	12.81	408.72	395.76	28.1	12.96	0.15	0.379017586
16	2		16:02:00 20	12.93	420.86	407.83	22	13.03	0.1	0.245200206
16	5		16:05:00 21	12.83	422.57	409.6	16.3	12.97	0.14	0.341796875
16	6.5		16:06:30 22	12.9	366.11	353.07	13.9	13.04	0.14	0.396521936
16	8		16:08:00 23	12.78	429.98	417.05	14	12.93	0.15	0.359669104
16	9.5		16:09:30 24	12.86	269.79	256.85	10.2	12.94	0.08	0.311465836
16	11		16:11:00 25	12.84	436.62	423.64	11	12.98	0.14	0.330469266
16	12		16:12:00 26	12.99	411.45	398.39	8.2	13.06	0.07	0.175707222
16	14.5		16:14:30 17	13.03	432.42	419.3	8.1	13.12	0.09	0.214643453
16	15	30	16:15:30 16	13.13	445.87	432.64	8.1	13.23	0.1	0.231139053
16	17		16:17:00 15	12.82	419.15	406.25	7.8	12.9	0.08	0.196923077
16	18		16:18:00 14	12.94	453.81	440.79	7.6	13.02	0.08	0.181492321
16	21	30	16:21:30 13	12.93	456.01	443.01	7.3	13	0.07	0.158009977
16	24		16:24:00 12	12.86	455.37	442.44	7.6	12.93	0.07	0.158213543
16	26		16:26:00 11	12.75	435.74	422.95	7.5	12.79	0.04	0.094573827
16	30		16:30:00 10	12.8	444.7	431.85	9.9	12.85	0.05	0.115780942
16	32		16:32:00 9	12.92	440.5	427.54	8.7	12.96	0.04	0.093558497
16	35		16:35:00 8	12.85	429.65	416.75	9.1	12.9	0.05	0.119976005
16	36		16:36:00 7	12.82	420.06	407.2	14.4	12.86	0.04	0.098231827
16	40		16:40:00 6	12.87	447.37	434.46	8.8	12.91	0.04	0.092068315
17	7		17:07:00 5	12.89	428.4	415.46	18.7	12.94	0.05	0.120348529
17	14		17:14:00 4	12.86	440.91	428.02	19.9	12.89	0.03	0.070090183
17	17		17:17:00 3	12.88	414.7	401.79	20.2	12.91	0.03	0.07466587
17	24		17:24:00 2	12.94	434.7	421.75	26.2	12.95	0.01	0.023710729
17	34		17:34:00 1	12.84	410.43	397.54	23.6	12.89	0.05	0.125773507
Total										2.06
mean										conc. = 0.198411076

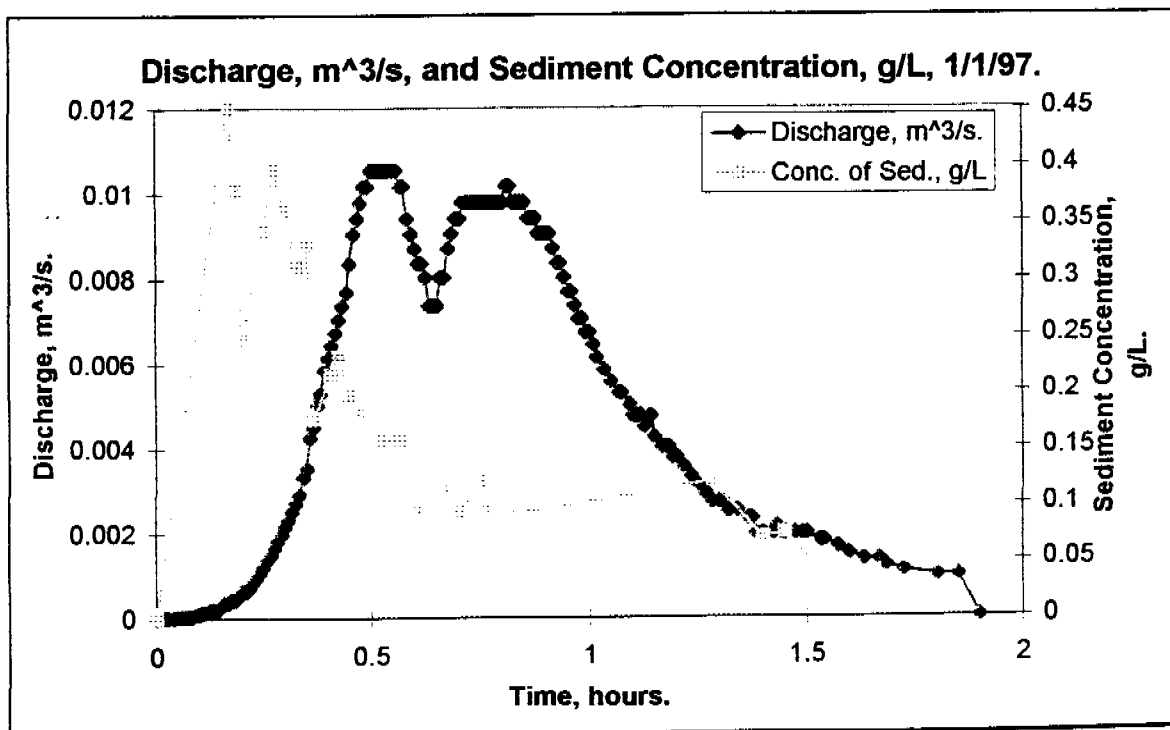


Figure 4.A.3: Plot of the discharge, (m³/s), and suspended sediment concentration, (g/L), for the storm event occurring on the 1st January on the natural field plot.

12th January 1st Event

Table 4.A.2: Suspended sediment analysis for the first storm event occurring on the 12th January.

Site Name:			Pit 1				Base level 5 uS/cm				
Date:			12 Jan 1997								
Time of storm:			17:08:00								
			TIME	SAMPLE NUMBER	CONT. WEIGHT	CONT. + SED+H2O	COND/CT	CONT. + SED.	WATER	SED.	CONC. OF SED.
Hrs	min	sec			g	g	uS/cm	g	g	G	g/L
17	15	30	17:15:30	13	13.14	350.87	78.2	13.21	337.66	0.07	0.20730913
17	16	30	17:16:30	14	13.01	407.3	93.1	13.06	394.24	0.05	0.1268263
17	18	0	17:18:00	16	12.83	372.1	80.7	12.88	359.22	0.05	0.13919047
17	19	0	17:19:00	19	13.11	352.17	129.4	13.11	339.06	0	0
17	20	0	17:20:00	21	12.97	337.29	70.8	13.03	324.26	0.06	0.1850367
17	21	0	17:21:00	22	12.97	366.94	71.5	13.02	353.92	0.05	0.14127486
Total sed. g.										0.28	
Mean Conc.											0.13327291

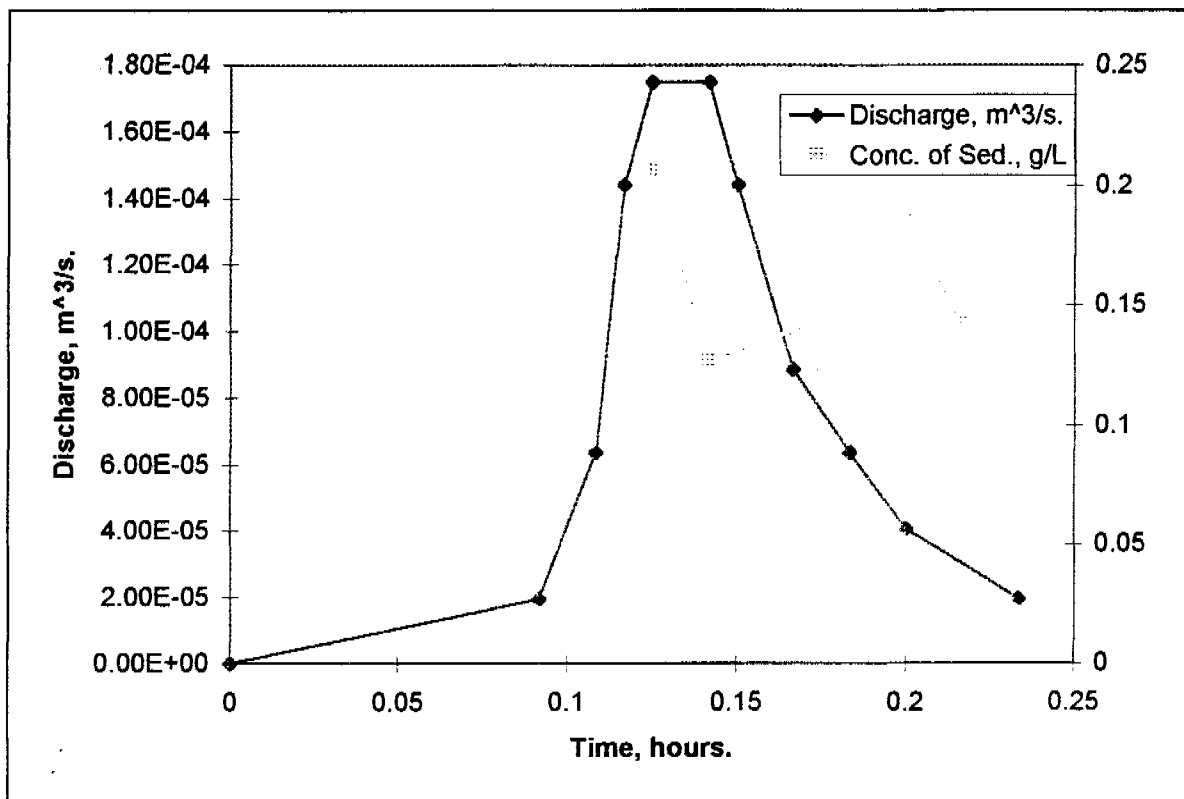


Figure 4.A.4: Plot of the discharge, (m³/s), and suspended sediment concentration, (g/L), for the first storm event occurring on the 12th January on the natural field plot.

12th January 2nd Event

Table 4.A.3: Suspended sediment analysis for the second storm event occurring on the 12th January.

Site Name: Pit1					Base Level		2.4 uS/cm				
Date: 12th Jan 1997											
Time of storm: 18:30:00											
			TIME	SAMPLE NUMBER	CONT. WEIGHT	CONT. + SED+H2O	COND/CT	CONT. + SED.	WATER	SED.	CONC. OF SED.
hrs	mm	sec			g	g	uS/cm	g	g	G	g/L
17	54	30	17:54:30	26	12.93	308.22	106	13	295.22	0.07	0.23711131
17	55	30	17:55:30	27a	12.92	327.75	108.4	13	314.75	0.08	0.25416998
17	56	30	17:56:30	25	12.79	373.36	105.8	12.89	360.47	0.1	0.2774156
17	57	30	17:57:30	24	12.81	388.22	106.9	12.87	375.35	0.06	0.15985081
17	59	30	17:59:30	27b	12.85	390.85	90	12.92	377.93	0.07	0.18521949
18	0	30	18:00:30	28	12.6	384.04	84.2	12.74	371.3	0.14	0.3770536
18	1	30	18:01:30	32	12.67	394.53	76.5	12.72	381.81	0.05	0.13095519
18	3	30	18:03:30	31	12.71	411.72	70.7	12.78	398.94	0.07	0.17546498
18	5	30	18:05:30	20	12.83	425.43	56	12.87	412.56	0.04	0.09695559
18	7	30	18:07:30	30	12.53	432.25	45.9	12.59	419.66	0.06	0.14297288
18	9	30	18:09:30	17	12.81	440.56	37.6	12.84	427.72	0.03	0.07013934
18	12	30	18:12:30	10	12.84	455.97	28.7	12.86	443.11	0.02	0.04513552
18	15	30	18:15:30	22	12.83	425.43	56	12.87	412.56	0.04	0.09695559
18	19	30	18:19:30	11	12.73	437.02	42.2	12.79	424.23	0.06	0.14143271
18	22	30	18:22:30	12	13	429.97	44.6	13.04	416.93	0.04	0.09593937
18	27	30	18:27:30	15	12.92	407.88	51.4	12.95	394.93	0.03	0.07596283
Total sed. g										0.96	
Mean Conc. =										0.16017092	

Discharge, m³/s, and Sediment Concentration, g/L, 12/1/97
2nd Event.

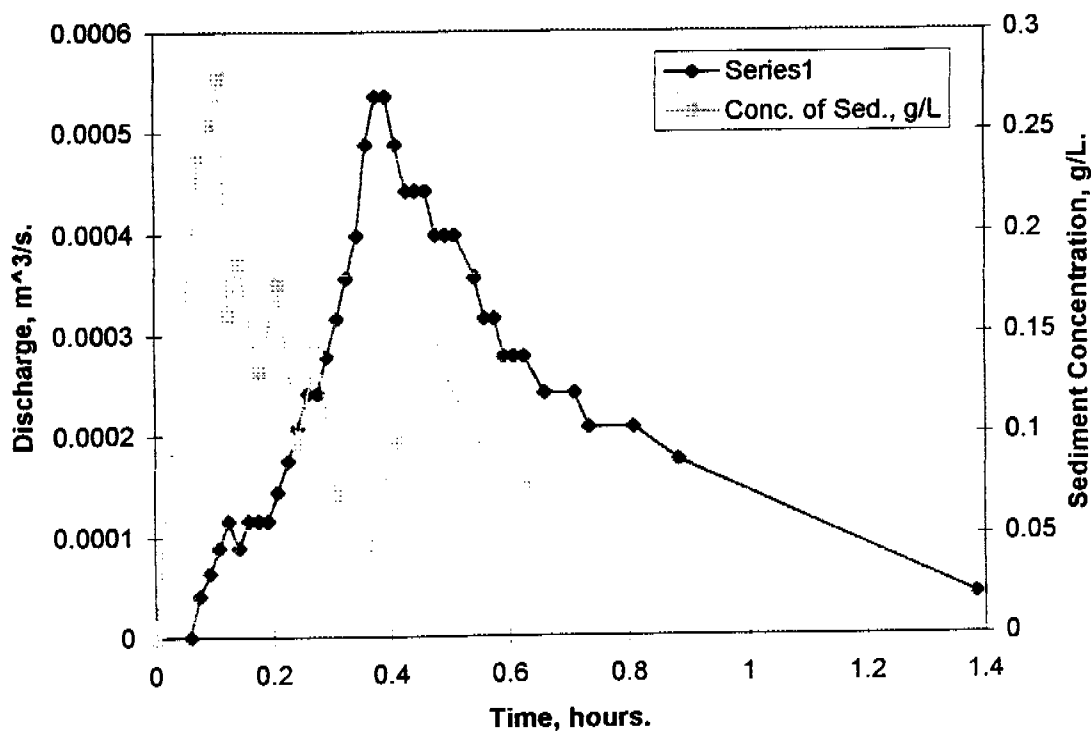


Figure 4.A.5: Plot of the discharge, (m³/s), and suspended sediment concentration, (g/L), for the second storm event occurring on the 12th January on the natural field plot.

17th January

Table 4.A.4: Suspended sediment analysis for the storm event occurring on the 17th January.

Site Name: Pit 1			Base Level 5 uS/cm									
Date: 17 Jan 1997												
Time of storm: 16:54:00												
hrs	min	sec	TIME	SAMPLE NUMBER	CONT. WEIGHT	CONT. + SED+H2O	COND/CT	CONT. + SED.	WATER	SED.	CONC. OF SED.	COMMENTS
					g	g	uS/cm	g	g	G	g/L	
17	17	30	17:17:30	2	12.98	334.53	76.2	13.06	321.47	0.08	0.248856814	
17	19	0	17:19:00	17a	12.58	401.97	73.6	12.67	389.3	0.09	0.231184177	Sample 17a on sheet.
17	20	30	17:20:30	12A	12.89	431.29	11.1	13.03	418.26	0.14	0.334720031	
17	21	30	17:21:30	17B	12.78	419.11	35.9	12.91	406.2	0.13	0.320039389	Sample 17b on sheet.
17	23	0	17:23:00	19	12.69	433.04	29.5	12.84	420.2	0.15	0.35697287	
17	23	30	17:23:30	18	12.95	430.61	23.9	13.15	417.46	0.2	0.479087817	
17	24	30	17:24:30	22	12.84	442.08	25	12.94	429.14	0.1	0.233024188	
17	26	0	17:26:00	23	12.79	435.93	22	12.91	423.02	0.12	0.283674531	
17	27	30	17:27:30	21	12.78	413.71	19	13.04	400.67	0.26	0.648913071	Container + sed could be 12.87
17	29	30	17:29:30	26	12.58	426.1	14.2	12.75	413.35	0.17	0.411273739	Inferred Value.
17	31	30	17:31:30	12B	12.89	408.12	47.4	13.03	395.09	0.14	0.354349642	Labelled 12B.
17	33	30	17:33:30	11	12.93	421.38	9.02	13.07	408.31	0.14	0.342876736	
17	35	30	17:35:30	3	12.81	411.19	8.5	12.98	398.21	0.17	0.426910424	
17	37	30	17:37:30	20	12.76	365.37	11.5	12.83	352.54	0.07	0.198559029	
17	41	0	17:41:00	24	12.9	390.11	15.1	12.96	377.15	0.06	0.159087896	
17	43	0	17:43:00	1	12.97	393.85	12	13.06	380.79	0.09	0.236350745	
17	46	0	17:46:00	16	12.61	380.29	14.1	12.77	367.52	0.16	0.435350457	
17	50	30	17:50:30	15	12.89	342.49	33.4	13.02	329.47	0.13	0.394573102	
										Total Sed.	Mean Conc.	
										2.4	0.338655814	

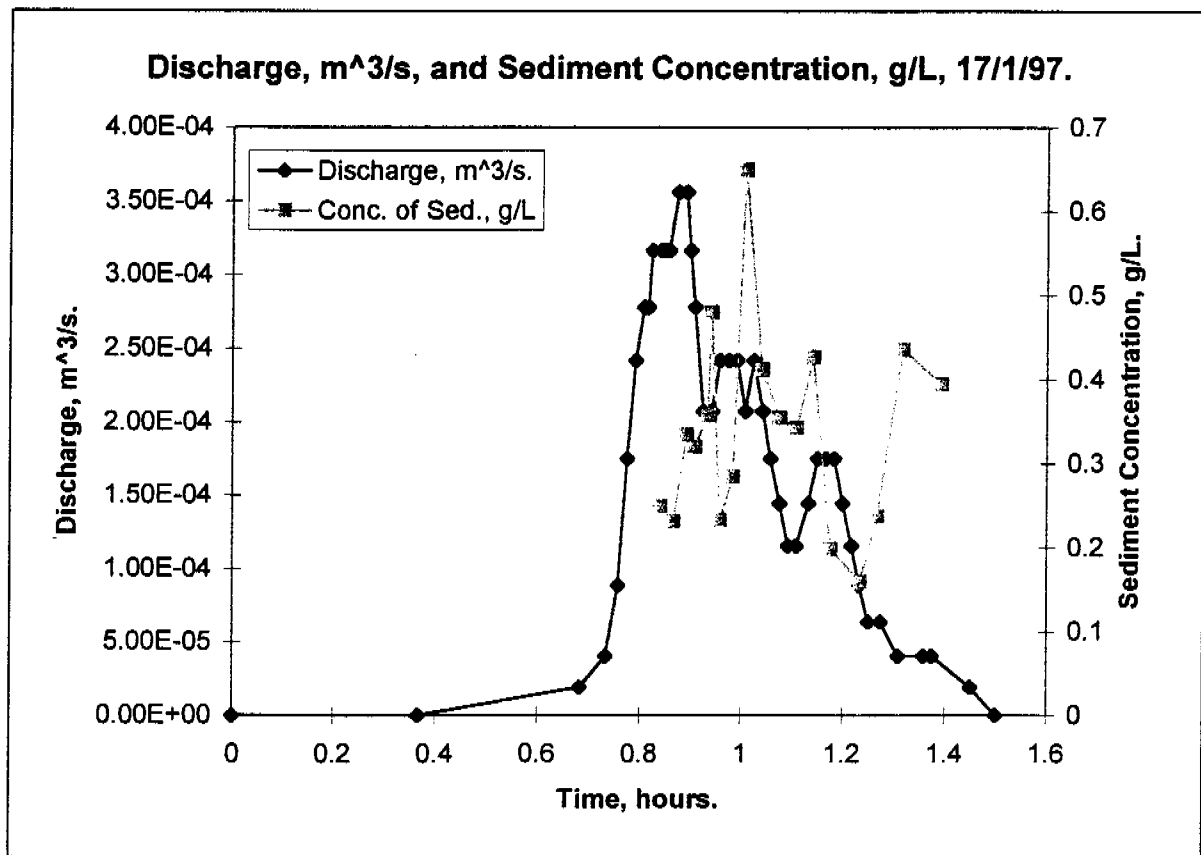


Figure 4.A.6: Plot of the discharge, (m³/s), and suspended sediment concentration, (g/L), for the storm event occurring on the 17th January on the natural field plot.

21st January 1st Event

Table 4.A.5: Suspended sediment analysis for the first storm event occurring on the 21st January.

Site Name:			Pit1		Base Level 5 uS/cm						
Date:			21stJan 1997								
Time of storm:			15:33:00								
			TIME	SAMPLE NUMBER	CONT. WEIGHT	CONT. + SED+H2O	COND/CT	CONT. + SED.	WATER	SED.	CONC. OF SED.
hrs	min	sec			g	g	uS/cm	g	g	G	g/L
15	43	30	15:43:30	8	12.85	360.05	115.5	12.85	347.2	0	0
15	44	30	15:44:30	11	12.73	366.87	100	12.77	354.1	0.04	0.112962
15	45	30	15:45:30	10	12.72	402.02	97.1	12.75	389.27	0.03	0.077067
15	46	30	15:46:30	6	12.82	408.74	70.5	12.86	395.88	0.04	0.101041
15	47	30	15:47:30	13	13.01	418.24	60.5	13.18	405.06	0.17	0.419691
15	48	30	15:48:30	28	12.82	437.3	50.8	12.93	424.37	0.11	0.259208
15	49	30	15:49:30	7	13.04	405.33	n/a	13.19	392.14	0.15	0.382516
15	50	30	15:50:30	14	12.89	400.89	23.7	13	387.89	0.11	0.283586
15	51	30	15:51:30	2	12.93	360.16	31.2	13.06	347.1	0.13	0.374532
15	52	30	15:52:30	27	12.91	364.85	27.6	12.99	351.86	0.08	0.227363
15	53	30	15:53:30	9	12.97	370.72	27	13.05	357.67	0.08	0.22367
15	54	30	15:54:30	5	12.94	358.67	30.2	13.01	345.66	0.07	0.202511
15	55	30	15:55:30	25	12.86	365.01	24.2	12.94	352.07	0.08	0.227228
15	57	30	15:57:30	31	12.99	344.14	37.3	13.06	331.08	0.07	0.211429
15	59	30	15:59:30	29	12.87	339.14	44.3	12.9	326.24	0.03	0.091957
16	3	0	16:03:00	26	12.86	341.39	48.4	12.91	328.48	0.05	0.152216
16	7	0	16:07:00	24	12.74	354.78	60.6	12.76	342.02	0.02	0.058476
16	13	0	16:13:00	32	12.87	330.49	61.2	12.91	317.58	0.04	0.125953
Tot sed, g										1.3	
mean=										0.196189	

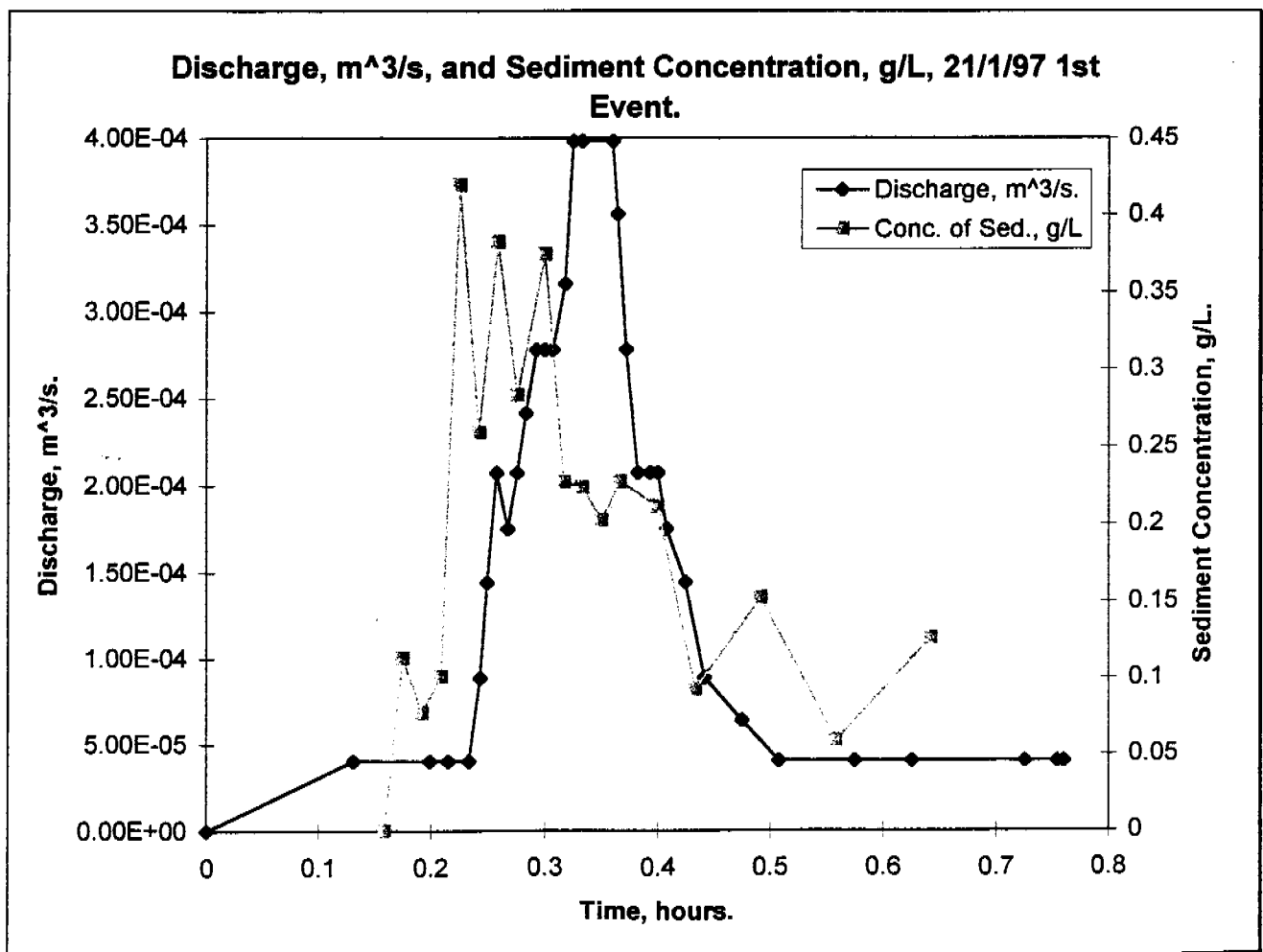


Figure 4.A.7: Plot of the discharge, (m³/s), and suspended sediment concentration, (g/L), for the first storm event occurring on the 21st January on the natural field plot.

21st January 2nd Event

Table 4.A.6: Suspended sediment analysis for the second storm event occurring on the 21st January.

Site Name: Pit1			Base Level 5 uS/cm									
Date: 21st Jan 1997												
Time of storm: 16:57:00												
Hrs	min	sec	TIME	SAMPLE NUMBER	CONT. WEIGHT g	CONT. + SED+H2O g	COND/CT uS/cm	CONT. + SED. g	WATER g	SED. G	CONC. OF SED. g/L	
17	0	0	17:00:00	11	12.95	301.45	65.6	13	288.45	0.05	0.17334	Not Faded.
17	1	0	17:01:00	10	13.19	325.74	61.2	13.23	312.51	0.04	0.127996	
17	2	0	17:02:00	16	12.98	359.44	64.2	12.98	346.46	0	0	
17	3	0	17:03:00	14	13.08	380.83	62.8	13.12	367.71	0.04	0.108781	
17	4	0	17:04:00	12	12.97	362.94	50.4	12.99	349.95	0.02	0.057151	
17	5	0	17:05:00	15	12.98	379.69	34	13.04	366.65	0.06	0.163644	
17	6	0	17:06:00	17	13.02	364.92	24.4	13.13	351.79	0.11	0.312687	
17	7	0	17:07:00	30	12.93	358.52	18.6	13.05	345.47	0.12	0.347353	
17	8	0	17:08:00	23	12.94	363.61	39.6	12.94	350.67	0	0	Top of sheet.
17	9	0	17:09:00	21	13.07	424.31	9.2	13.16	411.15	0.09	0.218898	Non faded.
17	10	0	17:10:00	22	13.22	401.15	5.3	13.32	387.83	0.1	0.257845	
17	11	0	17:11:00	24	12.94	405.97	5.6	13.01	392.96	0.07	0.178135	
17	12	0	17:12:00	19	13.14	415.1	5.1	13.21	401.89	0.07	0.174177	
17	13	0	17:13:00	18	12.81	402.91	6.1	12.84	390.07	0.03	0.076909	
17	14	0	17:14:00	27	12.78	391.61	6.3	12.82	378.79	0.04	0.105599	
17	15	0	17:15:00	32	12.94	384.69	7.3	12.99	371.7	0.05	0.134517	
17	16	0	17:16:00	26	13	390.2	8.2	13.02	377.18	0.02	0.053025	
17	17	0	17:17:00	20	12.91	370.19	9.6	12.94	357.25	0.03	0.083975	
17	18	0	17:18:00	28	13.32	414.92	9.6	13.32	401.6	0	0	
17	19	0	17:19:00	31	12.87	398.38	20.7	12.91	385.47	0.04	0.103769	
17	20	30	17:20:30	25	13	395.92	12.3	13.01	382.91	0.01	0.026116	Non faded.
17	22	0	17:22:00	29	12.68	396.51	14.2	12.68	383.83	0	0	Non faded.
17	24	0	17:24:00	13	12.79	400.96	13.1	12.79	388.17	0	0	
17	26	0	17:26:00	29	12.96	403.75	16.3	12.97	390.78	0.01	0.02559	Faded.
17	28	0	17:28:00	11	13.06	392.56	16.3	13.07	379.49	0.01	0.026351	Faded.
17	30	0	17:30:00	31	12.91	417.52	10.4	12.92	404.6	0.01	0.024716	Faded.
17	32	0	17:32:00	21	12.98	379.69	21.9	12.98	366.71	0	0	Faded.
17	36	0	17:36:00	23	12.76	343.04	28.2	12.76	330.28	0	0	Approx zero grams.
17	40	0	17:40:00	28	12.96	367.46	28.2	12.97	354.49	0.01	0.02821	
17	46	0	17:46:00	19	12.95	342.8	30.5	12.98	329.82	0.03	0.090959	Faded.
17	52	0	17:52:00	29	12.96	403.75	16.3	12.97	390.78	0.01	0.02559	Faded.
18	0	0	18:00:00	4	12.92	361.19	41.3	12.96	348.23	0.04	0.114867	
18	6	0	18:06:00	25	12.92	372.72	43.8	12.93	359.79	0.01	0.027794	Faded.
18	20	0	18:20:00	24	12.94	405.97	5.6	13.01	392.96	0.07	0.178135	Faded.
Tot Sed.g										1.19		
Mean Conc.										0.095474		
Extras										0.02	0.051787	Faded.
				20	12.95	399.17	55.6	12.97	386.2			

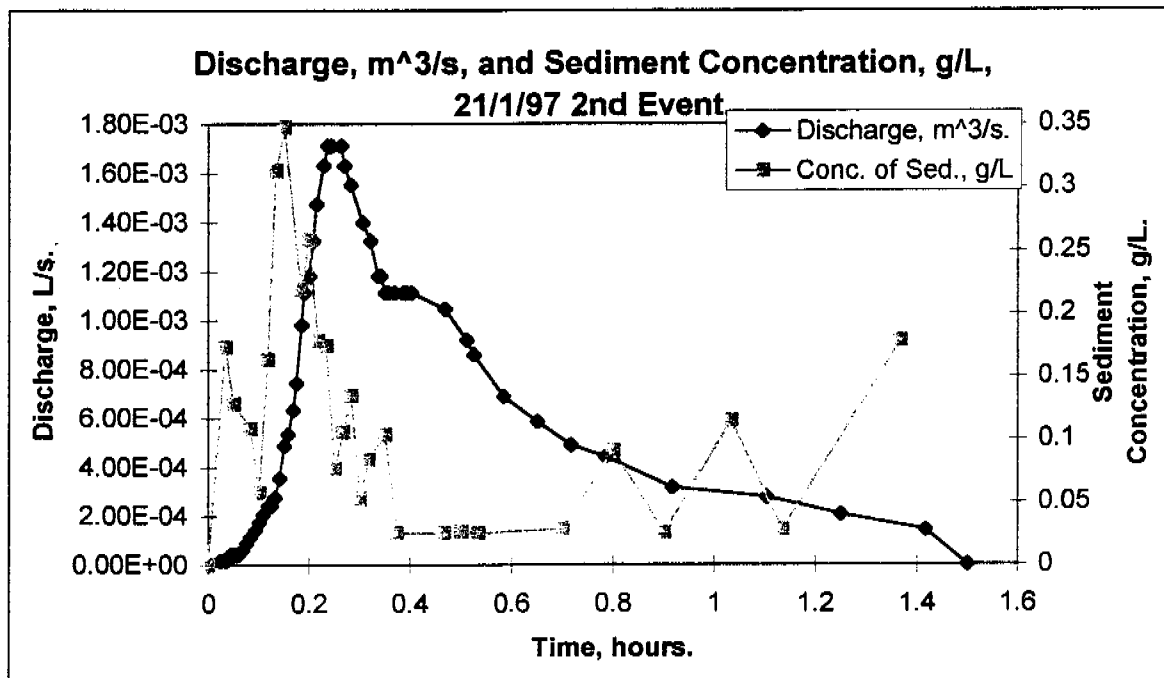


Figure 4.A.8: Plot of the discharge, (m³/s), and suspended sediment concentration, (g/L), for the second storm event occurring on the 21st January on the natural field plot.

23rd January

Table 4.A.7: Suspended sediment analysis for the storm event occurring on the 23rd January.

Site Name: Pit 1			Base Level 5 uS/cm									
Date: 23 Jan 1997												
Time	of	16:20:00	TIME	SAMPLE	CONT.	CONT. +	COND'CT	CONT. +	WATER	SED.	CONC. OF	
storm:				NUMBER	WEIGHT	SED+H2O		SED.			SED.	
hrs	min	sec			g	g	uS/cm	g	g	G	g/L	
16	28	30	16:28:30	13	12.92	376.73	31.3	13.06	363.67	0.14	0.384964	
16	30	0	16:30:00	25	13.18	403.33	20.8	13.31	390.02	0.13	0.333316	
16	31	0	16:31:00	31	12.9	412.18	15.4	13.06	399.12	0.16	0.400882	
16	32	0	16:32:00	23	13.01	426.27	10.4	13.13	413.14	0.12	0.290458	
16	33	0	16:33:00	14	12.76	429.4	9.3	12.88	416.52	0.05	0.120042	
16	34	0	16:34:00	19	12.79	427.57	8	12.89	414.68	0.1	0.24115	
16	35	0	16:35:00	20	12.83	406.71	8	13.01	393.7	0.18	0.457201	
16	36	0	16:36:00	29	13.17	419.07	8.3	13.3	405.77	0.13	0.320379	
16	36	30	16:36:30	16	12.79	412.23	7	12.86	399.37	0.07	0.175276	
16	37	30	16:37:30	21	12.8	414.18	21.6	12.84	401.34	0.04	0.099666	
16	38	30	16:38:30	27	13.02	432.72	4.6	13.11	419.61	0.09	0.214485	
16	39	30	16:39:30	24	13.06	411.97	4.2	13.1	398.87	0.04	0.100283	
16	40	30	16:40:30	28	12.9	448.76	4.3	12.94	435.82	0.04	0.091781	
16	41	30	16:41:30	30	12.74	431.22	4.5	12.75	418.47	0.01	0.023897	
16	42	30	16:42:30	17	12.77	454.55	5.3	12.78	441.77	0.01	0.022636	
16	43	30	16:43:30	32	12.71	408.26	21.8	12.68	395.58	-0.03	-0.07584	approx zero
16	44	30	16:44:30	15	13.06	405.71	34.3	13.09	392.62	0.03	0.07641	faded not on raw
16	46	0	16:46:00	26	12.99	418.45	30.5	13.02	405.43	0.03	0.073996	
16	47	0	16:47:00	22	13.01	451.18	34.2	13.02	438.16	0.01	0.022823	
16	48	0	16:48:00	67					0	0		Not on weigh sheet
16	49	0	16:49:00	63	12.76	428.1	10.4	12.76	415.34	0	0	
16	50	0	16:50:00	70	12.7	424.16	11.7	12.68	411.48	-0.02	-0.04861	
16	51	0	16:51:00	66	12.95	430.5	12.9	12.95	417.55	0	0	
16	52	0	16:52:00	64	12.92	433.23	15.1	12.93	420.3	0.01	0.023793	
16	53	0	16:53:00	65	12.98	397.89	15.9	12.99	384.9	0.01	0.025981	
16	54	0	16:54:00	60	12.95	421.39	17	12.98	408.41	0.03	0.073456	
16	55	0	16:55:00	61	12.83	424.01	16.3	12.83	411.18	0	0	
16	56	0	16:56:00	68	12.78	392.88	18	12.78	380.1	0	0	
16	57	0	16:57:00	62	12.95	421.39	20	12.96	408.43	0.01	0.024484	
16	58	30	16:58:30	32	12.71	408.26	21.8	12.68	395.58	-0.03	-0.07584	Approx zero
17	0	0	17:00:00	16	12.93	411.07	26.3	12.95	398.12	0.02	0.050236	
17	1	30	17:01:30	26	13.01	454.02	131	13.04	440.98	0.03	0.06803	Exchange with ss26
17	3	0	17:03:00	9	12.83	427.96	28.7	12.86	415.1	0.03	0.072272	
17	4	30	17:04:30	15	12.87	390.15	8.2	12.9	377.25	0.03	0.079523	another 15
17	6	0	17:06:00	1	12.79	261.9	33.8	12.77	249.13	-0.02	-0.08028	
17	8	0	17:08:00	18	12.72	422	50.8	12.68	409.32	-0.04	-0.09772	Approx zero
17	10	0	17:10:00	30	12.89	412.79	30.9	12.9	399.89	0.01	0.025007	box 2
17	12	0	17:12:00	13	12.83	400.54	34	12.84	387.7	0.01	0.025793	box 2 12 or 13
17	14	0	17:14:00	13	13.16	408.08	35.3	13.17	394.91	0.01	0.025322	box2
17	17	0	17:17:00	28	13.07	414.35	38.7	13.1	401.25	0.03	0.074766	box 2
17	21	0	17:21:00	29	12.93	381.28	41.7	12.94	368.34	0.01	0.027149	box2
17	25	0	17:25:00	25	12.98	458.28	43.6	13	445.28	0.02	0.044916	box 2
17	30	0	17:30:00	10	13.1	389.09	50.5	13.13	375.96	0.03	0.077996	box2
17	35	0	17:35:00	23	13.13	400.82	49.9	13.15	387.67	0.02	0.05159	box2
17	52	0	17:52:00	15	12.88	405.6	55.8	12.9	392.7	0.02	0.050929	box 2
17	58	0	17:58:00	11	13.07	373.7	58.9	13.1	360.6	0.03	0.083195	box2
										Corrected	1.77	
										Mean conc. =	0.08647	
										Corrected (with -ve's taken out)	0.096422	

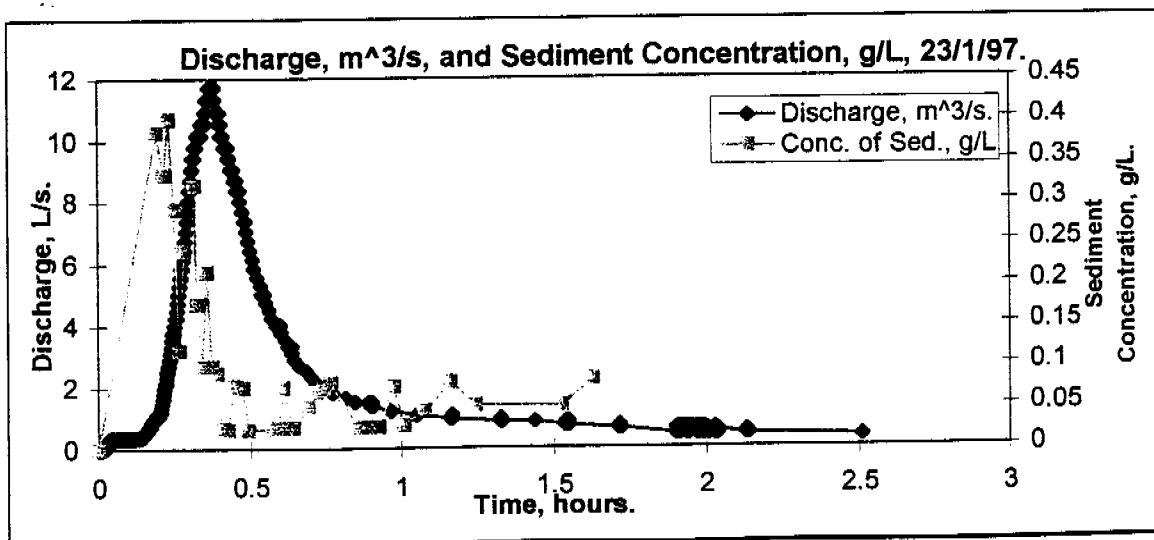


Figure 4.A.9: Plot of the discharge, (m³/s), and suspended sediment concentration, (g/L), for the storm event occurring on the 23rd January on the natural field plot.

28th January

Table 4.A.8: Suspended sediment analysis for the storm event occurring on the 28th January.

Site Name:			Pit1		Base Level		5 uS/cm				
Date:			28th Jan 1997								
Time of storm:			13:05:00								
			TIME	SAMPLE NUMBER	CONT. WEIGHT	CONT. + SED+H2O	COND'CT	CONT. + SED.	WATER	SED.	CONC. OF SED.
hrs	min	sec			g	g	uS/cm	g	g	G	g/L
13	9	30	13:09:30	24	13.07	408.55	39	13.15	395.4	0.08	0.202326758
13	10	30	13:10:30	21	13.13	433.8	48.7	13.21	420.59	0.08	0.190208992
13	11	30	13:11:30	14	12.83	453.87	36	12.93	440.94	0.1	0.226788225
13	12	30	13:12:30	5	12.88	443.42	35.6	12.94	430.48	0.06	0.139379298
13	13	30	13:13:30	17	12.77	452.45	31.5	12.85	439.6	0.08	0.181983621
13	14	30	13:14:30	8	12.83	422.06	28.5	12.91	409.15	0.08	0.195527313
13	15	30	13:15:30	22	12.61	457.7	26.7	12.69	445.01	0.08	0.179771241
13	16	30	13:16:30	18	12.65	443.72	16.1	12.8	430.92	0.15	0.348092453
13	17	30	13:17:30	19	12.8	456.36	21.7	12.94	443.42	0.14	0.315727752
13	18	30	13:18:30	23	13.09	432.62	9.7	13.27	419.35	0.18	0.429235722
13	19	30	13:19:30	31	12.84	443.92	15.6	12.9	431.02	0.06	0.139204677
13	20	30	13:20:30	32	12.69	402.91	14.5	12.74	390.17	0.05	0.128149268
13	21	30	13:21:30	31 faded	13.1	414.19	10.9	13.15	401.04	0.05	0.124675843
13	22	30	13:22:30	29	13.12	457.04	14.4	13.15	443.89	0.03	0.067584311
13	23	30	13:23:30	15	13.07	428.26	10.6	13.11	415.15	0.04	0.096350717
13	24	30	13:24:30	9	12.67	451.02	11	12.7	438.32	0.03	0.068443147
13	25	30	13:25:30	16	12.8	444.07	16.2	12.77	431.3	-0.03	-0.069557153
13	26	30	13:26:30	2	12.69	446.74	12.8	12.73	434.01	0.04	0.092163775
13	27	30	13:27:30	3	13.11	434.97	9.9	13.21	421.76	0.1	0.237101669
13	28	30	13:28:30	1	13.17	416.53	9.3	13.2	403.33	0.03	0.07438078
13	29	30	13:29:30	7	12.58	430.66	17.2	12.61	418.05	0.03	0.071761751
13	30	30	13:30:30	10	12.73	444.44	10.5	12.75	431.69	0.02	0.046329542
13	32	0	13:32:00	11	12.72	439.99	17.5	12.73	427.26	0.01	0.023404952
13	33	0	13:33:00	12	12.69	446.74	12.8	12.71	434.03	0.02	0.046079764
13	34	0	13:34:00	4	12.77	429.51	13.7	12.82	416.69	0.05	0.11999328
13	36	0	13:36:00	20	12.83	444.01	20.6	12.84	431.17	0.01	0.023192708
13	39	0	13:39:00	28	12.84	441.27	25.3	12.84	428.43	0	0
13	42	0	13:42:00	25	12.74	449.48	31.6	12.75	436.73	0.01	0.022897442
13	45	0	13:45:00	27	12.81	417.47	36.8	12.83	404.64	0.02	0.049426651
13	50	0	13:50:00	6	12.58	414.55	43.7	12.59	401.96	0.01	0.024878097
										Total	mean=
										1.61	0.126516753
										Corrected	1.61 0.126815

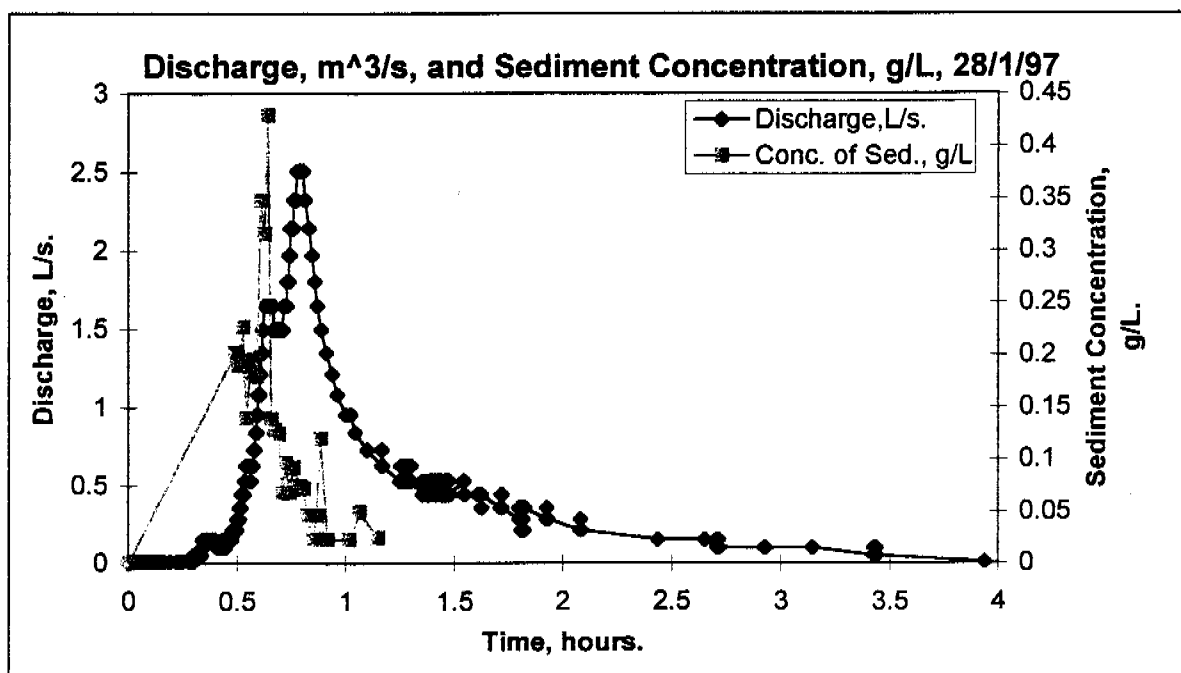


Figure 4.A.10: Plot of the discharge, (m³/s), and suspended sediment concentration, (g/L), for the storm event occurring on the 23rd January on the natural field plot.

Bedload Sediment Data

Table 4.A.9: Collected bedload sediment data from natural field plot over 1996/1997 wet season.

Sample Name.	Container Mass.	Sediment + Container.	Sediment.
19/12/96			
1	12.8	18.84	6.04
2	12.87	69.89	57.02
3	12.92	661.19	648.27
		Total Bedload Mass=	711.33
21/12/96			
1	12.78	17.82	5.04
2	12.68	242	229.32
		Total Bedload Mass=	234.36
24/12/96			
1	12.9	15.65	2.75
2	12.77	359.3	346.53
3	12.76	442.96	430.2
		Total Bedload Mass=	779.48
26-27/12/97			
1	12.67	460.82	448.15
2	12.65	1406	1393.35
		Total Bedload Mass=	1841.5
1/1/97 Before Event			
1	12.79	107.66	94.87
2	12.76	82.93	70.17
3	12.73	16.41	3.68
4	12.86	143.45	130.59
5	12.63	157.41	144.78
		Total Bedload Mass=	444.09
1/1/97 After Event.			
1	12.89	13.6	0.71
2	12.69	25.06	12.37
3	12.72	189.06	176.34
4	12.95	226.96	214.01
5	12.8	493.39	480.59
6	12.66	111.85	99.19
7	12.86	942.85	929.99
		Total Bedload Mass=	1913.2
2/01/97			
1	12.82	50.62	37.8
2	12.92	12.92	0
3	12.94	376.06	363.12
4	12.6	85.17	72.57
5	12.76	993.85	981.09
		Total Bedload Mass=	1454.58
4/01/97			
1	12.79	13.4	0.61
2	12.83	13.54	0.71
3	12.89	14.14	1.25
4	12.95	13.88	0.93
5	12.9	348.78	335.88
		Total Bedload Mass=	339.38
6/01/97			
1	12.74	99.77	87.03
2	12.81	14.65	1.84
3	12.93	13.91	0.98
4	12.73	12.99	0.26
		Total Bedload Mass=	90.11
7/01/97			
1	12.87	13.28	0.41
2	12.93	13.32	0.39
3	13	15.15	2.15
4	13.1	183.77	170.67
		Total Bedload Mass=	173.62
8/1/97 10am			
1	12.82	13.22	0.4
2	12.83	44.26	31.43
3	12.77	24.4	11.63
		Total Bedload Mass=	43.46
10/01/97			
1	12.79	13.02	0.23
2	12.83	13.02	0.19
3	12.88	13.09	0.21
4	12.87	13.63	0.76
5	12.83	128.33	115.5
		Total Bedload Mass=	116.89
11/1/97 6.30pm			
1	12.66	12.84	0.18
2	12.58	12.74	0.16
3	12.59	12.77	0.18
4	12.66	13.12	0.46
5	12.76	12.9	0.14
6	12.52	12.8	0.28
7	12.51	12.65	0.14
8	12.44	12.57	0.13
9	12.48	54.21	41.73
10	12.45	308.7	296.25
		Total Bedload Mass=	339.65

Table 4.A.9: (Continued) Collected bedload sediment data from natural field plot over 1996/1997 wet season.

Sample Name	Container Mass	Sediment + Container	Sediment
12/1/97 4pm			
1	12.54	13.33	0.79
2	12.39	47.84	35.45
3	12.55	14.79	2.24
4	12.56	15	2.44
5	12.49	101.78	89.29
6	12.89	13.34	0.45
7	12.85	682.24	669.39
8	12.9	84.68	71.78
		Total Bedload Mass=	871.83
12/1/97 5.30pm			
1	12.78	13.67	0.89
2	12.75	13.18	0.43
3	12.66	12.89	0.23
4	12.63	12.84	0.21
5	12.7	782.02	769.32
		Total Bedload Mass=	771.08
12/1/97 6.30pm			
1	12.84	41.58	28.74
2	12.88	13.96	1.08
3	12.86	13.16	0.3
4	12.86	48.04	35.18
		Total Bedload Mass=	65.3
16/01/97			
1	12.86	17.13	4.27
2	12.66	13.53	0.87
3	12.6	228.85	216.25
		Total Bedload Mass=	221.39
17/1/97 5.30pm			
1	12.92	13.85	0.93
2	13.02	177.44	164.42
3	12.98	144.44	131.46
4	29.49	35.4	5.91
		Total Bedload Mass=	302.72
19/1/97 5pm			
1	29.41	30.91	1.5
2	12.74	248.94	236.2
		Total Bedload Mass=	237.7
21/1/97 Storm 1			
1	28.25	220.92	192.67
2	28.8	219.5	190.7
3	12.89	59.89	47
		Total Bedload Mass=	430.37
21/01/97			
1	12.89	13.28	0.39
2	12.8	154.72	141.92
3	12.73	13.75	1.02
4	12.86	41.82	28.96
		Total Bedload Mass=	172.29
23/01/97			
1	29.44	31.45	2.01
2	29.64	1173.1	1143.46
		Total Bedload Mass=	1145.47
23/01/97			
1	28.68	36.94	8.26
2	28.53	255.02	226.49
		Total Bedload Mass=	234.75
24/01/97			
1	28.38	31.58	3.2
2	12.82	407.73	394.91
		Total Bedload Mass=	398.11
27/01/97			
1	29.63	296.01	266.38
		Total Bedload Mass=	266.38
28/01/97			
1	28.56	34.29	5.73
2	28.6	71.49	42.89
3	28.64	57.3	26.66
4	28.51	319.75	291.24
		Total Bedload Mass=	368.52
1/02/97			
1	28.66	30.24	1.58
2	12.53	13.56	1.03
3	12.55	153.61	141.06
4	12.77	144.06	131.29
		Total Bedload Mass=	274.96

Appendix 4.B

Particle Size Analysis.

Figure 4.B.1, illustrates the position of all of the particle size analysis samples that were collected from the natural field plot.

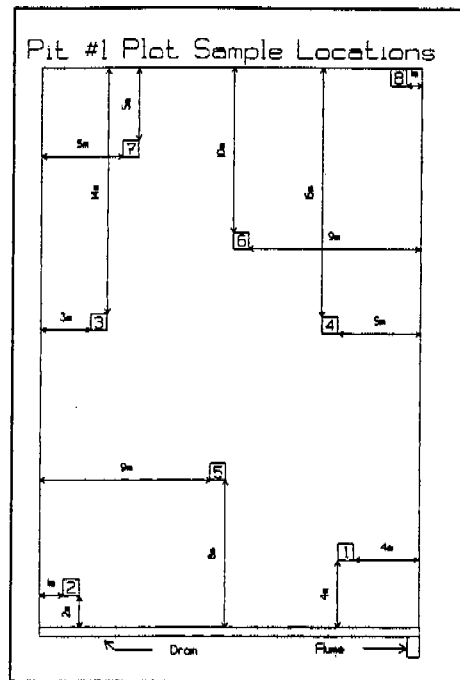


Figure 4.B.1: Distribution of particle size samples from the natural site, (Smith, 1997).

The average particle size distribution over all the samples collected, Smith (1997), is illustrated in Figure 4.B.2.

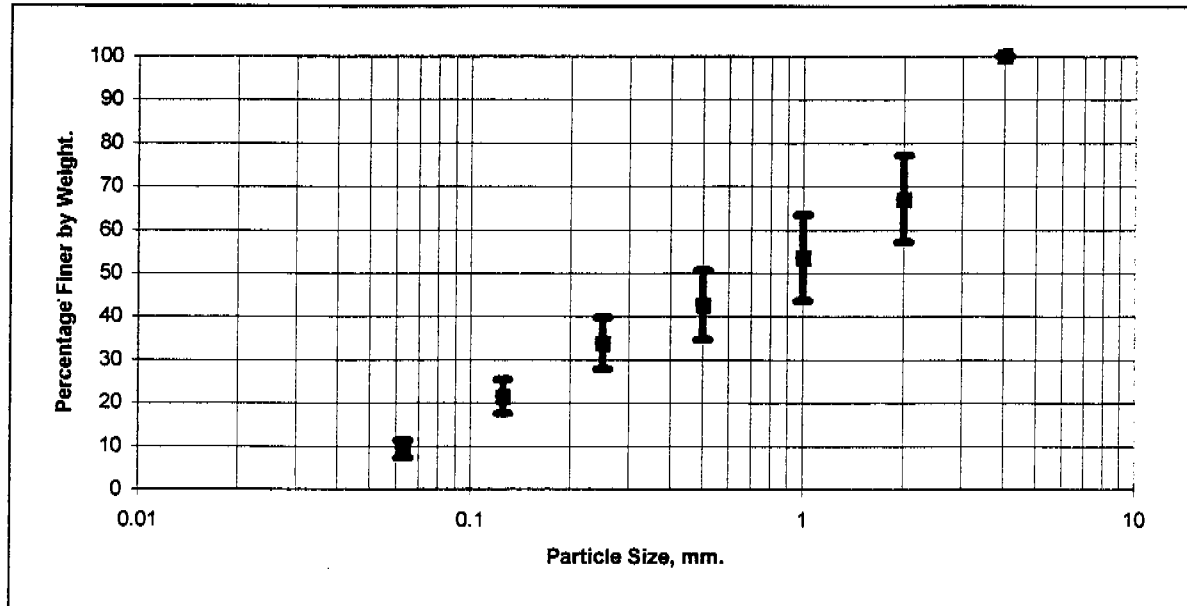


Figure 4.B.2: Average percentage finer particle size analysis derived from samples collected from a random number of locations around the natural field plot.

The d_{50} for the natural site was determined to be approximately 0.8 mm, which is comparable to that reported for the cap and batter sites.

Appendix 4.C

Regression Analysis For Overland Flow Erosion and Total Sediment Loss Models.

Table 4.C.1: Log-Log regression analysis for the overland flow erosion model, Section 4.3.

SUMMARY OUTPUT						
<i>Regression Statistics</i>						
Multiple R	0.859162116					
R Square	0.738159541					
Adjusted R Square	0.736600967					
Standard Error	0.358506217					
Observations	170					
ANOVA						
	<i>df</i>	<i>SS</i>	<i>MS</i>	<i>F</i>	<i>Significance F</i>	
Regression	1	60.87180068	60.87180068	473.6120737	9.30572E-51	
Residual	168	21.59248694	0.128526708			
Total	169	82.46428762				
	<i>Coefficients</i>	<i>Standard Error</i>	<i>t Stat</i>	<i>P-value</i>	<i>Lower 95%</i>	<i>Upper 95%</i>
Log10(K)	-0.929432869	0.027974295	-33.22453227	9.37168E-76	-0.984659319	-0.87420642
m1	0.853360152	0.039212179	21.76263021	9.30572E-51	0.775948034	0.930772271

Table 4.C.2: Log-Log regression analysis for the total sediment loss model, Section 4.3.

Log regression analysis for the total sediment loss model, Section 4.3.

SUMMARY OUTPUT						
Regression Statistics						
Multiple R	0.999718938					
R Square	0.999437955					
Adjusted R Square	0.999250607					
Standard Error	0.01799414					
Observations	5					
ANOVA						
	df	SS	MS	F	Significance F	
Regression	1	1.727301869	1.727301869	5334.651495	5.65612E-06	
Residual	3	0.000971367	0.000323789			
Total	4	1.728273236				
	Coefficients	Standard Error	t Stat	P-value	Lower 95%	Upper 95%
Log 10(K)	-0.822985506	0.052293776	-15.73773345	0.000557657	-0.989407795	-0.656563216
Log 10(Total of $\int(Q^m)dt$)	0.996980202	0.013650027	73.03869861	5.65612E-06	0.953539683	1.04042072